UNIVERSIDADE DE LISBOA
FACULDADE DE CIÊNCIAS
DEPARTAMENTO DE BIOLOGIA ANIMAL

Understanding the differentiation process of western Mediterranean butterflies: the case studies of *Lycaena* and *Melanargia*

Miguel Simões Nunes

Mestrado em Biologia Evolutiva e do Desenvolvimento

Dissertação orientada por:
Dr. Octávio Paulo
Msc. Eduardo Marabuto

2019

Acknowledgements

Um agradecimento à família pela paciência, ajuda e compreensão do tempo que levou a chegar a este resultado final. Foi difícil explicar a razão pela qual dediquei tanto tempo a um projecto que ia mais longe do que se pedia, trocando esforço, tempo e saúde por algo que não dá muito em retorno.

Agradeço também aos dois orientadores desta tese, Octávio Paulo e Eduardo Marabuto.

Agradeço em primeiro lugar ao Professor Octávio pelo facto de me ter aceite no grupo CoBIG2. No início do meu percurso universitário em Biologia percebi que gostaria de vir a integrar este grupo após ver uma apresentação sua sobre *Lacerta schreiberi* (lagarto de água). Perseguindo essa vontade, tal acabaria por acontecer, e fiquei feliz quando integrei por fim o leque de investigadores do CoBIG2 e me pude sentar entre cientistas que respeitava e ouvia atentamente nas reuniões, tentando absorver o maior conhecimento possível.

Sobre a tese, agradeço o seu incentivo de me fazer pegar no projecto das *Lycaena* quando o objectivo inicial estava somente delineado para as *Melanargia*. Foi um projecto trabalhoso, complexo, e que tomou conta da maior parte do meu tempo desta tese, mas foi também um projecto que fez sentir que estava a produzir algo de interessante e com um impacto real no conhecimento do mundo que nos rodeia e de que me orgulharia mais tarde.

Ao Eduardo deixo um agradecimento especial, pois acompanhou o progresso desta tese desde o início ao fim, transmitindo todo o seu conhecimento em prol da discussão de ideias e da interpretação do que passo a passo íamos descobrindo. Ao começar este projecto, o meu conhecimento sobre borboletas era quase inexistente, e a maior parte do que hoje sei e aprendi nesta área devo-o aos seus ensinamentos. Espero ter sido um bom padawan Mestre Marabuto.

Um agradecimento também especial aos restantes membros do CoBIG2. Aos que integravam o grupo quando eu apareci pela primeira vez, aos que vieram de passagem, e aos membros que chegaram recentemente. Todos contribuíram para o lado bom e positivo de se perseguir uma tese de mestrado neste grupo de investigação, e todos contribuíram para a união que se sente entre as pessoas que fazem este grupo. Foi um prazer trabalhar ao vosso lado.
Às pessoas que de forma um pouco mais directa ajudaram e contribuíram para que se atingisse este resultado final, um obrigado especial (Francisco Pina-Martins, Tatiana Moreira, João Raimundo e Raquel Mendes).

Agradeço ainda a todas as pessoas que contribuíram para o crowfunding online, organizado pela nossa equipa ExpedMarrocos, que financiou a nossa expedição de duas semanas a Marrocos e que tinha como um dos seus objectivos colectar espécimes do género *Melanargia* para este estudo. Um agradecimento especial à Associação Bioliving, ao Trilhos da Terra, Quinta da Mariposa, Noesis, Ria Prestige, MTL Estúdios, ASTRO Travel e NAUTA, bem como aos nossos amigos Patrícia Alegria, Carlos Moreira da Silva, Sara Raquel Fernandes, Teresa Cruz Santos, Jorge Garzón Gutiérrez, Ana Valadares, Andreia Moreira, Diana Moreira e Pedro Pires.

Por último, mas não menos importante, um agradecimento sentido a quem se prepara para ler esta tese. A sua coragem é de louvar. Obrigado!

Abstract

The western Mediterranean region is responsible for generating and keeping a great amount of interspecific and intraspecific variation among numerous groups of species. Choosing butterflies as a model organism, this study aims to unravel the differentiation process of a few species from this Mediterranean region, belonging in two different genera: *Lycaena* and *Melanargia*. Therefore, the present work is divided in two case-studies, both focusing on different but complementary problematics: The first deals with the speciation and relationship between the two Sooty Copper butterflies, *L. tityrus* (the Sooty Copper, widespread in Europe) and *L. bleusei* (the Iberian Sooty Copper, an Iberian endemic), which has been considered as a subspecies of the former; the second studies the phylogenetic relationships and genetic differentiation of the whole subgenus *Argeformia*, belonging in the genus *Melanargia*, in particular the species *Melanargia ines* (widespread in Iberia and North Africa), *M. occitanica* (found in South of France + North Italy, Iberia, North Africa and Sicily) and *M. arge* (Italian endemic). While the first deals with two sister taxa and goes through different analyses (Genetics, Geometric Morphometrics and Species Distribution Modeling (SDM)) in one integrative study to infer if these should be considered as independent species, the second tries to confirm the current phylogenetic relationships among the species of *Argeformia*, and analyse the gene flow across the different land and sea barriers of the western Mediterranean region. Overall, each analysis conducted for *Lycaena* allowed us to clearly differentiate both Sooty Coppers and conclude that these should be considered as different species. Nonetheless, their reproductive barriers appear not to be fully developed and two *L. tityrus* specimens displayed introgressed *L. bleusei* genetic material. Additionally, the combination of Genetics and SDM results support the hypothesis of a post glacial population and genetic bottleneck for *L. bleusei*. Regarding *Melanargia*, our phylogeny agrees with the current classification and relationships within *Argeformia*, with *M. occitanica* sister to *M. arge* and both closely related to *M. ines*. The western Mediterranean barriers displayed different roles and capacities to isolate populations gene flow, with the Gibraltar Strait being the most influential barrier. Different evolutionary history scenarios are here presented for both the Sooty Coppers and *Argeformia* species, which seem to have a differentiation process fundamentally driven by isolation in allopatry across the geographic barriers and climatic oscillations in a first phase, and different ecological adaptations later.

Key words: Butterflies; Western Mediterranean; Lycaena; Melanargia

Resumo

Tendo como objectivo geral compreender o processo de diferenciação das espécies de borboletas da região oeste do Mediterrâneo, o presente trabalho divide-se em dois casos de estudo independentes, mas complementares, que se focam no processo de diferenciação particular de dois géneros de borboletas desta região paleártica: os géneros *Lycaena* e *Melanargia*. Estes géneros pertencem a famílias de borboletas distintas e com características diferentes, a família Lycaenidae no caso das *Lycaena* e Nymphalidae no caso das *Melanargia*, mas cujo estudo nos permitirá olhar para o complexo processo de diferenciação através de diferentes perspectivas, de uma forma mais abrangente.

No primeiro caso de estudo, o presente trabalho procura desvendar a verdadeira relação filogenética e taxonómica de dois taxa do género *Lycaena*: *Lycaena tityrus* e *Lycaena bleusei*; que têm ora sido classificados como uma única espécie, sendo *L. bleusei* considerada uma subespécie de *L. tityrus*, ora atribuído o estatuto de espécie a cada uma. *Lycaena tityrus* é uma espécie com uma distribuição alargada, estendendo-se desde a Rússia até à Europa ocidental, chegando à Península Ibérica, onde ocupa a região Norte e algumas regiões montanhosas do centro de Portugal. Esta espécie possui diferentes morfotipos ao longo da sua distribuição, tendo ainda uma subespécie isolada nos Alpes, *L. t. subalpinus*. Por outro lado, *Lycaena bleusei* é um endemismo Ibérico, estando restrita à região montanhosa do centro da Península.

A relação entre os dois taxa é aqui analisada através de uma abordagem integrativa, que une ferramentas e análises de diferentes disciplinas para chegar a uma conclusão robusta e suportada. Assim sendo, as duas entidades biológicas são primeiramente enquadradas numa análise filogenética do género *Lycaena*, numa inferência mais abrangente recorrendo aos genes COI e EF-1α, e posteriormente enquadradas num grupo mais restrito de espécies que se encontram filogeneticamente mais próximas, adicionando à matriz dos genes anteriores os genes 16S, Wingless e CAD2. Estas filogenias permitiram confirmar a próxima relação taxonómica de *L. tityrus* e *L. bleusei*. Foi também realizada uma estimativa dos tempos de divergência entre as diferentes espécies do género *Lycaena*, sendo que *Lycaena tityrus* e *Lycaena bleusei* obtiveram uma estimativa de divergência na ordem dos 6.5 milhões de anos atrás.

Ainda a nível genético é analisada a variabilidade dos genes COI e EF-1α para os dois taxa, bem como a segregação geográfica dessa mesma variação ao longo da sua distribuição. *Lycaena bleusei* apresenta apenas dois haplótipos do gene mitocondrial COI mas curiosamente possui um número maior de haplótipos nucleares EF-1α. *Lycaena tityrus*, aparenta ter dois haplótipos do gene mitocondrial COI exclusivos da Península Ibérica, e o seu haplótipo mais comum está também presente na região da Catalunha. Surpreendentemente, dois indivíduos com fenótipo de *L. tityrus* e haplotipos COI do gene pool de *L. tityrus* revelaram sinais de introgressão ao apresentarem haplótipos nucleares EF-1α do gene pool de *L. bleusei*. Esta descoberta revela que *L. tityrus* e *L. bleusei* têm ainda a capacidade de se reproduzir e hibridar, ainda que esta introgressão possa ser antiga.

Como forma alternativa de olhar para os dados genéticos, é ainda utilizada a medida de diferenciação genética populacional Fst para comparar os níveis de diferenciação entre populações dentro de cada taxon, mas também entre ambos ao incluir *L. bleusei* como uma

população de *L. tityrus*. São igualmente comparados os valores de Fst entre as três entidades mais relevantes e consideradas como subespécies da mesma espécie: *L. t. tityrus*, *L. t. subalpinus* e *L. bleusei*. Adicionalmente, é também utilizada a Análise de Variação Molecular (AMOVA – Analysis of Molecular Variation) para comparar os valores de diferenciação genética obtidos agrupando as diferentes populações destes taxa em diferentes combinações hierárquicas. Todas estas análises revelam não só uma enorme diferenciação entre *L. bleusei* e *L. t. tityrus* como também entre *L. bleusei* e *L. t. subalpinus*.

Numa abordagem diferente, são também analisadas e comparadas as diferenças morfológicas de tamanho e forma da asa posterior entre *Lycaena tityrus* e *Lycaena bleusei* através da técnica de Morfometria Geométrica. Esta análise permite verificar que de uma forma sistemática, *L. bleusei* tem a asa posterior maior do que *L. tityrus*, e que as fêmeas da primeira têm esta asa maior do que os machos. É também verificado que o taxon *Lycaena bleusei* apresenta uma pequena cauda na região final da asa posterior, mais pronunciada nas fêmeas do que nos machos, e mais evidente na sua forma de verão. Esta cauda não está presente em *L. tityrus*.

Por fim, numa terceira abordagem é realizada uma modelação dos nichos climáticos dos dois taxa, com recurso aos pontos de ocorrência de ambos e às variáveis bioclimáticas da WorldClim para o Presente e para o último máximo glacial (LGM - Last Glacial Maximum). Desta forma, é feita uma análise das potenciais zonas de nicho climático favorável para cada uma das entidades na sua área de distribuição, tanto no Presente como no LGM, comparando-as entre si e com as distribuições actuais de cada uma. Esta inferência permite identificar não apenas zonas onde as espécies poderiam ocorrer actualmente, mas também possíveis zonas de refúgio durante o LGM. No geral, a previsão para o Presente não altera consideravelmente os locais dados como favoráveis para a ocorrência dos dois taxa em relação à sua distribuição actual. O mesmo acontece com a previsão de distribuição de *L. tityrus* no LGM mas, surpreendentemente, isso não acontece com *L. bleusei* que mostra uma grande expansão da sua potencial distribuição durante o período glacial. Esta potencial expansão glacial e menor distribuição interglacial associada à maior variabilidade do gene nuclear EF-1α em relação ao gene mitocondrial COI levanta a questão: estará a *Lycaena bleusei* neste momento a atravessar um bottleneck populacional e genético pós-glacial? Finalmente, tendo em conta os resultados das diferentes abordagens que de uma forma integrativa tornam este estudo mais suportado chegamos à conclusão de que as duas entidades *Lycaena tityrus* e *Lycaena bleusei* devem ser tratadas como espécies distintas.

O segundo caso de estudo foca-se em três espécies do género *Melanargia* que em conjunto compõem o subgénero *Argeformia*: *Melanargia ines*, *Melanargia occitanica* e *Melanargia arge*. As duas primeiras têm distribuições alargadas na região Oeste do Mediterrâneo, ocorrendo ambas na Península Ibérica e Norte de África, e estando *Melanargia occitanica* ainda presente no sul de França, norte de Itália e Sicília. *Melanargia arge* por outro lado está restricta ao centro e sul de Itália. As suas relações filogenéticas, apesar de previamente analisadas por outros autores, aparentavam ser contraditórias consoante o gene estudado tendo ainda pouco suporte estatístico. Desta forma, adicionámos mais um gene nuclear (EF-1α) à matriz de genes já estudada numa tentativa de resolver ou consolidar estatisticamente as suas relações filogenéticas e taxonómicas. No entanto, a nossa filogenia corrobora a filogenia obtida em estudos anteriores, sendo *Melanargia occitanica* e *Melanargia arge* filogeneticamente mais próximas uma da outra, e *Melanargia ines* a espécie que divergiu primeiro neste clade. Foi igualmente feita uma estimativa dos tempos de divergência entre estas espécies, sendo que foi obtida uma estimativa média de divergência à volta dos 5.7 milhões de anos entre *M. occitanica* e *M. arge* e de 14.5 milhões de anos entre *M. ines* e as anteriores.

Este trabalho teve também o objectivo de estudar a variabilidade do gene COI nas espécies *M. ines* e *M. occitanica* bem como a segregação geográfica dessa mesma variabilidade genética ao longo da sua distribuição. Através desta análise pudemos confirmar a já conhecida relação genética próxima entre a população de *M. occitanica* da Sicília (subespécie *M. o. pherusa*) e as populações do Norte de África, sugerindo uma colonização da Sicília a partir desta região. Tendo estas espécies uma distribuição alargada na região oeste do Mediterrâneo foi também analisada a influência de diferentes barreiras geográficas no "gene flow" entre populações da mesma espécie. Assim, as grandes barreiras geográficas dos Pirenéus, montanhas do Atlas, e Mar Mediterrâneo (estreitos de Gibraltar e da Sicília) foram estudadas do ponto de vista da sua capacidade de fragmentar e isolar populações através das diferenças genéticas encontradas entre as mesmas. Foram mais uma vez usadas as medidas de diferenciação genética populacional Fst e AMOVA, e o estreito de Gibraltar revelou o maior efeito isolador entre populações. As restantes barreiras estudadas apesar de demonstrarem ser menos eficazes que o estreito de Gibraltar, tendo permitido a passagem de alguns indivíduos desde a fragmentação inicial das populações, aparentam conseguir isolar de forma consistente as populações e os clusters genéticos dos dois lados. Por fim, foi igualmente realizada a modelação dos nichos climáticos para as três espécies do subgénero *Argeformia*. Esta modelação revelou poucas diferenças para a distribuição actual das três espécies, mas revelou uma distribuição mais alargada em redor do Mediterrâneo para *M. occitanica* e *M. ines* durante o LGM. Curiosamente a modelação de *M. arge* para o LGM não encontra qualquer região climaticamente adequada para a sua ocorrência.

A junção das diferentes abordagens em cada caso de estudo permitiu a elaboração de diferentes cenários para a história evolutiva destas espécies. Esta metodologia demonstrou ainda a importância e a vantagem de realizar um estudo integrativo englobando diferentes áreas da Ciência como apoio ao tradicional estudo de Filogeografia. Os dois casos de estudo permitiram a análise de diferentes fases de um processo de diferenciação complexo entre populações e espécies nesta região Mediterrânica. Um processo que nos casos de estudo analisados aparenta ser essencialmente despoletado pela topologia desta região geográfica, bem como pelos eventos climáticos do passado que, em fases diferentes deste processo, levam as espécies a fragmentar as suas populações e a evoluir diferencialmente em alopatria, com avanços e recuos, adaptando-se de forma distinta a novos estímulos ambientais e ecológicos e acumulando diferenças genéticas.

Palavras-chave: Borboletas; Mediterrâneo; *Lycaena*; *Melanargia*

Index

Tables and Figures Index

1. Introduction

1.1. The importance of the Mediterranean region on promoting and keeping diversity

The Mediterranean is the richest and most heterogeneous biogeographical region of the Palaearctic in habitats and biodiversity[1]. Its geomorphology is the result of an expressive transformation over time, with its shape, ecosystems and biota being severely influenced by tectonics and orography, as well as the climatic oscillations over time. The convergence of the Eurasian and African plates starting around 170-175 Mya gave rise to the uplift of big orogenic belts and mountain ranges within the Mediterranean, as well as to important connections between the two continents, such as the land connection between Iberia and North Africa around 6-5.3 Mya, which caused the evaporation of most of the Mediterranean sea, an event designated as Messinian salinity crisis (MSC) [2–4]. This event allowed for the interchange of many species, either by land or due to the proximity of the two continents with lower sea level in between, influencing the distribution patterns of many taxa we observe today[5–11].

The climatic oscillations of the Quaternary period (< 2.3 Mya) have also played a major role in shaping many species distribution, as well as their genetic diversity[7,8,12,13]. The Mediterranean basin has been a retreat ground for biodiversity, especially during glacial periods, with many taxa escaping from the extreme cold felt in northern latitudes. As such, several areas of this region served as refugia for species seeking southern latitudes and warmer temperatures, being especially important the Iberian, Italic and Balkan Peninsulas, as well as North Africa[4,14–16], although other extra-Mediterranean refugia have also been important and should not be ignored[17,18].

For many refuged species, a big part of their genetic diversity has been eroded with the extinction of genetic lineages, given the shrinkage into smaller population pockets and the action of selection and genetic drift. In the end, many populations survived the glacial periods isolated in their own refuges, and potentially representing only a subset of the initial gene pool. These refugia served later as the source for several species' northern recolonizations during glacial-interglacial transitions, where previous rear edge populations became now the expanding leading edge[17,19–21]. However, not all species followed this pattern during glacial periods, and some of them with a greater cold tolerance were able to resist in stable populations in more northern latitudes[21–24], or even expand their range due to favourable colder conditions[13,25–27].

Overall, for most taxa, refugia acted not only as biodiversity reservoirs but also as promoters of differentiation by splitting populations apart in different isolated pockets, and leading to their genetic divergence with time, genetic drift and mutations. This has thus influenced the patterns of geographic structure observed for many species' genetic diversity, and increased the rates of speciation in the Mediterranean basin, as seen for the Iberian Peninsula with an endemicity rate that surpasses 30% [14,28–30]. However, not only glacials promote the differentiation of populations and the Mediterranean region has a wide diversity of topologies and barriers that keep promoting diversity even in interglacial periods. From big mountains to rivers, islands and sea barriers, the variable orography together with favourable climatic conditions have made the Mediterranean region a centre of diversification for fauna and flora.

In fact, this biogeographic region combines a wide range of different habitats, sheltering 10% of all plant species in the world and 80% of all endemic European plants, some of which are restricted

to small ranges[31]. Its own flora richness allied with the orography and climate allowed for the emergence of specific ecosystems as well as a wide range of phytophagous species dependent on them. Small scale subsistent farming activities and agroforestry practices also exerted a big influence within this region by creating a complex mosaic of semi-natural habitats in different succession stages, rich in wildlife. Ultimately, the resulting vegetation structure and plant diversity of the Mediterranean is particularly important to insects, like butterflies, and 75% of the total European insect fauna is found in this area[29,32].

Furthermore, butterfly species richness was shown to be mostly correlated to actual evapotranspiration, a measure of water–energy balance, being the richness higher on warm and wet areas close to the Mediterranean sea[33]. Also, climate has been considered the main factor shaping the range limits of butterflies, directly[34–36] or indirectly by affecting the viability of their hostplants or the timing of these plants' growth[37]. Many species are dependent on a single hostplant species or a single genus (monophagous) and display smaller distribution ranges than their hostplants[38–40]. Thus, they become very scarce or inexistent when these are absent, although some maintain the capacity to shift hostplant or become polyphagous when in need[40,41].

However, the Mediterranean region is already being affected by climate change and is foreseen to experience an increase in temperature (2-4° C), aridity and desertification, as well as a decrease in precipitation in a near future[32]. Habitat types known today are likely to shift, with African and Asian species possibly arriving and current Mediterranean species expected to move northwards or higher in altitude[36]. In the driest parts of the Mediterranean, short spring and autumn seasons are critical periods for plant growth, and consequently for many insects feeding on them as well. Changes in timing and length of these short seasons may have severe consequences on wildlife and ecosystem food-webs all over the region[32,37].

1.2. Case-study 1 - *Lycaena* and the Sooty Copper butterflies

Lycaena is a large and widespread butterfly genus, with approximately 64 species spread around Palaearctic, Nearctic and Oriental biogeographic regions, but also in South Africa and New Zealand. This genus belongs in the Lycaeninae subfamily, which comprises two recognized tribes: Lycaenini (Leach, 1815) and Heliophorini (Geyer, 1832). The focus of this study is on the Lycaenini tribe and most particularly on the taxa *Lycaena tityrus* (Poda, 1761) and *Lycaena bleusei* (Oberthür, 1884). The former, commonly known as the Sooty Copper, is a widespread Palaearctic species, extending from Central Asia to the northern region of the Iberian Peninsula and parts of central Portugal. Alternatively, *L. bleusei*, known as the Iberian Sooty Copper, is an Iberian endemism, restricted to the central part of this Peninsula (Figure 1.1).

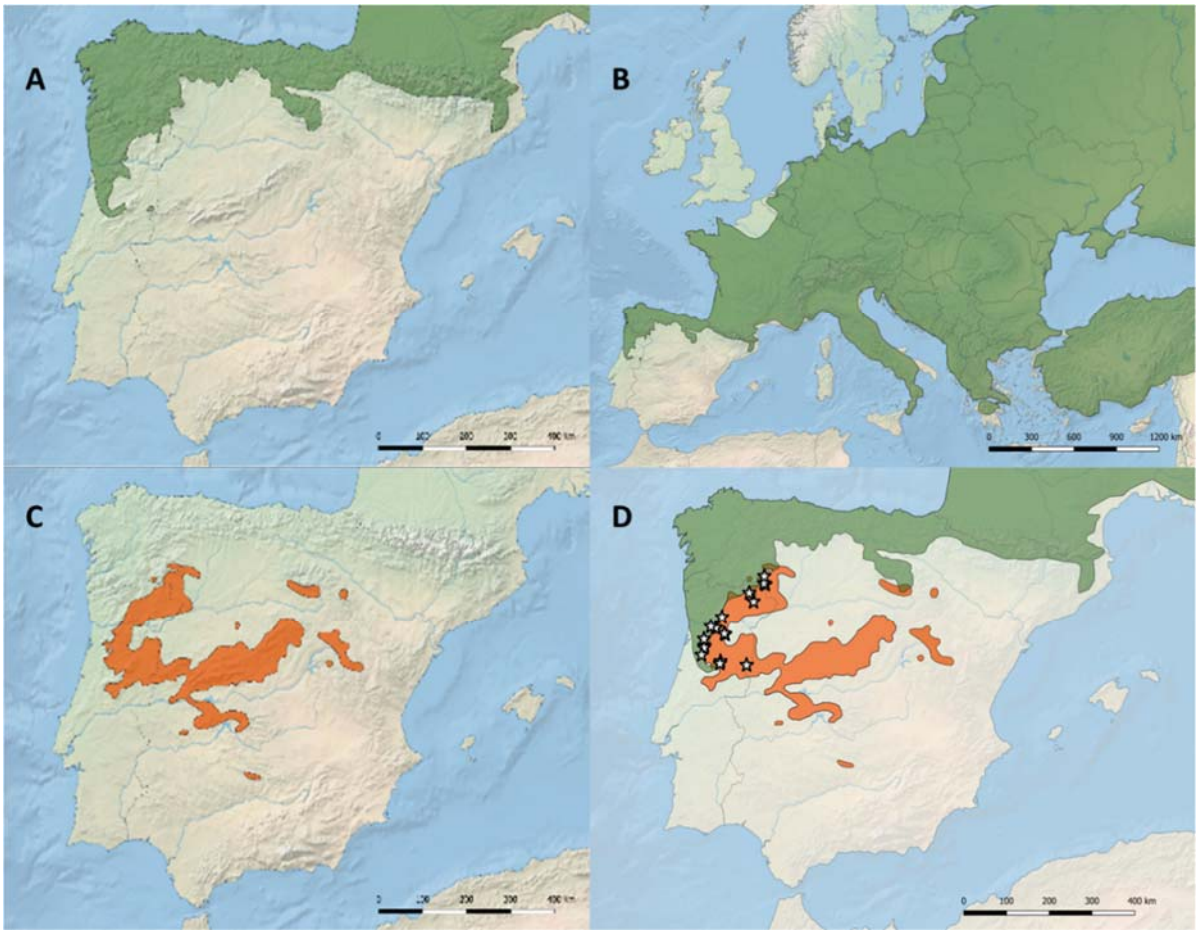

Figure 1.1 – Distribution range of: *L. tityrus* in Iberia (A) and Europe (B); *Lycaena bleusei* (C); Both taxa in Iberia with sympatric locations represented by stars (D).

Both taxa are phenotypically similar (Figure 1.2) and *L. bleusei* has many times been considered a subspecies or a race of *Lycaena tityrus* during the past decades[42–44]. Even so, based on some well-defined diagnostic morphological characters, *L. bleusei* was raised to species level at the end of the 20th century[45,46]. However, morphological characters are still considered to provide insufficient resolution for a correct phylogenetic inference[47] and the taxonomic position of this taxon hasn't been stable, and it has still been branded as a mere subspecies of *L. tityrus* on some taxonomic list updates[48,49]. Nonetheless, a published barcode study has later suggested the species status for *L. bleusei*[50], and the number of publications recognising it have also been growing in recent years, following a better understanding of both Sooty Copper populations and their interaction[51–56]. Additionally, *Lycaena tityrus* has another recognised subspecies isolated in the Alps, *Lycaena t. subalpinus* (Speyer, 1851) (Figure S1.1), but its taxonomic status has also been largely discussed and debated[46,57–59].

Figure 1.2 – Male (A) and female (B) *L. tityrus* upperside; *L. tityrus* underside (C); Male (D) and female (E) *L. bleusei* upperside; *L. bleusei* underside (F).

Overall, *Lycaena* are small-sized species, averaging 20-30 mm wingspan, and can have 1-3 generations per year although 2 generations are more usual. The hostplant choice is not constant within the genus and for the Sooty Coppers is mostly *Rumex acetosa*, but also *R. acetosella* and *R. scutatus*[44,60], while adult butterflies predominantly feed on composite plants (Compositae). The morphology of our two focal taxa is only slightly different and often difficult to assess, especially within spring generations, but in general, males of *L. tityrus* have a dark brown upper side colouration (sooty appearance), contrasting with most of the other more brightly coloured *Lycaena*. This species exhibits a distinct sexual dimorphism with female upper side wings showing a more pronounced orange colouration, though variable. On the underside, both sexes exhibit a similar pattern of small black spots and a row of orange spots near the margin over a grey/sand-coloured background. *Lycaena bleusei* shares many of these traits, but in the second annual generation (and beyond) both sexes show a small but distinct tail in the hindwing anal edge, as well as more pronounced black spots on a bright orange background in both wings upper side and a more yellowish colour on the underside. Moreover, this species is not as sexually dimorphic as *L. tityrus* and males are similar to females in many aspects, such as the presence of a golden or orange background on the upper side where darker spots stand out (Figures 1.2 and S1.1).

Still, these taxa' phenotype can be quite variable, especially in such a widespread species as *L. tityrus*[42,43,57,61]. In fact, apart from the sexual dimorphism already mentioned, the males of this species display several different morphotypes throughout its distribution (Figure S1.2), while females display at least two. These morphotypes are not taxonomically relevant, representing phenotypic variations mostly perceived in the upper wing colouration. However, the complexity concerning these taxa is only the tip of the iceberg for this genus, which also shares a lot of taxonomic and phylogenetic uncertainties and currently lacks a comprehensive and unifying phylogeny. In truth, few molecular studies have been carried so far, attempting to clarify the relationships between the Nearctic species[62], the Nearctic and Palaearctic species[63] or the whole genus[47,64]. While the latter managed to gather representative species from most of the *Lycaena* distribution range (except the Oriental region), but used only mitochondrial genes in their inference, the most recent study by Oliver & Stein (2011) managed to use both

mitochondrial and nuclear genes but lacked on species representation. Even so, the dataset from both studies is far from being representative of the total amount of taxa within *Lycaena* and missed the inclusion of *Lycaena bleusei* in their phylogenies.

In the end, *L. bleusei* is one of many misunderstood taxa and cryptic diversity cases, generated through time in suitable places promoting diversity like Iberia, hidden from common knowledge and waiting to be studied and understood. Are these Sooty Coppers really different species? This should only be answered through a multi approach integrative study, as shown ahead.

1.3. Case-study 2 – *Melanargia* and the subgenus *Argeformia*

The genus *Melanargia* (Meigen, 1828) belongs in the subfamily Satyrinae, and in the tribe Satyrini. It is the only genus of the subtribe Melanargiina, and comprises 24 species with a Palaearctic distribution, from the western Mediterranean region to the far east of Russia[65]. It is usually divided in three subgenera: *Melanargia* (Meigen, 1828), *Argeformia* (Verity, 1955) and *Halimede* (Oberthur and Houlbert, 1922)[66]. The present work focusses only on the *Argeformia* subgenus, endemic to the western part of the Mediterranean area. It includes three allopatric or partially sympatric species, whose relationships are not well studied: *Melanargia ines* (Hoffmannsegg, 1804), *Melanargia occitanica* (Esper, 1793), and *Melanargia arge* (Sulzer, 1776).

While *M. arge* is restricted to the Italian Peninsula, the other two have a wider geographic distribution: *M. ines* is found in the Iberian Peninsula and in the Maghreb, from Morocco to Libya; and *M. occitanica* occupies Iberia, Mediterranean southern France to extreme western Italy (Liguria), small patches in North Africa (Morocco and Algeria) and an isolated population in Sicily (Figure 1.3). The latter population is attributed to subspecies *M. o. pherusa*[46,49,65], often treated as a distinct species due to little larvae differences in early stages[58,67,68]. Within *Argeformia*, intraspecific variation has been considered relevant to the elevation of some populations to subspecies level and both *M. ines* and *M. occitanica* are considered to include three subspecies each[49,65], while *M. arge* is monotypic. The list of currently accepted *Argeformia* subspecies[65] and respective type localities are shown in Supplementary Material (Table S1.1).

Figure 1.3 – Distribution ranges of *Melanargia ines*, *Melanargia occitanica* and *Melanargia arge* in the western Mediterranean region.

Argeformia species use several genera of Poaceae as host plants, while adult stages feed on Compositae and Dipsacaceae plant species[49,67–69]. They occupy mostly grasslands and have a single annual generation[49] with two larvae diapauses: from June to August-October in the larvae stage L1 and from November to January/February in L3[67–69]. These taxa fly earlier than other *Melanargia*, mostly between April-June, and females tend to be larger independently of the species. Curiously, *Argeformia* females have different wingspan ranges for each species: *M. ines* 41-47 mm; *M. occitanica* 48-50 mm; *M. arge* 54-57 mm[49]. *Melanargia* is a morphologically consistent group of Satyrinae butterflies, bearing a distinctive black and white wing pattern, not sexually dimorphic. The specific configuration of these patterns, as well as their egg structure separate the *Argeformia* species from other *Melanargia*, displaying also consistent differences between each other and between some of their own populations[49,65,66,68–70] (Figure 1.4 and S1.3).

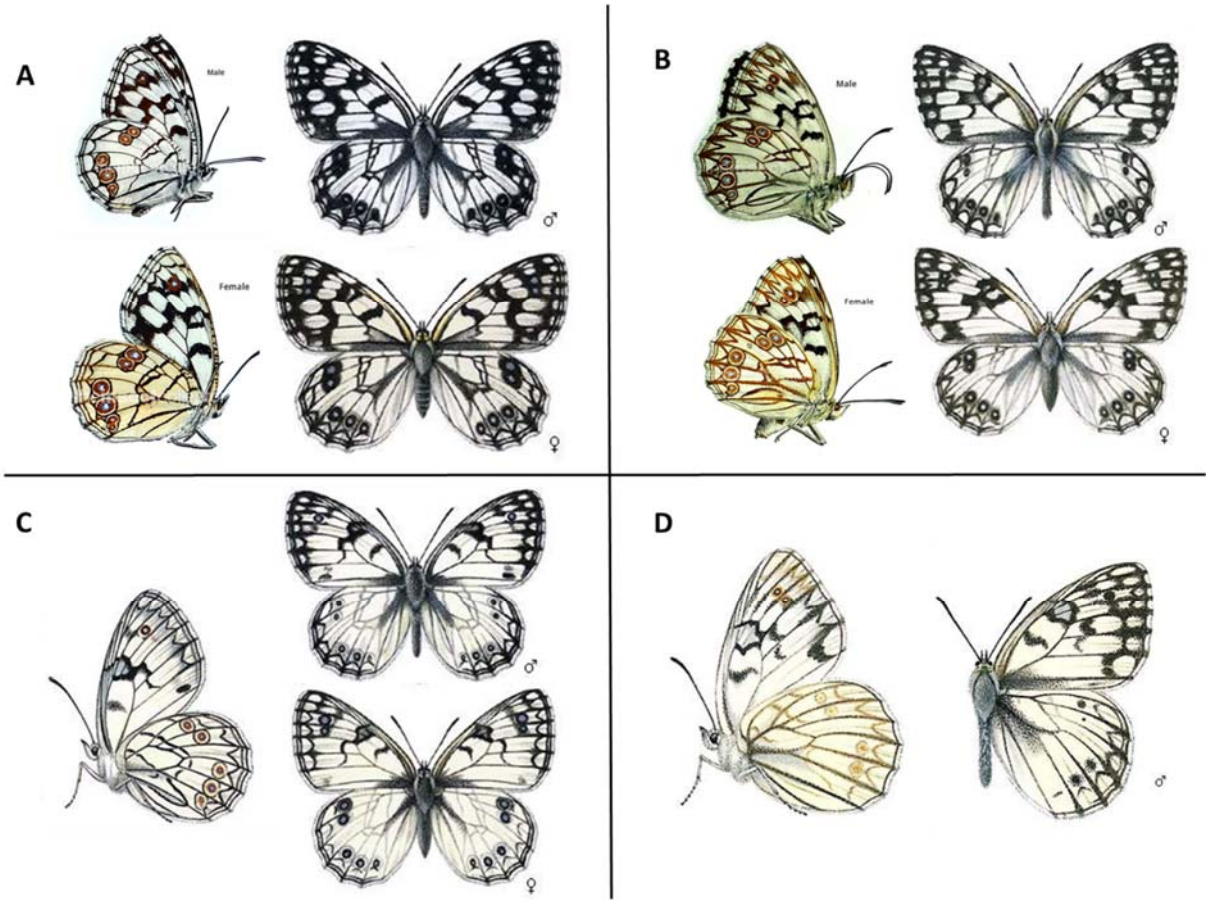

Figure 1.4 – Phenotypic differences between *Melanargia ines* (A), *Melanargia occitanica* (B), *Melanargia arge* (C) and *Melanargia o. pherusa* (D).

Nazari *et al*. (2010) constructed the most complete phylogeny of *Melanargia* so far, using both mitochondrial and nuclear DNA sequences, while corroborating information from morphology and geography[65]. Three molecular markers were studied in their work (cytochrome oxidase I, 16S and Wingless) and the species dataset included the *Argeformia* group with 20 *M. ines* individuals, 18 *M. occitanica* (including 3 *M. o. pherusa*) and 4 *M. arge* specimens. The resulting species tree corroborated morphological affinities and placed *Melanargia arge* as closely related to *Melanargia occitanica*, which

together with *Melanargia ines* formed a sister clade to all other Melanargia. However, not all genes supported this result and the statistical support was low. A great genetic distance was also found within *M. ines* and *M. occitanica*, separating African and European populations, currently considered different subspecies (Table S1.1), being that distance more pronounced in the mitochondrial gene. The African lineage of *Melanargia occitanica* was also genetically closer to the Italian population of Sicily (*M. o. pherusa*) suggesting a Sicilian colonization from North Africa.

Additionally, Habel *et al*. (2011) aimed to test for the importance of an Atlanto-Mediterranean refugium for *M. ines* (Iberia + Maghreb), using both polymorphic allozyme data and species distribution models (SDMs) to portray the potential Last Glacial Maximum (LGM) distribution of this species[71]. Molecular data showed very low genetic diversity between the three populations sampled (Iberia, Western Maghreb and Eastern Maghreb), and SDM results were almost identical when comparing current and past distributions, with a slight deviation southward during LGM. Nevertheless, this study was not pioneer in constructing SDMs for this taxon since models of our three *Argeformia* species had been previously represented in the Climatic Risk Atlas of European Butterflies[72]. However, the North African populations were ignored in this work and the range grid used for pinpointing the species distribution was too broad (50 km*50 km), leading to a probable mismatch of the climatic variables' correlation with actual species presence.

Therefore, despite representing ground-breaking advances for *Argeformia* species' knowledge, these past studies have their own flaws, like sampling efforts that do not reflect the variation within these species and lack representatives of many populations, required for a complete and extensive population genetic screening. Such screening is needed to understand both the divergence and diversity of these taxa, but also their relationships and the importance of great western Mediterranean barriers to populations gene flow (Figure 1.5), shaping the evolutionary history of this species group. Overall, the present work gathers the relevant knowledge achieved so far for *Argeformia* in past studies and takes one step forward to unravel these species' evolutionary history with new and improved analysis.

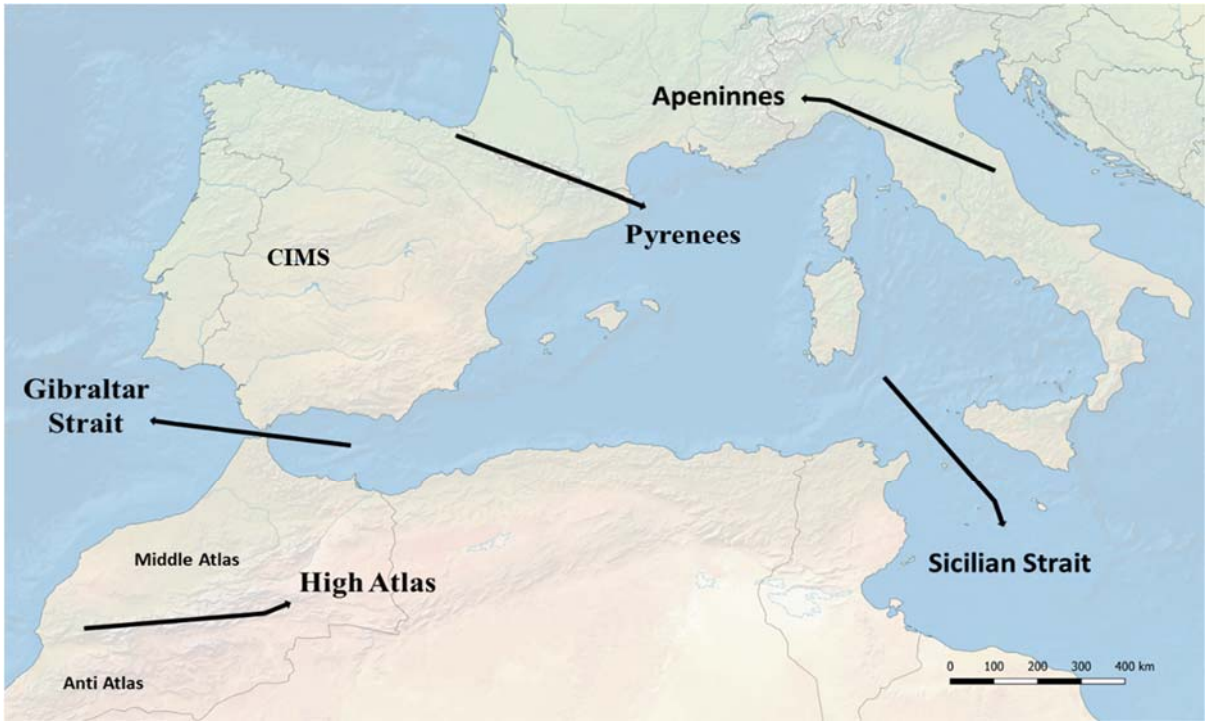

Figure 1.5 – Most influent land and sea geographical barriers of the western Mediterranean region.

2. Case-Study goals

1. *Lycaena*:

- To infer an improved and comprehensive phylogeny for *Lycaena*, using mitochondrial and nuclear markers (COI and EF-1α) and estimate the divergence times among taxa.
- To estimate the genetic diversity and population differentiation of *L. bleusei* and *L. tityrus* (COI and EF-1α).
- To infer the taxonomic relationship between both Sooty Coppers with an integrative approach using Genetics, Geometric Morphometrics and Species Distribution Models.
- To understand *L. bleusei* and *L. tityrus* biogeography and hypothesize their evolutionary history in Iberia.

2. *Melanargia*:

- To infer an improved phylogeny for the *Argeformia* clade and estimate the divergence times within this subgenus.
- To estimate the genetic diversity and population differentiation of *M. ines*, *M. occitanica* and *M. arge* (COI and EF-1α).
- To hypothesize an evolutionary history scenario for the *Argeformia* species and understand their biogeography combining Genetics, Divergence Times and SDMs.

3. Materials and Methods

* – Applied only to the *Lycaena* case-study

3.1. Sampling and genetic analysis

The sampling process of the first case-study was mainly focused on the Sooty coppers *Lycaena tityrus* and *Lycaena bleusei* although several other *Lycaena* species have also been collected or obtained through colleagues. Samples of the Sooty Coppers were captured throughout their distribution range in the Iberian Peninsula and some other regions of Europe for *Lycaena tityrus* in a total of 45 locations sampled between May 2011 and August 2018, while different phenotypes of *L. tityrus* were also distinguished after sampling (Table S3.1). Most of the sampling was carried throughout the time course of a previous master's thesis project entitled "On the evolutionary history of the Iberian Sooty Coppers", by Renata Martins in 2011. In Iberia, the sampling sites spanned both known and predicted distributions of each taxon, with special emphasis on their potential contact zone in the western part of the Central Iberian Mountain System (CIMS) (Figure 1.5).

The sampling effort for the second case-study focused on both *Melanargia occitanica* and *Melanargia ines*. All samples used were collected between May 2011 and May 2018 in 47 locations throughout the Iberian Peninsula, South of France, Italy and Morocco (Table S3.2). Due to the lack of available samples, we used only one previously collected specimen of the Italian endemic *Melanargia arge* for genetic analysis.

Individuals of both cases studies were collected alive using an entomological net and scored to morphospecies in the field. These were then kept at -20°C until DNA extraction. Two legs per specimen were used in DNA extraction and the rest of the body was preserved dry for future morphological analyses. DNA extraction was performed with E.Z.N.A® Tissue DNA Kit (Omega, Biotek) following manufacturer's protocol. In total, two mitochondrial genes (Cytochrome Oxidase I (COI) and 16S ribosomal RNA) and three nuclear genes (Elongation Factor-1α (EF-1α), Wingless (Wg) and CAD (carbamoyl-phosphate synthetase 2, aspartate transcarbamylase, and dihydroorotase)) were amplified for *Lycaena* samples, while only two of these (COI and EF-1α) were amplified for *Melanargia*. All molecular markers here used have already proved to be good indicators of differentiation between and within species and have been widely used in similar studies[65,73–75].

The primers and Polymerase Chain Reaction (PCR) protocols required for the amplification of each gene are described in Supplementary material (Table S3.3). PCR products were checked for the presence of amplified DNA with correct band weight on 1% agarose gel, stained with 2x Red Safe™ Nucleic Acid Staining Solution (iNtRON Biotechnology, Inc), and fragments were then purified using SureClean (Bioline) following manufacturer's protocol. The samples were later sequenced by Macrogen, and chromatograms were manually checked for errors in Sequencher v.4.0.5 (Gene Codes Co.). Nucleotide ambiguities, considered as heterozygous sites, were classified accordingly to IUPAC ambiguity codes. All sequences were aligned using MAFFT online[76] and trimmed in BioEdit[77]. For the nuclear sequences of *Lycaena* the phase of heterozygotic ambiguities was determined using SeqPhase online and PHASE v.2.1.1[78].

Several publicly available sequences of both *Lycaena* and *Melanargia* from NCBI Genbank and Barcode of Life Data (BOLD) systems were used to complement our genetic dataset on both case studies (Tables S3.1 and S3.2). Overall, we used genetic data of 60 *Lycaena bleusei* specimens, of which 11 sequences were taken from Genbank/BOLD, and 106 *L. tityrus* (52 from Genbank/BOLD). For the second case-study we used genetic data of 78 *Melanargia ines* specimens (37 from Genbank/BOLD), 64 *Melanargia occitanica* (30 from Genbank/BOLD) and 1 *Melanargia arge*. Although only two genes were amplified using our *Melanargia* samples we were able to use online available sequences from two other genes (16S and Wingless) in our genetic inferences, mostly from the previous work of Nazari *et al*. (2010).

3.2. Phylogenetic analysis and haplotype networks

To understand the phylogenetic relationships within *Lycaena* and *Melanargia* clades we analysed our genetic data under a phylogenetic framework. Two different analyses were carried for both case studies: a maximum likelihood inference (ML) using raxmlGUI v.1.5b2[79] and a Bayesian inference (BI) using MrBayes v.3.2.6[80].

For *Lycaena* two different phylogenies were constructed using both maximum likelihood and Bayesian inference analysis: a comprehensive phylogeny of the genus using all *Lycaena* sequences available (COI and EF-1α), and a smaller one using only the closest species to the Sooty Coppers but with more genes (COI, 16S, CAD, EF-1α and Wg). For each, both individual and concatenated datasets were used and analysed. Additionally, for the individual *Lycaena* COI dataset and the COI partition of the combined analysis, the third position of each codon was analysed separately to account for mitochondrial DNA saturation. For *Melanargia*, a phylogenetic tree was constructed under each of the two phylogenetic inferences mentioned above using a concatenated matrix of four genes (COI, 16S, EF-1α and Wg), as well as each gene individually. Detailed information of each dataset and what specimens are included is given in Tables S3.4 and S3.5.

Conversion between file formats and concatenation of all genes was accomplished using Concatenator v.1.1.0[81]. For each gene, the best-fit evolution model for Bayesian analysis was selected with jModelTest v.2.1.10[82] under the Akaike Information Criterion (AIC), and for ML the default GTR Gamma model was used. Both analyses were performed with multiple replicates: 10 000 bootstraps for ML and two runs of four Monte Carlo Markov Chain (MCMC) iterated for 6M generations for BI. The phylogenetic trees posterior editing steps were carried in FigTree v1.4.4. Furthermore, the sequences of outgroup species chosen for both case studies (*Lampides boeticus*, *Curetis barsine*, *Papilio paris* for *Lycaena*; *Maniola jurtina* for *Melanargia*), were taken from NCBI Genbank (Tables S3.1 and S3.2).

Maximum parsimony median-joining haplotype networks were built for both *Lycaena* (COI and EF-1α individual datasets; Dataset 1 and 4) and *Melanargia* (COI dataset; Dataset 5 and 6) combining collected specimen sequences and online database sequences, with PopArt v.1.7[83]. Once more, no *M. arge* haplotype network was included in our main analysis due to our lack of samples and lack of online genetic sequences. In *Lycaena* networks, the species were displayed together and COI sequences of the subspecies *L. tityrus subapinus* were also included. For *Melanargia*, *M. ines* and *M. occitanica* were analysed individually. Haplotypes generated for *Lycaena* and *Melanargia* were then projected into representative maps of Iberia and Europe according to their specific geographic structuring for a better

understanding of these species' genetic diversity distribution, using Google Earth maps as background and Inkscape v.0.92.1 as editing software.

3.3. Population genetic differentiation

Analysis of molecular variance (AMOVA), nucleotide diversity (π), haplotype diversity (h) and F_{st} pairwise differences were all assessed with ARLEQUIN v.3.5[84] using the mitochondrial COI datasets. Pairwise genetic distances were calculated with MEGA 7[85] for all genes, using datasets 1-4 for *Melanargia* and the ingroup datasets (Datasets 6-10) for *Lycaena*, except COI and EF-1α genes for which the datasets with all our *L. bleusei* and *L. tityrus* specimens (Datasets 2 and 4, respectively) were also used. For both studies, the population groups used in Arlequin were defined based on geographic proximity of sampling sites or according to perceived geographic structure (Tables S3.6 and S3.7). Within each genus the groups established are different between species as they also have overall different distribution ranges, although with overlap. *Melanargia arge* was excluded from these inferences due to its limited distribution range and lack of genetic sequences.

For the AMOVA of *Lycaena*, the population groups of *L. tityrus* and the entities *L. tityrus subalpinus* and *L. bleusei* were aggregated in different hierarchical combinations. For *Melanargia*, species were once more analysed individually. Pairwise F_{st} values were calculated among populations within each species for both case studies. However, for a better comparison between the two Sooty Coppers, *L. bleusei* was also included as one of *L. tityrus* populations. Additionally, a pairwise F_{st} analysis was also carried between the three major Sooty Copper taxa groups: *Lycaena tityrus*, *L. tityrus subalpinus* and *Lycaena bleusei*.

3.4. Divergence time estimates

Both *Lycaena* and *Melanargia* combined gene datasets (datasets 3+5 and 1+2+3+4, respectively) were subjected to a partitioned Bayesian analysis in the software BEAST v2.5.2[86] to infer the estimated divergence times between taxa. The datasets were partitioned by genes, with two partitions for *Lycaena* and four partitions for *Melanargia*. For *Lycaena*, the COI partition was assigned with the JC69 + I + G substitution model and the EF-1α partition with the TIM2 + I + G. For *Melanargia*, the COI, 16S, EF-1α and Wingless partitions were assigned with the JC69 + I + G, TPM2uf, TN93 + G and HKY + G, respectively. The parameters were estimated separately for each partition (Tables S3.8 and S3.9). The relaxed clock log normal model was assigned to every partition on both datasets, with non-estimated different clock rates for each gene: COI - 0.0115; 16S - 0.0086; EF-1α - 0.001277; Wingless - 0.007044. Partitions of both datasets were also linked to share the same tree topology, and while the *Lycaena* tree prior was set to the Birth Death Model, the *Melanargia* tree prior was set to the Yule Model. All the remaining priors were left with default options. Although there are no known fossil records of *Lycaena* and *Melanargia*, recent studies on the radiation of Satyrini butterflies (subfamily Satyrinae) and a whole dated phylogenomic study of butterflies used fossils on their phylogeny

calibrations, estimating a divergence time of ~33 mya between *Maniola* and *Melanargia*[87,88] and ~60 mya between *Lampides* and *Lycaena*[88]. These ages were used as calibrations points between our focal taxa and the outgroups chosen for each case-study, with monophyly, and uniform distributions between [57-63] mya for *Lycaena* and [32-36] mya for *Melanargia*. The analysis was run six times for both datasets, for 20000000 iterations of MCMC each and sampling every 1000 iterations. The validation of each run's quality and the concatenation of the six runs with 10% discarded as burn-in was obtained with Tracer[89]. Annotation of the trees was carried in TreeAnnotator of the BEAST software package, and the editing steps in FigTree.

3.5. Geometric Morphometric analysis*

A total of 182 specimens were chosen for morphometric analysis (n=82 *Lycaena bleusei* and n=100 *Lycaena tityrus*; Table S3.10 and S3.11), mainly from Iberian Peninsula but also from other European locations. Differences in shape between groups were analysed using landmark-based geometric morphometric procedures. We used a combination of 18 type I landmarks (Bookstein 1991) applied to both vein intersections with the wing margin and around the cell of the left hindwing on each *L. tityrus* and *L. bleusei* specimen (Figure S3.1). Hindwing underside was chosen for its clear pattern and discriminant power in differentiating both species, where a small tail-like projection is present in most *L. bleusei* individuals. Chosen landmarks follow Zelditch *et al*. (2004) criteria of independence, homology among specimens and ease of identification[90]. Similar landmarks have previously been used in butterflies[91].

For each specimen, a picture was taken on a fixed set and the acquisition of two-dimensional coordinates of these landmarks was accomplished using FIJI[92]. To reduce measurement error, specimens were digitised by a single user. Analysis of shape and size were implemented with the R package geomorph v.3.0.7 and raw coordinates were superimposed using a Generalized Procrustes Analysis (GPA) to standardise the size and to translate and rotate the configurations of landmark coordinates[93]. We used centroid size (CS) to analyse wing size variation, which is defined as the square root of the sum of the squared distances between the centre of the configuration of landmarks and each separate landmark (Bookstein 1991). Centroid sizes of different groups were after compared by means of ANOVA and pairwise t-tests. Principal Component Analysis (PCA) were also conducted for a better visualization of data.

The relationship between shape and size (allometry) was examined through multivariate regression of the shape variables (Procrustes coordinates) onto natural log-transformed CS, through a Procrustes ANOVA with randomised residual permutation procedures (RRPP), as well as a test of homogeneity of slopes between groups (geomorph: procD.allometry). To test for shape differences between groups, we used Procrustes ANOVA with pairwise tests, using centroid size as a factor to account for the allometric effect.

3.6. Species distribution modeling

To evaluate differences in the current and past distributions of both *Lycaena* Sooty Coppers and *Melanargia* species in relation to Quaternary climatic fluctuations, we performed species distribution modeling (SDM) independently, using maximum entropy analysis in MAXENT v.3.4.1[94]. These models were restrained to the Iberian Peninsula for *Lycaena* SDMs and to the entire western Mediterranean region for *Melanargia*.

For the occurrence data of *Lycaena* in Iberia, we included all published and accessible information whenever possible, as well as our own personal records. However, data had to be severely filtered since the two taxa are not distinguished in many of the records. Thus, *L. bleusei* was considered for data described in the Spanish Central Mountain System from Ayllon to Gata ranges, Moncayo range and both provinces of Castilla la Mancha and Caceres, but ignored for Portugal and Badajoz. On the other hand, *L. tityrus* was considered for data coming from Catalonia to Galicia, Zamora, Burgos, and La Rioja provinces but not considered for Portugal. We also considered many of the source references of Garcia Barros *et al*. (2004)[95] and other references of later publication, especially if relating explicitly to *L. bleusei*[51–54,96–100]. In fact, as there was an uncertainty to the species assignment of previously published Portuguese records, most of these presence points for Portugal were omitted. Therefore, most records, either belonging to *L. tityrus* or *L. bleusei* presented here for Portugal are posterior to published sources, original and accurately verified, as we did not consider published records prior to Marabuto *et al*. (2004)[51].

For *Melanargia* we included most of published occurrence data available for the three Argeformia. All Atlas and paper records represented as grid points in illustrated maps were translated into Google Earth coordinates, and later all distribution coordinates gathered were filtered to a single occurrence point per 10km^2 grids and centred on those grids' midpoint. We also included many unpublished photographic or voucher records by the authors and colleague contributors, georeferenced and/or photographically supported citations in GBIF, Observation.org and Naturdata online databases for species of both case studies. Overall, the usable database totals 1023 *Lycaena* distribution points for Iberia, of which 534 belong to *L. tityrus* and 489 belong to *L. bleusei*, and 2104 *Melanargia* distribution points for the western Mediterranean region, of which 885 belong to *M. ines*, 1054 belong to *M. occitanica* (16 from *M. occitanica pherusa*) and 165 belong to *M. arge*.

We used 19 current bioclimatic variables from the WORLDCLIM website (www.worldclim.org)[101], clipped to the western Mediterranean area. For the estimation of current potential distribution of species, we ran 5 bootstrap replicates using 75% of species localities as training data, and the remaining 25% to test the model. Then, we projected the resulting distribution models to past climatic conditions assuming niche conservatism through time, at least in the last climatic cycle[102]. Projections to the LGM (ca. 21 kyr before present) were performed using paleoclimate data obtained from the Community Climate System Model (CCSM4)[103] and the MaxPlanck-Institut Earth System Model (MPI-ESM-P)[104] of atmospheric circulation, as available in WORLDCLIM.

Case-study 1 – *Lycaena* and the Sooty Copper butterflies

4. Results

4.1. Data characterization

The matrices of our samples were obtained through direct PCR sequencing. Amplification and editing of DNA sequences yielded 657 base pairs for the alignment of COI, 584 for EF-1α, 618 for 16S, 402 for Wingless and 453 for CAD2, including BOLD and Genbank sequences.

The dataset containing all *L. tityrus* + *L. bleusei* COI sequences (Dataset 1) displayed 632 invariable sites and 25 variable sites, from which 21 are parsimoniously informative and 4 are singletons. A second dataset (Dataset 2) without the online database COI sequences, yielded 636 invariable sites and 21 variable ones, being 19 parsimoniously informative and 2 singletons. For the same gene but using the dataset with all *Lycaena* species available (Dataset 3) we found 435 invariable sites among these and 222 variable ones (153 parsimoniously informative and 69 singletons). On the other hand, the dataset with all *L. tityrus* + *L. bleusei* EF-1α sequences after phase determination (Dataset 4) displayed 572 invariable sites and 12 variable ones, from which 10 are parsimoniously informative and 2 are singletons. The heterozygotic sites of this alignment before phase determination varied from 0 to 3 for both *L. tityrus* and *L. bleusei*. The EF-1α dataset with all *Lycaena* species (Dataset 5) displayed 424 invariable sites and 160 variable ones (104 parsimoniously informative and 56 singletons).

As for the remaining genes (16S, Wg and CAD2), a smaller dataset including only two specimens for both Sooty Coppers revealed: 578 invariable sites, 16 variable sites (8 parsimoniously informative and 8 singletons) and 24 sites with missing data for 16S (Dataset 6); 381 invariable sites, 8 variable sites (singletons) and 13 sites with missing data for Wingless (Dataset 7); and 448 invariable sites, 4 variable ones (parsimoniously informative) and 1 site with missing data for CAD2 (Dataset 8).

The pairwise distances (p-distances) between *L. tityrus* and *L. bleusei* are of: 2,3 to 3,1% for COI; 1,6 to 2,4% for 16S; 0,9 to 1,9% for EF-1α; 2,1% for Wingless; and 0,9% for CAD2. All p-distance matrices calculated with the ingroup datasets are shown in Tables S4.1-S4.5. Additionally, p-distances for COI and EF-1α genes between other *Lycaena* sister taxa are also shown in Tables S4.6 and S4.7.

4.2. Phylogenetic analysis and haplotype networks

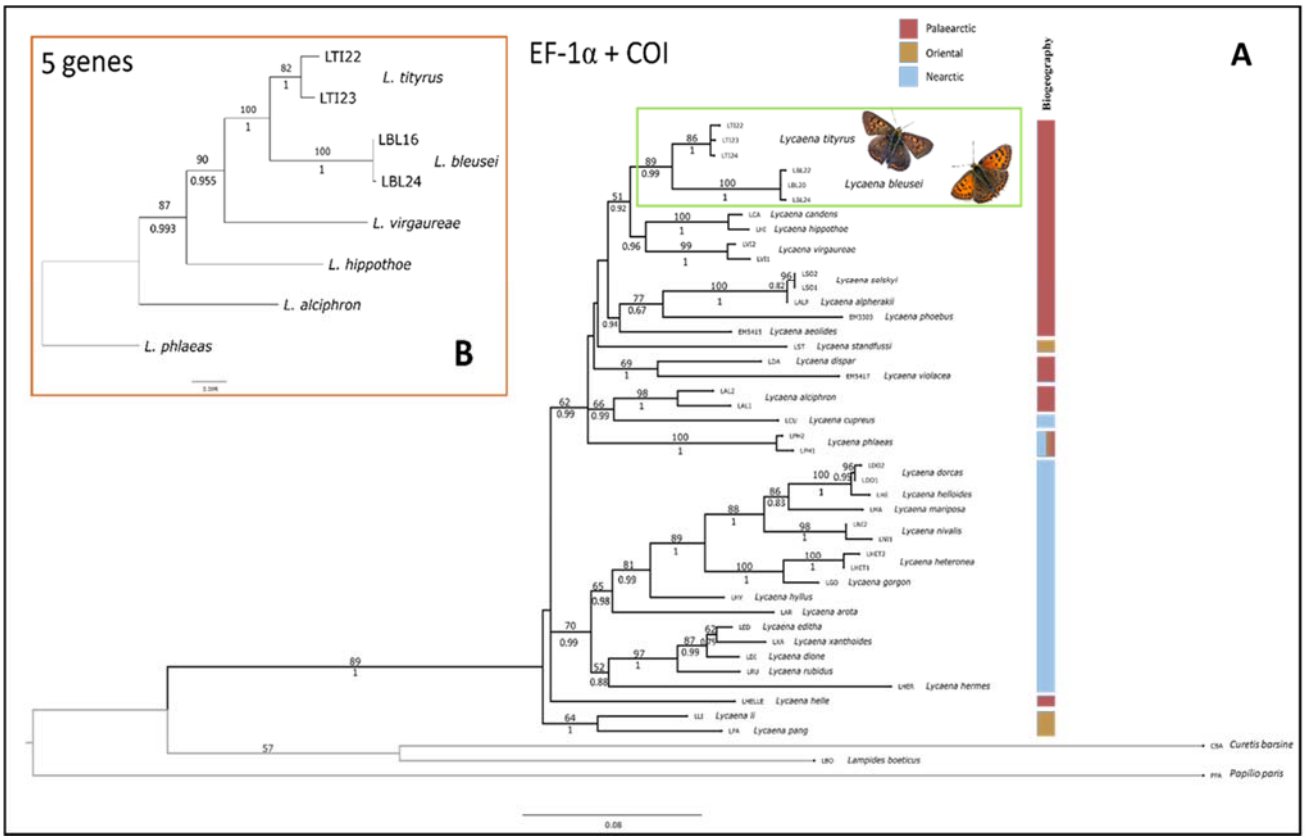

Figure 4.1 – (**A**): Maximum Likelihood phylogeny of *Lycaena* based on the combined analysis of COI and EF-1α gene haplotypes (Datasets 3 + 5). Bootstrap values above 50 and Bayesian posterior probabilities higher than 0.7 are shown along branches. The names of all taxa included are shown at the tip of the topology. (**B**): Five gene (COI, 16S, EF-1α, Wg, CAD) Maximum Likelihood phylogeny of the Sooty Coppers ingroup clade (Datasets 6 + 7 + 8 + 9 + 10). Bootstrap values above 50 and Bayesian posterior probabilities higher than 0.7 are shown along branches. The names of the taxa are shown at the tip of the topology.

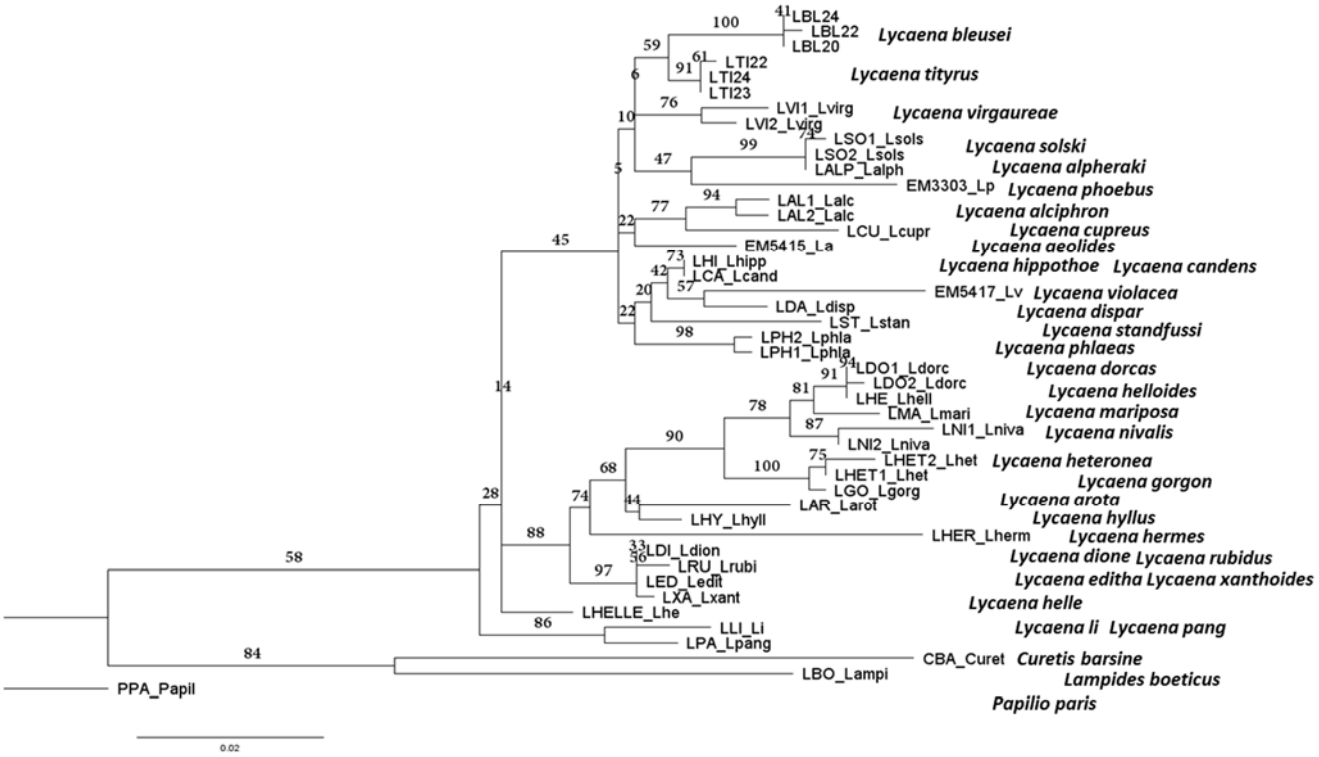

Figure 4.2 – Maximum Likelihood phylogeny of *Lycaena* based on the EF-1α gene haplotypes (Dataset 5). Bootstrap values above 50 are shown along branches. The names of all taxa included are shown at the tip of the topology.

The ML phylogenetic tree of all *Lycaena* species combining COI + EF-1α genes (Figure 4.1A) gave a similar topology of the one obtained under Bayesian inference (Figure S4.1), thus only the first is presented. Additionally, as we observed topological differences between combined COI + EF-1α and single EF-1α trees, affecting the sister clade of the Sooty Coppers, the ML tree built only with the nuclear dataset (Dataset 5) is also shown (Figure 4.2). The phylogenies comprise 31 species of Palaearctic, Nearctic and Oriental origin, out of the currently recognised 64 species in the genus[46,105]. *Lycaena phoebus*, *L. aeolides*, *L. standfussi*, *L. violacea* and *L. pang* are here included in a genetic analysis for the first time. The individual ML COI gene tree and Bayesian trees are also shown in Supplementary Material, as well as the list of current subgenus attribution for every *Lycaena* species used in our analyses and their respective biogeographic region distribution (Figures S4.2-S4.4, Table S4.8).

Within *Lycaena*, three major groups appear: 1) an Oriental, encompassing the Chinese species *Lycaena li* and *Lycaena pang*; 2) a Nearctic group, encompassing all North American species except *L. cupreus* and *L. phlaeas*; and 3) a Palaearctic group, including the North American *L. cupreus* and encompassing all European species except *L. helle*, which appears in an undefined position equally diverging from the three clusters of species (Figure 4.1A).

Lycaena tityrus and *Lycaena bleusei* appear deeply nested within the Palaearctic clade as sister taxa with high bootstrap. The closest related species to this pair is *Lycaena virgaureae* and the couple *Lycaena hippothoe* and *Lycaena candens* in the combined analysis (Figure 4.1A) but *L. virgaureae*, *L. solski*, *L. alpheraki* and *L. phoebus* in the nuclear one (Figure 4.2). Despite the low bootstrap support, *L. hippothoe* and *L. candens* always group together and *L. virgaureae* either groups with these or with *L. tityrus* + *L. bleusei* (Figure 4.1A). Among the other Palaearctic subclades, bootstrap usually increases from the base to the tips of the topology. *Lycaena solski* and *Lycaena alpheraki* also group together as

sister taxa, clustered with *L. phoebus* as in the nuclear analysis (Figure 4.2) but also with the Central Asian *L. aeolides*, which is placed close to *L. alciphron* and *L. cupreus* in the EF-1α gene tree. The latter two pair weekly in the combined analysis, and the widespread *L. dispar* groups with *L. violacea*, while in the nuclear tree these two species are placed with *L. candens* and *L. hippothoe*, the sister clade of the Sooty Coppers in the COI + EF-1α tree. The Chinese species *L. standfussi* appears to have no close relative in our study, showing also low bootstrap values, while the Holarctic and most adaptable *Lycaena phlaeas* appears as one of the most basal taxa of this Palearctic clade in Figure 4.1A.

All North American (Nearctic) species, except for the previously mentioned *L. cupreus* and *L. phlaeas*, group together in a very diverse clade with two internal branches. One includes *L. dorcas*, *L. helloides*, *L. mariposa* and *L. nivalis* as a sister clade to *L. heteronea* + *L. gorgon,* with *L. hyllus* and *L. arota* outgrouping all the previous. Excluding the latter two, all bootstrap values are equal or above 75, making this phylogenetic clade statistically well supported in both trees (Figures 4.1A and 4.2). The second clade is another strong cluster with *L. xanthoides*, *L. editha*, *L. dione*, and *L. rubidus*. The only difference between analyses within the Nearctic group is the placement of *L. Hermes*, which relates with the second clade in the nuclear tree (Figure 4.2), and with the first clade in the combined one (Figure 4.1A).

Finally, the representatives of the Oriental *Lycaena*, *L. li* and *L. pang*, appear as sister taxa and did not seem to relate closely with other Asian species such as the also Chinese *L. standfussi* or the widespread but phenotypically similar *L. helle*. The latter was always placed in a polytomy with the Palaearctic and Nearctic clades.

A more extensive dataset of five genes (Datasets 6 to 10 combined) centred on the Sooty Coppers ingroup taxa resulted in a more supported phylogeny (Figure 4.1B), having a similar topology to the first (Figure 4.1A), except for *Lycaena virgaureae* placement as the clear sister species of the Sooty Coppers with strong bootstrap support. The Bayesian five gene ingroup phylogeny is shown in Supplementary Material (Figure S4.5). This phylogeny does not include the potential sister clade of *L. solski*, *L. alpheraki* and *L. phoebus* shown in Figure 4.2 given the lack of genetic sequences for these species. Nonetheless, *Lycaena tityrus* and *Lycaena bleusei* are clearly separated as two independent sister taxa in all sampled individual genes (Figures S4.6 – S4.15), as well as in trees combining only mtDNA genes (Figures S4.16 and S4.17) and nuclear genes (Figures S4.18 and S4.19).

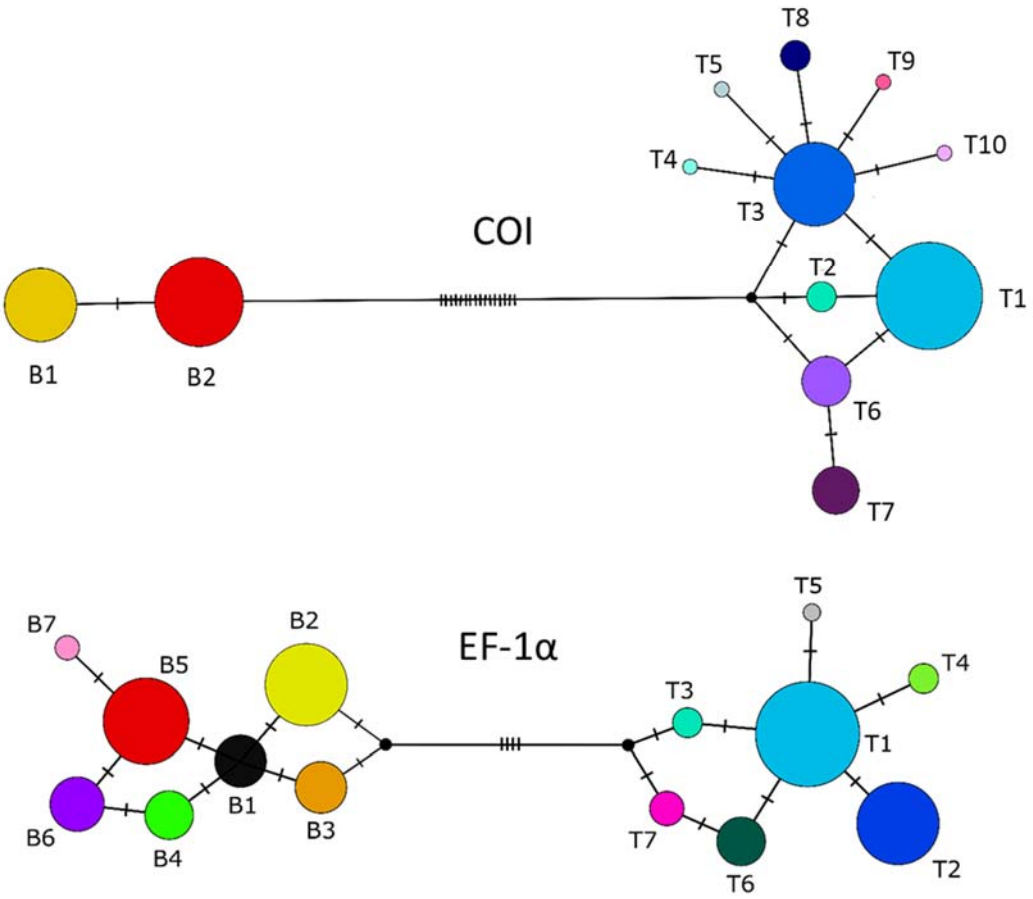

Figure 4.3 – Haplotype networks of *Lycaena tityrus* (**T**) and *Lycaena bleusei* (**B**) using COI and EF-1α genes.

Haplotype networks of both COI (Dataset 1) and EF-1α (Dataset 4, except LBL 19 and LTI 44 which presented issues with phase determination) genes are concordant by showing a clear separation between both taxa, as two divergent genetic entities (Figure 4.3). Seventeen mutational steps separate the two coppers' gene pools on COI network, while six mutations separate these on EF-1α. For *L. tityrus* (n=106 on COI; n=52 on EF-1α), a total of ten different haplotypes were found throughout Europe for mtDNA COI, while only seven haplotypes were found for the nuclear EF-1α. Conversely, for the Iberian *L. bleusei* (n=60 on COI; n=51 on EF-1α) only two haplotypes were found for the mitochondrial COI gene, while EF-1α displays a diversity of seven different haplotypes.

No shared haplotypes were found between taxa in the mitochondrial gene, although one COI-EF-1α mismatch was noticed. In fact, two *L. tityrus* specimens displaying a correspondent *L. tityrus* COI haplotype, have conversely both displayed the B2 and B4 nuclear haplotypes (after phase determination) from *L. bleusei*'s gene pool (Figure 4.3). Information about which specimens display each haplotype is detailed in Supplementary Material (Table S4.9).

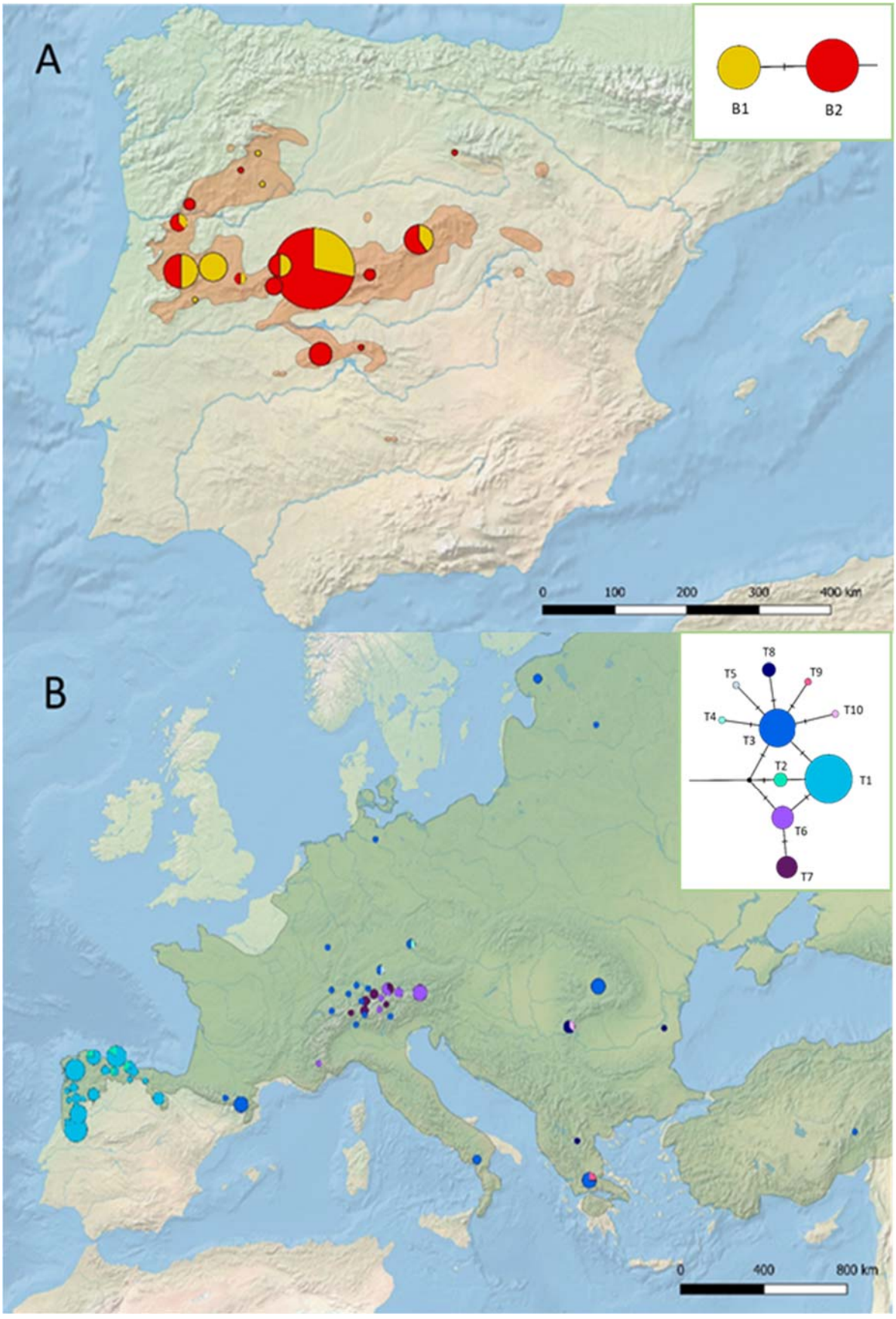

Figure 4.4 – Geographic segregation of *L. bleusei* (A) and *L. tityrus* (B) COI haplotypes in Iberia and Europe, respectively. Haplotype colours are identical to Figure 4.3.

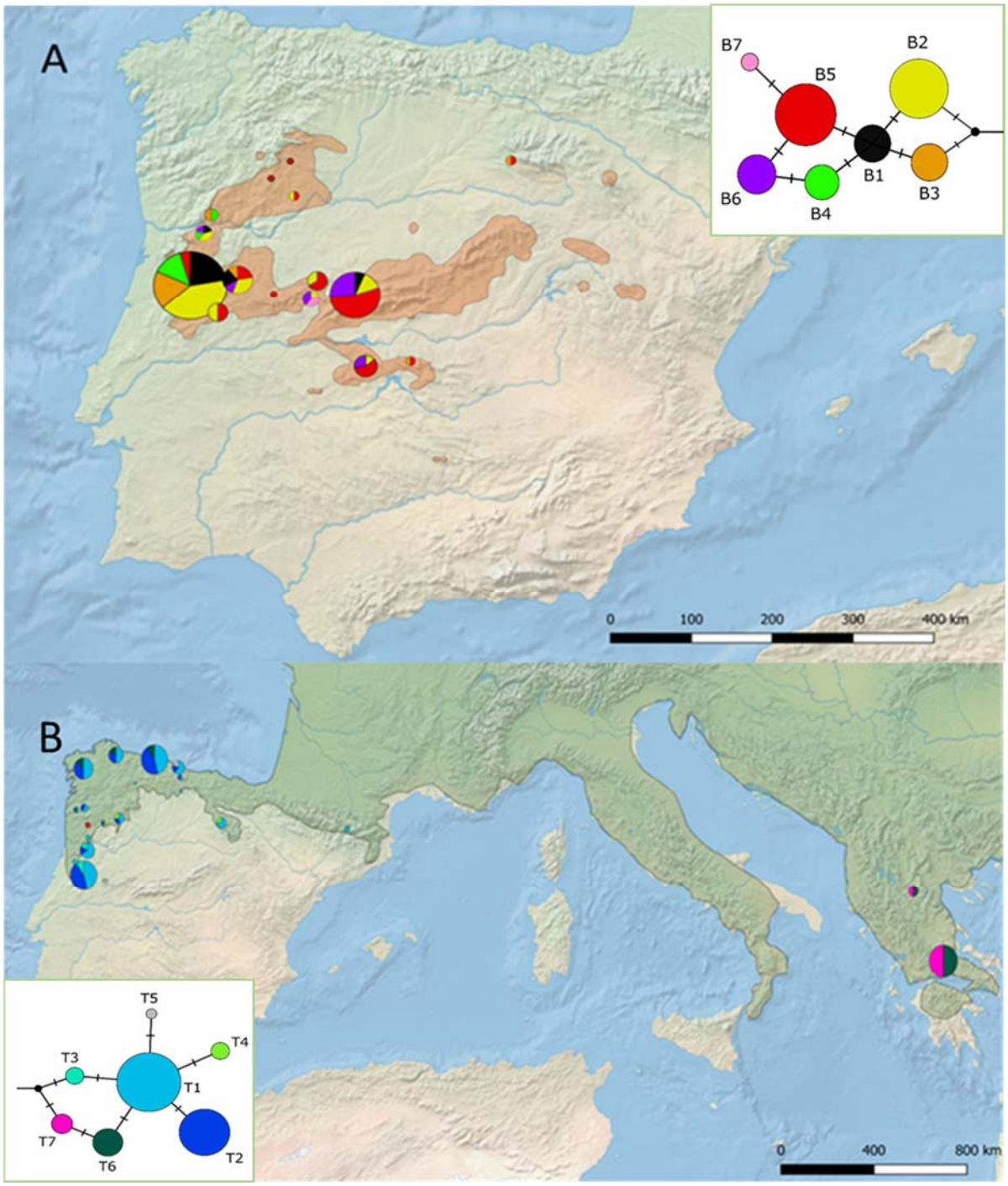

Figure 4.5 – Geographic segregation of *L. bleusei* (A) and *L. tityrus* (B) EF-1α haplotypes in Iberia and Europe, respectively. Haplotype colours are identical to Figure 4.3.

The geographic structure of *L. bleusei* and *L. tityrus* genetic variation can be analysed by the haplotype segregation of these two genes across Iberia and Europe, as seen in Figures 4.4 and 4.5. While there is no evidence for geographic structure of the two *L. bleusei* COI haplotypes throughout Iberia, being both well mixed and widespread, *L. tityrus* shows a bigger structuring of its genetic variation throughout its wider distribution range (Figure 4.4). In fact, from all ten *L. tityrus* COI haplotypes found, two of them appear to be exclusive from the Iberian Peninsula: T1 and T2. The former is the most abundant haplotype in Iberia, while T2 appears to be confined to a narrow region north of the Peninsula (Asturias). The only Iberian haplotype shared with the rest of Europe is T3, the most widespread *L. tityrus* haplotype, extending from western Russia and Estonia, all the way down to the southwestern Mediterranean region. In Iberia, T3 has so far only been found in northeast Catalonia, close to the Pyrenees range. The individuals phenotypically classified as *Lycaena tityrus ssp. subalpinus* carry the haplotypes T6 and T7 and appear to be restricted to the Alpine mountain range. Haplotype T8 is confined to south-eastern European countries, and the remaining haplotypes are represented by singletons from Germany (T4 and T5), Greece (T9) and Romania (T10).

Regarding the nuclear gene EF-1α, *L. bleusei*'s haplotypes show only little evidence for geographic structuring, with most of them present in the western part of Iberia but only a few reaching the centre and north of Spain (B3, B5 and B6, Figure 4.5). On the other hand, *L. tityrus* displays five EF-1α haplotypes restricted to the Iberian Peninsula, either widespread (T1 and T2) or confined to smaller regions (T3, T4 and T5), and two other haplotypes present in Greece, either exclusive (T7) or shared with the Iberian Peninsula (T6).

4.3. Divergence time estimates

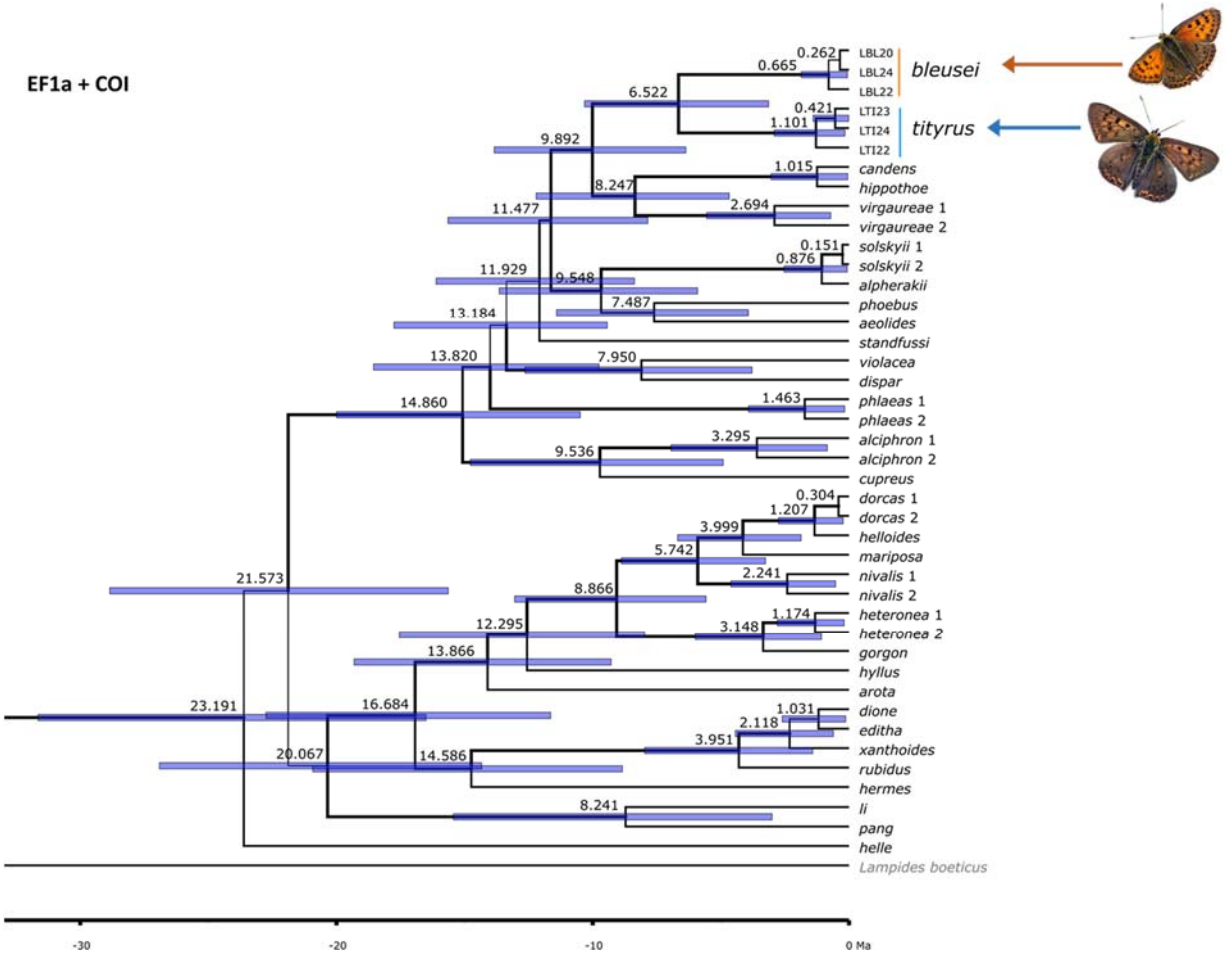

Figure 4.6 – Bayesian phylogeny of *Lycaena* with BEAST mean divergence time estimates based on the combined analysis of COI and EF-1α gene haplotypes (Datasets 3 + 5). The names of all taxa included are shown at the tip of the topology.

A BEAST Bayesian phylogenetic tree with the mean divergence time estimates for *Lycaena* is shown in Figure 4.6. While the primary divergence and radiation of *Lycaena* butterflies seems to have started around 23 mya (95% HPD: 16.51 – 31.65 mya), the initial divergence between the ancestral population of the Sooty Coppers and the ancestral population of its sister taxa clade might have occurred around 9.9 mya (95% HPD: 6.37 – 13.85 mya). The subsequent divergence between the entities *L. bleusei* and *L. tityrus* appear to have started soon after that, around 6.5 mya (95% HPD: 3.14 – 10.32 mya). As comparison, the divergence within the Nearctic *L. editha* complex seems to have started around 3.95 mya (95% HPD: 1.42 – 7.97 mya). The same Bayesian phylogeny with BEAST divergence time estimates of *Lycaena* but including the 95% HPD time intervals is given in Supplementary Material (Figure S4.20).

4.4. Hybridization and molecular introgression

The DNA sequences base calling and alignment revealed the presence of two likely hybrid individuals. Specimens LTI32 and LTI33, morphologically scored as *L. tityrus* in the field, were captured in the same date and on the same meadow (Table S3.1) within an *L. tityrus* exclusive area, although not far from *Lycaena bleusei* closest known location. Both individuals display the same mitochondrial and nuclear gene haplotypes, but each gene belongs to a different taxa gene pool, carrying an *L. tityrus* COI haplotype and two *L. bleusei* EF-1α phase determined haplotypes. No other individuals have shown this marker mismatch, not even the ones sampled within sympatric populations. Unfortunately, we were not able to amplify more nuclear genes from these two specimens besides EF-1α. Still, we were able to amplify the mitochondrial 16S ribosomal RNA for one of them, which as expected displayed an haplotype belonging to *L. tityrus* gene pool, such as COI.

4.5. Population genetic differentiation

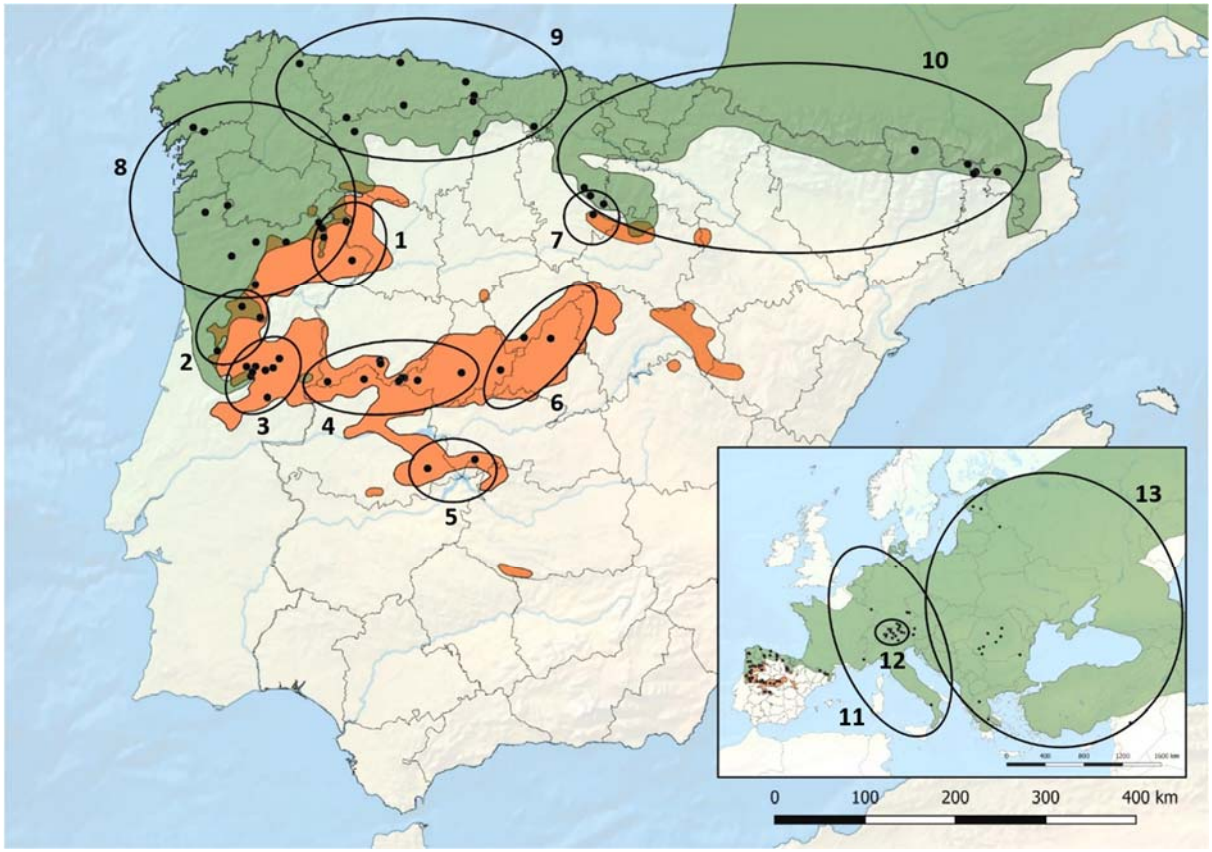

Figure 4.7 – Sampling site locations of the specimens used in this study (black dots) as well as population group division areas delimited for each species (black circles): 1 – Bragança (bleusei); 2 – Douro (bleusei)/South of Douro except Estrela (tityrus); 3 –Western CIMS (bleusei)/Estrela (tityrus); 4 – Central CIMS; 5 – Toledo Mountains; 6 – Eastern CIMS; 7- Burgos; 8 – North of Douro + Galicia; 9 – Cantabrian; 10 – Eastern Spain; 11 – Western Europe; 12 - *Lycaena t. subalpinus*; 13 – Eastern Europe.

The group divisions defined for *Lycaena* are highlighted in Figure 4.7 (Table S3.6). These groups and their correspondent values of nucleotide and haplotype diversities are also shown in Supplementary Material (Table S4.10). Within the population groups established for *L. tityrus*, the highest haplotype and nucleotide diversity values (h and π, respectively) were found in "Eastern Europe", "Eastern Spain" and "*L. tityrus subalpinus*" (Table S4.10), while in *L. bleusei*, the highest values were found among "Bragança" and "Eastern CIMS" populations. Note that "Burgos" haplotype diversity is in fact an artefact caused by one single specimen represented in this population.

Table 4.1 – Analysis of Molecular Variance (AMOVA) between *Lycaena tityrus*, *Lycaena t. subalpinus* and *Lycaena bleusei* in different hierarchical combinations.

	AMOVA1	**Degrees of freedom**	**Sum of squares**	**Variance components**	**Percentage of variation**
***L. tityrus* Iberia** • Western Iberia • Eastern Iberia • *Lycaena bleusei* ***L. tityrus* Non Iberia** • Western Europe • Eastern Europe • *Lycaena t. subalpinus*	Among groups	1	132.259	-0.22925 Va	-4.02
	Among populations within groups	4	562.937	5.71293 Vb	100.25
	Within populations	160	34.418	0.21511 Vc	3.77
	Total	165	729.614	5.69879	100
	AMOVA2	**Degrees of freedom**	**Sum of squares**	**Variance components**	**Percentage of variation**
L. tityrus* Iberia** • Western Iberia • Eastern Iberia ***L. tityrus* Non Iberia** • Western Europe • Eastern Europe ***Lycaena bleusei ***Lycaena t. subalpinus***	Among groups	3	691.956	5.90637 Va	95.03
	Among populations within groups	2	3.240	0.09357 Vb	1.51
	Within populations	160	34.418	0.21511 Vc	3.46
	Total	165	729.614	6.21505	100

Lycaena tityrus • Western Iberia • Eastern Iberia • Western Europe • Eastern Europe ***Lycaena bleusei*** ***Lycaena t. subalpinus***	**AMOVA3**	**Degrees of freedom**	**Sum of squares**	**Variance components**	**Percentage of variation**
	Among groups	2	677.416	6.83778 Va	92.75
	Among populations within groups	3	17.780	0.31959 Vb	4.33
	Within populations	160	34.418	0.21511 Vc	2.92
	Total	165	729.614	7.37248	100
Lycaena tityrus • Western Iberia • Eastern Iberia • *Lycaena t. subalpinus* • Western Europe • Eastern Europe ***Lycaena bleusei***	**AMOVA4**	**Degrees of freedom**	**Sum of squares**	**Variance components**	**Percentage of variation**
	Among groups	1	660.988	8.33235 Va	92.63
	Among populations within groups	4	34.208	0.44824 Vb	4.98
	Within populations	160	34.418	0.21511 Vc	2.39
	Total	165	729.614	8.99571	100
L. tityrus • Western Iberia • Eastern Iberia • *Lycaena bleusei* • Western Europe • Eastern Europe ***Lycaena t. subalpinus***	**AMOVA5**	**Degrees of freedom**	**Sum of squares**	**Variance components**	**Percentage of variation**
	Among groups	1	54.644	-2.33984 Va	-57.46
	Among populations within groups	4	640.552	6.19677 Vb	152.18
	Within populations	160	34.418	0.21511 Vc	5.28
	Total	165	729.614	4.07204	100

The sequential set of AMOVAs, mixing all population groups and major Sooty Copper taxonomic entities (*L. t. tityrus*, *L. t. subalpinus* and *L. bleusei*) in different hierarchical combinations, are shown in Table 4.1. The populations aggregated in the groups of Eastern and Western Iberia are detailed in Table S3.6. Within all group arrangements, the highest percentage of variation among groups was achieved in AMOVA 2, slightly above AMOVA 3 and 4, while the lowest variation among groups was obtained with AMOVA 5. Individual AMOVA for *L. tityrus* and *L. bleusei* are shown in Tables S4.11 and S4.12.

Table 4.2 – Pairwise F_{st} between *Lycaena tityrus* populations (including *L. bleusei*). Values above 0.5 are highlighted.

Lycaena tityrus	Estrela	South of Douro*	North of Douro + Galicia	Cantabrian	Eastern Spain	Western Europe	Eastern Europe	*L. tityrus subalpinus*	*Lycaena bleusei*
Estrela	-								
South of Douro*	0.00000	-							
North of Douro + Galicia	-0.06567	-0.08127	-						
Cantabrian	0.02026	0.00382	-0.00129	-					
Eastern Spain	0.43047	0.40807	**0.50788**	0.44056	-				
Western Europe	**0.79624**	**0.78297**	**0.82257**	**0.75540**	0.26529	-			
Eastern Europe	**0.63422**	**0.62154**	**0.69537**	**0.65950**	0.20703	0.04903	-		
L. tityrus subalpinus	**0.65104**	**0.63877**	**0.71059**	**0.67639**	**0.65211**	**0.75288**	**0.72019**	-	
Lycaena bleusei	**0.97614**	**0.97577**	**0.97810**	**0.97597**	**0.97217**	**0.97262**	**0.96962**	**0.96980**	-

Table 4.3 – Pairwise F_{st} between *Lycaena tityrus*, *L. tityrus subalpinus* and *Lycaena bleusei*.

Lycaena tityrus	*Lycaena tityrus*	*Lycaena tityrus subalpinus*	*Lycaena bleusei*
Lycaena tityrus	-		
Lycaena tityrus subalpinus	0.59661	-	
Lycaena bleusei	0.96492	0.96980	-

F_{st}, a measure of population differentiation, shows a convergent result to the AMOVA set. For a matter of comparison, the *Lycaena tityrus* pairwise F_{st} includes *L. bleusei* as another *L. tityrus* population (Table 4.2). Pairwise F_{st} values of *L. bleusei* populations alone are shown in Supplementary Material (Table S4.13). Overall, the F_{st} values between populations are generally high (>0.5), with "Western Europe", "Eastern Europe" and "*L. tityrus subalpinus*" being some of the most differentiated populations. Nonetheless, the highest scores belong to *L. bleusei* with all pairwise F_{st} values reaching almost 1 (>0.96) no matter the population (Table 4.2). "Western Europe" is genetically closer to "Eastern Europe" and to "Eastern Spain" with low F_{st} values (<0.27), but more differentiated from both western Iberian populations and *L. tityrus subalpinus* (>0.75). "Eastern Europe" shows the same pattern of differentiation towards West Iberia and *L. t. subalpinus* (>0.62 and 0.72, respectively), but is closer to "Eastern Spain" (0.20703), which stands in an intermediate position between West Iberia populations and the rest of Europe. On the other hand, *L. tityrus subalpinus* displays high values of differentiation from all the other populations (>0.63).

The pairwise F_{st} values between the major Sooty Copper groups *L. t. tityrus*, *L. tityrus subalpinus* and *L. bleusei* followed the same pattern seen in Table 4.2, after merging all *Lycaena tityrus* populations (Table 4.3). The highest values obtained are between *Lycaena bleusei* and both *Lycaena tityrus* and *Lycaena tityrus subalpinus* (0.96492 and 0.96980, respectively), while F_{st} between *Lycaena tityrus* and *L. t. subalpinus* is considerably lower, yet significant (0.59661).

4.6. Morphological analysis

Morphotype observations

All specimens were correctly identified as *L. bleusei* or *L. tityrus* on the field, except for 6 *L. bleusei* individuals incorrectly identified as *L. tityrus* (LTI 10, LTI 12, LTI 15, LTI 17, LTI 18 and LTI 21; Table S3.1). Throughout our sampling and research on *Lycaena tityrus* we found that male individuals occurring in western Iberia (Portugal and the western range of its Spanish distribution) consistently display a different phenotype from the ones occurring elsewhere in Europe, except for some regions of central and southern France where the western Iberian male phenotype is also present. While other European male phenotypes usually display a darker ground colour in the forewings upper side, the western Iberian individuals have a brighter colouration of the same surface with a bigger expression of orange and yellow, being closer to the phenotype presented by *Lycaena bleusei* (Figure S1.1). Females

throughout Europe usually display two alternative phenotypes, a brighter and a darker one, although in Iberia only the brighter one is known to occur.

This western Iberian male phenotype had previously been described as the race *praebleusei* (Verity, 1934) (Figure S1.2), with Asturias as its type locality. A second morphotype, described as race *pallidepicta* from the region of Mont Ventoux (France) (Verity, 1934) (Figure S1.2), was considered by Roger Verity as the linkage step between *praebleusei* and the northern darker morphotypes, such as the original *tityrus* morphotype (Figure S1.1), within the geographical phenotypic cline presented by this species. *Pallidepicta* is nonetheless much darker than *praebleusei*, and is also present in north-eastern Iberia, reaching the Cantabrian range where both *praebleusei* and *pallidepicta* morphotypes seem to meet. In fact, through a visual inspection of specimens and online records, we were able to confirm that the *pallidepicta* morphotype does not expand further west than the Cantabrian range, and conversely, the *praebleusei* morphotype does not go further East than the region of Burgos in Iberia, being then also present in some regions of France.

Many races or morphotypes of *L. tityrus* have been described through time and along the European range of this species, but their interpretation or validation is complex, based on small phenotypic colour variations or on the strength of wing patterns, which is not always constant. Thus, for a matter of simplicity and for the purpose of this work, we will only take in consideration the two Iberian *L. tityrus* morphotypes here mentioned: *praebleusei* and *pallidepicta*.

Geometric Morphometric Analyses

Allometry

The Procrustes ANOVA for allometry rejected the null hypothesis of parallel slopes, indicating that at least one group displays a different allometric pattern. Subsequent pairwise comparisons showed that this group corresponds to *L. tityrus* females, which differ significantly from males of *L. tityrus* and *L. bleusei* in vector length (magnitude) and from *L. bleusei* females in angle between slope vector (direction) (Figure S4.21).

Shape analysis

Pairwise comparisons of wing shape showed that all groups differ from all other groups. The highest difference was found between *L. tityrus* males and *L. bleusei* females, with a Procrustes distance of 0.08, and the smallest between males of the two taxa with a Procrustes distance of 0.04 (Table S4.14). A graphic comparison between the two coppers' wing shapes highlight the differences between these entities in wing silhouettes and tail projection (Figure 4.8). Additionally, wing shape comparisons between sexes within species are shown in Supplementary Material (Figure S4.22).

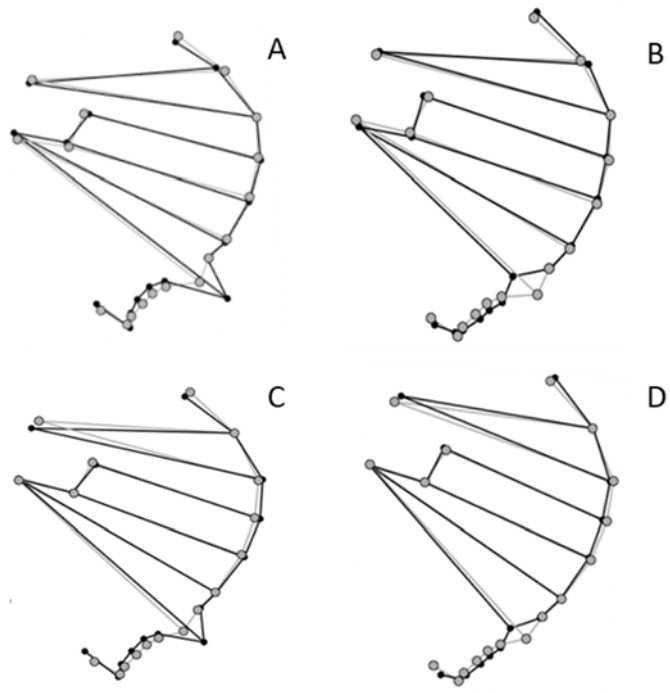

Figure 4.8 – Differences between means of both coppers' females/males (grey lines) against individual groups (black lines). A – Mean of all females against the mean of *L. bleusei* females. B - Mean of all females against the mean of *L. tityrus* females. C - Mean of all males against the mean of *L. bleusei* males. D - Mean of all males against the mean of *L. tityrus* males.

Centroid Size

ANOVA analysis on centroid size showed that there are significant differences between groups. Pairwise t-test with bonferroni correction for multiple comparison further indicated that all groups differ from the others, except males and females of *L. tityrus* (Figure S4.23). Females of *L. bleusei* display the biggest wings with an average centroid size of 1871, followed by males of the same species with 1684. Both are significantly different from males and females of *L. tityrus*, which have smaller wings, with a centroid size of 1511 and 1561 respectively (Figure 4.9; Table S4.15). The ANOVA analysis also indicated a small influence of season on centroid size, illustrated in Figure S4.24 (Table S4.16). For a better conception of data differences and similarities between the Sooty Coppers, an additional PCA is shown in Supplementary Material, where PC1 and PC2 display an overlap of both taxa, while PC3 reasonably separates them (Figure S4.25).

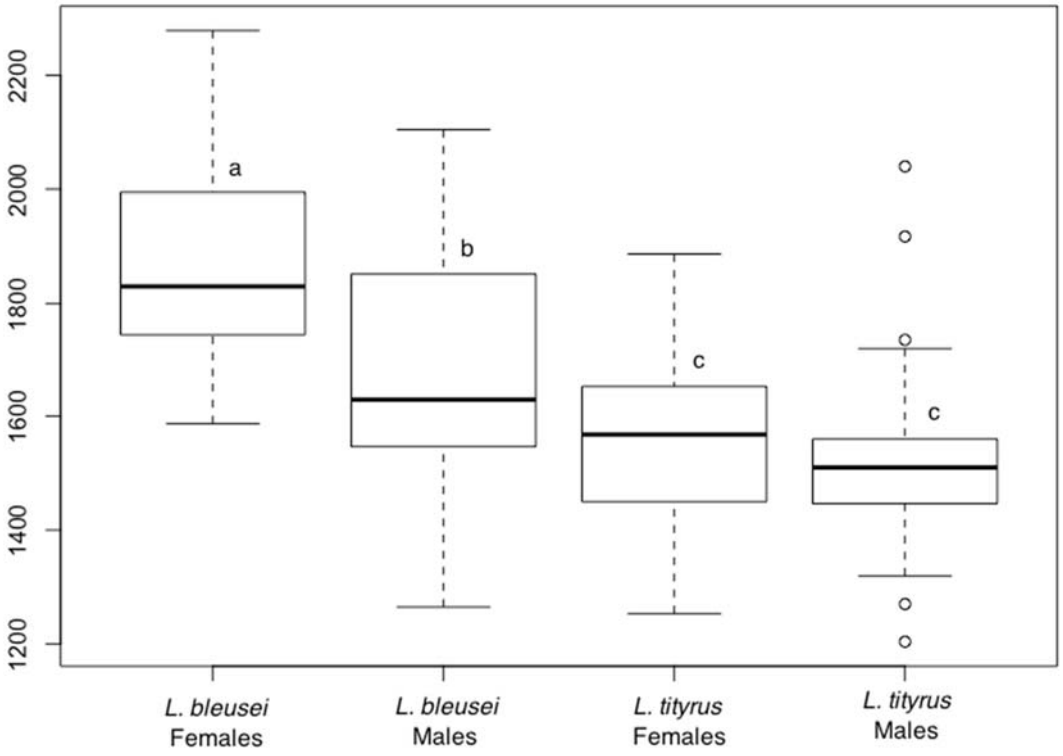

Figure 4.9 – Boxplot graphic of hindwing centroid size variation within the four *Lycaena* groups analysed. Groups which are not statistically different display the same letter (a, b, c).

4.7. Species Distribution Modeling

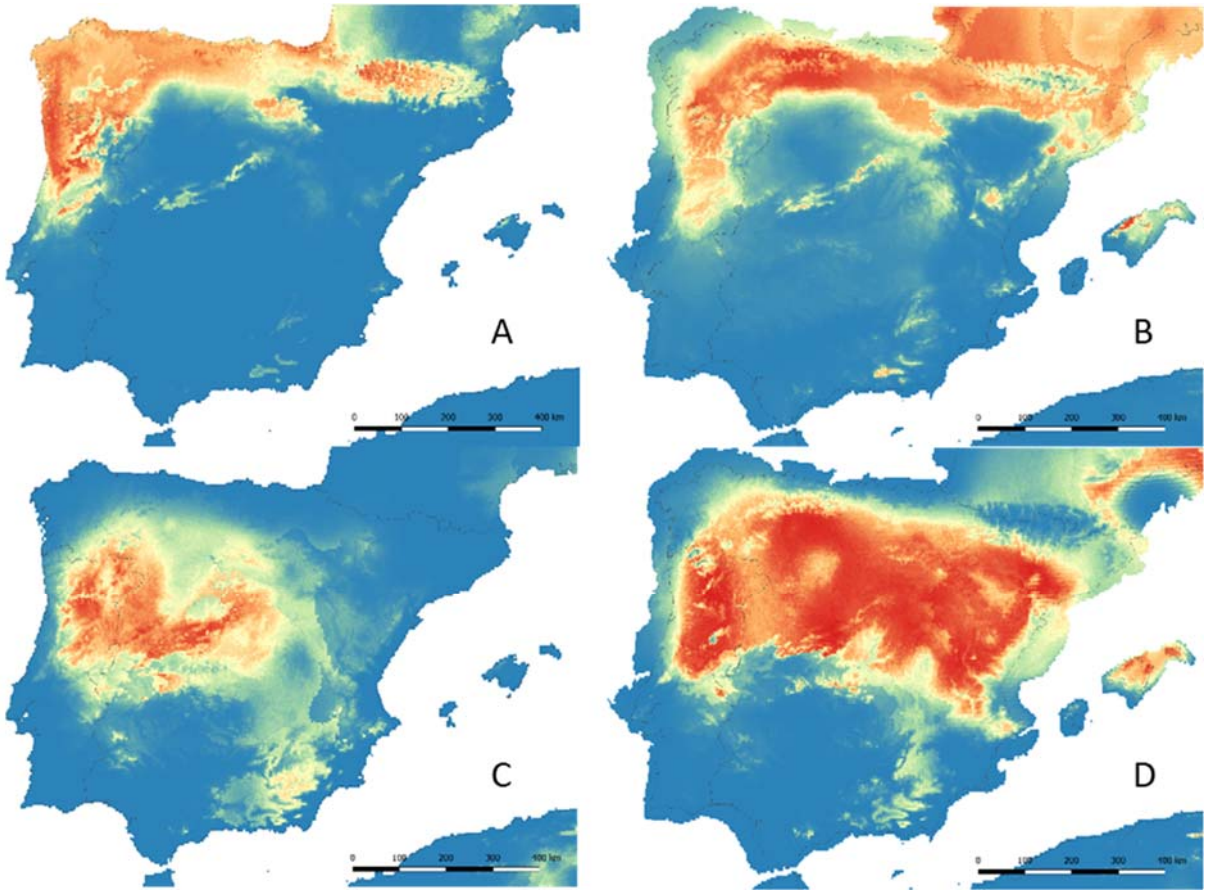

Figure 4.10 – SDM maps for both *L. tityrus* Present (A) and LGM (B) distributions and *L. bleusei* Present (C) and LGM (D) distributions.

The Sooty Coppers SDM analysis yielded an AUC of 0,977 for *L. tityrus* and 0,978 for *L. bleusei*, with a standard deviation of 0 for both. *Lycaena tityrus* Present model distribution displayed a very sharp correlation with the actual range of this species (Figure 4.10A). Thus, the model did not predict the occurrence of *L. tityrus* in places where it does not exist or where its occurrence is unlikely and, conversely, did not miss current distribution areas of this species. The bioclimatic variables that best explain *L. tityrus* distribution are temperature seasonality (BIO 4), temperature annual range (BIO 7), mean temperature of the driest quarter (BIO 9) and annual precipitation (BIO 12) (Figures S4.26 and S4.27). The variable which causes more loss to the model when omitted is temperature seasonality (BIO 4). A list of all WorldClim bioclimatic variables and respective codes is given in Supplementary Material (Table S4.17).

The correlation was not so precise with *L. bleusei*, for which the prediction map correctly foresees the species presence throughout the Central Iberian Mountain System in a continuous range but fails to predict some isolated southern and eastern areas where this species also occurs (Figure 4.10C; Figure 1.1). The variables that best explain *L. bleusei* distribution are precipitation of the warmest quarter (BIO 18), precipitation of the driest quarter (BIO 17), precipitation of the driest month (BIO 14)

and mean temperature of driest quarter (BIO 9) (Figures S4.28 and S4.29). The variable which causes more loss to the model when omitted is mean diurnal range (BIO 2).

Regarding LGM models, the range of *L. tityrus* did not change considerably from the Present map, with its projected distribution extending only slightly further away from the Atlantic coast in western Iberia and approaching the Catalonian Mediterranean coast (Figure 4.10B). On the other hand, the LGM model for *Lycaena bleusei* is drastically different from the Present prediction. In fact, the model projected a past distribution much more expanded to the northern half of the Peninsula, south of the Cantabrian belt, and more expanded to the East and West (Figure 4.10D). This projection spans a continuous Iberian range between the western Atlantic coast and the eastern Mediterranean coast, including areas of isolated *L. bleusei* populations (in the East) that the Present model was unable to predict. However, neither Present or LGM models have included some current southern isolated populations in Sierra Madrona and surroundings. The model also predicts other suitable LGM areas for *L. bleusei* outside of Iberia such as Provence, Corsica, Sardinia, Sicily, Southern Italy or Greece, where the species does not occur.

5. Discussion

5.1. Phylogenetic analysis

All Palaearctic, Nearctic and Oriental groups were overall clearly sorted out according to current species distribution in both tree inferences presented, except for *Lycaena cupreus*, an exclusive North American species phylogenetically placed in the Palaearctic clade (Figures 4.1A and 4.2). The Sooty Coppers *L. bleusei* and *L. tityrus* appear nested within the Palaearctic group as differentiated sister species and with high bootstrap support (BS), while still having three different haplotypes of each included in the analysis to account for intraspecific diversity. Their mean divergence time estimate places the beginning of their separation around 6.5 mya (95% HPD: 3.14 – 10.32 mya). This estimate is not as recent as we could initially expect from taxa regarded as the same species. However, their sister clade is less resolved in both combined and nuclear trees, with phylogenies displaying different topologies, polytomies and lower BS on its root. In fact, the different topologies obtained with COI + EF-1α and EF-1α trees (mito-nuclear discordance) show that these molecular markers are telling different stories when it comes to infer the phylogenetic relationships of *Lycaena*. The single use of mtDNA is not consensual within the scientific community when it comes to identify and differentiate species and races[50,106,107] or resolve phylogenies[47,108]. As such, we presented both combined and separated analyses for comparison.

Furthermore, the phylogeny constructed for the Sooty Coppers ingroup (Figure 4.1B) served not only to infer the direct relationship between *L. tityrus* and *L. bleusei* in a more supported analysis but also to take a deeper look into the possible closer taxon to this clade. This phylogeny returned the same general topology of Figure 4.1A, strengthening the separation of the Sooty Coppers (100% BS), but also placing *Lycaena virgaureae* as their sister taxon. This result is in line with the ones of De Jong & Van Dorp (2006)[47] and Oliver & Stein (2011)[63] (COI + COII and COI + EF-1α phylogenies, respectively) who also grouped *L. virgaureae* with *L. tityrus*, although the second had considerably less Palaearctic taxa in their analysis. In fact, the present *Lycaena* phylogeny also lacks the inclusion of many species, some of them possibly relatives to the Sooty Coppers ingroup. Similarly, the ingroup phylogeny (Figure 4.1B) was also limited by the amount of gene sequences available for the closer ingroup taxa and consequently lacked the inclusion of other important species as the EF-1α *L. solski* clade. Hence, any conclusions must be taken cautiously until further improved analysis with more species and more genes.

Lycaena phoebus and *Lycaena aeolides* had never been included in a molecular analysis and have clustered with *Lycaena solskyi* and *Lycaena alpherakyi* in the combined gene tree (Figure 4.1A), which are usually placed in the subgenus *Thersamonia* (Table S4.8). This seems to agree with *L. phoebus* and *L. aeolides* phenotypic resemblances to *Thersamonia*, while the latter has even a matching distribution with *L. solski* and *L. alpheraki* in the eastern Mediterranean and western Asia. *Lycaena phoebus* is, however, isolated in Morocco (North Africa), which raises interesting biogeographical hypotheses for these species' common ancestor and its past distribution range. However, such hypotheses are not further discussed in this study. The placement of *L. aeolides* in the nuclear tree topology is nonetheless different (Figure 4.2), next to *L. cupreus* and *L. alciphron*. *Lycaena aeolides* (= *aeolus*) had previously been pointed out as morphologically close to *L. cupreus*[62], while the latter shares similarities in their genitalia and facies with *Lycaena alciphron*[62], with their proximity being discussed in other studies[62,109–111]. The placement of *Lycaena cupreus* within the Palaearctic clade and its close

relation to *L. alciphron* suggests a fairly recent colonization of the Nearctic region by this species (or one of its ancestor lineages), with a later extinction of its Palaearctic populations.

Lycaena standfussi does not appear to have a direct relation to any other sampled *Lycaena* and the additional low bootstrap support over its placement does not allow for further interpretations without an improved phylogeny. *Lycaena dispar* had previously been associated with *L. splendens*[47] (not included in our analysis) and with *L.* cupreus[63]. However, its clustering with *L. violacea* in our phylogeny agrees with the morphological assignment of Bozano & Weidenhoffer (2001)[46]. Furthermore, in agreement with De Jong & Van Dorp (2006)[47] and Oliver & Stein (2011)[63], *Lycaena phlaeas* appears as one of the most basal taxa of our Palaearctic clade in the combined gene analysis (Figure 4.1A). It is the most widespread *Lycaena* species ranging across the entire Holarctic region but also in eastern Africa, Arabian Peninsula and some Atlantic islands. Its basal position as one of the first diverging lineages within the Palaearctic group supports its wider distribution and its diverse ecological adaptations to different environmental conditions[47]. Miller & Brown (1979) pointed *L. phlaeas* and *L. cupreus* as the most primitive *Lycaena* in North America (after morphological analysis), proposing that *L. phlaeas* must have reached the Nearctic during the Pleistocene by dispersal through the land bridge of Beringia[111]. In fact, a study on Beringia demonstrated the probable existence of a biogeographical corridor, serving as a route for larger animals during the Pleistocene glaciations[112], which certainly may have allowed for the interchange of many butterfly species.

Another interesting result is the phylogenetic position of *Lycaena helle*, standing in a polytomy with the Palaearctic and Nearctic clades, after the divergence from the Oriental species. Despite having a widespread Palaearctic distribution, this species has a remarkable phenotypic resemblance to the Oriental taxa and has thus often been included in this species group[46]. Furthermore, its position in our tree topology raises the hypothesis of this species possibly being an important key piece of the evolutionary connection between both clades, although more gene coverage is required to accurately support this statement. Still, its distance from the other sampled species indicate an old divergence from its theoretically closest relatives[46].

Both internal branches of the Nearctic species group appear well structured in our inferences (Figures 4.1A and 4.2). One encompasses mostly species attributed to the subgenus *Epidemia*[105], although *L. heteronea*, *L. gorgon* (*Chalceria*) and *L. arota* (*Tharsalea*) are also included (Table S4.8). Miller & Brown (1979) considered *Lycaena dorcas* as morphologically similar to *Lycaena helloides*, with only egg morphology distinguishing between the two[111]. This agrees with both our molecular results and the ones of Oliver & Stein (2011) which clustered the two species[63]. Moreover, the well supported inclusion of the closely related species *L. gorgon* and *L. heteronea* in this clade may not be a surprise since *L. gorgon* has been considered very different from other *Chalceria* species by its venation and male genitalia. *Lycaena heteronea*'s is however still similar to Chalceria in this regard[111]. Pratt & Wright (2002) allozyme phylogenies placed these two species in the *Chalceria* clade, although in a separated cluster, mentioning that the branch length between these and the remaining *Chalceria* is virtually the same as the branch lengths leading to other subgenera[62]. In fact, these two species display larvae differences from the rest of their subgenus species group and made a non-reversible host plant shift to *Eriogonum*, while other *Chalceria* species kept *Rumex* as host plant[62]. De Jong & Van Dorp (2006) and Oliver & Stein (2011) analysis have also integrated these species in the *Epidemia* clade, although with less support[47,63]. Overall, genetics seem to discredit the current formal taxonomic position of these two taxa, suggesting they might belong in *Epidemia*.

Lycaena hyllus had its own genus in the past, *Hyllolycaena* (Miller & Brown 1979)[111], and despite similar to *Chalceria* coppers on some characters, it is currently attributed to the subgenus

Epidemia[105]. Indeed, our results and the ones of Pratt & Wright (2002) and Oliver & Stein (2011) also place *L. hyllus* closer to *Epidemia*[62,63]. *Lycaena arota*, on the other hand, is currently placed in its own subgenus *Tharsalea*[105] and outgroups the first Nearctic branch, suggesting an earlier differentiation. Miller & Brown (1979) also considered this species a primitive copper of North America due to its venation and leg morphology[111]. To these authors, *L. arota*'s male phenotype resembles no other copper in the American continent. Our phylogeny, however, disagrees with the ones of Oliver & Stein (2011), which placed *L. arota* outgrouping the Editha complex clade, but agrees with Pratt & Wright (2002) distance tree phylogenies[62,63]. Nevertheless, the latter concluded that this species might require a different grouping above species level due to the allozyme differentiation. In the light of our molecular results we believe that *L. arota* current attribution to the genus *Lycaena* and under its own subgenus *Tharsalea* might be correct for this species, supported by genetic distance and morphological differences to other taxa.

The second Nearctic clade assembles the monophyletic *Chalceria* group, including the Editha species complex. The topology of the Editha complex clade agrees with Pratt *et al*. (1991) in which a phylogeny using 30 morphological characters pointed out *L. rubidus* as the likely most primitive species of the complex, and that *L. editha* and *L. xanthoides* would have evolved independently from a common ancestor with *L. dione*[62]. The allozyme phylogeny of Pratt & Wright (2002) and the gene phylogeny (COI + COII) of Oliver & Stein (2011) confirm this result[62,63].

On the other hand, *Lycaena hermes* (subgenus *Hermelycaena*) was not well resolved in either of the analysis (Figure 4.1A and 4.2), and it is the most ecologically and phenotypically divergent *Lycaena* species in North America due to its wing pattern and venation. Additionally, its larvae feed on *Rhamnus crocea* (Rhamnaceae), a different host plant family from most of the other Lycaeninae[62,111]. Thus, it is currently attributed to its own subgenus, *Hermelycaena*, but its position within *Lycaena* has been debated over time. In fact, Miller & Brown (1979) considered that the separation of *L. hermes* from the other North American *Lycaena* must have occurred in the Old World with a later extinction of the remaining *Hermelycaena*[111]. The phylogenies of Oliver & Stein (2011) placed *L. hermes* closer to the *Epidemia* clade[63], as in our nuclear tree topology (Figure 4.2). Nonetheless, more genes are required to understand the true phylogenetic position of this species and to infer its origin.

Finally, outgrouping both Palaearctic and Nearctic clades is the Oriental (East Asia) species clade. It includes *Lycaena pang* and *Lycaena li*, two species with a strict oriental distribution and both phenotypically similar, which makes their phylogenetic affinity an expected result. The Oriental species are considered as a phenotypic link to other Lycaeninae, especially the genus *Heliophorus* or even the Theclinae[110]. The basal position of this clade in relation to all the remaining *Lycaena* might suggest an origin of the whole group in this biogeographic region, and from where the rest of the world could have been colonized. Moreover, given its variety of habitats and species, this region may be seen as a diversification hotspot for *Lycaena*. However, we cannot infer the evolutionary history of an entire species group without a complete and significative sampling. Therefore, a true and comprehensive biogeographic inference of *Lycaena* must wait for an improved phylogeny, which should include more key taxa such as the South African (*L. clarki* and *L. orus*) and New Zealand (*L. salustius*, *L. boldenarum*, etc) clades. In fact, these missing species might completely alter our perception of this genus evolutionary history.

5.2. Haplotype networks and geographic structure

We found an unmistakably high genetic differentiation between both Sooty Coppers, as previously seen in Figures 4.1 and 4.2, with no genetic overlap or shared haplotypes between them (Figure 4.3). The mitochondrial COI gene displays more mutational steps separating the two entities than the nuclear elongation factor 1α. Given its higher mutation rate we could also expect a higher haplotypic diversity and richness for the mitochondrial gene than the nuclear one, and that was observed for *Lycaena tityrus* but not for *Lycaena bleusei*. The latter shows a surprisingly inverted result, with a higher haplotypic diversity in the nuclear gene EF-1α. Such mismatch is uncommon since nuclear genes take longer to accumulate mutations, due to their double copy and heritage from both parents. However, the lack of mitochondrial variation could possibly be explained by this species recent evolutionary history, like the occurrence of a genetic bottleneck affecting mostly the mitochondrial genome. If true, the genetic variability of the mitochondrial gene would be affected in a faster way than the genetic variability of the nuclear marker, and this could help explain the disparity observed between both markers' diversity in *L. bleusei*. This mismatch has been found in other organisms, including the human species, which are also thought to have undergone population and genetic bottlenecks throughout their history[113,114]. Other species might display the same mismatch pattern but resulting from selection[115] or from a recent species origin followed by expansion[116].

Regarding the genetic structure of our markers, we can only deeply discuss the results obtained for COI, as the nuclear EF-1α is considerably less sampled throughout Europe, having also limited DNA sequences available in online databases. As such, despite showing a minimal geographic structure for both species' haplotypes, this nuclear marker may still be hiding new unknown haplotypes exclusive from the eastern part of the CIMS for *L. bleusei* or from eastern Europe for *L. tityrus* as our sampling did not reach these eastern regions. As for COI, the lack of geographic structure for *L. bleusei* haplotypes is not surprising (Figure 4.4) given its small distribution range, its potential expansion in LGM and its general range connectivity for both Present and LGM ranges. *Lycaena tityrus*, on the other hand, is genetically structured for this mitochondrial gene throughout its wider distribution. Its most widespread haplotype, T3, is represented in the central position of this species star-like COI network (Figure 4.3), suggesting that it may possibly be the most ancestral haplotype from which all the others eventually diverged[117,118]. This mitochondrial lineage reaches Iberia, and its secondary contact zone with T1 in the north eastern part of the Peninsula (Figure 4.4) falls into a previously detected pattern of post glacial lineages meeting point along the main range of Pyrenees[7,21]. On the other hand, T2 is confined to the Asturias region and was first discovered by Dinca *et al*. (2015) from a single individual[50]. Our study found 3 other individuals displaying this rare haplotype and therefore confirming its existence in this region of Iberia. Bearing in mind the ranges of both *L. tityrus* COI T1 and T2 haplotypes and the Iberian ranges of the *praebleusei* and *pallidepicta* morphotypes, we could think of a possible correlation between T1 + T2 and *praebleusei*, and between T3 and *pallidepicta*. However, we didn't find this correlation as T1 individuals can be found associated with both *praebleusei* and *pallidepicta* morphotypes (Table S4.9). Interestingly, haplotypes T6 and T7, exclusive from *L. tityrus subalpinus* and from the Alpine range have T1 as their genetically closest haplotype, separated by one mutation, while separated by two mutations from the commonest T3.

It is possible that western and eastern Palaearctic regions may have had a stronger geographical segregation of *L. tityrus* COI haplotypes in the past, perhaps caused by the Quaternary climatic cycles. A population potentially carrying a common ancestor of all extant haplotypes could have been initially separated, originating the divergence between a western and eastern haplotype, which could be T1 and T3 due to their range representation and position within the COI network. As such, while T1 would be

mainly distributed throughout the southwestern Mediterranean area, giving rise later to T2 in Iberia, and to T6 and T7 in the Alps, T3 would be spread in the eastern range. The latter must have likely been the source origin for the isolated singleton haplotypes found in north and eastern Europe, probably originated in different refugia during the Pleistocene glaciations through the geographical fragmentation of the ancestral T3 population. Still, a larger T3 group must have persisted elsewhere in Europe, most likely in the Balkans or the Carpathians[7,21,119–122], conserving this haplotype in higher population frequencies. Later, during the glacial-interglacial transition, this larger T3 population could have had a more favourable expansion route out of its refugia, without major geographic barriers conditioning its dispersal[17,28,121–123], and recolonized central and western Europe into the previous range of T1. The latter, possibly more restrained in Iberia during the glacial periods, may have taken longer to expand, falling into the post glacial range expansion "Butterfly Paradigm", a reference to the biogeographical incapacity to cross the barriers of the Pyrenees and Alps by Iberian populations while central Europe is recolonized by populations from the Italian and Balkans refugia[21,124]. Nonetheless, the mutational difference between the groups of T1, T3 and T6+T7 is rather small, and an almost simultaneous split of these three populations during the glacial periods cannot also be excluded, with the latter likely being initially isolated in the southern slopes of the Alps, in a climatically buffered pocket, as shown for other species[121,125], before adapting to high altitude.

5.3. Populations genetic differentiation

The lower values of haplotype and nucleotide diversity for *L. tityrus* western Iberian populations were expected as there are only two *L. tityrus* COI haplotypes in western Iberia and one of them is restricted to Asturias (Figure 4.4B). As for *L. bleusei*, these statistics are not very informative since there are only two COI haplotypes in all its Iberian range, and both are widespread and mixed. Moreover, the values obtained for *L. bleusei* are tendentiously biased by the low number of individuals encompassed in each group, with some exceptions. "Burgos", for example, displays a maximum haplotype diversity value of 1 when there is only one individual sampled from this location. The establishment of these group divisions was carried in a way to achieve the most reasonable biogeographic range partitions for *L. bleusei*. Alternatively, with the same sampling but different group categories, and each of them assembling an equivalent number of individuals, we would have had a biased biogeographic inference.

The sequence of different AMOVA highlights the relationship between *Lycaena tityrus* and *Lycaena bleusei*, using the subspecies *L. tityrus subalpinus* as a measure scale in terms of differentiation levels (Table 4.1). The first two AMOVA show that treating both *L. bleusei* and *L. t. subalpinus* as simple *Lycaena tityrus* populations, respectively under the groups *L. tityrus* Iberia and *L. tityrus* Non-Iberia, makes the differentiation levels among populations within groups raise to extremely high values, as these populations are very different from each other. On the other hand, this makes the differentiation among groups so irrelevant that it drops to negative values. However, by considering both entities as something other than simple *L. tityrus* populations, attributing them a major group for their own, the results are inverted. The third AMOVA simply aims at proving that the high differentiation levels among groups seen with the second AMOVA are not being caused by the differences between the Iberian and Non-Iberian *L. tityrus* divisions, but by the establishment of the two new major groups *L. bleusei* and *L. tityrus subalpinus*. Finally, the fourth and fifth AMOVA were useful to distinguish which of the two entities, *L. bleusei* or *L. tityrus subalpinus*, was causing this high differentiation values among groups and the results were clear. In fact, the differentiation values stay virtually the same when we include the

subspecies *L. tityrus subalpinus* as one population of *L. tityrus* and keep *L. bleusei* as a distinct major group. However, it drastically changes to maximum values of differentiation obtained among populations within groups when *L. bleusei* and *L. tityrus subalpinus* change places. This highlight the major influence *Lycaena bleusei* has over these differentiation levels and, consequently, how much differentiated it is when compared to the recognized subspecies *L. tityrus subalpinus*.

The pairwise F_{st} values obtained follow the same tendency of the AMOVA, with *L. bleusei* displaying the highest differentiation from the other groups when included as a population of *L. tityrus* (Table 4.2). The high F_{st} levels displayed by western and eastern Europe populations are partially due to the larger assemble of different haplotypes inside their own range divisions, which consequently raises the differentiation levels of these populations. Additionally, the closer genetic proximity (lower F_{st} values) between "Eastern Spain" and both western and eastern European populations is caused by the presence of T3 in the north-eastern part of Iberia. Overall, the same F_{st} pattern was obtained when using a dataset reduced to the major Sooty Copper entities analysed: *L. bleusei*, *L. tityrus* and *L. t. subalpinus* (Table 4.3). Here, the pairwise F_{st} obtained illustrate once more the higher differentiation status of *L. bleusei*. In fact, the pairwise F_{st} observed between *L. tityrus* and *L. t. subalpinus* turns insignificant when both are compared to *Lycaena bleusei*, as their pairwise Fst with this taxon just slightly differ from each other (0.96980-0.96492=0.00488), despite all differences between them subspecies.

Although the fixation index F_{st} is mostly used to access differentiation levels among populations, it may also be of interest to investigate what could be the threshold for species and subspecies delimitation[126]. Furthermore, as *L. bleusei* has been treated as a mere race/form or subspecies of *L. tityrus* for a long time since its description, we intended to put this taxon in that same category throughout these population differentiation analyses and observe the outcome. Previous studies have also used pairwise F_{st} and AMOVA as tools to infer the true relationships within species complexes and unstudied polytypic species, obtaining similar results to ours and unveiling the presence of cryptic diversity[11,122]. In the end, even though we are only analysing one molecular marker, and with no recognized or valid threshold for measuring species delimitation using F_{st}, our results still stand as another solid proof that *Lycaena bleusei* should not be treated as a simple population of *Lycaena tityrus* nor its subspecies.

5.4. Geometric Morphometric Analyses

Geometric Morphometric Analyses have proven to be useful and capable of distinguishing closely related taxa, populations or even sexes and seasonal dimorphisms in some studies analysing wing shape and size[122,127–130]. However, it also proved to be conversely inefficient in others[75,131,132]. As mentioned before, the Sooty Coppers display a sexual dimorphism visible within several phenotypic characters such as coloration, size and wing shape. Still, pairwise comparisons exposed differences between all four groups (males and females of *L. bleusei* and *L. tityrus*) showing that there is also a significant variance in wing shape between individuals of the same sex but different taxa (Table S4.14). Wing shape differences between the means of each *L. bleusei* males and females to the mean of both species combined is clear and especially remarkable over the tail projection (Figure 4.8). Nonetheless, while *L. bleusei* individuals seem to consistently display this hindwing feature, more prominent in females, *L. tityrus* doesn't seem to have it in neither of the sexes. Even so, males of both coppers are similar to each other in wing shape, likely due to the overall contour of the wing (Table S4.14). Conversely, the most divergent groups are *L. bleusei* females and *L. tityrus* males, likely due to the

cumulative differences between both species and sexes. It should also be noted that the different allometric pattern found in *L. tityrus* females didn't seem to have had any influence in wing shape analysis, probably because the allometric difference, although significant, is not enough to express major changes in the mean wing shape of this group.

In centroid size analysis (intrinsically correlated with wing size), the considerable gap between *L. bleusei* females and all other groups (Figure 4.9) could be explained by their distinctive big tail projection (seen in Figure 4.8), especially pronounced in summer generations (Figure S4.24). *Lycaena bleusei* males, however, with their smaller tail projection and their overall wing shape similarities with *L. tityrus* males, appear closer to *L. tityrus* butterflies in wing size. The wide boxplot variation of *L. bleusei* and *L. tityrus* females in Figure 4.9 is highly associated with the intrinsic seasonal variation displayed by these groups (Figure S4.24). Males of both coppers don't change as much as females from Spring to Summer generations, but still display a slight deviation towards smaller centroid sizes (Figure S4.24). Curiously, females of the two taxa display an opposite pattern of size variation: while females of *L. bleusei* tend to be bigger in summer generations, females of *L. tityrus* are bigger in spring generations, approaching the size of its correspondent males during the summer (Figure S4.24).

Environmental cues such as thermal clines have proven to directly influence butterfly's phenotype and physiology, influencing also seasonal size variation within different annual generations[133–136]. The general pattern of temperature-size rule (TSR) for most Lepidoptera, suggest that individuals grow larger with colder temperatures and smaller with increasing temperatures[134]. In fact, considering the current distribution of *L. tityrus*, the Iberian Peninsula could be at the limit range of what are the tolerable conditions for this widespread and temperate species (although the influence of potential competition with *L. bleusei* may also shape its range, not studied in this work). As such, the warmer Mediterranean environment, intensely felt in Iberia, could perhaps be affecting the size of this species females in summer generations. However, in that case, we could ask why was *L. bleusei* getting bigger when the temperatures were raising. Despite being sister taxa, *L. bleusei* is an Iberian endemism and could be more adapted to such environmental conditions. Furthermore, similar cases of butterfly seasonal size variation with inverted TSR have been discovered[137]. In the end, with no other geometric morphometric study on *Lycaena tityrus* hindwings outside of Iberia, it is currently impossible to deeply discuss any further hypothesis.

On the other hand, the size decrease presented by males in summer generations (Figure S4.24) is in accordance with the TSR and with the laboratorial experiments conducted by Fisher & Fiedler (2000), which showed that with higher temperatures during development time, males of *L. tityrus subalpinus* emerge earlier and display a considerable drop in corporal weight in comparison with males developed in colder temperatures[133]. This is thought to be related with fitness traits, namely the fact that by compromising the development time and consequently reducing their corporal weight (possibly also correlated with a size decrease) males can emerge earlier in the summer, translating in more chances of occupying and defending a territory against other males, while also having higher chances to increase the number of annual generations[133].

Overall, considering our results, we may conclude that despite sharing many morphological traits, as expected from sister taxa, these coppers display consistent and important differences separating them as different biological entities, as here highlighted for wing shape and size.

5.5. Species Distribution Modeling

Species Distribution Modeling is a very useful tool to predict current, past and future ecological niches of many taxa, being used in this study as one more essential approach to the inference of the Sooty Coppers evolutionary history and relationship. The predictive maps obtained for the Present time conditions were very accurate with species current known distributions, except for a few isolated *L. bleusei* populations in eastern and southern Spain not included by this species predictive model (Figure 4.10C). Predictions for the LGM conditions were also interesting, and during this period *Lycaena tityrus* might have been more disseminated in the Catalonian region (Figure 4.10B), possibly suffering some population extinctions in those peripherical locations until the present day. Even so, the SDM results for *L. bleusei* LGM distribution were the most unexpected, as instead of being constraint during this glacial cycle, it appears to have possibly expanded and occupied the northern half of the Peninsula, south of the Cantabrian range (Figure 4.10D). According to Schmitt (2007), species adapted to Mediterranean conditions were expected to suffer more from the temperature drop during the LGM while continental adapted species would suffer from the lack of precipitation and general dryness[21]. While the Iberian population of *L. tityrus* might have resisted the dryness by maintaining its distribution relatively close to the northern mountain ranges of Cantabria and Pyrenees, the result obtained for *L. bleusei* goes against what Schmitt's theory would predict. In fact, this result may be supportive of the idea that *Lycaena bleusei* might have gone through or be currently going through a process of population bottleneck and consequent genetic bottleneck, having experienced a considerable range reduction from the LGM to the Present. This hypothesis first arose with the finding of a molecular marker mismatch in this species, and SDM maps for LGM might also be pointing in the same direction. Curiously, additional demographic inference tests also confirm this pattern, with positive Tajima' D values suggesting a population numbers decrease for *L. bleusei* and a population number increase for *L. tityrus* (negative Tajima' D values) when analysing the whole populations COI dataset for each taxon (Table S5.1)[113]. The nuclear gene EF-1α was not analysed for demographic tests.

An LGM range expansion has been documented in other species, although rare and expected from alpine or arctic species and not Mediterranean ones[13,25,26]. Even so, the Iberian Peninsula was much less affected by the Quaternary glacial periods than northern European latitudes, with glaciated and permanent snow areas mostly restricted to some ocean-land transition areas and to the big mountain systems of the Pyrenees, CIMS, Cantabrian range, Betic range and north-western mountains in Peneda-Gerês[138–143]. The Peninsula has thus maintained reasonable conditions during LGM for many species to persist or expand within a wide range of its extension, even with the general temperature drop of 6ºC to 10-12ºC, more severe during winter months[144,145].

Nonetheless, with *L. bleusei* theoretical expanded range, both Sooty Coppers must have likely co-occurred in much larger sympatric areas, with potential for hybridization and introgression events occurring between them. The predicted *L. bleusei* LGM distribution also includes the current eastern isolated populations that the model map built for the Present conditions was unable to predict but fails to include the southern isolated populations. This may suggest a maintenance of these eastern populations since the glaciation period and until the present day, while the surrounding *L. bleusei* populations suffered an extinction during the LGM-interglacial transition. These places may have had optimal ecological conditions in the past, and remain now suitable for this species to resist, although in possible different ecological conditions from the rest of *L. bleusei*'s range, causing this model results disparity in Present time maps. On the other hand, the Southern populations not predicted by both models may possibly represent post glacial dispersions.

Finally, although the LGM model for *L. bleusei* also predict a potential distribution in many regions of Southern Europe, the dispersal of this species to these regions outside of Iberia has likely never happened since there are currently no relict populations of *L. bleusei* in this southern Mediterranean region, which maintain similar ecological conditions to Iberia.

5.6. Evolutionary history scenario for the Sooty Coppers

Based on the different results obtained for both *Lycaena bleusei* and *Lycaena tityrus* and their relationship, we hypothesize here alternative evolutionary history scenario hypothesis for the Sooty Coppers:

Hypothesis nr.1

1. Initially, a Palaearctic common ancestor of both *L. tityrus* + *L. bleusei* and the clade of their sister taxa (not specified due to the uncertainty of the phylogenetic results), could have been possibly expanding to western Europe and colonized the Iberian Peninsula around 9.9 million years ago (95% HPD: 6.37 – 13.85 mya) (Figure 4.6), originating two allopatric populations: one in Iberia and another outside of Iberia. Although environment can have a strong effect on butterfly's phenotype and promote its rapid change within short geological time frames, this ancestral population could have carried a brighter colour phenotype, resembling the brighter phenotype of some of the species that might have possibly arisen from this lineage: *L. bleusei, L. virgaureae*, *L. candens*, *L. hippothoe*. Still, without a more gene inclusive phylogeny of *Lycaena* we cannot further infer more details over the descendants of this ancestral lineage as well as their phenotype heritage.
2. An extended period of allopatry between the two populations might have led to the separation of the clades containing the ancestral lineage of *L. tityrus* + *L. bleusei* in Iberia and the one of their sister clade outside of Iberia.
3. After being possibly isolated for a long period of time, the ancestral population of *L. tityrus* + *L. bleusei* might have crossed once more the geographical barrier of the Pyrenees, this time leaving Iberia, around 6.5 mya (95% HPD: 3.14 – 10.32 mya), being thus split one more time in two new allopatric populations: in Iberia and outside of Iberia.
4. With time, both allopatric populations of *L. tityrus* + *L. bleusei* common ancestor must have differentiated genetically from each other, becoming later the biological entities of *L. bleusei* in Iberia and *L. tityrus* outside of Iberia. Subsequently, the population differentiating on *L. tityrus* must have expanded and reached northern latitudes, possibly splitting into different geographic European subpopulations. This could have originated the initial divergence between T1 and T3 COI haplotypes. Also, during its expansion and adaptation to more temperate and colder regions, one of its northern populations could have possibly assimilated a darker phenotype for both males and females (as seen for the darker *L. tityrus subalpinus* population isolated in the Alps), although females would have also kept an ancestral brighter form, displaying therefore two phenotypes throughout Europe and maintaining a sexual dimorphism within this species' European populations. Conversely, southern *L. tityrus* lineages would have kept a resembling ancestral and brighter phenotype (*praebleusei*), phenotypically closer to the one that might have persisted in

the Iberian *L. bleusei*. This agrees with the findings of Roger Verity, who considered the morphotype *L. bleusei*, at that time seen as another *L. tityrus* race, as the likely ancestral phenotypic state[61].

5. Later, with the different climatic cycles of the Quaternary period and consequently the different waves of contraction and expansion, the southwestern and brighter *praebleusei* populations must have recolonized the North of the Iberian Peninsula and established secondary contact zones with populations of *L. bleusei*, possibly more than once as it has been suggested for Iberian sister species[4]. With their reproductive system barriers not yet established, hybridization events must have likely occurred between both taxa, something we can still observe today with the two hybrid individuals found in our study. The recolonization of Iberia by a potential T1 population might have also allowed for the later differentiation of T2, possibly in a refuge within the refuge of Iberia[15], during one of the glacial periods of the Quaternary. Still, a relict population displaying the *praebleusei* phenotype would have persisted and survived in southern France, as it is currently observed in this region. Conversely, the European T3 lineage might have been divided in different subpopulations during the glacial periods, giving rise to the different singleton COI haplotypes.

Hypothesis nr.2

Same as Hypothesis nr.1 (1-4), except: the initial European *L. tityrus* population could have collectively assimilated a darker phenotype soon after its divergence from *L. bleusei*, resembling the current morphotype *pallidepicta*. Afterwards, throughout its expansion to northern latitudes it would have adapted to even colder environments and strengthened this dark colouration.

5. The southern *pallidepicta* population could have then recolonized Iberia where it had to adapt to the conditions of this region, and consequently assimilated a brighter phenotype for the males of its leading edge in western Iberia (morphotype *praebleusei*), getting closer to the one of *L. bleusei* due to the similar environmental conditions (as shown to occur in other organisms[146]), and thus reducing the strong sexual phenotypic dimorphism displayed by *L. tityrus* populations throughout Europe. Alternatively, the morphotype *pallidepicta* could have also hybridized with the brighter *L. bleusei* when expanding in northern Iberia, giving thus origin to the western Iberian *L. tityrus* morphotype *praebleusei*. This new lineage could have maintained its closer identity to *L. tityrus*, as well as its mitogenome as seen for COI haplotype T1, suggesting a one-way direction for the hybrid relations (females of *L. tityrus* with males of *L. bleusei*, the same direction of our two introgressed specimens LTI32 and LTI33), but assimilated some phenotypic characters of *L. bleusei* through this adaptive introgression event. Consequently, the newly introgressed *L. bleusei* characters could have given this newly formed *praebleusei* lineage some fitness advantage, making it more adapted to the Iberian environment than its parental lineage of *L. tityrus* and become completely established in the western Iberian range, while pushing the morphotype *pallidepicta* to the eastern range of Iberia. Nonetheless, such hypothesis of an adaptive introgression event could only be tested and confirmed with future more extensive nuclear gene inference, ideally at a genomic level.
6. Afterwards, with the contraction and expansion events imposed by the climatic cycles of the Quaternary, the morphotype *praebleusei* could have reached France and established a population that persisted until today, with a possible extinction of the populations connecting it to Iberia.

Hypothesis nr.3

1. The common ancestor of *L. tityrus* + *L. bleusei* could have been present in Europe, carrying a phenotype similar to the one currently observed in *L. bleusei*. It could have then eventually reached Iberia and colonized it around 6.5 mya (95% HPD: 3.14 – 10.32 mya), thus originating two allopatric populations: inside and outside of Iberia.
2. With time, the two populations differentiated from each other and originated the biological entities *L. bleusei* in Iberia and *L. tityrus* outside of Iberia.

Same as hypothesis 1 (4 and 5) or,

Same as hypothesis 2 (4-6).

Case-study 2 – *Melanargia* and the *Argeformia* subgenus

6. Results

6.1. Data characterization

The matrices of our samples were obtained through direct PCR sequencing. Amplification and editing of DNA sequences yielded 657 base pairs for the alignment of COI, 617 for 16S, 578 for EF-1α and 403 for Wingless. Also, the dataset containing *M. occitanica* + *M. ines* + *M. arge* COI sequences (Dataset 1, without the outgroup sequence) displayed 558 invariable sites, 99 variable sites, from which 75 are parsimoniously informative and 24 are singletons. The dataset with the same species 16S sequences (Dataset 2) displayed 486 invariable sites, 25 variable ones (14 parsimoniously informative and 11 singletons) and 6 sites with missing data. The dataset with these species EF-1α sequences (Dataset 3) displayed 547 invariable sites and 31 variable sites, from which 22 are parsimoniously informative and 9 are singletons. Most of *M. ines* individuals displayed between 0 and 2 heterozygotic sites, while one specimen had 6. The number of heterozygotic sites in *M. occitanica* individuals ranged between 0 and 1, while the only *M. arge* EF-1α sequence had none. Finally, the dataset with these species' Wingless sequences (Dataset 4) displayed 376 invariable sites and 27 variable sites, from which 9 are parsimoniously informative and 16 are singletons. The few samples that we were able to amplify from this nuclear gene revealed no heterozygotic sites. The list of all datasets used in this study can be seen in Table S3.5. The pairwise distances between the three *Argeformia* species, as well as between the different populations defined for *M. occitanica* and *M. ines* are also shown in Supplementary Material for all genes analysed (Figures S6.1-S6.4).

6.2. Phylogenetic analysis and haplotype networks

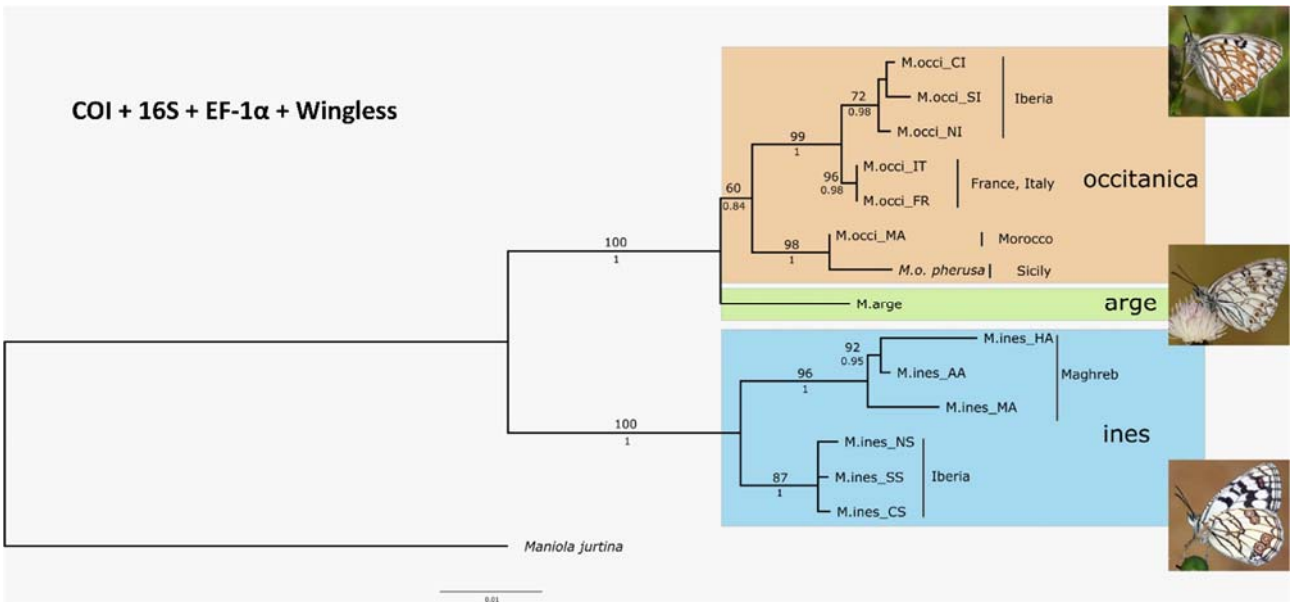

Figure 6.1 – Maximum Likelihood phylogenetic tree using the concatenated dataset of 2 nuclear and 2 mitochondrial genes (Datasets 1 + 2 + 3 + 4). NI = North Iberia; CI = Central Iberia; SI = South Iberia; IT = Italy; FR = France; MA = Middle Atlas; HA = High Atlas; AA = Anti Atlas; NS = North Spain; CS = Central Spain; SS = South Spain.

The Maximum Likelihood phylogenetic tree is the only one here presented (Figure 6.1) as the Bayesian Inference analysis recovered the same general tree topology, except for a basal polytomy (Figure S6.5). Additional trees for each gene with both ML analysis and Bayesian inference are given in Supplementary Material (Figures S6.6-S6.13).

The ML phylogeny recovers three well differentiated clades, corresponding to the three recognized species of *Argeformia*: *M. ines*, *M. occitanica* and *M. arge*. The latter appears closely related to *M. occitanica* as likely sister species (60% BS, PP = 0.839). *Melanargia occitanica* comprises two differentiated lineages: one including the Moroccan and Sicilian populations, and another comprising the European populations from Iberia to north western Italy. The second group is still divided in two well supported clades (99% BS, PP = 1): the Iberian and the France + North Italy clades. Western and Central Iberian populations are genetically closer to each other than to North Iberia, although with low support (46% BS, PP = 0.719), while the Maghreb-Sicilian clade is conversely very well supported (98% BS, PP = 1). Within *Melanargia ines* there is once more a demarked separation between Iberian and Moroccan populations (96% and 87% BS, PP = 1). Additionally, the Moroccan populations sampled are well differentiated, with High and Anti Atlas clades appearing as phylogenetically closer to each other than to the Middle Atlas one (92% BS, PP = 0.945).

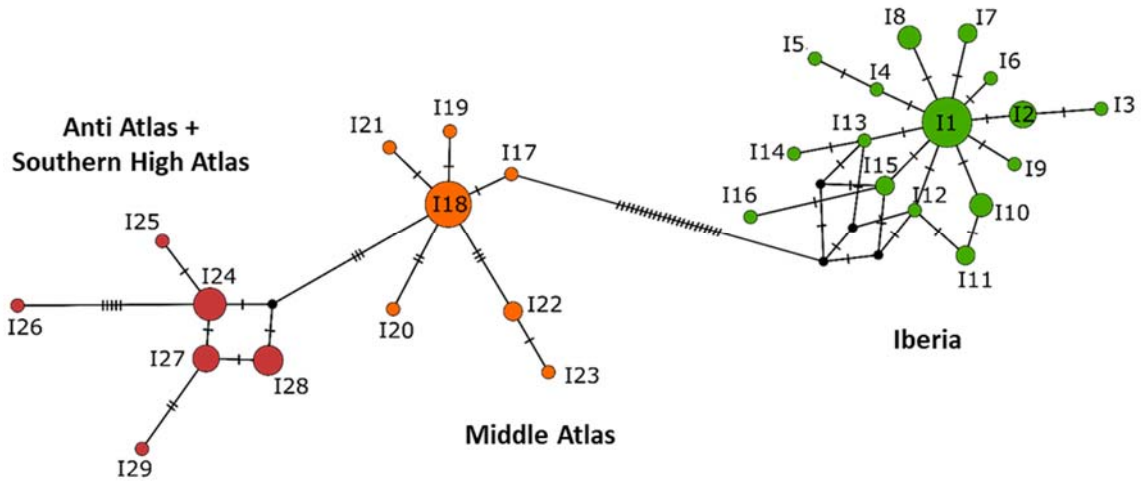

Figure 6.2 – Haplotype network of *Melanargia ines* for mitochondrial COI gene using Dataset 5. Different colours represent different genetic clusters.

The mitochondrial COI haplotype network for *M. ines* displays a clear and pronounced differentiation between the Iberian (I1-I16) and Moroccan (I17-I29) groups with twenty-five mutational steps (Figure 6.2) and a different structure for both. The Iberian cluster is diverse, showing a star-like pattern with sixteen different haplotypes, yet little differentiated from each other with only one or two mutations distancing them from the commonest I1. We found no significative geographical structure of the Iberian haplotypes as several common haplotypes are spread through the whole area. Interestingly, the closest Iberian haplotypes to the Moroccan group are found exclusively in the South of the Iberian Peninsula (I12, I13 and I15; Table S6.1).

In Morocco, there are two clusters separated by four mutations: one exclusive from the region north of the High Atlas range with seven represented haplotypes (I17-I23), and another comprising individuals from both south and north of the High Atlas range, with six different haplotypes (I24-I29). The first cluster can be further divided in two other sub clusters with three and four mutational steps separating, respectively, I22 and I23 from the remaining haplotypes. Similarly, another divergence is visible within the second cluster, with one High Atlas haplotype (I26) displaying a deep differentiation of five mutational steps from the closest one (I24). The spatial segregation of these haplotypes throughout *M. ines* distribution is shown in Figure 6.3.

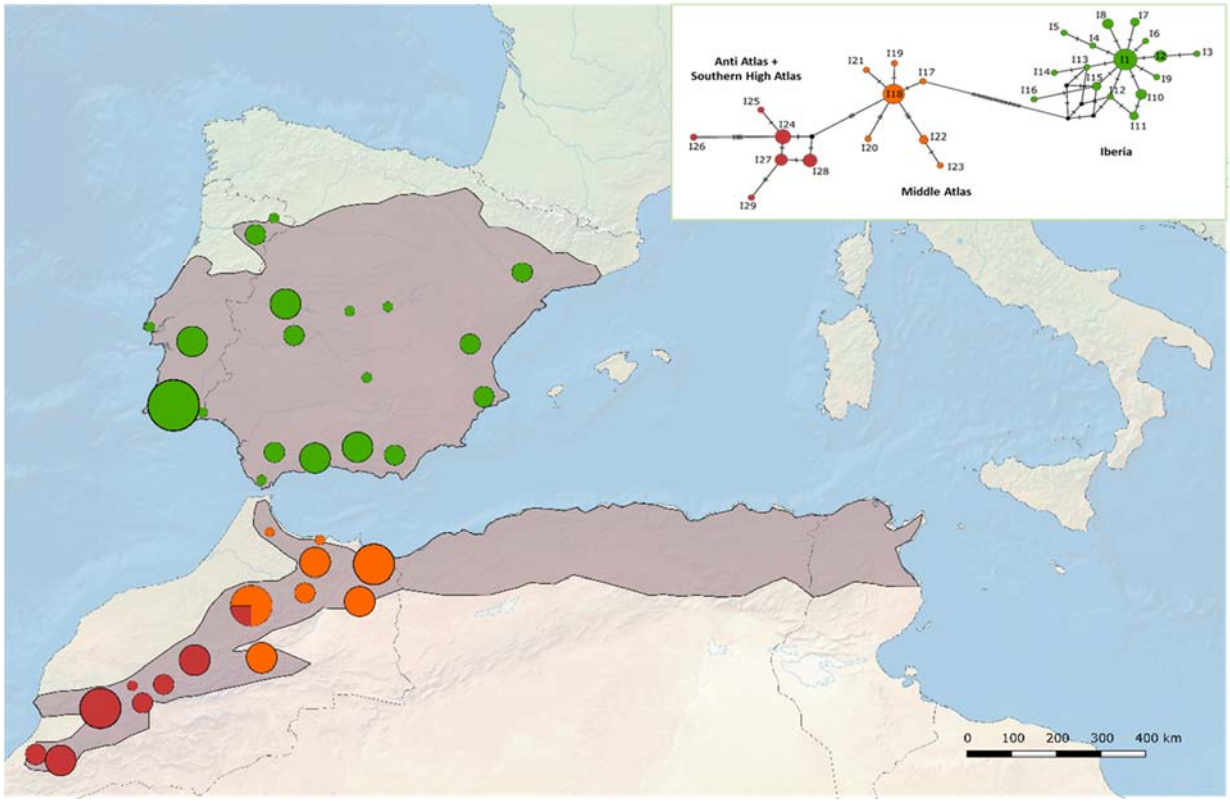

Figure 6.3 – Geographic segregation of *M. ines* COI haplotypes in the western Mediterranean region. Haplotype colours are identical to Figure 6.2 and represent the three different clusters of this Figure.

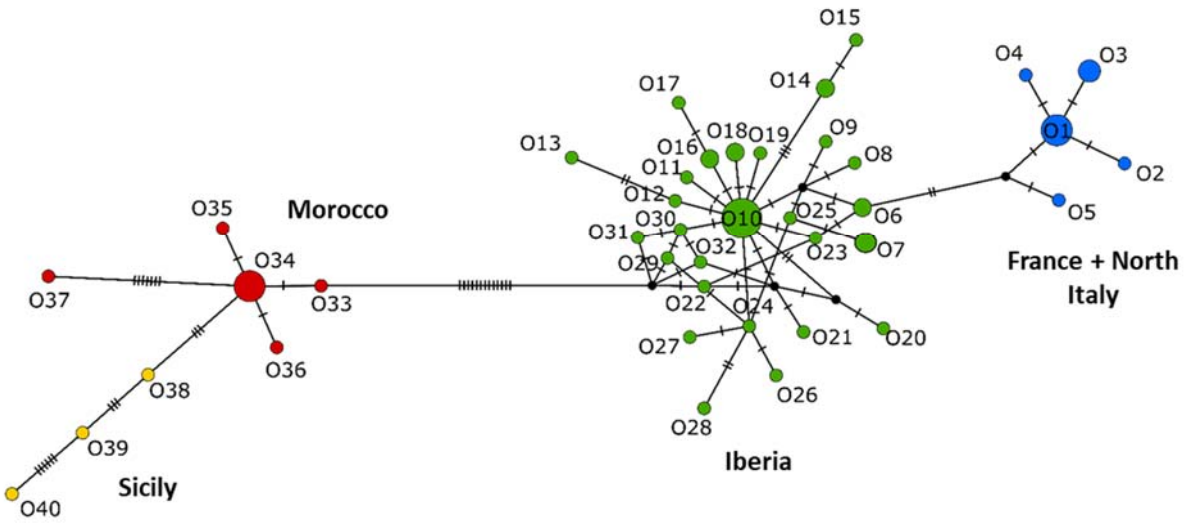

Figure 6.4 – Haplotype network of *Melanargia occitanica* for COI gene using Dataset 6. Different colours represent different genetic clusters.

The haplotype network obtained for *Melanargia occitanica* shows a pronounced differentiation between European and Maghreb haplotypes as well, with thirteen mutational steps between them, and with the Sicilian group being clustered with the Maghreb haplotypes (Figure 6.4).

Within the European clade two different clusters appear: an Iberian and a French-Italian. The Iberian is the most diverse cluster with thirty-two different haplotypes represented in a star-like pattern, separated by one to four mutations from the central and most common haplotype O10. Just like for *M. ines*, there is no evident geographical structure of the genetic diversity in Iberia for *M. occitanica* except for a few more differentiated haplotypes from the southeast (O7, O14 and O15; Table S6.1). The French-Italian cluster encompasses five haplotypes (O1-O5) with little differentiation among them, although differentiated from the Iberian cluster by three and four mutations (five and six mutations to the commonest haplotype 010). Even though there is no genetic overlap between the gene pools of both groups, the French-Italian haplotype O1 was found in the Northeast region of Iberia (Table S6.1).

The Morocco + Sicily cluster can be further divided in one Moroccan lineage with five haplotypes (O33-O37) and a Sicilian one with three (O38-O40). Both clusters are separated by a minimum of three mutational steps. The Moroccan haplotypes are all genetically close from each other except for O37, which surprisingly distances itself from the commonest haplotype O34 by seven mutations. On the other hand, the three Sicilian haplotypes are all distant from each other, separated by three to nine mutational steps from each other. The haplotypes from both groups are well separated geographically with no genetic overlap.

The geographic segregation of *M. occitanica* COI haplotypes can be seen in Figure 6.5. Additionally, an *M. occitanica* COI network including one COI sequence of *M. arge* is shown in Supplementary Material, where the latter appears genetically closer to the Moroccan cluster of *M. occitanica* (Figure S6.14).

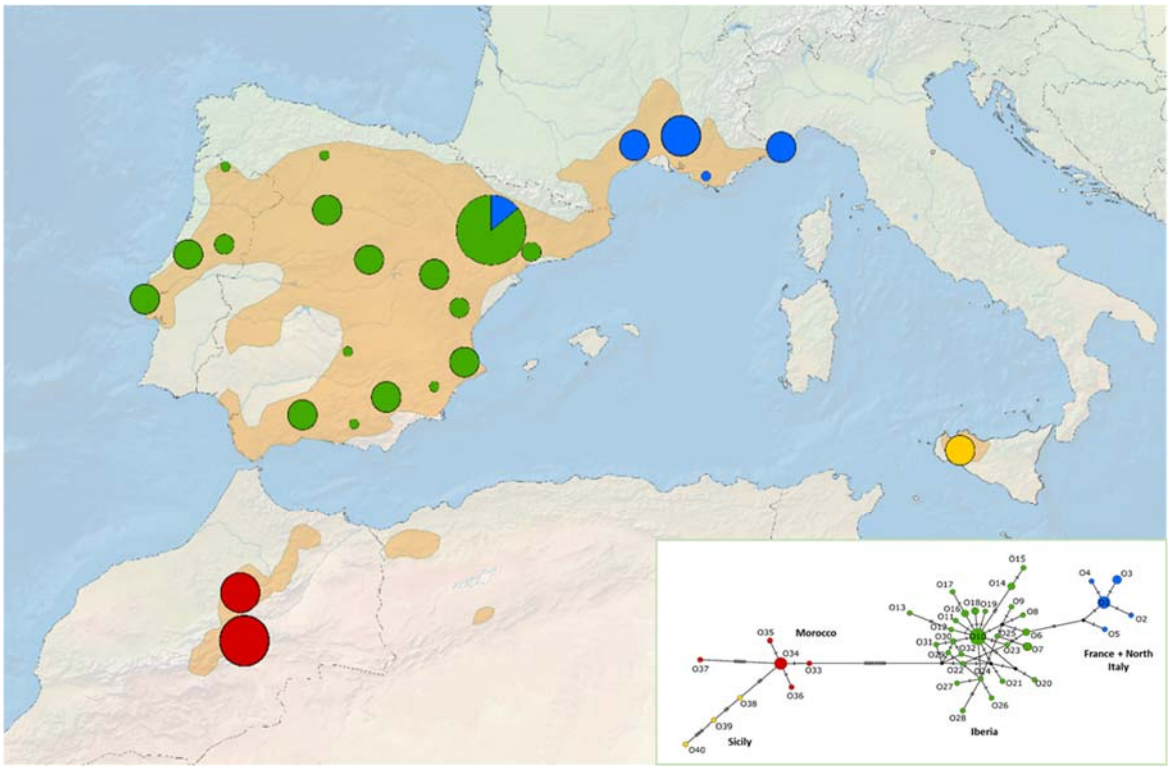

Figure 6.5 – Geographic segregation of *M. occitanica* COI haplotypes in the western Mediterranean region. Haplotype colours are identical to Figure 6.4. and represent the four different clusters of this Figure.

6.3. Divergence time estimates

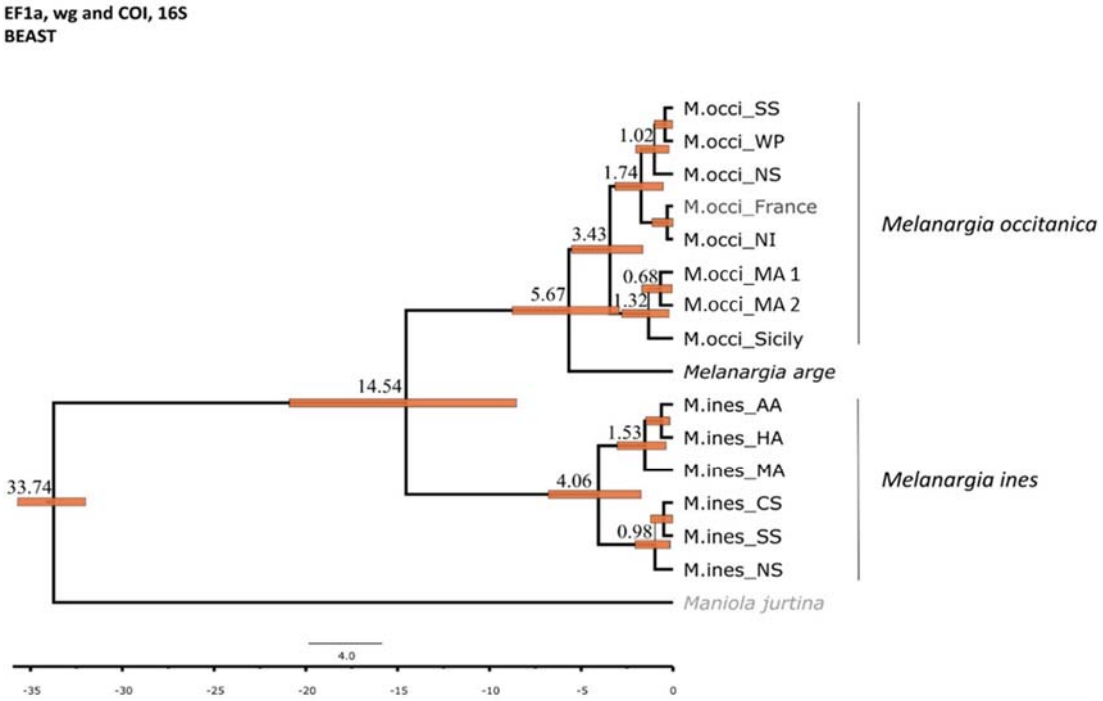

Figure 6.6 – BEAST mean divergence time estimates for the *Melanargia* combined gene dataset (Datasets 1 + 2 + 3 + 4). SS = South of Spain; CS = Central Spain; NS =North of Spain; WP = Western Portugal; NI = North Italy; MA1 = Middle Atlas 1; MA2 = Middle Atlas 2; MA = Middle Atlas; AA = Anti Atlas; HA = High Atlas;

The divergence between the ancestral lineage of *M. ines* and the ancestral lineage of *M. occitanica* + *M. arge* is predicted to have taken place around 14.5 mya (95% HPD: 8.5 – 20.9 mya) (Figure 6.6). On the other hand, the ancestral lineages of *M. arge* and *M. occitanica* display an estimated mean divergence time of 5.67 mya (95% HPD: 2.9 – 8.8 mya).

The subsequent inner split of *M. occitanica* into the current European and African clades appears to have occurred short after, around 3.4 mya (95% HPD: 1.6 – 5.5 mya), while the European and African clades of *M. ines* have a similar divergence time estimate, of around 4 mya (95% HPD: 1.7 – 6.8 mya). Additionally, the age of divergence between *M. occitanica* populations separated by the barriers of the Pyrenees (around 1.74 mya, 95% HPD: 0.5 – 3.2 mya) and Sicilian Strait (1.33 mya, 95% HPD: 0.2 – 2.8 mya) or the *M. ines* clusters separated by the High Atlas Mountains (1.5 mya, 95% HPD: 0.38 – 3 mya) seem to fall more or less within the same geological time interval.

6.4. Populations genetic differentiation

Within *M. ines* populations, the highest values of haplotype diversity are found in Central and South Iberia, as well as in Northern Middle Atlas, while the highest nucleotide diversity values belong to Northern Middle Atlas, Southern Middle Atlas, and Southern High Atlas border populations (Table S6.2). *Melanargia occitanica* has several populations with high values of both haplotype and nucleotide diversity such as Sicily, Central Iberia and South Iberia (Table S6.2).

Table 6.1 – Analysis of Molecular Variance (AMOVA) within *Melanargia ines* and *Melanargia occitanica* populations with different geographical group combinations using Datasets 5 and 6.

	AMOVA 1 (*M. ines*)	**Degrees of freedom**	**Sum of squares**	**Variance components**	**Percentage of variation**
Iberia • North Iberia • Central Iberia • South Iberia **Above High Atlas** • Rif Mountain Range • Oriental Region • Northern Middle Atlas • Southern Middle Atlas **Below High Atlas** • Southern High Atlas border • Anti Atlas	Among groups	2	526.461	11.25147 Va	91.09
	Among populations within groups	6	18.118	0.27764 Vb	2.25
	Within populations	68	55.927	0.82246 Vc	6.66
	Total	76	600.506	12.35158	100
	AMOVA 2 (*M. ines*)	**Degrees of freedom**	**Sum of squares**	**Variance components**	**Percentage of variation**
Iberia • North Iberia • Central Iberia • South Iberia **Morocco** • Rif Mountain Range	Among groups	1	505.890	12.93368 Va	89.99
	Among populations within groups	7	38.689	0.61589 Vb	4.29

• Oriental Region • Northern Middle Atlas • Southern Middle Atlas • Southern High Atlas border • Anti Atlas	Within populations	68	55.927	0.82246 Vc	5.72
	Total	76	600.506	14.37203	100
Above Pirenees • North Italy • France **Iberia** • North Iberia • Central Iberia • South Iberia **Middle Atlas** **Sicily**	**AMOVA 1 (*M. occitanica*)**	**Degrees of freedom**	**Sum of squares**	**Variance components**	**Percentage of variation**
	Among groups	3	198.526	5.56155 Va	79.60
	Among populations within groups	3	5.520	0.04222 Vb	0.60
	Within populations	59	81.606	1.38315 Vc	19.80
	Total	65	285.652	6.98692	100
Above + Below Pirenees • North Italy • France • North Iberia • Central Iberia • South Iberia **Middle Atlas** **Sicily**	**AMOVA 2 (*M. occitanica*)**	**Degrees of freedom**	**Sum of squares**	**Variance components**	**Percentage of variation**
	Among groups	2	162.726	7.26072 Va	76.26
	Among populations within groups	4	41.320	0.87762 Vb	9.22
	Within populations	59	81.606	1.38315 Vc	14.53
	Total	65	285.652	9.52149	100
	AMOVA 3 (*M. occitanica*)	**Degrees of freedom**	**Sum of squares**	**Variance components**	**Percentage of variation**

Above + Below Pirenees • North Italy • France • North Iberia • Central Iberia • South Iberia **Middle Atlas + Sicily**	Among groups	1	151.281	7.19328 Va	75.02
	Among populations within groups	5	52.764	1.01261 Vb	10.56
	Within populations	59	81.606	1.38315 Vc	14.42
	Total	65	285.652	9.58904	100

The different AMOVA carried for each species differed only in the hierarchical groups defined (Table 6.1). For *Melanargia ines*, the two AMOVA display similar results with a high percentage of variation among groups (91.09% - AMOVA 1, and 89.99% - AMOVA 2). For *M. occitanica*, all three AMOVA show also similar results although with some differences between the first AMOVA and the others regarding variation among groups (79.60% - AMOVA 1, 76.26% - AMOVA 2 and 75.02% - AMOVA 3), variation among populations within groups (0.60%, 9.22% and 10.56%), and within populations (19.80%, 14.53% and 14.42%).

Table 6.2 – Pairwise F_{st} between *Melanargia ines* populations using Dataset 5. Values above 0.5 are highlighted.

M. ines	North Iberia	Central Iberia	South Iberia	Rif Mountain range	Oriental Moroccan region	Northern Middle Atlas	Southern Middle Atlas	Southern High Atlas border	Anti Atlas
North Iberia	-								
Central Iberia	0.15396	-							
South Iberia	0.16524	0.08369	-						
Rif Mountain range	**0.98244**	**0.95999**	**0.94991**	-					
Oriental Moroccan region	**0.97869**	**0.96066**	**0.95132**	-0.01083	-				

Northern Middle Atlas	**0.90276**	**0.93432**	**0.92684**	0.19004	0.23945	-			
Southern Middle Atlas	**0.92928**	**0.94183**	**0.93465**	0.47077	0.49895	0.32351	-		
Southern High Atlas border	**0.91917**	**0.94124**	**0.93367**	**0.65309**	**0.68082**	0.46610	0.25601	-	
Anti Atlas	**0.98394**	**0.96340**	**0.95425**	**0.92000**	**0.90135**	**0.62838**	0.38455	0.04000	-

Table 6.3 – Pairwise F_{st} between *Melanargia occitanica* populations using Dataset 6. Values above 0.5 are highlighted.

M. occitanica	North Italy	France	North Iberia	Central Iberia	South Iberia	Middle Atlas	Sicily
North Italy	-						
France	-0.06282	-					
North Iberia	**0.66308**	**0.66818**	-				
Central Iberia	**0.60304**	**0.62816**	0.01055	-			
South Iberia	0.46450	**0.52562**	0.07249	0.05680	-		
Middle Atlas	**0.90157**	**0.89541**	**0.87626**	**0.85099**	**0.81302**	-	
Sicily	**0.87500**	**0.89369**	**0.88370**	**0.86014**	**0.80708**	**0.59773**	-

The pairwise F_{st} conducted for *M. ines* shows a pattern of small differentiation levels between land connected and geographically close populations (e.g. within Iberia, Northern Morocco, or Southern Moroccan populations) and a progressive increase of differentiation levels towards more distant populations. The Southern Middle Atlas population, however, shows a closer proximity to the population of Southern High Atlas border than to the Northern Middle Atlas one. The highest differentiation values are found between all Moroccan populations and the Iberian ones ($F_{st} > 0.9$). Conversely, the lowest pairwise F_{st} values are found between Rif Mountain range and Oriental Moroccan region, between Anti Atlas and Southern High Atlas, and between South Iberia and Central Iberia.

M. occitanica displays the same correlation pattern between geographic proximity and F_{st} values with low scores between France and North Italy, or within the Iberian populations, and a progressive increase with distance. Interestingly, the populations of France and North Italy display lower pairwise F_{st} values with South Iberia than with North and Central Iberia. The highest values stand between the clades of Morocco + Sicily and Europe.

6.5. Species distribution modeling

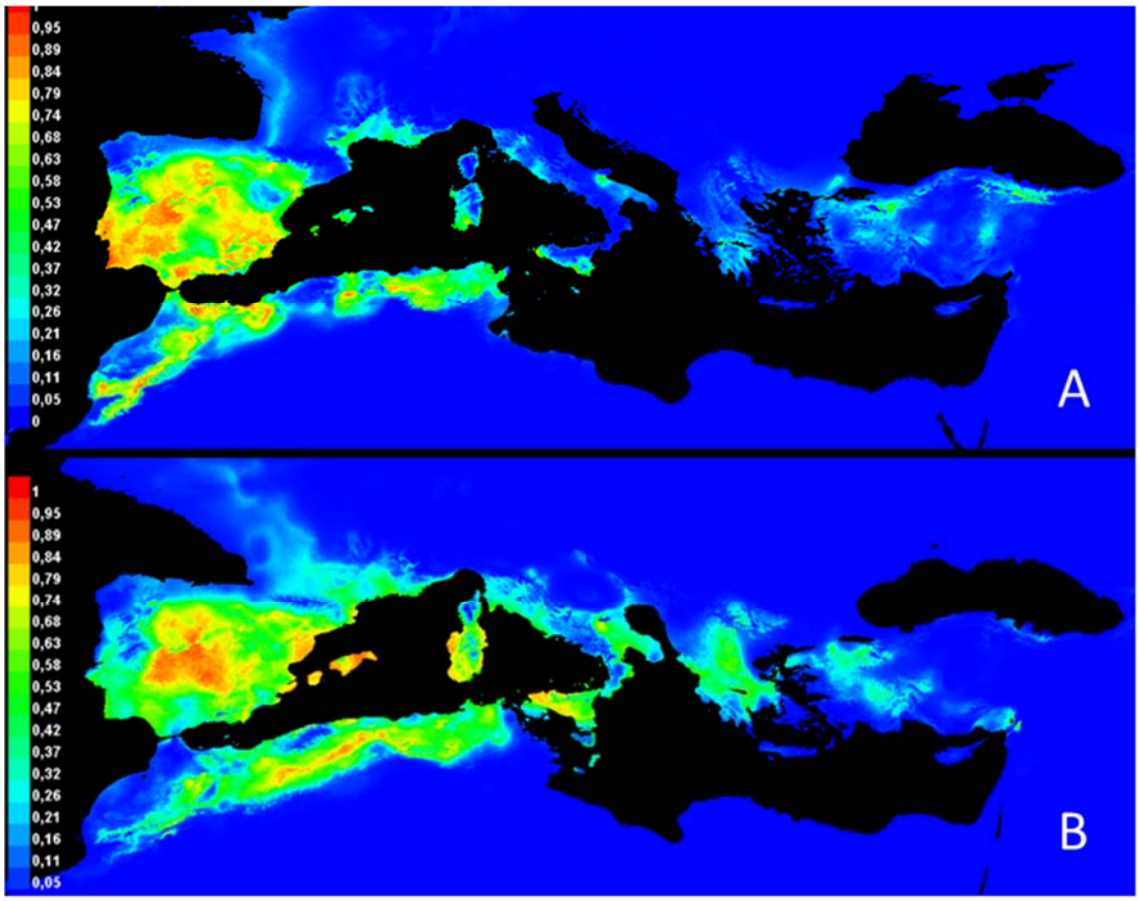

Figure 6.7 – SDM maps for *M. ines* Present (A) and LGM (B) distributions.

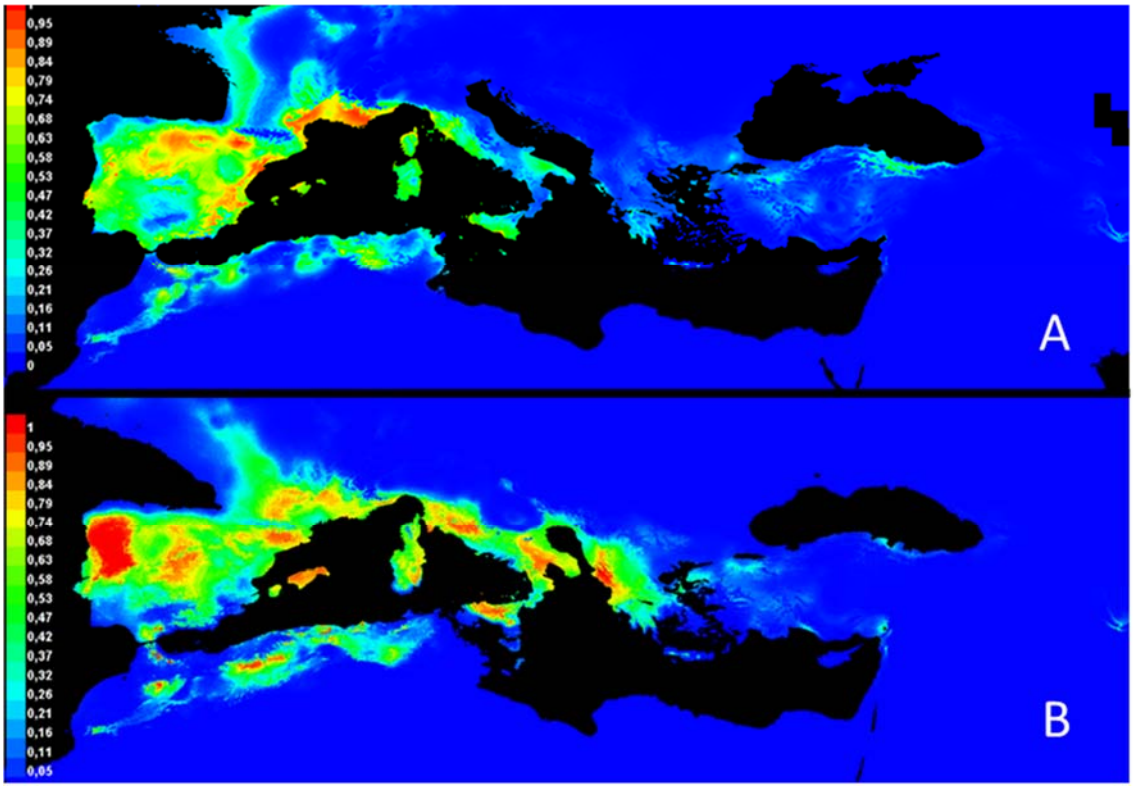

Figure 6.8 – SDM maps for *M. occitanica* Present (A) and LGM (B) distributions.

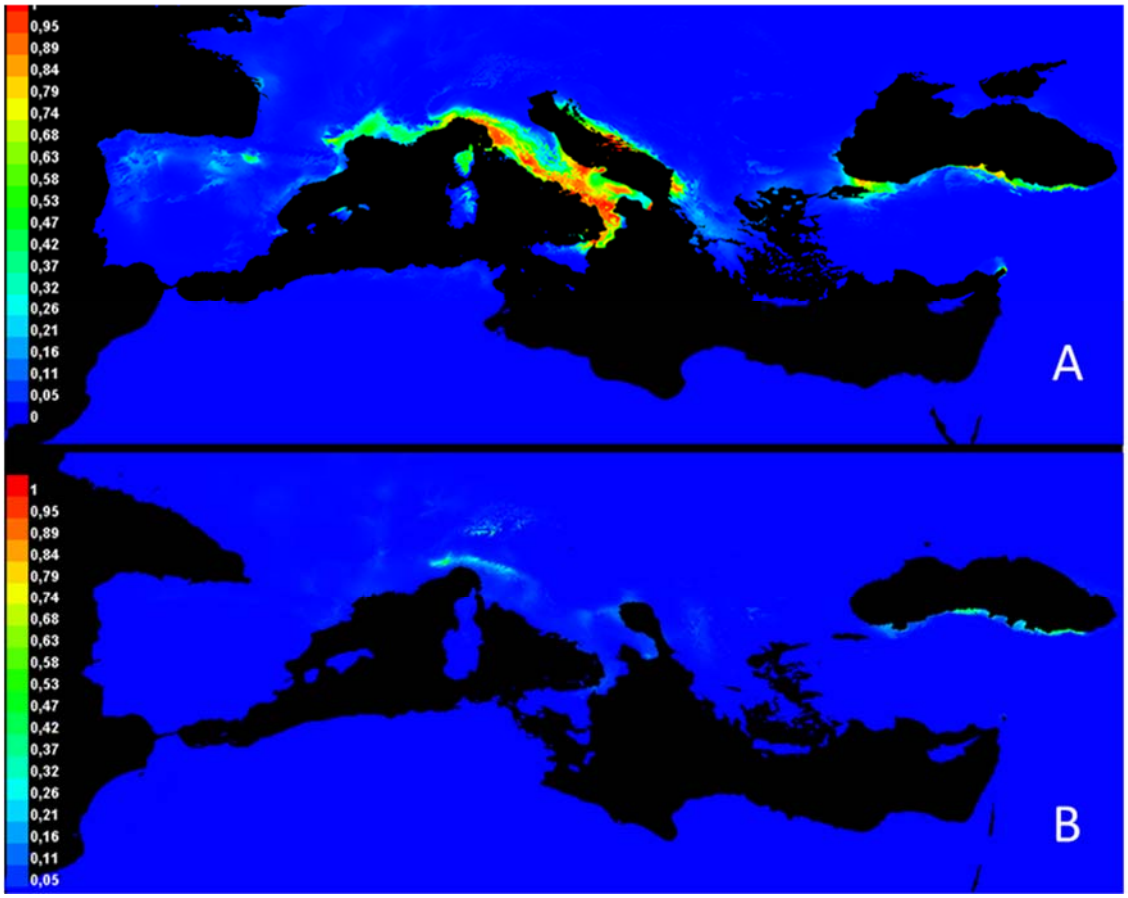

Figure 6.9 – SDM maps for *M. arge* Present (A) and LGM (B) distributions.

M. ines

The SDM analysis yielded an AUC of 0,936 and a standard deviation of 0,003. According to the models, the bioclimatic variables that best explain *M. ines* current distribution are, in order of importance: precipitation of warmest quarter (BIO18), mean temperature of the driest quarter (BIO9) and annual mean temperature (BIO1) (Figures S6.15 and S6.16). On the other hand, the variable which causes the most loss to the model when omitted is temperature seasonality (BIO4).

The Present distribution map for this species seem to be accurate with its current range except for Libya, not predicted by the model (Figure 6.7A). The occurrence of *M. ines* was also moderately predicted (green colour in the occurrence probability scale) for regions where it does not currently occur such as southern France (Mediterranean coast and Atlantic coast), Balearic Islands, the south of Sardinia and Sicily, some areas in North and centre Italy, southeast Europe, and Turkey near the Black Sea.

The LGM map displays a more unified higher probability range around the entire Western Mediterranean region and a slight deviation from the Atlantic coast. In Iberia, there are no major changes from the Present model except for a higher probability of occurrence in the eastern Mediterranean coast and in the centre of the Peninsula, cut in half by the Central Iberian Mountain System (CIMS) (Figure 6.7B). In North Africa, the range is more continuous and shifted to the East, not reaching the southwestern region of the Moroccan Anti Atlas where the species is currently present. The additional predicted areas are the same of Present model but with extended ranges such as the South of France, Balkan Peninsula, or even higher occurrence probabilities for the Balearic Islands, Sardinia + Corsica and Sicily.

M. occitanica

The *Melanargia occitanica* SDM analysis yielded an AUC of 0,934 and a standard deviation of 0,004. The bioclimatic variables that best explain the distribution of this species are, in order of importance: temperature seasonality (BIO4), mean temperatures of the driest (BIO9) and coldest (BIO11) quarters, and precipitation of warmest quarter (BIO18) (Figures S6.17 and S6.18). Additionally, the variable causing the most loss to the model when omitted is precipitation of driest month (BIO14).

M. occitanica Present model spans almost accurately the area in Iberia where this species occurs, as well as in Morocco except for the most southwestern predicted Atlas range (Figure 6.8A). The model also predicts the presence of this species in two other African regions: north western Algeria and north eastern Algeria + Tunisia, where there is uncertain evidence of its presence nowadays. As expected, the species presence is strongly predicted in South of France near the Mediterranean Sea, where it is widespread, but also in the Atlantic Ocean coast and centre of France, where it is not. Additionally, the model predicts *M. occitanica*'s presence in Sicily, where the differentiated population of *M. o. pherusa* occurs. *Melanargia occitanica* and *M. o. pherusa* are here modeled together, with input occurrence records mixing both entities, while independent model maps are shown in Supplementary Material Figures S6.19 and S6.20). *Melanargia occitanica* presence is further predicted in the Balearic Islands, Sardinia and Corsica, North and Central Italy, South East Europe and Turkey, near the Black Sea.

For LGM, the predicted distribution doesn't change considerably from the Present but is slightly expanded further North (Figure 6.8B). The strongest predicted area is in northern Portugal, central and northeast Spain and the Betic range. The CIMS cut once more through the predicted range of this species in central Iberia, just like the Pyrenees which stand as a thin climatic barrier, less contrasting during LGM. The South of France is kept as a region of relatively high probability of this species occurrence, but its range prediction expands inland during LGM. In North Africa, the predicted occurrence is still fragmented in Morocco but more continuous in Algeria when compared to the Present map. Sicily is also strongly predicted, alongside central and northern Italy. Many additional regions also predicted in the Present model are included in the LGM map but with increased areas and probabilities such as the Balearic Islands, Sardinia + Corsica and South East Europe.

M. arge

Finally, for *Melanargia arge* we obtained an AUC of 0,984 and a standard deviation of 0,002. In order of importance, the bioclimatic variables contributing more to the model are: precipitation of warmest quarter (BIO18), temperature seasonality (BIO4) and temperature annual range (BIO7) (Figures S6.21 and S6.22). The variable which causes more loss to the model when omitted is temperature seasonality (BIO4).

This species Present SDM predicts Italy as the most suitable region for its occurrence, with strong probabilities along the coast. This prediction matches its current distribution except for the area north of Tuscany where the species is not present (Figure 6.9A). As other potential suitable regions outside of its current range, the model highlights northeast Sicily, Corsica, southern France, Balkans (Mediterranean coast), and the Black Sea coast of northern Turkey. On the other hand, the LGM distribution of this species has been surprisingly reduced to an almost inexistent suitable area, with only a weak occurrence prediction close to the Alps and in the Black Sea coast of Northern Turkey (Figure 6.9B).

7. Discussion

7.1. Phylogenetic analysis and haplotype networks

The three species that make up the subgenus *Argeformia* are well segregated into three separated clades in our phylogenetic analyses (Figure 6.1), supporting their current taxonomic status. The placement of *Melanargia arge* as *M. occitanica* sister species in our topology strengthens the previous phylogeny of Nazari *et al*. (2010)[65] and the previous morphological studies and notes of other authors[68,70,147–149].

The new addition of the elongation factor 1-α gene to the phylogenetic analysis represents another step forward to understand these species evolutionary history, as well as the history of *Argeformia*. Unfortunately, we were not able to amplify the EF-1α gene from our single Sicilian *M. o. pherusa* specimen and with no other gene sequences available online from this subspecies apart from COI we were not able to deeply infer its phylogenetic relationships with both the Moroccan *M. occitanica pelagia* populations and *M. arge*. Even so, through the analysis of the mitochondrial COI gene, the population of Sicily appears to be derived from the African *M. o. pelagia* populations (Figures 6.1 and 6.4), as previously shown by Nazari *et al*. 2010[65].

The divergence between the ancestral populations of *M. ines* and *M. arge* + *M. occitanica* appears to have occurred early on, around 14.5 mya (HPB 95% 8.5 – 20.9 mya), while the separation between the ancestral populations of *M. arge* and *M. occitanica* seem to have taken place more recently, around 5.67 mya (HPB 95% 2.9 – 8.8 mya), roughly coincident with the MSC. By the time of *M. ines* divergence the continents of Europe and Africa might have been close to each other through the existence of several islands where later would be formed the Italian Peninsula[150]. However, by the time of *M. arge* divergence this Peninsula hadn't yet achieved its current geological form, although there was already a land mass making up most of what would later be part of Italy.

The major lineage splits within *M. occitanica* and *M. ines* are between continental Europe and African populations (Figures 10-12), and here the Gibraltar Strait appears to be the main barrier to gene flow, in agreement with Nazari *et al*. 2010 who found significative differences in genitalia structures between *M. ines* populations on both sides of this Strait[65]. In fact, this pattern is observed within population genetic studies of many organisms, which were able to colonize either side of this Strait during the MSC or some other time, remaining after isolated in both separate sides when the gene flow was interrupted or constrained[6,7,151–154]. The divergence times between African and European populations of *M. ines* (around 4 mya, HPB 95% 1.7 – 6.8 mya) and of *M. occitanica* (around 3.4 mya, HPB 95% 1.6 – 5.5 mya) do not fall with certainty within the predicted geological time interval of the MSC, although a colonization during the duration of this event cannot be excluded. Nonetheless, the Gibraltar Strait is nowadays 15 km long[11,122,155] and these species might have still been able to cross the sea Strait by flight, as it has been shown for other Nymphalidae species which appear to have a great capacity for long range dispersals throughout their evolutionary history[6,121,156].

Other barriers have also proven to be of great importance for *Melanargia* species' biogeography such as the Sicilian Strait, the Pyrenees and the Atlas Mountains. The Sicilian Strait seems to exert a reasonably strong influence over the differentiation observed between *M. occitanica pherusa* and Moroccan *M. occitanica pelagia* populations (Figure 6.4). Our divergence time estimates using BEAST suggest a colonization of Sicily and consequent divergence of both populations around 1.33 mya (HPB

95% 0.2 – 2.8 mya). Therefore, this may have happened during the Quaternary and likely during one of its glacial periods when the water level dropped and reduced the channel size to an estimated 50 km[157], with potential stepping stone islands facilitating the dispersal by flight. Moreover, the west-east winds felt in this region have been suggested to have possibly helped other butterfly species doing this exact traverse[158]. In fact, more butterfly species and other organisms have used this Sicilian connection route between Africa and Europe, in both directions[122,132,159,160], highlighting how important this pathway between both continents was for many species' biogeography, by allowing the interchange of taxa between continents through a different route than Iberia. However, it is impossible to say with our sampling if this sea barrier is currently preventing gene flow between Sicily and Africa, and thus promoting a true geographical segregation of both *M. o. pelagia* and *M. o. pherusa* haplotype clusters, since we were not able to sample the Algerian *M. o. pelagia* populations or any other population further East. Additionally, the high levels of differentiation found between the three Genbank *M. o. pherusa* COI sequences are intriguing and perhaps derived from a long presence of this population in Sicily, with demographic fluctuations and local isolation of subpopulations. Even so, a more extensive sampling of this subspecies must be carried out in the future, as well as the analysis of nuclear markers to infer its real genetic diversity and whether it truly deserves or not the subspecies level.

The land barriers of Pyrenees and Atlas Mountains, on the other hand, have an arguable effect on population divergence. These barriers appear to have had a reasonable influence on the genetic differentiation of *Melanargia* populations, yet not as strong as the ones imposed by the Sea. In fact, both Pyrenees and Atlas Mountains seem to have been fairly permeable for the passage and dispersal of individuals, making us question their isolating capacity (Figures 6.2 and 6.4). Even so, such dispersal events are likely rare, and these land barriers are still imponent and able to separate populations and promote differentiation. The Pyrenees barrier effect is visible through the separation of the well supported *M. occitanica* Iberian and French-Italian clades (Figure 6.1), estimated to have occurred around 1.74 mya (HPB 95% 0.5 – 3.2 mya), as well as the geographic structure of most haplotypes north of this barrier (Figure 6.4). This divergence falls too within the Quaternary period and within the demographic range contractions and expansions associated with the climatic cycles, which might have enabled the dispersal of individuals north of the Pyrenees, as possibly supported by the *M. occitanica* LGM map (Figure 6.8B).

The origin of the French-Italian O1 in Iberia can be discussed, but the hypothesis of a southern dispersal event by an individual(s) carrying this haplotype seems more likely than its long-term evolution in both sides of the Pyrenees, as shown to have also likely occurred in other organisms[161]. If so, this haplotype would now likely be found in a wider range of Iberia, and we would see slight variations of it from other Iberian regions in the French-Italian haplotype cluster (Figure 6.4). Still, this option cannot be totally excluded as the sampling of *M. o. occitanica* in Northern Iberia was limited and O1 is also not genetically very distant from the Iberian haplotypes (only two mutations away from the closest Iberian one – Figure 6.4). Furthermore, the pattern of an Iberian range expansion beyond the Pyrenees, shown by *M. occitanica*, has also been found in other western Mediterranean species adapted to the slightly warmer conditions of this biogeographical region, although not expanding much further due to the more temperate environmental conditions felt in northern latitudes[9].

Another interesting result is the proximity between *M. i. ines* south Iberian haplotypes and *M. i. fathme* Middle Atlas haplotypes since the climate and habitat are similar between these regions. Within the extensive Atlas Mountains, the most effective barrier appears to be the High Atlas, which promoted some differentiation between the two *M. ines* Moroccan clusters (Figure 6.2) as well as a supported clade assemblage of High and Anti Atlas populations in our ML phylogeny (Figure 6.1). It must be

noted that the specimens caught in the northern border of the High Atlas carrying the two Anti Atlas/southern High Atlas haplotypes I24 and I25 (EM6552, EM6553, EM6559, VNMB143-08, VNMB239-08 and VNMB238-08; Table S6.1) were still within the geographic range of what we could technically call High Atlas. As such, if we were to include these specimens in the High Atlas + Anti Atlas gene pool we wouldn´t have the barrier permeability issue mentioned above, except for the specimen EM1418 (Table S6.1) which also carried the I24 haplotype and was caught further north in plain Middle Atlas region. However, to test the importance of High Atlas as an effective barrier, all individuals caught north of the highest altitude mountain range were considered as part of Middle Atlas, such as the individuals mentioned above.

Moreover, although we didn't find any individuals below the High Atlas carrying a Middle Atlas haplotype, it doesn't mean that individuals can't cross the High Atlas during southern dispersals. In fact, the first colonization of this southern area by *M. ines* might have likely been carried by individuals coming from the North, probably during the demographic population expansion and contraction events enhanced by the climatic cycles of the Quaternary, as supported by a BEAST divergence time of 1.53 mya between both Moroccan clusters (HPB 95% 0.38 mya – 3 mya). The leading-edge population, able to find a passage through the mountains into southern Morocco, must have then persisted isolated in this region and diversified genetically throughout the High and Anti Atlas into the variety of haplotypes seen today and to the taxonomic status of perhaps different subspecies. The divergence time estimates between *M. ines* Anti and High Atlas populations, as well as within *M. occitanica* Middle Atlas populations show similar values (0.63 mya (HPB 95% 0.17 – 1.48 mya) and 0.68 mya (HPB 95% 0.05 – 1.7 mya), respectively), representing clusters that are not constrained by geographical barriers and are capable of mixing with each other despite showing genetic differences.

Both species networks display one highly differentiated Moroccan haplotype that stands out from the genetic pool, I26 for *M. ines* and O37 for *M. occitanica*. These might be part of isolated High Atlas populations, which can only be confirmed or interpreted with further sampling. Additionally, the lack of genetic differentiation as well as the star-like pattern observed for the Iberian haplotype networks of both *Melanargia* species suggest that these Iberian clusters might have grown and expanded from a reduced genetic diversity state, possibly resulting from a founder effect event or a genetic bottleneck. The smaller geographical barriers in the Iberian Peninsula might not be strong enough to prevent the dispersal of individuals, allowing for the consequent lack of geographical structuring of the Iberian haplotypes and maintain these clusters star-like structure through time.

7.2. Populations genetic differentiation

The higher haplotype diversity seen for the Iberian populations of both *M. ines* and *M. occitanica* (Table S6.2) is caused by the also higher diversity represented in both species' Iberian haplotype clusters. Regarding the AMOVA, the high percentage of variation among groups obtained for *M. ines* show that major groups were well established, splitting the most genetically distinct populations (Table 6.1). Also, the fact that there are little differences between both *M. ines* AMOVAs suggest that the bulk of differentiation observed among groups is being caused by the Gibraltar Strait and not by the High Atlas Mountains, which show an insignificant influence when the two AMOVAs are compared. The genetic diversity differences between the two *M. ines* Moroccan clusters is causing the slight increase observed in percentage of variation among populations within groups from first to second AMOVA.

The AMOVAs conducted for *M. occitanica* display a much higher variation within populations than *M. ines* AMOVA (Table 6.1) and this is likely being caused by the high differentiation levels observed within the population of Sicily, where all three individuals analysed have unique and genetically differentiated haplotypes. The observed differences of variation among groups between the three AMOVAs confirm that the Gibraltar Strait is the major barrier influencing the differentiation levels among groups, although the Pyrenees also display a strong influence on populations differentiation, as already seen in *M. occitanica* haplotype network. Indeed, the pronounced increase in percentage of variation among populations within groups from first to second AMOVA was caused by the agglutination of both above and below Pyrenees populations under the same major group. This percentage of variation also increased slightly from second to third AMOVA with the merging of Sicilian and Moroccan groups. However, the major land barriers here studied (Atlas Mountains and Pyrenees) have a reduced impact on populations differentiation when compared to the sea barrier of the Gibraltar Strait, which is the great promotor of long-term populations isolation and thus camouflages the influence exerted by all other barriers.

The pairwise F_{st} obtained for *M. ines* and *M. occitanica* show that geographically proximal and connected populations display lower pairwise F_{st} values, as expected (Tables 6.2 and 6.3). Within *Melanargia ines*, the low pairwise F_{st} value between Southern Middle Atlas and Southern High Atlas Border populations suggest connectivity among them, as confirmed in Figure 6.2. However, pairwise F_{st} gives us only another perspective of the same genetic data and although confirms the sharing of haplotypes observed between both sides of this mountain range, it does not disprove the major geographical structure observed for the two Moroccan genetic lineages seen in Figure 6.2. As for *M. occitanica*, the lower F_{st} value between populations north of Pyrenees and South Iberia (instead of North Iberia for example) was also expected as shown by Figure 6.4, in which the closest Iberian haplotype to the French-Italian populations is from the southern Iberian region of Alicante (Table S6.1). This suggest that an ancestral population carrying this haplotype might have been more expanded in Iberia in the past, and been able to cross the Pyrenees, establishing a new population in Southern France.

Alternatively, it could have been the French-Italian haplotype cluster colonizing Iberia and originating the diversity seen today within the Peninsula. However, this seems unlikely as the haplotype O6 is not the central haplotype of the Iberian network and the French-Italian cluster display a low diversity and a limited distribution range. Nonetheless, this hypothesis should not be completely ruled out as the haplotype O6 could have given origin to the central O10, which could have later experienced a great expansion in the Peninsula, and the French-Italian population could have had its genetic diversity eroded during the Quaternary climatic oscillations.

7.3. Species Distribution Modeling

M. ines

The most influent bioclimatic variables in *M. ines* distribution model suggest that this species is mostly positively dependent on the increasing temperatures of the driest quarter alongside a residual precipitation during the warmest one, as well as on low temperature seasonality during the year. This might indicate an adaptation to the warmer and drier Mediterranean conditions, experiencing also less rigorous winters than northern latitudes, which could be expected from a strictly Mediterranean species (Figure S6.16). Nonetheless we must not ignore the effect that these bioclimatic variables might have

on other ecological key pieces of these butterflies' lifecycle, such as their hostplants, not modulated in this work.

The SDM accuracy with this species' current distribution suggest that the model training and the inference of bioclimatic variables were appropriate. For *M. ines* the model only misses the prediction of the species' presence in Libya, from where it is currently known. This might be related with the lack of precise occurrence records for the Eastern part of its North African range in our input data (Figure 6.7A). It could also mean that despite occurring in Libya, the bioclimatic conditions of this region might be suboptimal for this species, which could possibly be persisting but not thriving in this region. Conversely, the model predicted some European areas outside of *M. ines* current distribution and near the Mediterranean Sea, suggesting that these areas might be climatically suitable, but the species is absent by some other reason (Figure 6.7A). Even so, if *M. ines* could disperse through existing geographical barriers such as the Pyrenees and the Sicilian Strait, there is no guarantee that it would persist at long term in those predicted areas since species distribution is ruled by more than just climate.

According to the LGM SDM maps, neither *M. ines* nor *M. occitanica* appear to have been severely constrained during the last glacial. Having their current distribution along the Western Mediterranean area and being this region a refuge zone itself for many European species could help explain this LGM pattern. Moreover, although some regions not occupied by *M. ines* may have been more accessible for dispersal during LGM (e.g. Balearic Islands closer to Iberia and Sicily closer to North Africa), it is unknown if this species has ever reached such regions (Figure 6.7B). Still, in case of dispersal those populations must have surely gone extinct. Furthermore, although unlikely, we cannot also exclude a scenario of competition between closely related species of this genus, which could lead to populations or even species loss from certain regions. In fact, large Mediterranean islands are in general continually occupied, with rare extinction events, which makes the invasion and colonization of such islands difficult for species with closed related taxa already occupying the island[158]. Even so, and except for the possible competition between *M. lachesis* and *M. galathea* in Iberia[121,122], scenarios of competition between *Melanargia* species are not currently evident in the Western Mediterranean region as *M. o. pherusa*, *M. galathea* and *M. russiae* coexist in Sicily; *M. occitanica*, *M. galathea*, *M. russiae* and *M. lachesis* coexist in South of France; *M. lucasi*, *M. ines* and *M. occitanica* coexist in the Maghreb, and *M. ines* and *M. occitanica*, *M. russiae* and *M. lachesis* coexist in Iberia. Nonetheless, despite coexisting, some of these taxa might still compete at a certain level and further ecological studies must be carried in the future to clarify such relationships between taxa.

The suitable occurrence area on central Iberia in the LGM map agrees with the star like pattern observed in the COI haplotype network (Figure 6.2) by identifying a single refugium for this species in this peninsula (Figure 6.7B). On the other hand, the haplotype cluster differentiation in North Africa suggests the possible existence of more refugia, although the LGM model predicts a more or less continuous range in this region. In fact, the differentiation observed between southern populations (High and Anti Atlas) and northern ones (Middle Atlas and Rif, which possibly extend to Algeria and Tunisia) must be older than the last glacial, possibly originated in the previous cycles given its pronounced genetic distance and structure (Figure 6.2). The region south of the High Atlas could have been a refugia for the population carrying the haplotypes of this cluster, while the northern lineage might have shifted its distribution to the East, where climatic conditions were more suitable. More recently, the southern clade may have dispersed north through the High Atlas and individuals carrying the I26 haplotype reached their current position in Middle Atlas. Here, they had a secondary contact with the northern lineage which must have expanded from the East and recolonized the western region of the Maghreb during the interglacial. Some COI sequences of Algerian and Tunisian specimens available online but

not published (and not included in our final analysis) seem to cluster with the Middle Atlas clade, thus supporting both this biogeographical hypothesis and the SDM results of an eastern unified LGM predicted range for the Maghreb. Cases of genetic differentiation between eastern and western north African populations have been reported for other butterfly species and other organisms, including *Melanargia lucasi*, restricted to the Maghreb and belonging in the *M. galathea* species group[9,11,122].

Overall, our map is not much different from the map obtained by Habel *et al*. 2011, although with some differences on the strength of the prediction in Iberia and the extension of the predicted range in eastern Maghreb[71].

M. occitanica

M. occitanica's most important bioclimatic variables used by the model suggest that this species is positively dependent on temperature seasonality until a certain degree, above which the species does not occur, but also on a little amount of precipitation in the warmest quarter, and a small range of favourable mean temperatures of the driest and coldest quarters. The latter may possibly be important for larvae survival during the winter estivation period. Overall, the bioclimatic factors shaping its distribution are similar to those of *M. ines* but seems less tolerant to high summer temperatures.

The SDM map for the Present matched the current patterns of *M. occitanica* distribution, not only for the European range but also the fragmented populations in North Africa (Figure 6.8A). The higher probability of occurrence in South of France is correlated with the many distribution records of this species available for this region, making it a very well sampled area with more presence points within the same range. This area's predicted range is also partially detached from the one in Iberia by the evident block imposed by the Pyrenees (Figure 6.8A). Despite the apparent suitable conditions in the Balearic Islands, Sardinia and Corsica, as well as the inexistence of other *Melanargia* competitors, this species has likely never colonized these islands, or otherwise it has gone extinct. In mainland Italy, *M. occitanica* is restricted to coastal Liguria and does not extend further East. In fact, the model displays a climatic gap between Liguria and the suitable areas in central and southern Italy for the Present map, which is likely being caused by the barrier effect of the Apennines (Figure 6.8A). These mountains display not only different climatic conditions but also different habitats, which may or may not include the butterfly species hostplants. Moreover, the Present model range as well as the LGM model prediction of a strong Western Mediterranean occupation, show that if this species had ever dispersed to the rest of Italy over these mountains during the LGM, it would have had a suitable climate to persist until today (Figures 6.8A and B). The same discussion could be applied to the South East region of Europe, also predicted in this model. Nonetheless, a scenario of competition with *M. arge* in Italy shouldn't be discarded, as cases of competition between species with similar ranges have been described[161].

Finally, the extended LGM range prediction in eastern Maghreb (Figure 6.8B) and the proximity between Sicily and Tunisia during this period support the hypothesis of a Sicily colonization by *M. occitanica* through the Sicilian Strait, already highlighted by the genetic data (Figure 6.4). A posterior interruption of gene flow and isolation in a novel ecosystem allowed the differentiation of the Sicilian population into *M. o. pherusa*. In fact, an alternative SDM map excluding all the *M. o. pherusa* records from the software input data kept Sicily as a suitable area for *M. occitanica* (even more evident in LGM), showing that this island was not only geographically closer but has been climatically suitable during both glacial and interglacial periods (Figure S6.19). Also, the fragmented LGM North African ranges could have intensified the genetic distance between a potential LGM western O37 haplotype population

and a potential LGM eastern O34 haplotype cluster, currently widely represented within Moroccan individuals (Figure 6.4). The second would have then colonized Sicily during a glacial eastern expansion, a scenario supported by the genetic proximity between Sicilian haplotypes and the O34 cluster.

M. arge

The most influent variables considered by *M. arge* model suggest that this species occurrence is very sensitive to the level of temperature seasonality, as well as positively dependent on some level of precipitation on the warmest quarter (Figure S6.22). These results might be correlated with the smaller and restrained distribution of this species in Italy, or alternatively, this species may simply have a narrow ecological niche.

The SDM map for the Present predicted some climatically favourable areas for this species in Northern Italy, below the Alps, which indeed seem to have a favourable habitat (personal observations) but where the species does not currently occur (Figure 6.9A). This could be due to the randomness associated with persistence and dispersal of populations or something else could be preventing the occupation of this northern region or been preventing it until recently. The predicted range also extends to the South of France, in a similar way but an inverted direction to the case of *M. occitanica*. The model map does not predict the species presence in Sicily and, conversely, the SDM map for *M. o. pherusa* (Figure S6.20) does not predict the presence of this population in mainland Italy. Therefore, the allopatric distribution of *M. arge* and *M. o. pherusa* could be caused by niche incompatibly rather than competition between both taxa. Indeed, niche specificity varies between species and has a great influence over current taxa distributions. The closely related *Melanargia galathea* occupies both mainland Italy and Sicily and the two populations seem to interbreed in the southern Italian region of Calabria[121].

The reason for the surprising lack of predicted range on the LGM map is not clear (Figure 6.9B). While it is highly unlikely to be reflecting the correct past distribution of this species, it also does not appear to be caused by a software caveat or an incorrect data model training as the model predicted correctly the species distribution for the Present. Moreover, it certainly does not mean that we cannot trust the modelling results obtained so far for the other species. Nonetheless, this model result for *M. arge* still needs to be confirmed.

7.4. Evolutionary history scenario for *Argeformia*

The different analyses conducted on this case-study allowed us to hypothesize alternative evolutionary history scenarios for the subgenus *Argeformia*.

Hypothesis nr.1

1. Initially, the common ancestor of all *Argeformia* species could have been present around southern Europe, sometime during the Miocene and likely within or before 8.5 – 20.9 mya, reaching the landmass present where later the Italian Peninsula would be formed, which also appeared to be closer to North Africa[150]. Nonetheless, it is uncertain if this population might have reached the western Mediterranean area through a northern or southern Mediterranean route coming from western Asia, where the bulk of diversity for this genus currently is (see Hypothesis nr 2).
2. Later, the stepping stone islands connecting Europe to North Africa in this area might have allowed this population to cross and expand to the Maghreb, somewhere around 14.5 mya (95% HPD: 8.5 – 20.9 mya).
3. The allopatric European and Maghrebian populations, could have accumulated genetic and ecological differences through time, becoming individually distinct and enhancing the primary divergence between the biological entity *M. ines* in North Africa and the common ancestor of *M. arge* + *M. occitanica* in Europe.
4. The ancestral population of *M. ines* would have then adapted and expanded within the Maghreb. Either by chance, constraints associated with dispersal or expansion into a territory already occupied by *M. ines*, or due to the progressive separation of Europe and North Africa in that same region, the ancestral population of *M. arge* + *M. occitanica* would only cross the same path into North Africa much later. This would have likely occurred during the MSC or temporally near that event (around 5.67 mya, 95% hpd: 2.9 – 8.7 mya), being this dispersal possibly facilitated by the water level reduction or by a land corridor forming from Italy to North Africa during this event. Moreover, since the primary divergence between *M. ines* and *M. occitanica* + *M. arge* both lineages would have then developed some reproductive barriers, avoiding a later gene flow and admixture of both taxa again into a single entity.
5. The corridor(s) between Europe and North Africa must have later become definitively disrupted, likely due to the refill of the Mediterranean at the end of the MSC, isolating the ancestor of both *M. arge* and *M. occitanica* in different sides of what would later be the Sicilian Strait. These two allopatric populations would have afterwards given rise to *M. arge*, in the landmass that would become Italy, and *M. occitanica* in North Africa.
6. Later, while *M. arge* would have likely been geographically restrained to mainland Italy by sea to the East, South and West, and by the Apennines and the Alps in the North, *M. occitanica* would have dispersed through the Maghreb wherever the conditions were favourable, and probably sharing part of its range with *M. ines*. However, perhaps due to its adaptation to colder European conditions, this species might not have been as expanded in North Africa as *M. ines*.
7. Whether or not *M. ines* reached northern Morocco before *M. occitanica*, the divergence time estimates between Moroccan and Iberian populations of both species are similar, and the colonization of Iberia might have happened for both within the same time period, possibly responding to the same stimulus. According to BEAST estimates, the Iberian colonization would have likely occurred after the end of the MSC, possibly overcoming the long sea distance by flight. However, the HPD time interval still covers the MSC time range, and the hypothesis of a dispersal facilitated by land connection must not be excluded. Through time, both species must have been able to expand their range within Iberia. The consequent isolation of Iberian and

Moroccan populations in allopatry would later give rise to the status of different subspecies recognized today for these taxa in separate continents.

8. More recently, the North African population of *M. occitanica* would have been able to disperse to the East and reach Sicily, likely during one of the glacial periods as suggested by the LGM SDM map, and when the coasts of Tunisia and Sicily were much closer, establishing there a new isolated population around 1.33 mya (95% HPD: 0.2 – 2.8 mya). Additionally, in a similar period of time but perhaps during an interglacial, the Iberian *M. occitanica* population might have been able to cross the Pyrenees and colonize the southern region of France around 1.74 mya (95% HPD: 0.53 – 3.16 mya), expanding later its range up to Liguria, in Italy.
9. Due to the favourable conditions found in Sicily the local *M. occitanica* population could persist there until today, differentiating genetically and phenotypically from the North African *M. o. pelagia* population, and thus being recognized as the subspecies *M. o. pherusa*.

Hypothesis nr.2

1. Initially, the common ancestor of all *Argeformia* species could have reached the western Mediterranean area through a southern Mediterranean route connecting western Asia with the Maghreb sometime during the Miocene, likely within or before 8.5 – 20.9 mya.
2. Later, the stepping stone islands approaching Europe to North Africa in the western/middle Mediterranean area might have allowed this population to cross into the European landmass located where later Italy would be formed, somewhere around 14.5 mya (95% HPD: 8.5 – 20.9 mya).

Same as hypothesis nr. 1 (3-9)

8. Final remarks and future perspectives

Phylogeography is a powerful tool to unveil the evolutionary history of species, enabling us to understand the processes occurring between and within populations as well as the process of speciation itself[162]. Butterflies have proven to be good model organisms for phylogeographical studies due to their dispersal capacity and susceptibility to climatic and geographical constraints, as well as biotic interactions[6,33,38,122,163]. As such, this work focused on two different butterfly genera and some of its western Mediterranean species, in order to understand their relationships, differentiation processes and evolutionary history. The different analyses conducted in each case-study allowed us to unveil most of our initial goals. Although there are different drivers of butterfly differentiation in the Western Mediterranean region, each playing a different role and in different timings or combinations for each species, the combined study of *Lycaena* and *Melanargia* enabled both a broader look and wide perspective into such processes, as well as a detailed look into their own cases of differentiation and lineage evolution. While the Sooty Coppers study allowed for a closer look into the relationship between two sister taxa at the threshold of what we may consider a different species, studying the subgenus *Argeformia* (*Melanargia*) allowed for an extended look across land and sea barriers, expanding from the cradle of Iberia and into the whole western Mediterranean biogeographic region. As such, both groups seem to complement each other when aiming to study and understand the differentiation process of the western Mediterranean butterflies.

Within *Lycaena*, we tried to tackle the question: Are *L. tityrus* and *L. bleusei* different species? However, in order to answer it, we must first consider other questions such as "What are different species, and what is the threshold to consider one entity different from another?". Nowadays, many different species concepts can be found, each having its own delimiting criteria, being thus difficult and limiting to choose one. The mostly used Biological Species Concept (Mayr 1942) does not allow for different species to interbreed. However, many species are known today to hybridize without putting in cause their species rank[164], including Lepidoptera, with many cases of gene introgression being recorded in butterflies and maybe even within other *Lycaena*[37,122,165–172]. As such, perhaps the nearest concepts to what we believe it could be the most fitting definition are the Phylogenetic Species Concept, which sees species as entities belonging to the same tip of the phylogeny, sharing a common ancestor and forming monophyletic clusters, or even the Evolutionary Species Concept (Simpson 1951) which defines a species as a "single lineage of ancestor-descendant populations of organisms which maintains its identity from other such lineages [in space and time] and which has its own evolutionary tendencies and historical fate" (Wiley, 1981). Overall, due to the difficulty of identifying a cryptic species based on single approaches, we chose to address the true relationship of the Sooty Coppers with an integrative and supported study, through multiple analyses, ideally leading us into the same answer. In the end, under the cap of the concepts above and considering our multi approach results, we propose that *L. tityrus* and *L. bleusei* are indeed different species and should be addressed as such due to their differences at many levels:

1) Beforehand, both species appear to have slightly different optimal ecological preferences, and while *L. bleusei* is apparently more adapted to the Mediterranean environment, withstanding a certain meadow summer drought, *L. tityrus* ecological preferences seem more shifted towards mountains ranges and humid regions in the centre and north of Portugal as it could be expected from a widespread European species.

2) Geometric morphometric analysis shows differences in wing shape and size between both taxa, revealing that *L. bleusei*'s hindwing is generally larger than *L. tityrus*'s, particularly females which tend to be always larger than males, more prominent in *L. bleusei*. Moreover, this analysis also highlighted some species phenotypic differences between seasons, especially in *L. bleusei*, which develops a small hindwing tail and a yellower underside colouration in its summer generation, as a possible adaptive trait in the drier habitats where it occurs. The Iberian population of *Lycaena tityrus* doesn't display these seasonal differences, but the multiple morphotypes found throughout its palaearctic distribution likely highlight different adaptations to different environments. In Iberia, we found both the exclusive western Iberian morphotype "*praebleusei*" (Verity, 1934) and the European morphotype "pallidepicta" (Verity, 1934), which meet in the region of Cantabria. However, when it comes to understand the real genetic differences and similarities between the several *L. tityrus* morphotypes, more research is needed. A future genomic approach may perhaps allow for a deeper understanding of the ecological differences and adaptations between both Sooty Coppers in Iberia and the different *L. tityrus* morphotypes in Europe.

3) In our genetic analyses, both Sooty Coppers appear clearly differentiated as sister taxa for COI and EF-1α. They show a maximum p-distance of 3.1% for COI, although the average interspecific distance for this gene in all Lycaenidae was estimated to be around 5%[173]. Even so, we find a stronger genetic differentiation between them than among some other *Lycaena* sister taxa (Table S4.1, S4.3, S4.6 and S4.7). Our *Lycaena* phylogenies, obtained with mtDNA and nuclear DNA separately, displayed different results, often falling into a "mito-nuclear discordance". Overall, the nuclear DNA phylogeny appears to fit better with the morphological traits and ecological preferences of the species affected by the mismatch, much in agreement with Pazhenkova & Lukhtanov (2018) for the genus *Brenthis* (Nymphalidae)[108]. In fact, although our *Lycaena* phylogeny is among the most complete studies on this genus so far, it still needs more genes and species to clarify the phylogenetic relationships between many taxa and improve the statistical support of the basal branches of the tree. Additionally, some key species must also be included as the New Zealand and South African *Lycaena*, as well as representative species of close related butterfly groups like *Melanolycaena*, *Hyrcanana*, *Athamanthia* or *Iophanus*, which still have an uncertain relationship and origin within the Lycaeninae subfamily.

Finding specimens with introgressed genetic material was an interesting result of this case-study and serve as proof that both taxa can likely still interbreed and haven't yet establish pre or post zygotic mating barriers. In fact, the likely recurrent secondary contacts and range overlaps through time might have helped delay the establishment of such barriers. Moreover, by finding no other cases of introgression in other specimens doesn't mean we don't have more introgressed individuals in our database, but simply that we might have been unable to find them with the genes studied due to the process of genetic recombination. We don't know if the two introgressed individuals represent the F1 generation of this hybrid cross or if they are carrying the remaining genetic evidence of an old interbreeding event, and neither the extent of genetic material introgressed. That can only be accessed in a future genomic study which will also enable us to differentiate these specimens as pure hybrids or the result of an adaptive introgression. Furthermore, a deeper study on these hybrid relations in a controlled environment will also perhaps allow us to understand if hybrid specimens acquire any kind of fitness advantage or disadvantage towards the parental lines, working against speciation by homogenising both lineages or favouring it by reinforcing parental premating barriers, respectively. A detailed comparison of both Sooty Coppers genitalia should also be carried in the future to infer if these species have already started developing different reproductive structures, although probably not different enough to prevent hybrid relations.

Another interesting result is the potential post glacial bottleneck hypothesis for *L. bleusei*. In fact, the possible extensive distribution of this species during LGM supports this scenario, suggesting a bigger adaptation to that colder and drier climate, consequently retracting and reducing its population size during the current interglacial period. However, this interpretation should be handled carefully as not only bioclimatic variables determine the presence or absence of a species. Thus, for a rigorous analysis of such occurrence at a macroecological scale the biotic interactions should be also taken into account, such as the interactions with the hostplant species[174] or the interspecific competition with close related species, no matter the organism[175,176]. Either way, the Iberian Peninsula seems to have been crucial for this species' development through time, with the several slopes of the CIMS in a wide range of gradients appearing to be a suitable refugia for this species to persist, adapting its distribution to the different climate oscillations. Moreover, the two exclusive *L. tityrus* Iberian COI haplotypes also highlight this role of Iberia on generating and keeping populations genetic diversity even within widespread European species with strongly connected populations.

Within the *Melanargia* case-study, our analysis of *Argeformia* confirmed the previous combined phylogeny and taxonomic classification presented by Nazari *et al*. 2010, with *M. arge* and *M. occitanica* coming as sister species, outgrouped by *M. ines*. The haplotypic diversity found for the mitochondrial COI gene also agrees with the number of subspecies currently proposed for both *M. ines* and *M. occitanica* (Table S1.1), although these might not be exactly the same as the ones considered by Nazari *et al*. 2010 for *M. ines*[65]. In fact, our results highlight two independent genetic clusters for *M. ines* in Morocco, separated by the High Atlas Mountains. The Anti Atlas + southern High Atlas cluster is geographically coincident with the once described subspecies *M. ines arahoui*. On the other hand, the Middle Atlas cluster does not seem to divide into two separated population groups as it could be expected for the divergence between *M. ines fathme* and *M. ines jahandiezi*, and therefore these two could, in this point of view, be synonymized. Moreover, the COI haplotype similarities between eastern maghrebian individuals (available sequences in online databases, not published) and the Middle Atlas cluster reinforce this idea. As such, a map with the subspecies that our own results suggest, is given in Supplementary Material for both *M. ines* and *M. occitanica* (Figures S8.1 and S8.2). Nonetheless, more research is needed to clarify the taxonomic classification of *Argeformia* subspecies, as we are only analysing one gene and highly divergent specimens were also found in the High Atlas region for both *M. ines* and *M. occitanica*, representing either a base calling artefact or new differentiated populations. Additionally, for a better understanding of the relationships and genetic differentiation within *Argeformia*, a future study must also include more specimens of the Sicilian *M. o. pherusa* and the eastern north African *M. ines* in both phylogenies and haplotype networks, as well as more individuals of the mainland Italian *M. arge* across its distribution.

Overall, all the *Argeformia* taxa appear to have slightly different ecological niches, that likely reflect their evolutionary history. The current species distribution and the SDM maps show that *Melanargia ines* appears to be more adapted to the warmer and drier conditions of the Mediterranean, with a bigger range extension in the Maghreb. The greatest COI haplotypic differences are also found in Morocco, suggesting a long-term management of genetic diversity in this region. Thus, we propose that this species might have had its origin in the Maghreb, adapting to its ecological conditions, and colonized Iberia in a more recent event, with its leading-edge population suffering a founder effect bottleneck that gave rise to the COI star-like pattern visible today in Iberia. On the other hand, the distribution and SDM maps of *M. occitanica* indicate that this species might be slightly less dependent on and adapted to the dry and warm conditions of the Maghreb, probably due to a later colonization of North Africa, and being still more adapted to the conditions felt in Italy when it shared a common ancestor with *M. arge*. Nonetheless, *M. occitanica* was able to expand in north Africa and reach Sicily,

likely during a glacial period, where it stayed isolated and differentiated into *M. o. pherusa*. Finally, *Melanargia arge* is the least expanded species of *Argeformia*, being restricted to Italy, and the genetic diversity of this species was not studied in detail in this work due to our lack of samples across its range. Its endemicity to the Italian mainland resulted also in a more restricted modulation of its distribution and optimal niche. Here, we propose that this species had its origin from an old common ancestor population with *M. occitanica* that stood isolated in Italy and differentiated with time into the new species *M. arge*. Since then, this taxon might have been unable to reconnect with its sister species, due to the presence of geographical barriers found all around the Italian Peninsula.

In fact, in agreement to Hewitt (1999) who considered the southern European mountains and seas as formidable barriers for most organisms today[17], our inference of the western Mediterranean geographical barriers and its influence over the differentiation of populations revealed an unmatched effect of the Gibraltar Strait, and also a weaker but still efficient isolation effect of the remaining barriers studied: Sicilian Strait, Pyrenees and High Atlas Mountains. However, it is always important to consider how long have these barriers been affecting the populations gene flow and the amount of genetic differentiation accumulated, so that we can properly compare their effect. In this regard, it is normal to see the greatest effect being caused by the Gibraltar Strait, since the Iberian and North African populations of *M. ines* and *M. occitanica* have been separated for a longer period of time and thus been able to accumulate the high number of genetic differences observed in our analysis.

Overall, by combining Genetics, Species Distribution Modeling, Geometric Morphometrics, as well as phenotype scoring of populations, we were able to propose different evolutionary history scenarios for both the Sooty Coppers and *Argeformia* species. More research and further studies are necessary to confirm or disprove them, adding more genes to this inference or even bigger parts of the genome and mitogenome, not only focused on the Sooty Coppers or the *Argeformia* but the whole *Lycaena* and *Melanargia* genera. Such approach will also likely resolve the conflict between molecular markers and clarifying all the mito-nuclear discordances.

In the end, the differentiation by allopatry created by both geographic barriers and climate constraints seems to be the main driver of species and populations differentiation within the Sooty Copper and *Argeformia* butterflies in the Western Mediterranean region. Thus, while leading populations to long-term isolation, it also promotes an independent genetic drift of both groups and adaptation to new environments. Still, climate shifts promote not only the isolation of populations and lineages but also their reunion and secondary contact along different time cycles, all of it shaping the patterns of distribution and genetic differentiation observed today. This present study represents one more step towards the understanding of all these species evolutionary histories, their differentiation process through time in this biodiverse region and, ultimately, their status in the Present. The past research of many authors stood as foundations for this work, which may hopefully be also the foundation for further studies, in a path that leads to the understanding of our surrounding world and to the knowledge of how to protect it.

9. References

1. Cuttelod, A., García, N., Malak, D. A., Temple, H. & Katariya, V. The Mediterranean: A biodiversity hotspot under threat. *IUCN* (2008).
2. Jong, H. D. E. In search of historical biogeographic patterns in the western Mediterranean terrestrial fauna. 99–164 (1998).
3. Krijgsman, W., Hilgen, F. J., Raf, I., Sierro, F. J. & Annunzio, Á. G. D. Chronology, causes and progression of the Messinian salinity crisis. 400**,** (1999).
4. Hewitt, G. M. Quaternary phylogeography: the roots of hybrid zones. 617–638 (2011).
5. Carranza, S. & Arnold, E. N. History of West Mediterranean newts, Pleurodeles (Amphibia: Salamandridae), inferred from old and recent DNA sequences. 2000**,** (2004).
6. Weingartner, E., Wahlberg, N. & Nylin, S. Speciation in Pararge (Satyrinae: Nymphalidae) butterflies – North Africa is the source of ancestral populations of all Pararge species. 621–632 (2006).
7. Wahlberg, N. & Saccheri, I. The effects of Pleistocene glaciations on the phylogeography of *Melitaea cinxia* (Lepidoptera: Nymphalidae). *Eur. J. Entomol.* 675–684 (2007).
8. Paulo, O. S. *et al.* The role of vicariance vs dispersal in shaping genetic patterns in ocellated lizard species in the western Mediterranean. 1535–1551 (2008).
9. Santos, X., Rato, C., Carranza, S., Carretero, M. A. & Pleguezuelos, J. M. Complex phylogeography in the Southern Smooth Snake (*Coronella girondica*) supported by mtDNA sequences. (2012).
10. Gibert, L. *et al.* Evidence for an African-Iberian mammal dispersal during the pre-evaporitic Messinian. 691–694 (2013).
11. Kindler, C. *et al.* Phylogeography of the Ibero-Maghrebian red-eyed grass snake (*Natrix astreptophora*). (2017).
12. Alexandrino, J., Froufe, E., Arntzen, J. W. & Ferrand, N. Genetic subdivision, glacial refugia and postglacial recolonization in the golden-striped salamander, *Chioglossa lusitanica* (Amphibia: Urodela). 771–781 (2000).
13. Martínez-Freiría, F., Velo-Antón, G. & Brito, J. C. Trapped by climate: interglacial refuge and recent population expansion in the endemic Iberian adder *Vipera seoanei*. 331–344 (2015).
14. Bilton, D. T. *et al.* Mediterranean Europe as an area of endemism for small mammals rather than a source for northwards postglacial colonization. (1998).
15. Gómez, A. & Lunt, D. H. Refugia within refugia: patterns of phylogeographic concordance in the Iberian Peninsula. (2007).
16. Husemann, M., Schmitt, T., Zachos, F. E., Ulrich, W. & Habel, J. C. Palaearctic biogeography revisited: evidence for the existence of a North African refugium for Western Palaearctic biota. 81–94 (2014).
17. Hewitt, G. M. Post-glacial re-colonization of European biota. *Biol. J. Linn. Soc.* 87–112 (1999).
18. Schmitt, T. & Varga, Z. Extra-Mediterranean refugia: The rule and not the exception 1–12 (2012).
19. Hewitt, G. The genetic legacy of the Quaternary ice ages. *Nature* (2000).
20. Taberlet, P., Fumagalli, L., Wust-Saucy, A.-G. & Cosson, J.-F. Comparative phylogeography and postglacial colonization routes in Europe. 453–464 (1998).
21. Schmitt, T. Molecular biogeography of Europe: Pleistocene cycles and postglacial trends. *Front. Zool.* 13**,** 1–13 (2007).
22. Stewart, J. R. & Lister, A. M. Cryptic northern refugia and the origins of the modern biota. 16**,**

608–613 (2001).
23. Rowe, G., Harris, D. J. & Beebee, T. J. C. Lusitania revisited: A phylogeographic analysis of the natterjack toad *Bufo calamita* across its entire biogeographical range. 39**,** 335–346 (2006).
24. Zeisset, I. & Beebee, T. J. C. Amphibian phylogeography: a model for understanding historical aspects of species distributions. 109–119 (2008).
25. Schmitt, T. & Hewitt, G. M. Molecular biogeography of the arctic-alpine disjunct burnet moth species *Zygaena exulans* (Zygaenidae, Lepidoptera) in the Pyrenees and Alps. 885–893 (2004).
26. Muster, C. & Berendonk, T. U. Divergence and diversity: lessons from an arctic – alpine distribution (*Pardosa saltuaria* group, Lycosidae). 2921–2933 (2006).
27. Varga, Z. S. & Schmitt, T. Types of oreal and oreotundral disjunctions in the western Palearctic. 415–430 (2008).
28. Hewitt, G. M. Some genetic consequences of ice ages and their role in divergence and speciation. *Biol. J. Linn. Soc.* 247–276 (1996).
29. Médail, F. & Quézel, P. Biodiversity Hotspots in the Mediterranean Basin: Setting Global Conservation Priorities. 13**,** 1510–1513 (1999).
30. Araújo, M. B., Lobo, J. M. & Moreno, J. C. The Effectiveness of Iberian Protected Areas in Conserving Terrestrial Biodiversity. 21**,** 1423–1432 (2007).
31. Comes, H. P. The Mediterranean region – a hotspot for plant biogeographic research. 1–16 (2004).
32. Pinborg, U. The Mediterranean biogeographical region. 1–54 (2008).
33. Hawkins, B. A. & Porter, E. E. Water – energy balance and the geographic pattern of species richness of western Palearctic butterflies. *Ecol. Entomol.* 678–686 (2003).
34. Bryant, S. R., Thomas, C. D. & Bale, J. S. Nettle-feeding nymphalid butterflies: temperature, development and distribution. 390–398 (1997).
35. Bryant, S. R., Thomas, C. D. & Bale, J. S. The influence of thermal ecology on the distribution of three nymphalid butterflies. 43–55 (2002).
36. Parmesan, C. *et al.* Poleward shifts in geographical ranges of butterfly species associated with regional warming. 399**,** 579–583 (1999).
37. Dennis, R. L. H. & Shreeve, T. G. Climatic Change and the British Butterfly Fauna: Opportunities and Constraints. *Biol. Conserv.* **55,** 1–16 (1991).
38. Quinn, R. M., Gaston, K. J. & Roy, D. B. Coincidence in the distributions of butterflies and their foodplants. *Ecography (Cop.).* 279–288 (1998).
39. Tiple, A. D., Khurad, A. M. & Dennis, R. L. H. Butterfly Larval Host Plant use in a Tropical Urban Context: Life history associations, herbivory, and landscape factors. (2010).
40. Habel, J. C., Meyer, M. & Schmitt, T. *Jewels in the Mist*. (2014).
41. Thompson, J. N. Variation in preference and specificity in monophagous and oligophagous swallowtail butterflies. 42**,** 118–128 (1988).
42. Querci, O. Contributo biologia alla conoscenza della dei rhopaloceri Iberici. XI**,** (1932).
43. Kudrna, O. An Annotated Catalogue of the Butterflies (Lepidoptera: Papilionoidea) Named by Roger Verity. (1982).
44. Asal, J. Beitrag zur Biologie und Ökologie von *Lycaena tityrus bleusei* (Oberthür, 1884) aus Spanien (Lepidoptera: Lycaenidae). 29**,** 15–18 (2008).
45. Cassulo, L., Mensi, P. & Balletto, E. Taxonomy and evolution in Lycaena (subgenus Heodes) (Lycaenidae). *Solutions* 53–84 (1989).
46. Bozano, G. C. & Weidenhoffer, Z. Lycaenidae Part 1. Subfamily Lycaeninae. Guide to the butterflies of the Palearctic Region. (2001).
47. de Jong, R. & van Dorp, K. The African copper connection. *Entomol. Ber.* 66**,** 124–129 (2006).

48. Kocak, A. Ö. & Kemal, M. Annotated List of the Lycaena Fabr . 1–8 (2007).
49. Leraut, P. *Butterflies of Europe and neighbouring regions*. (2016).
50. Dincă, V. *et al.* DNA barcode reference library for Iberian butterflies enables a continental-scale preview of potential cryptic diversity. *Sci. Rep.* **5,** 12395 (2015).
51. Marabuto, E., Pires, P. & Cardoso, J. P. Contribuição para o conhecimento dos Macrolepidópteros do Parque Natural da Serra da Estrela, Portugal (Lepidoptera). *Boletín S.E.A.* 34**,** 171–175 (2004).
52. Vicente Arranz, J. C., Hernández Rodríguez, J. A. & Hernández Martín, H. Primeros registros de *Lycaena bleusei* Oberthür, 1884 en Valladolid y Zamora (Castilla y León: España), y Bragança (Portugal) (Lepidoptera: Lycaenidae). *Arq. Entomolóxicos* 14**,** 227–234 (2015).
53. Vicente Arranz, J. C., Hernández Rodríguez, J. A., Manceñido-González, D. C. & Parra Arjona, B. Primeros registros de *Lycaena bleusei* Oberthür, 1884 en las provincias de Burgos y León (Castilla y León: España) (Lepidoptera: Lycaenidae). *Arq. Entomolóxicos* 16**,** 217–224 (2016).
54. Hernández Martín, H. & Vicente Arranz, J. C. Primeros registros de *Lycaena bleusei* Oberthür, 1884 para Galicia (N.O. España) (Lepidoptera: Lycaenidae). *Arq. Entomolóxicos* 16**,** 173–174 (2016).
55. Numa, C. *et al. The status and distribution of Mediterranean butterflies*. (2016).
56. Wiemers, M. *et al.* An updated checklist of the European Butterflies. 45**,** 9–45 (2018).
57. Descimon, H. *Heodes tityrus tityrus* Poda et *H. tityrus subalpina* Speyer (Lycaenidae): un probleme de speciation en milieu alpin. 2**,** 123–125 (1980).
58. Parenzan, P. & Porcelli, F. I macrolepidotteri italiani. 1–1051 (2006).
59. Balletto, E., Cassulo, L. A. & Bonelli, S. *An annotated checklist of the Italian butterflies and skippers (Papilionoidea, Hesperiioidea)*. *Zootaxa* 3853**,** (2014).
60. Munguira, M. L., García-Barros, E. & Martín, J. Plantas nutricias de los licénidos y satirinos españoles (Lepidoptera: Lycaenidae y Nymphalidae). 21**,** 29–53 (1997).
61. Verity, R. Sous-genre Chrysophanus. (1948).
62. Pratt, G. F. & Wright, D. M. Allozyme phylogeny of North American coppers (Lycaeninae: Lycaenidae). 4**,** (2002).
63. Oliver, J. C. & Stein, L. R. Evolution of influence: signaling in a lycaenid-ant interaction. 1205–1216 (2011).
64. Dorp, van, K. Molecular systematics of Lycaena F., 1807 (Lepidoptera: Lycaenidae) - some preliminary results. *Proc. Netherlands Entomol. Soc. Meet.* 15**,** 65–70 (2004).
65. Nazari, V., Hagen, W. Ten & Bozano, G. C. Molecular systematics and phylogeny of the 'Marbled Whites' (Lepidoptera: Nymphalidae, Satyrinae, Melanargia Meigen). *Syst. Entomol.* 35**,** 132–147 (2010).
66. Mensi, P., Lattes, A., Cassulo, L., Cinti, R. & Baletto, E. Electrophoretic studies in the genus Melanargia Meigen, 1828 (lepidoptera: Satyridae). *Journal of Research on the Lepidoptera* 29**,** 11–20 (1990).
67. Nardelli, U. & Benedetto, G. *Melanargia pherusa* Boisduval 1833: Biologie, Ökologie, Morphologie und Verbreitung im Vergleich mit Melanargia arge Sulzer 1776 (Lepidoptera: Nymphalidae, Satyrinae). 15**,** (1994).
68. Jutzeler, D., Grillo, N., Russo, L., Nardelli, U. & De Bros, E. Position taxinomique et biologie de *Melanargia pherusa* (Boisduval, 1833) de Sicile selon les stades pré-imaginaux (Lepidoptera:Nymphalidae, Satyrinae). *Linneana Belgica* (1996).
69. Nardelli, U., Olivares, J. & Jutzeler, D. Études sur l´écologie et le développement de *Melanargia ines* (Hoffmannsegg, 1804) en Andalousie et comparaison avec les espèces les plus proches (Lepidoptera: Nymphalidae, Satyrinae). (1998).

70. Oberthur, C. Lépidoptérologie comparées. 358–363 (1906).
71. Habel, J. C., Husemann, M., Rödder, D. & Schmitt, T. Biogeographical dynamics of the Spanish Marbled White *Melanargia ines* (Lepidoptera: Satyridae) in the Western Mediterranean: Does the Atlanto-Mediterranean refuge exist? *Biol. J. Linn. Soc.* 104**,** 828–837 (2011).
72. Settele, J. *et al.* Climatic Risk Atlas of European Butterflies (2008).
73. Wahlberg, N., Brower, A. V. Z. & Nylin, S. Phylogenetic relationships and historical biogeography of tribes and genera in the subfamily Nymphalinae (Lepidoptera: Nymphalidae). 227–251 (2005).
74. Wahlberg, N. & Wheat, C. W. Genomic Outposts Serve the Phylogenomic Pioneers: Designing Novel Nuclear Markers for Genomic DNA Extractions of Lepidoptera. 57**,** 231–242 (2008).
75. Barão, K. R., Gonçalves, G. L., Mielke, O. H. H., Kronforst, M. R. & Moreira, G. R. P. Species boundaries in Philaethria butterflies: an integrative taxonomic analysis based on genitalia ultrastructure, wing geometric morphometrics, DNA sequences, and amplified fragment length polymorphisms. *Zool. J. Linn. Soc.* 690–709 (2014).
76. Katoh, K., Rozewicki, J. & Yamada, K. D. MAFFT online service: multiple sequence alignment , interactive sequence choice and visualization. 1–7 (2018).
77. Hall, T. BioEdit: a user-friendly biological sequence alignment editor and analysis program for Windows 95/98/NT. (1999).
78. Stephens, M., Smith, N. J. & Donnelly, P. A New Statistical Method for Haplotype Reconstruction from Population Data. *Am. J. Hum. Genet.* 68**,** 978–989 (2001).
79. Silvestro, D. & Michalak, I. RaxmlGUI: A graphical front-end for RAxML. *Org. Divers. Evol.* 12**,** 335–337 (2011).
80. Huelsenbeck, J. P. & Ronquist, F. MRBAYES: Bayesian inference of phylogenetic trees. *Bioinformatics* 17**,** 754–755 (2001).
81. Pina-Martins, F. & Paulo, O. S. Concatenator: Sequence data matrices handling made easy. *Mol. Ecol. Resour.* 8**,** 1254–1255 (2008).
82. Darriba, D., Taboada, G. L., Doallo, R. & Posada, D. jModelTest 2: more models, new heuristics and parallel computing CircadiOmics: integrating circadian genomics, transcriptomics, proteomics. *Nat. Methods* 9**,** 772 (2012).
83. Leigh, J. W. & Bryant, D. POPART: full-feature software for haplotype network construction. 1110–1116 (2015).
84. Excoffier, L. & Lischer, H. E. L. Arlequin suite ver 3.5: a new series of programs to perform population genetics analyses under Linux and Windows. *Mol. Ecol. Resour.* 564–567 (2010).
85. Kumar, S., Stecher, G. & Tamura, K. MEGA7 : Molecular Evolutionary Genetics Analysis Version 7.0 for Bigger Datasets Brief communication. *Mol. Biol. Evol.* **33,** 1870–1874 (2016).
86. Drummond, A. J. & Bouckaert, R. R. Bayesian Evolutionary Analysis with BEAST. *Cambridge Univ. Press* (2014).
87. Pena, C., Nylin, S. & Wahlberg, N. The radiation of Satyrini butterflies (Nymphalidae: Satyrinae): A challenge for phylogenetic methods. *Zool. J. Linn. Soc.* (2013).
88. Espeland, M. *et al.* A Comprehensive and Dated Phylogenomic Analysis of Butterflies. *Curr. Biol.* 1–9 (2018).
89. Rambaut, A., Drummond, Al. J., Xie, D., Baele, G. & Suchard, M. A. Posterior Summarization in Bayesian Phylogenetics Using Tracer 1.7. *Syst. Biol.* 67**,** 901–904 (2018).
90. Zelditch, M. L., Swiderski, D. L., Sheets, H. D. & Fink, W. L. Geometric Morphometrics for Biologists. in (2004).
91. Breuker, C. J., Gibbs, M., Dyck, H. V. A. N., Brakefield, P. M. & Klingenberg, C. P. Integration of Wings and Their Eyespots in the Speckled Wood Butterfly *Pararge aegeria*. 463**,** 454–463

(2007).
92. Schindelin, J. *et al.* Fiji: an open-source platform for biological-image analysis. 9**,** (2012).
93. Rohlf, F. J. & Slice, D. Extensions of the Procrustes Method for the Optimal Superimposition of Landmarks. *Syst. Zool.* 39**,** 40–59 (1990).
94. Phillips, S. J., Anderson, R. P. & Schapire, R. E. Maximum entropy modeling of species geographic distributions. *Ecol. Modell.* 190**,** 231–259 (2006).
95. García-Barros, E. *et al.* Atlas of the butterflies of the Iberian Peninsula and Balearic Islands (Lepidoptera: Papilionoidea and Hesperioidea). 228 (2004).
96. Valverde, A. J., Cano, J. M. & Munguira, M. L. Patrones de diversidad de la fauna de mariposas del Parque Nacional de Cabañeros y su entorno (Ciudad Real, España central) (Lepidoptera, Papilionoidea, Hesperioidea). *Anim. Biodivers. Conserv.* 2**,** 15–24 (2004).
97. Díaz-Regañón, A. Datos sobre la fauna de mariposas diurnas de la Sierra de San Vicente, Toledo, España (Lepidoptera: Papilionoidea). *SHILAP Revista de Lepidopterologia* (2012).
98. De Arce-Crespo, J. I. & Sánchez-Fernández, P. Ampliación de la información sobre la distribución de las mariposas de la Serranía de Cuenca, España (Lepidoptera: Papilionoidea). *SHILAP Revista de Lepidopterologia* (2013).
99. Blázquez-caselles, Á. Análisis de la información conocida sobre los lepidópteros de Cáceres (España), con aportación de nuevos datos. (Insecta: Lepidoptera). *Arq. Entomolóxicos Galegos* 3–130 (2014).
100. Vidal, E. H. F. Lepidópteros de O Courel (Lugo, Galicia, España, N.O. Península Ibérica) XII: Papilionidae, Pieridae y nota adicional sobre Hesperiidae y Lycaenidae. (Insecta: Lepidoptera). *Arq. Entomolóxicos Galegos* 79–96 (2017).
101. Fick, S. E. & Hijmans, R. J. WorldClim 2: new 1-km spatial resolution climate surfaces for global land areas. *Int. J. Climatol.* (2017).
102. Nogués-Bravo, D. Predicting the past distribution of species climatic niches. *Glob. Ecol. Biogeogr.* 18**,** 521–531 (2009).
103. Gent, P. R. *et al.* The Community Climate System Model Version 4. *J. Clim.* 4973–4991 (2011).
104. Giorgetta, M. A. *et al.* Climate and carbon cycle changes from 1850 to 2100 in MPI-ESM simulations for the Coupled Model Intercomparison Project phase 5. *J. Adv. Model. EARTH Syst.* 5**,** 572–597 (2013).
105. Pohl, G. R., Patterson, B. & Pelham, J. P. Annotated taxonomic checklist of the Lepidoptera of North America, North of Mexico. (2016).
106. Brower, A. V. Z. Rapid morphological radiation and convergence among races of the butterfly *Heliconius erato* inferred from patterns of mitochondrial DNA evolution. *Evolution (N. Y).* (2014).
107. Moritz, C. & Cicero, C. DNA Barcoding: Promise and Pitfalls. *Plos Biol.* 2**,** (2004).
108. Pazhenkova, E. A. & Lukhtanov, V. A. Nuclear genes (but not mitochondrial DNA barcodes) reveal real species: Evidence from the Brenthis fritillary butterflies (Lepidoptera, Nymphalidae). *J. Zool. Syst. Evol. Res.* (2018).
109. Klots, A. B. The Interrelationships of the species of the genus Lycaena Fabricius (Lepidoptera, Lycaenidae). *Bull. Brooklyn Entomol. Soc.* 31**,** (1936).
110. Sibatani, A. A new genus for two new species of Lycaeninae (S. STR.) (Lepidoptera: Lycaenidae) from Papua New Guinea. *J. Aust. ent. Soc* 5**,** 57–58 (1974).
111. Miller, L. D. & Brown, F. M. Studies in the Lycaeninae (Lycaenidae). *Allyn Museum Entomol.* (1979).
112. MacDonald, G. M. & McLeod, T. K. The holocene closing of the 'ice-free' corridor: a biogeographical perspective. *Quat. Int.* 32**,** 87–95 (1996).

113. Fay, J. C. & Wu, C.-I. A human population bottleneck can account for the discordance between patterns of mitochondrial versus nuclear DNA variation. *Mol. Biol. Evol.* (1999).
114. Ji, Y., Wu, D., Wu, G., Wang, G. & Zhang, Y. Multi-Locus Analysis Reveals A Different Pattern of Genetic Diversity for Mitochondrial and Nuclear DNA between Wild and Domestic Pigs in East Asia. *PLoS One* 6**,** (2011).
115. Hung, C. & Zink, R. M. Distinguishing the effects of selection from demographic history in the genetic variation of two sister passerines based on mitochondrial – nuclear comparison. *Heredity (Edinb).* 113**,** 42–51 (2014).
116. Dantas, G. P. de M., Meyer, D., Godinho, R., Ferrand, N. & Morgante, J. S. Genetic variability in mitochondrial and nuclear genes of *Larus dominicanus* (Charadriiformes, Laridae) from the Brazilian coast. *Genet. Mol. Biol.* 885**,** 874–885 (2012).
117. Cann, R. L., Stoneking, M. & Wilson, A. C. Mitochondrial DNA and human evolution. *Nature* (1987).
118. Templeton, A. R., Routman, E. & Phillips, C. A. Separating population structure from population history: a cladistic analysis of the geographical distribution of mitochondrial DNA haplotypes. *Genet. Soc. Am.* (1995).
119. Schmitt, T. & Seitz, A. Intraspecific allozymatic differentiation reveals the glacial refugia and the postglacial expansions of European *Erebia medusa* (Lepidoptera: Nymphalidae). *Biol. J. Linn. Soc.* (2001).
120. Schmitt, T., Rákosy, L., Abadjiev, S. & Muller, P. Multiple differentiation centres of a non-Mediterranean butterfly species in south-eastern Europe. *J. Biogeogr.* 939–950 (2007).
121. Habel, J. C., Lens, L., Rödder, D. & Schmitt, T. From Africa to Europe and back: refugia and range shifts cause high genetic differentiation in the Marbled White butterfly *Melanargia galathea*. *BMC Evol. Biol.* 215**,** (2011).
122. Habel, J. C. *et al.* Differentiation in the marbled white butterfly species complex driven by multiple evolutionary forces. *J. Biogeogr.* 433–445 (2017).
123. Hewitt, G. M. Genetic consequences of climatic oscillations in the Quaternary. *R. Soc.* 183–195 (2004).
124. Habel, J. C., Schmitt, T. & Muller, P. The fourth paradigm pattern of post-glacial range expansion of European terrestrial species: the phylogeography of the Marbled White butterfly (Satyrinae, Lepidoptera). *J. Biogeogr.* 1489–1497 (2005).
125. Gratton, P., Konopinski, M. K. & Sbordoni, V. Pleistocene evolutionary history of the Clouded Apollo (*Parnassius mnemosyne*): genetic signatures of climate cycles and a 'time-dependent' mitochondrial substitution rate. *Mol. Ecol.* 4248–4262 (2008).
126. Hey, J. & Pinho, C. Population genetics and objectivity in species diagnosis. *Evolution (N. Y).* 66, 1413–1429 (2012).
127. Wells, C., Munn, A. & Woodworth, C. Geomorphic morphometric differences between populations of Speyeria diana (Lepidoptera: Nymphalidae). *Florida Entomol.* 101**,** 195–202 (2018).
128. Benítez, H. A., Parra, L. E., Sepulveda, E. & Sanzana, M. J. Geometric perspectives of sexual dimorphism in the wing shape of Lepidoptera: the case of *Synneuria sp.* (Lepidoptera: Geometridae). *J. Entomol. Res. Soc.* 13**,** 53–60 (2011).
129. Khaghaninia, S. *et al.* An analysis of seasonal dimorphism in codling moths, Cydia pomonella, from Iran using geometric morphometrics. *Bull. Insectology* 67**,** 43–50 (2014).
130. Bai, Y., Ma, L. Bin, Xu, S.-Q. & Wang, G.-H. A geometric morphometric study of the wing shapes of Pieris rapae (Lepidoptera: Pieridae) from the Qinling Mountains and adjacent regions: An Environmental and distance-based consideration. *Florida Entomol.* 98**,** 162–169 (2015).

131. Dapporto, L. & Strumia, F. The thorny subject of insular endemic taxonomy: morphometrics reveal no evidence of speciation between *Coenonympha corinna* and *Coenonympha elbana* butterflies (Lepidoptera: Nymphalidae). *Zootaxa* 56**,** 47–56 (2008).
132. Dincă, V., Dapporto, L. & Vila, R. A combined genetic-morphometric analysis unravels the complex biogeographical history of *Polyommatus icarus* and *Polyommatus celina* Common Blue butterflies. *Mol. Ecol.* 3921–3935 (2011).
133. Fischer, K. & Fiedler, K. Sex-related differences in reaction norms in the butterfly *Lycaena tityrus* (Lepidoptera: Lycaenidae). *OIKOS* 2**,** 372–380 (2000).
134. Angilletta, M. J. & Dunham, A. E. The Temperature-Size Rule in Ectotherms: Simple Evolutionary Explanations May Not Be General. *Am. Nat.* (2003).
135. De Jong, M. A., Collins, S., Beldade, P., Brakefield, P. M. & ZWAAN, B. J. Footprints of selection in wild populations of *Bicyclus anynana* along a latitudinal cline. *Mol. Ecol.* 341–353 (2013).
136. Mateus, A. R. A. *et al.* Adaptive developmental plasticity: Compartmentalized responses to environmental cues and to corresponding internal signals provide phenotypic flexibility. *BMC Biol.* 1–15 (2014).
137. Oliveira, N. The adult body size variation of *Dryas iulia* (Lepidoptera, Nymphalidae, Heliconiinae) in different populations is more influenced by temperature variation than by host-plant availability during the seasons. *Entomol. Sci.* 376–387 (2014).
138. Daveau, S. La glaciation de la Serra da Estrela. *Finisterra* (1971).
139. Coudé, A., Coudé-Gaussen, G. & Daveau, S. Nouvelles observations sur la glaciation des montagnes du nord-ouest du Portugal. (1983).
140. Daveau, S. & Devy-Vareta, N. Gélifraction, nivation et glaciation d'abri de la Serra da Cabreira (Portugal). in (1985).
141. Ferreira, A. de B., Romaní, J. R. V., Zêzere, J. L. & Rodrigues, M. L. A glaciação plistocénica da Serra do Gerês. *Finisterra* 39–68 (2000).
142. Pereira, P. & Pereira, D. Geomorfologia glaciária e periglaciária: contributo para a inventariação do património geológico português. *Assoc. Port. Geomorfólogos* (2009).
143. Peixoto, L. & Alves, M. I. C. Quantificação do património geomorfológico – glaciário no Parque Nacional da Peneda-Gerês (Portugal). *Assoc. Port. Geomorfólogos* VI**,** 265–268 (2009).
144. Frenzel, B., Pécsi, M. & Velichko, A. A. Atlas of paleoclimates and paleoenvironments of the northern hemisphere: late pleistocene - holocene. (1992).
145. Ferreira, A. de B. Considerações acerca do arrefecimento plistocénico em Portugal. *Finisterra* 89–101 (2000).
146. Gvozdík, V., Moravec, J. & Kratochvíl, L. Geographic morphological variation in parapatric Western Palearctic tree frogs, *Hyla arborea* and *Hyla savignyi*: are related species similarly affected by climatic conditions? *Biol. J. Linn. Soc.* (2008).
147. Eitschberger, U. & Racheli, T. Die rasterelektronische Darstellung des Eis von *Melanargia arge* (SULZER, 1776). 338–343 (1984).
148. Jutzeler, D. & Leestmans, R. La signification des variantes vertes et brunes des chenilles de *Melanargia lachesis* (Hübner, 1790) (Lepidoptera: Nymphalidae, Satyrinae). (1994).
149. Jutzeler, D., Russo, L. & De Bros, E. Observations sur la vie de *Melanargia occitanica* (Esper, 1793) de la Riviera franco-italienne, dans la nature et en élevage (Lepidoptera: Nymphalidae, Satyrinae). *Linneana Belgica* (1995).
150. van Hinsbergen, D. J. J. *et al.* Orogenic architecture of the Mediterranean region and kinematic reconstruction of its tectonic evolution since the Triassic. *Gondwana Res.* (2019).
151. Burban, C., Petit, R. J., Carcreff, E. & Jactel, H. Rangewide variation of the maritime pine bast

scale *Matsucoccus feytaudi* Duc. (Homoptera: Matsucoccidae). *Mol. Ecol.* 1593–1602 (1999).
152. Percy, D. M. Radiation, diversity, and host-plant interactions among islands and continental legume-feeding psyllids. *Evolution (N. Y).* 57**,** 2540–2556 (2003).
153. Hundsdoerfer, A. K., Kitching, I. J. & Wink, M. The phylogeny of the *Hyles euphorbiae* complex (Lepidoptera: Sphingidae): Molecular evidence from sequence data and ISSR-PCR fingerprints. *Org. Divers. Evol.* 5**,** 173–198 (2005).
154. Wiemers, M. & Fiedler, K. Does the DNA barcoding gap exist? - a case study in blue butterflies (Lepidoptera: Lycaenidae). *Front. Zool.* 16**,** 1–16 (2007).
155. Zazo, C. *et al.* Coastal uplift in continental collision plate boundaries: data from the Last Interglacial marine terraces of the Gibraltar Strait area (south Spain). *Tectonophysics* 301**,** 95–109 (1999).
156. Vandewoestijne, S., Baguette, M., Brakefield, P. M. & Saccheri, I. J. Phylogeography of *Aglais urticae* (Lepidoptera) based on DNA sequences of the mitochondrial COI gene and control region. *Mol. Phylogenet. Evol.* 31**,** 630–646 (2004).
157. Manzi, V. *et al.* Age refinement of the Messinian salinity crisis onset in the Mediterranean. *Terra Nov.* 315–322 (2013).
158. Dapporto, L., Bruschini, C., Dincă, V., Vila, R. & Dennis, R. L. H. Identifying zones of phenetic compression in West Mediterranean butterflies (Satyrinae): refugia, invasion and hybridization. *Divers. Distrib.* 1066–1076 (2012).
159. Cosson, J.-F. *et al.* Phylogeographical footprints of the Strait of Gibraltar and Quaternary climatic fluctuations in the western Mediterranean: a case study with the greater white-toothed shrew, *Crocidura russula* (Mammalia: Soricidae). *Mol. Ecol.* 1151–1162 (2005).
160. Habel, J. C., Dieker, P. & Schmitt, T. Biogeographical connections between the Maghreb and the Mediterranean peninsulas of southern Europe. *Biol. J. Linn. Soc.* 1**,** 693–703 (2009).
161. Guicking, D., Joger, U. & Wink, M. Molecular phylogeography of the viperine snake *Natrix maura* (Serpentes: Colubridae): Evidence for strong intraspecific differentiation. *Org. Divers. Evol.* 8**,** 130–145 (2008).
162. Buckley, D. Toward an organismal, integrative, and iterative phylogeography. *Phylogenetics Syst.* 784–793 (2009).
163. Dapporto, L. Speciation in Mediterranean refugia and post-glacial expansion of *Zerynthia polyxena* (Lepidoptera, Papilionidae). *J. Zool. Syst. Evol. Res.* 48**,** 229–237 (2010).
164. Eckert, A. J. & Carstens, B. C. Does gene flow destroy phylogenetic signal? The performance of three methods for estimating species phylogenies in the presence of gene flow. *Mol. Phylogenet. Evol.* 49**,** 832–842 (2008).
165. Oliver, J. C. & Shapiro, A. M. Genetic isolation and cryptic variation within the *Lycaena xanthoides* species group (Lepidoptera: Lycaenidae). *Mol. Ecol.* 4308–4320 (2007).
166. Mavárez, J. *et al.* Speciation by hybridization in Heliconius butterflies. *Nature* 441**,** 868–871 (2006).
167. Mallet, J., Beltrán, M., Neukirchen, W. & Linares, M. Natural hybridization in heliconiine butterflies: the species boundary as a continuum. *BMC Evol. Biol.* 16**,** 1–16 (2007).
168. Schmidt, B. C. & Sperling, F. A. H. Widespread decoupling of mtDNA variation and species integrity in Grammia tiger moths (Lepidoptera: Noctuidae). *Syst. Entomol.* 613–634 (2008).
169. Talavera, G., Dincă, V. & Vila, R. Factors affecting species delimitations with the GMYC model: insights from a butterfly survey. *Methods Ecol. Evol.* 1101–1110 (2013).
170. Dupuis, J. R. & Sperling, F. A. H. Repeated reticulate evolution in North American *Papilio machaon* group swallowtail butterflies. *PLoS One* 1–26 (2015).
171. Capblancq, T., Després, L., Rioux, D. & Mavárez, J. Hybridization promotes speciation in

Coenonympha butterflies. *Mol. Ecol.* 6209–6222 (2015).
172. Capblancq, T., Mavárez, J., Rioux, D. & Després, L. Speciation with gene flow: Evidence from a complex of alpine butterflies (Coenonympha, Satyridae). *Ecol. Evol.* 6444–6457 (2019).
173. Hebert, P. D. N., Ratnasingham, S. & DeWaard, J. R. Barcoding animal life: cytochrome c oxidase subunit 1 divergences among closely related species. *Biol. Lett.* 96–99 (2003).
174. Araújo, M. B. & Luoto, M. The importance of biotic interactions for modelling species distributions under climate change. *Glob. Ecol. Biogeogr.* 743–753 (2007).
175. Davis, A. J., Lawton, J. H., Shorrocks, B. & Jenkinson, L. S. Individualistic species responses invalidate simple physiological models of community dynamics under global environmental change. *J. Anim. Ecol.* (1998).
176. Leathwick, J. R. & Austin, M. P. Competitive interactions between tree species in New Zealand's old-growth indigenous forests. *Ecology* 82**,** 2560–2573 (2001).

10. Supplementary Material

10.1 Figures

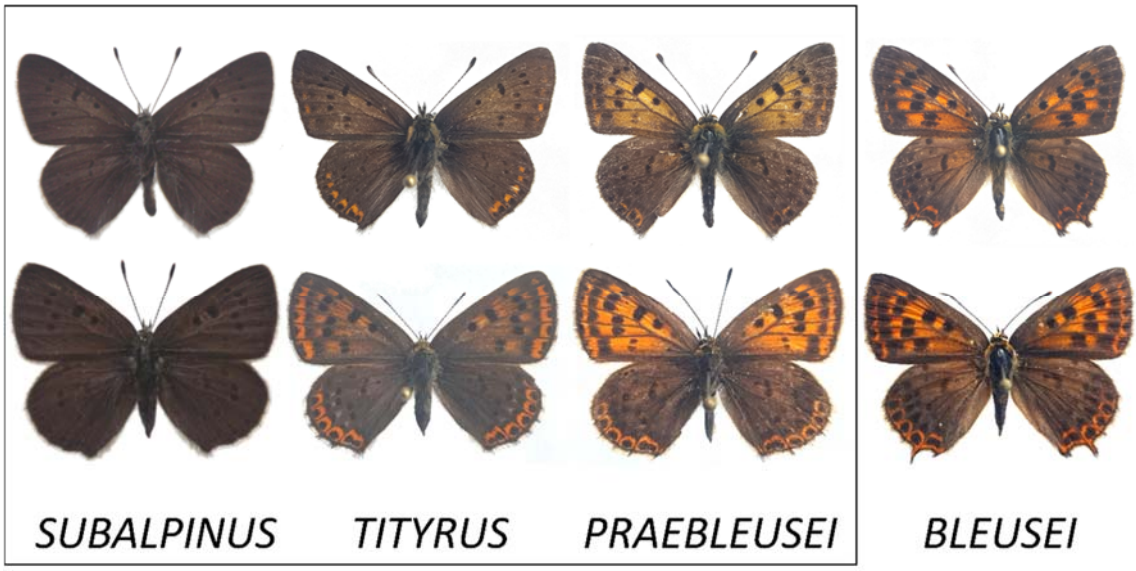

Figure S1.1 – Male (top figures) and female (below figures) phenotype differences between *L. t. subalpinus*, *L. t. tityrus* morphotype *tityrus*, *L. t. tityrus* morphotype *praebleusei* and *Lycaena bleusei*.

Figure S1.2 – *L. tityrus* morphotypes throughout its distribution range in Europe with type locality (small dots at the end of black lines) and date of description.

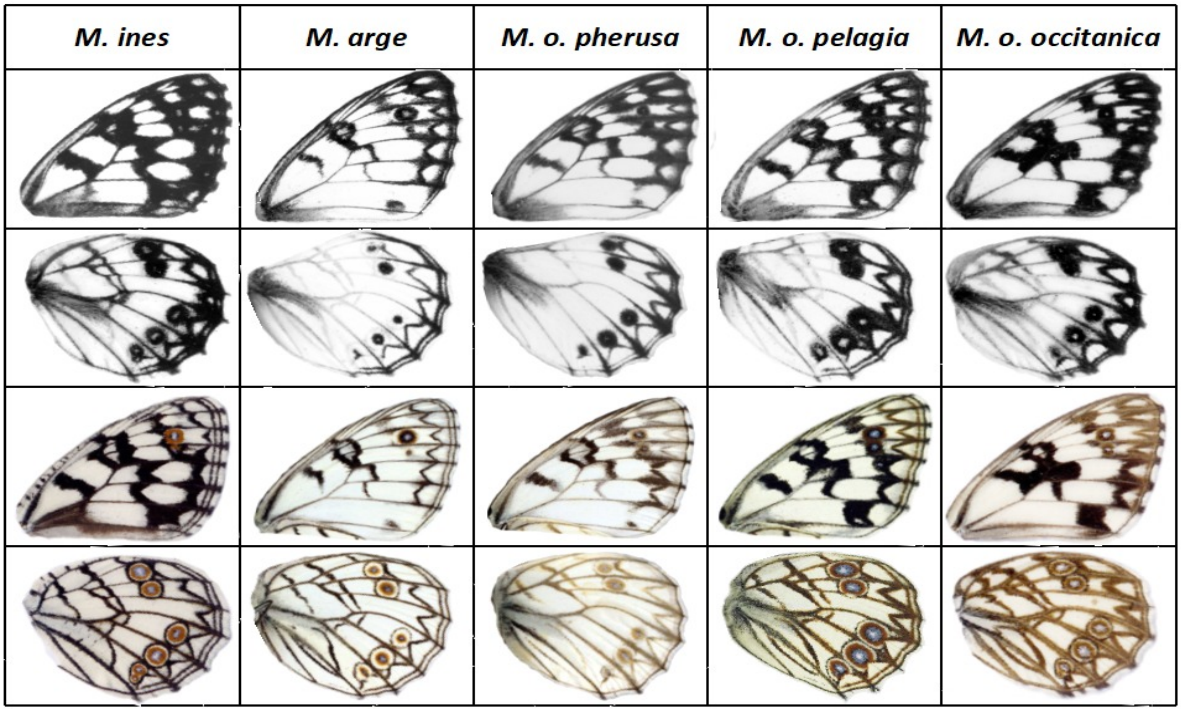

Figure S1.3 – Phenotypic differences between *Melanargia ines*, *Melanargia arge*, *M. o. pherusa*, *M. o. pelagia* and *M. o. occitanica*.

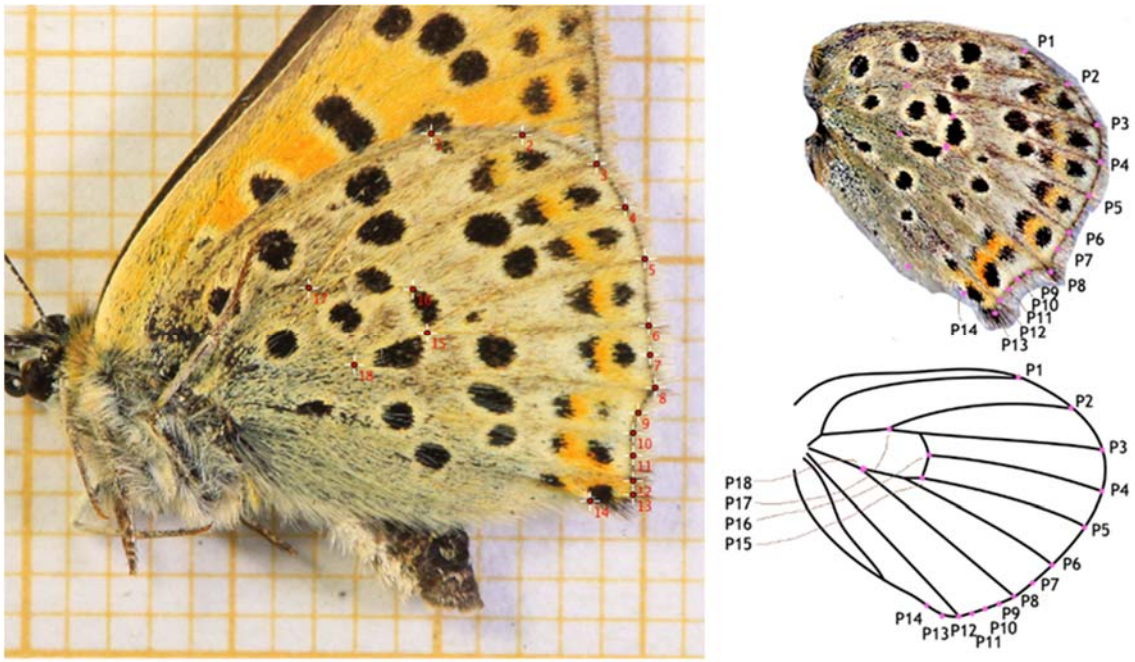

Figure S3.1 – Landmarks disposition on the *Lycaena* hindwing for the Geometric Morphometrics analysis.

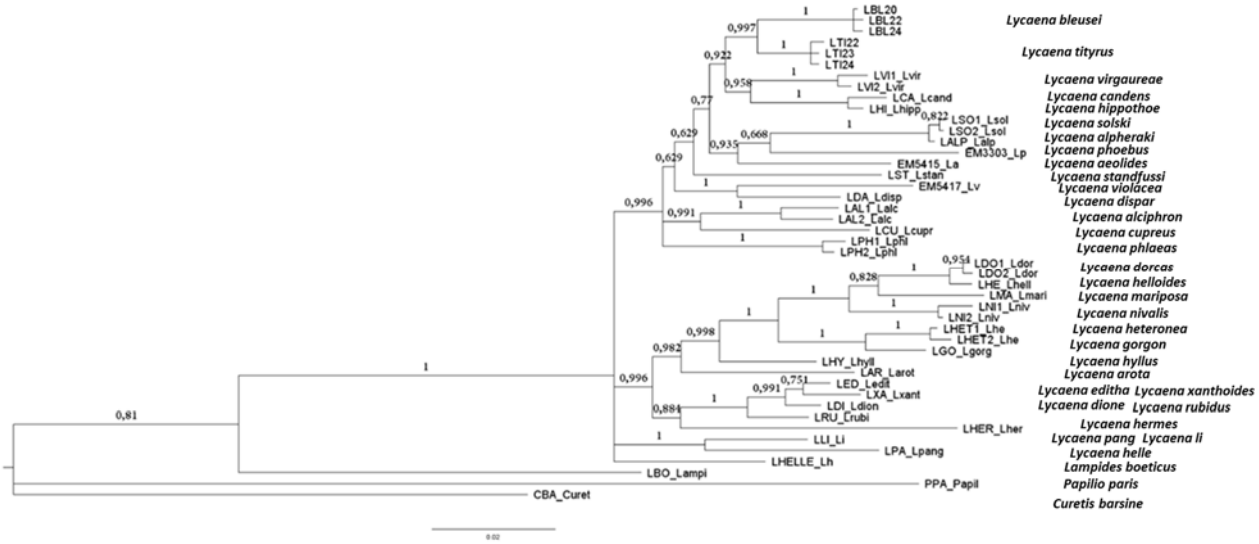

Figure S4.1 – Bayesian inference phylogeny of *Lycaena* based on the combined analysis of COI and EF-1α gene haplotypes (Datasets 3 + 5). Bayesian posterior probabilities higher than 0.7 are shown along branches.

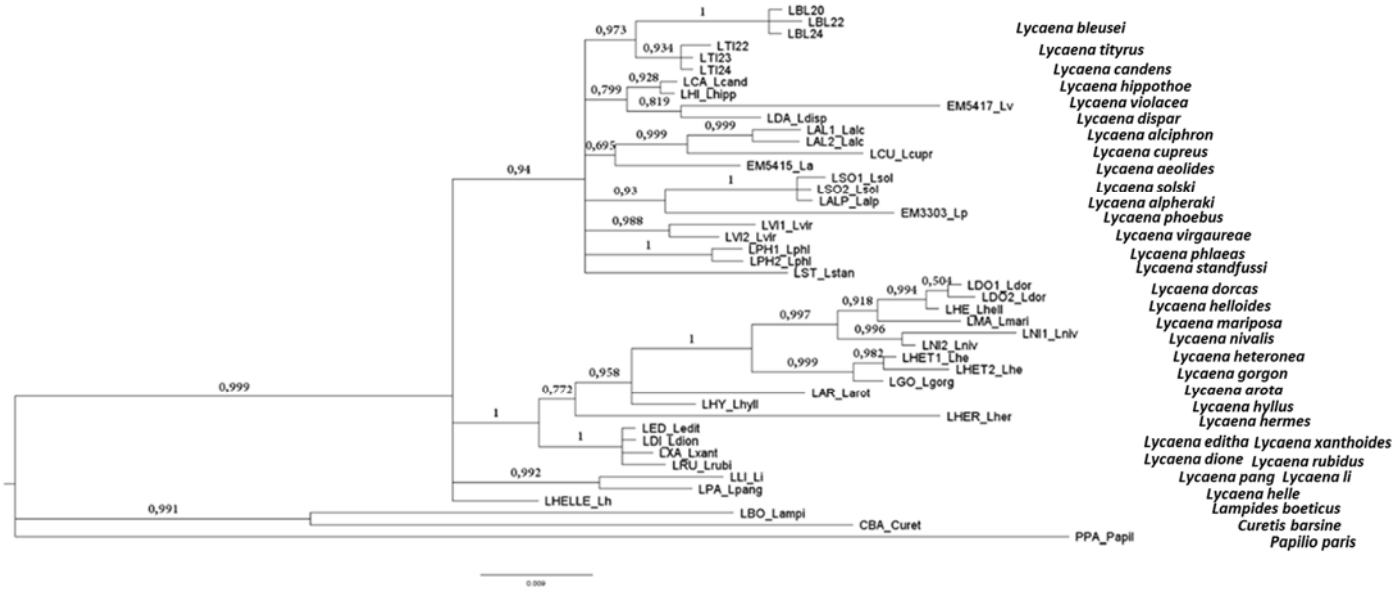

Figure S4.2 – Bayesian inference phylogeny of *Lycaena* based on the analysis of EF-1α gene haplotypes (Dataset 5). Bayesian posterior probabilities higher than 0.7 are shown along branches.

Figure S4.3 – Maximum likelihood phylogeny of *Lycaena* based on the analysis of COI gene haplotypes (Dataset 3). Bootstrap values above 50 are shown along branches.

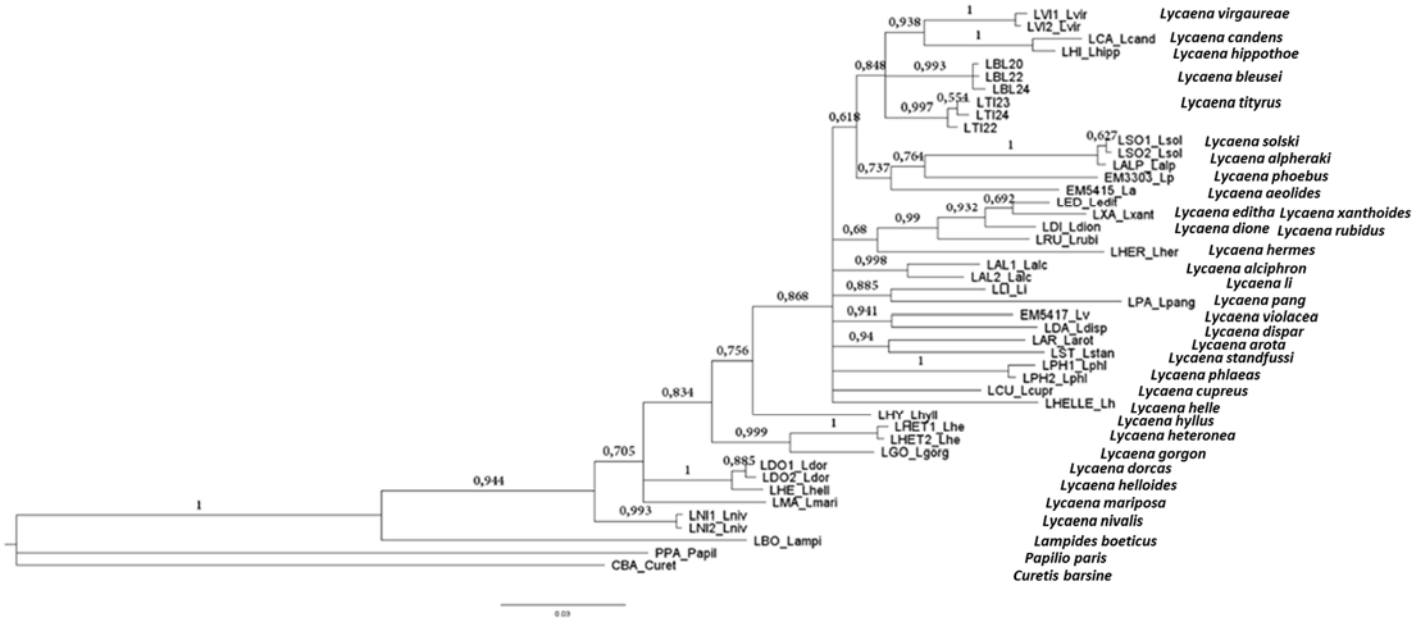

Figure S4.4 – Bayesian inference phylogeny of *Lycaena* based on the analysis of COI gene haplotypes (Dataset 3). Bayesian posterior probabilities higher than 0.7 are shown along branches.

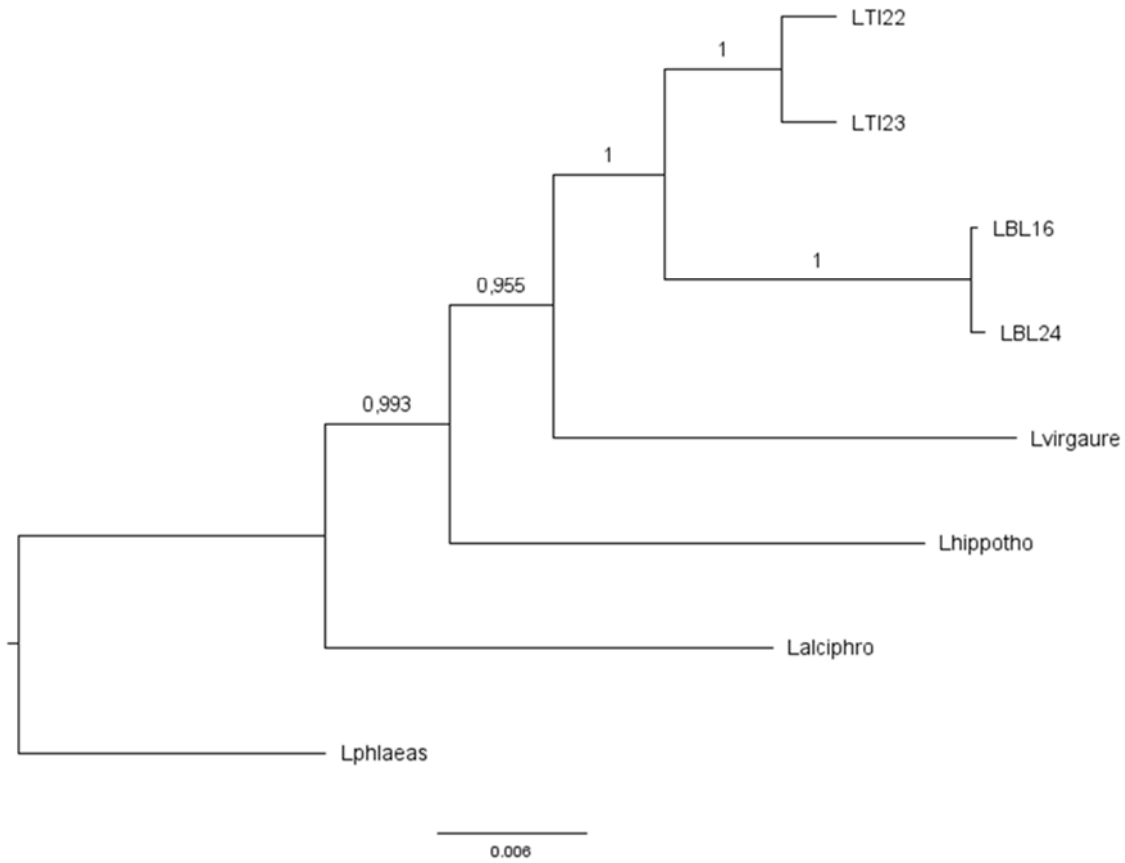

Figure S4.5 – Five gene (COI, 16S, EF-1α, Wg, CAD2) Bayesian inference phylogeny of the Sooty Coppers ingroup clade (Datasets 6 + 7 + 8 + 9 + 10). Bayesian posterior probabilities higher than 0.7 are shown along branches. The names of the taxa are shown at the tip of the topology.

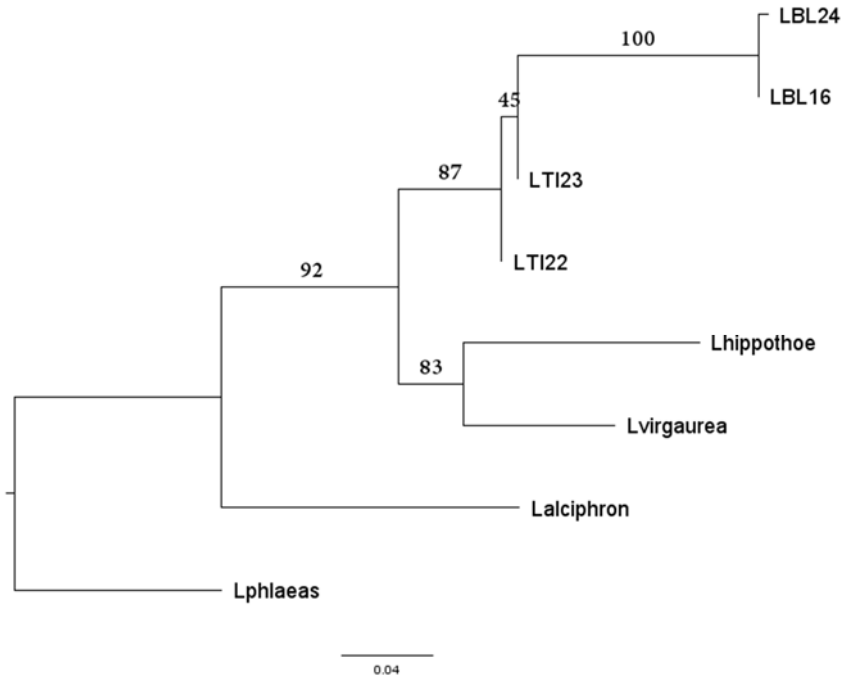

Figure S4.6 – Maximum likelihood phylogeny of the Sooty Coppers ingroup clade based on the COI gene haplotypes (Dataset 9). Bootstrap values above 50 are shown along branches. The names of the taxa are shown at the tip of the topology.

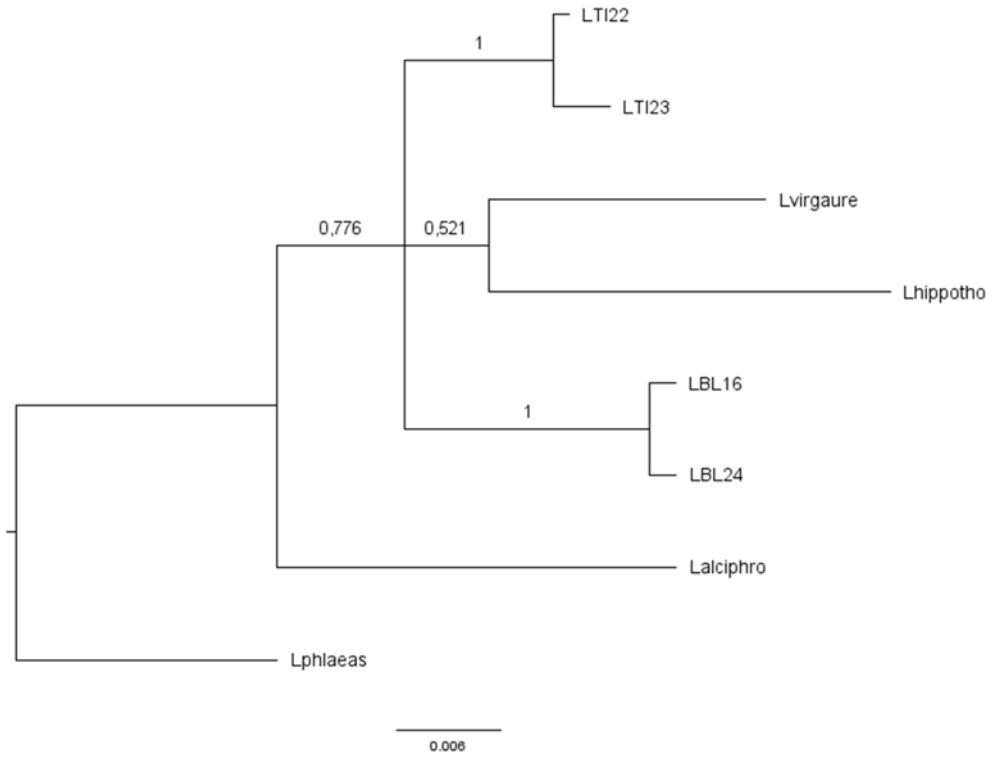

Figure S4.7 – Bayesian inference phylogeny of the Sooty Coppers ingroup clade based on the COI gene haplotypes (Dataset 9). Bayesian posterior probabilities higher than 0.7 are shown along branches. The names of the taxa are shown at the tip of the topology.

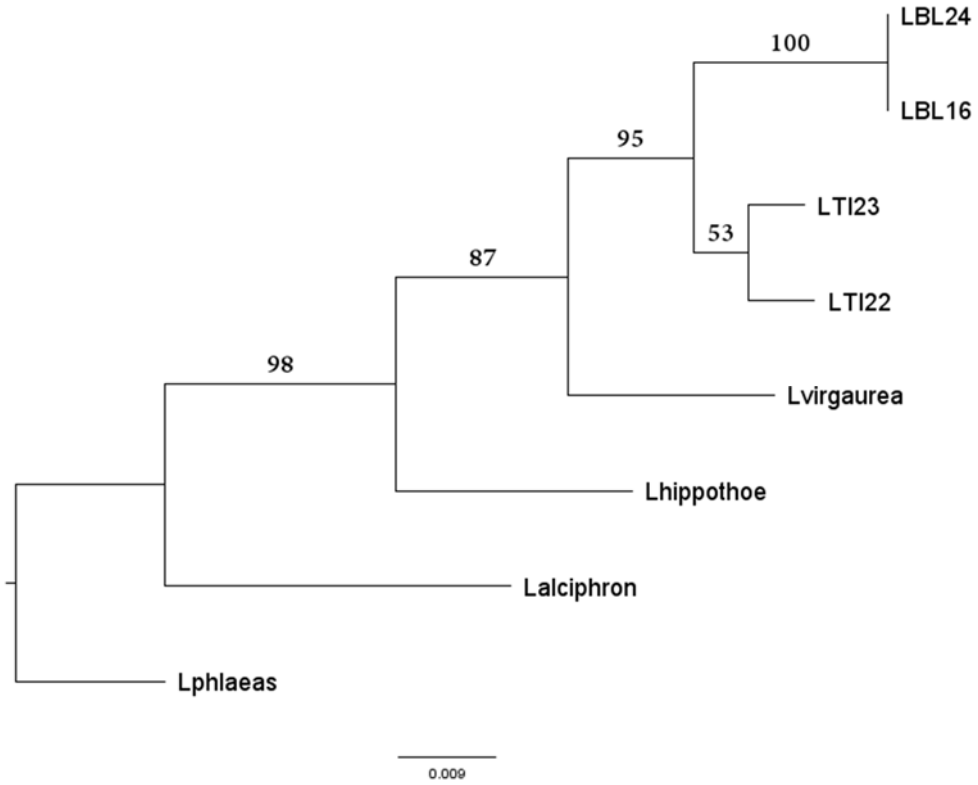

Figure S4.8 – Maximum likelihood phylogeny of the Sooty Coppers ingroup clade based on the 16S gene haplotypes (Dataset 6). Bootstrap values above 50 are shown along branches. The names of the taxa are shown at the tip of the topology.

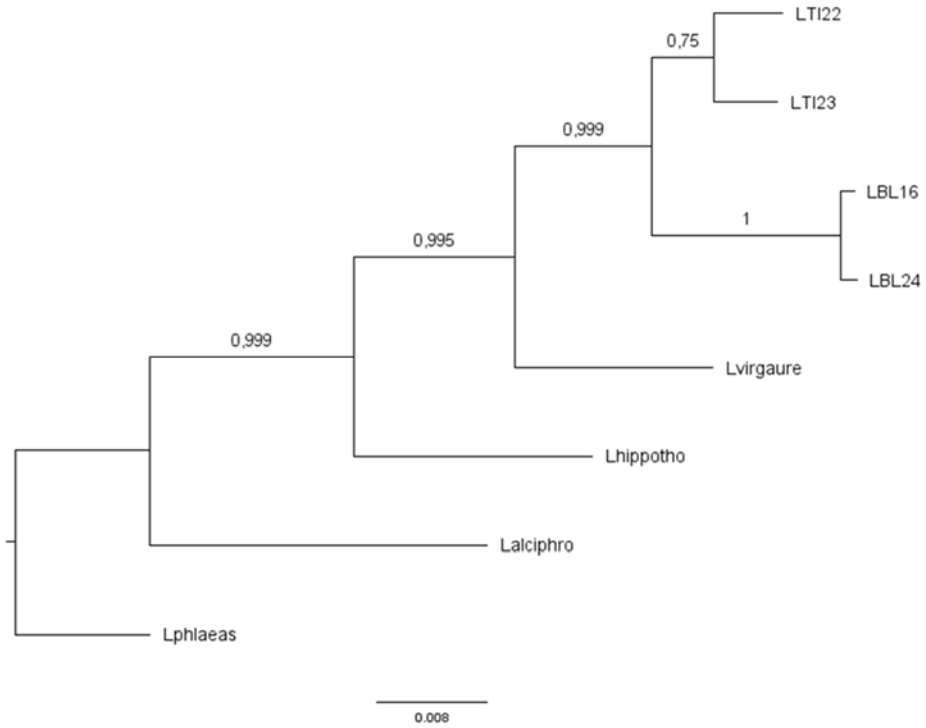

Figure S4.9 – Bayesian inference phylogeny of the Sooty Coppers ingroup clade based on the 16S gene haplotypes (Dataset 6). Bayesian posterior probabilities higher than 0.7 are shown along branches. The names of the taxa are shown at the tip of the topology.

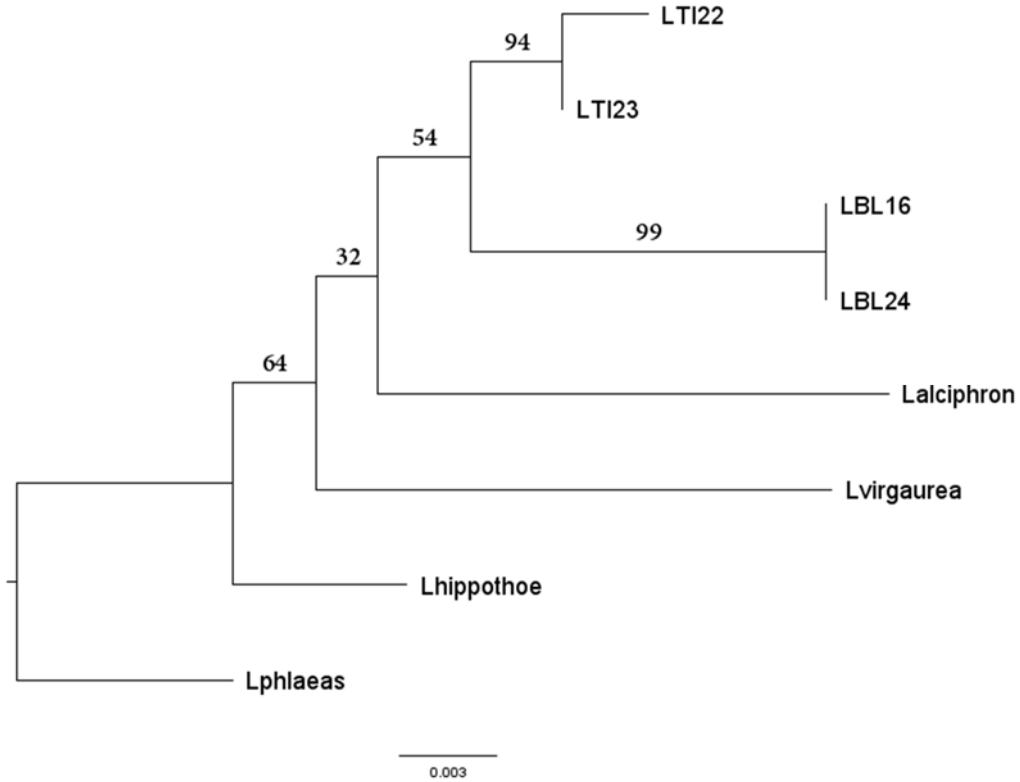

Figure S4.10 – Maximum likelihood phylogeny of the Sooty Coppers ingroup clade based on the EF-1α gene haplotypes (Dataset 10). Bootstrap values above 50 are shown along branches. The names of the taxa are shown at the tip of the topology.

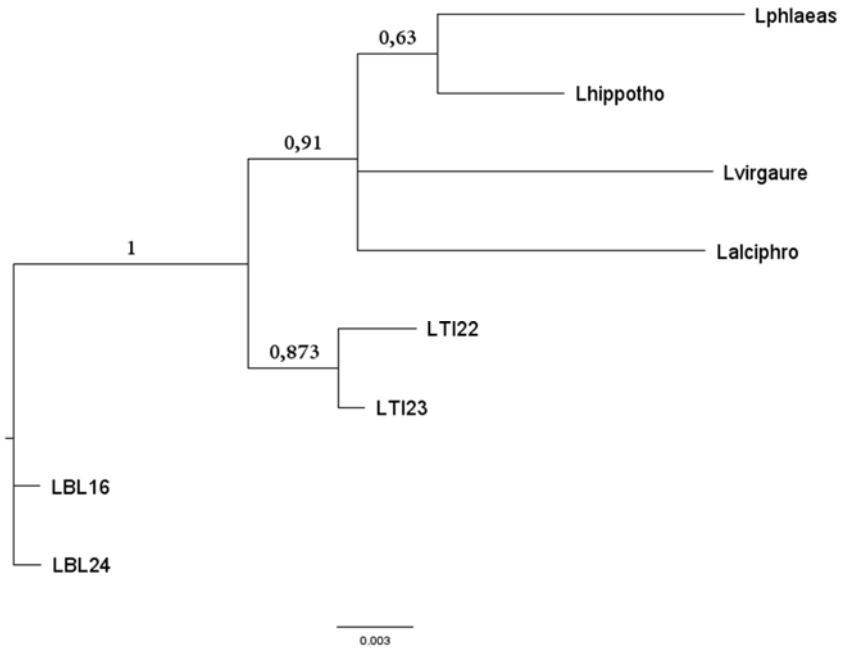

Figure S4.11 – Bayesian inference phylogeny of the Sooty Coppers ingroup clade based on the EF-1α gene haplotypes (Dataset 10). Bayesian posterior probabilities higher than 0.7 are shown along branches. The names of the taxa are shown at the tip of the topology.

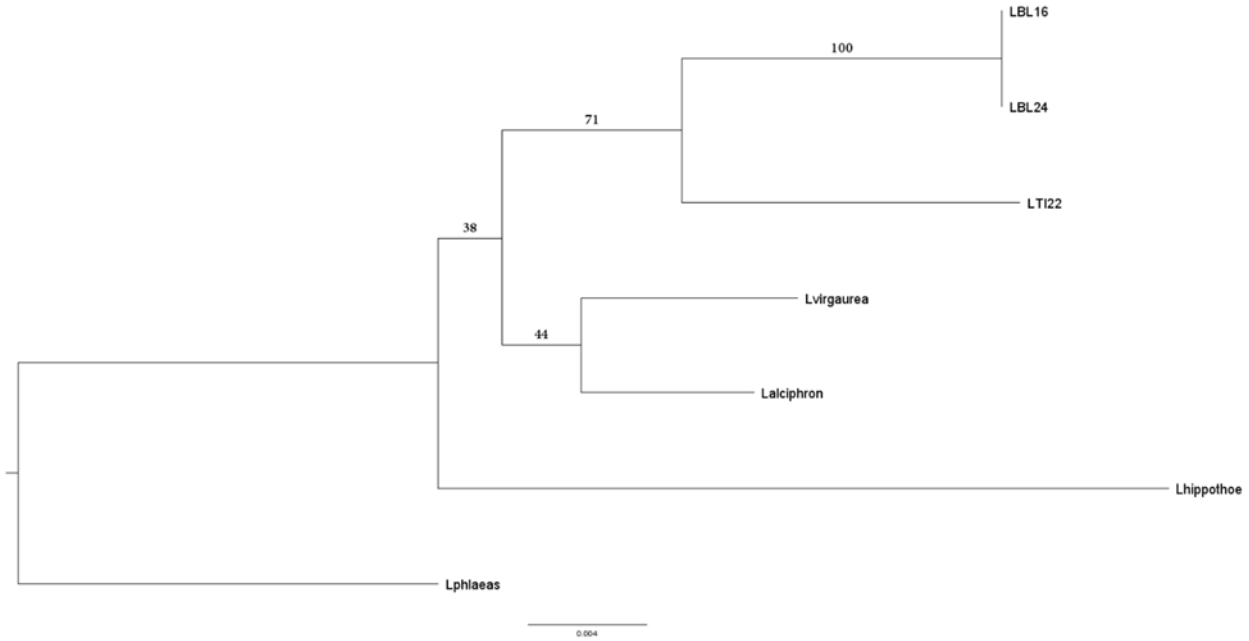

Figure S4.12 – Maximum likelihood phylogeny of the Sooty Coppers ingroup clade based on the Wingless gene haplotypes (Dataset 7). Bootstrap values above 50 are shown along branches. The names of the taxa are shown at the tip of the topology.

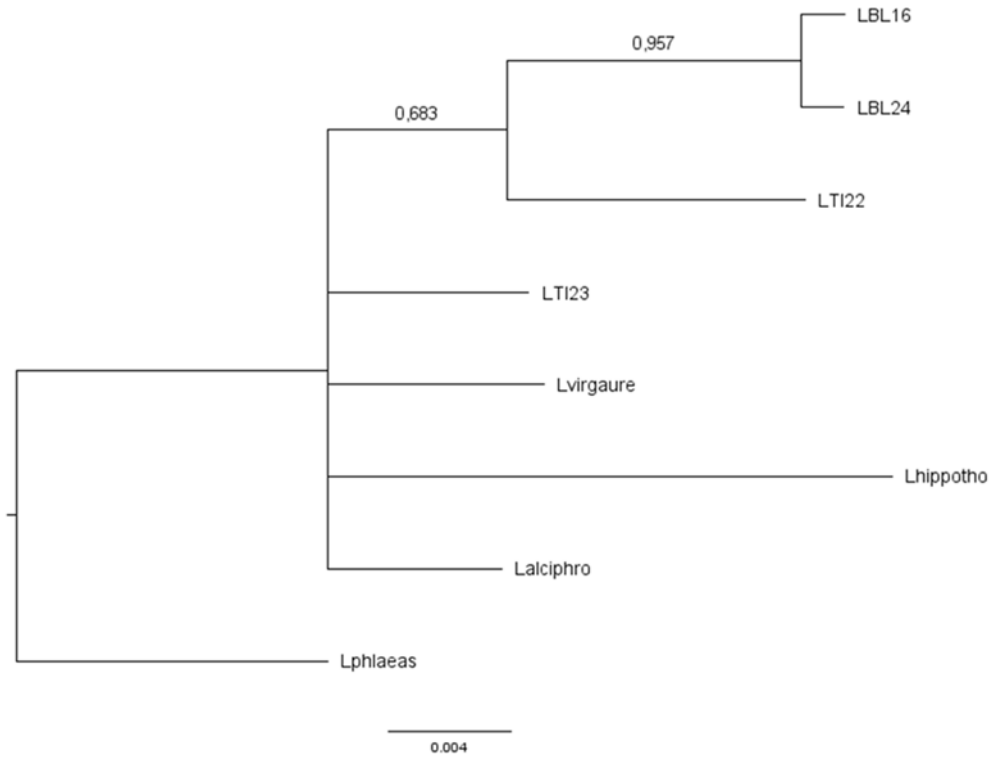

Figure S4.13 – Bayesian inference phylogeny of the Sooty Coppers ingroup clade based on the Wingless gene haplotypes (Dataset 7). Bayesian posterior probabilities higher than 0.7 are shown along branches. The names of the taxa are shown at the tip of the topology.

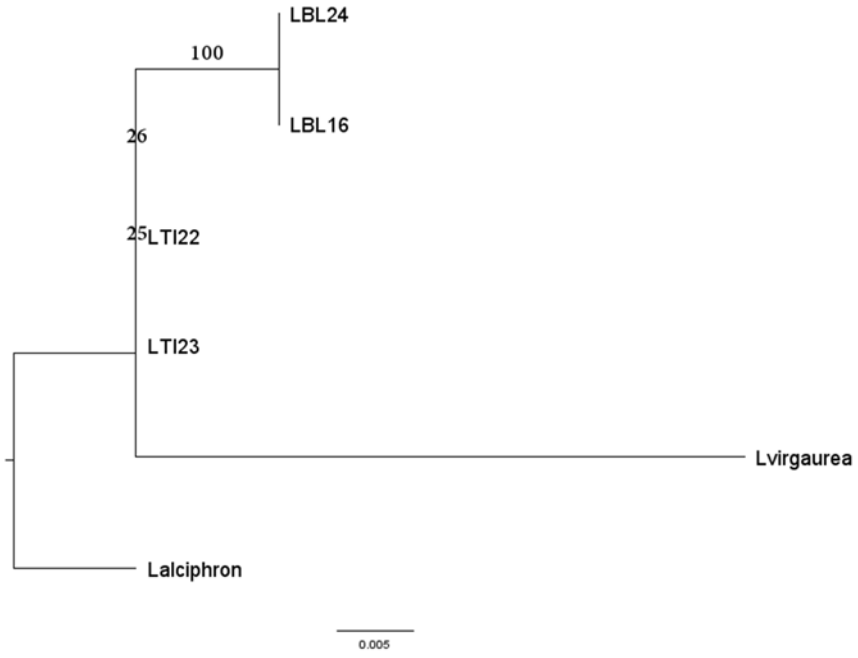

Figure S4.14 – Maximum likelihood phylogeny of the Sooty Coppers ingroup clade based on the CAD2 gene haplotypes (Dataset 8). Bootstrap values above 50 are shown along branches. The names of the taxa are shown at the tip of the topology.

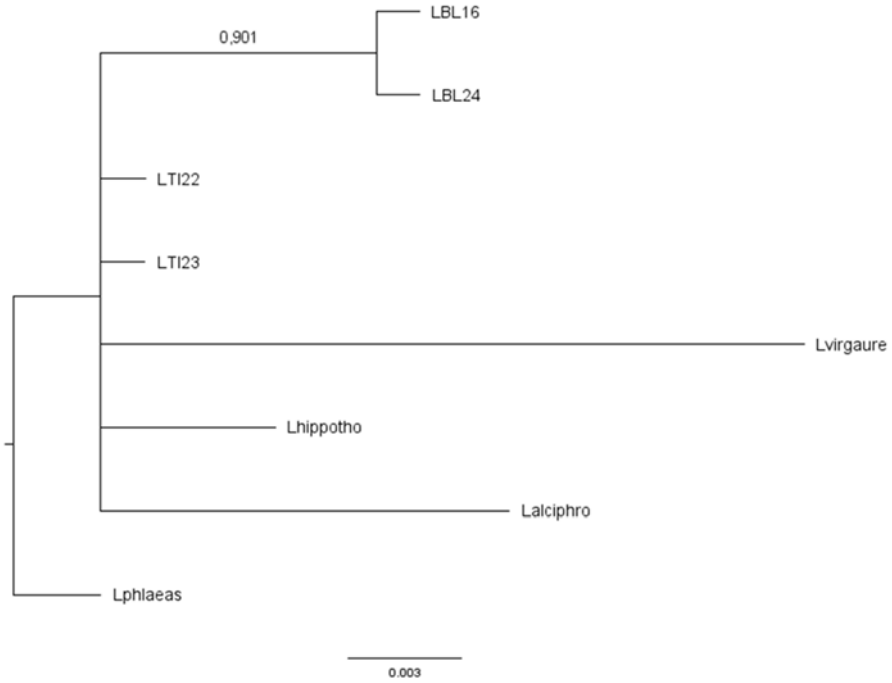

Figure S4.15 – Bayesian inference phylogeny of the Sooty Coppers ingroup clade based on the CAD2 gene haplotypes (Dataset 8). Bayesian posterior probabilities higher than 0.7 are shown along branches. The names of the taxa are shown at the tip of the topology.

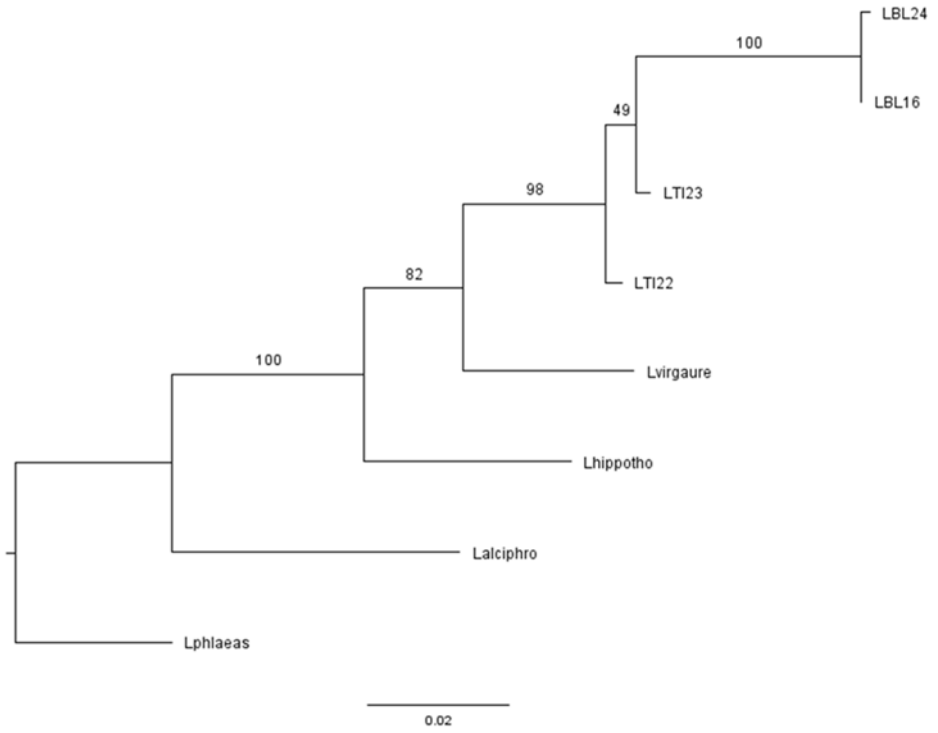

Figure S4.16 – Mitochondrial gene (COI + 16S) Maximum likelihood phylogeny of the Sooty Coppers ingroup clade (Datasets 6 + 9). Bootstrap values above 50 are shown along branches. The names of the taxa are shown at the tip of the topology.

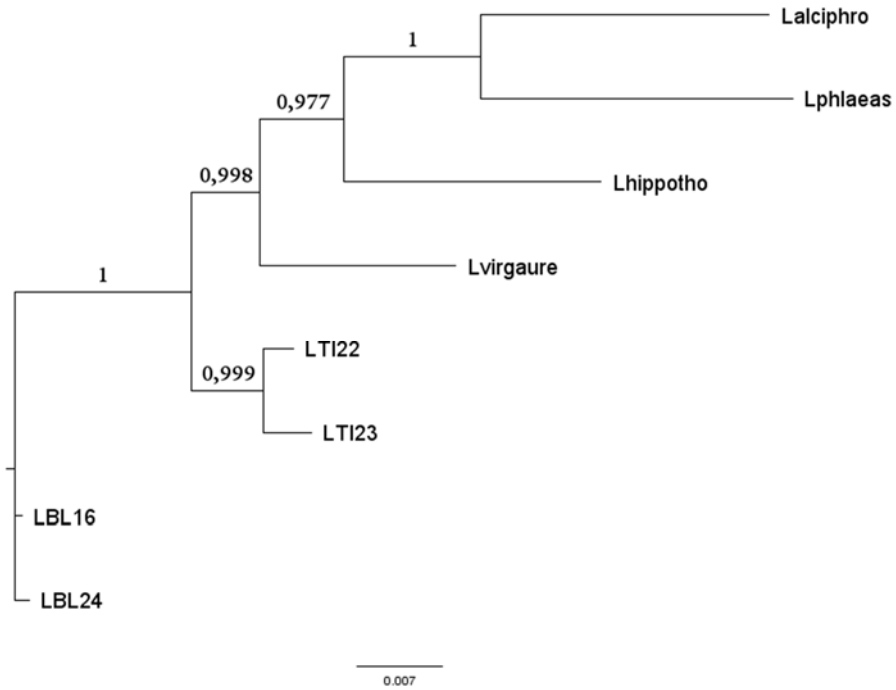

Figure S4.17 – Mitochondrial gene (COI + 16S) Bayesian inference phylogeny of the Sooty Coppers ingroup clade (Datasets 6 + 9). Bayesian posterior probabilities higher than 0.7 are shown along branches. The names of the taxa are shown at the tip of the topology.

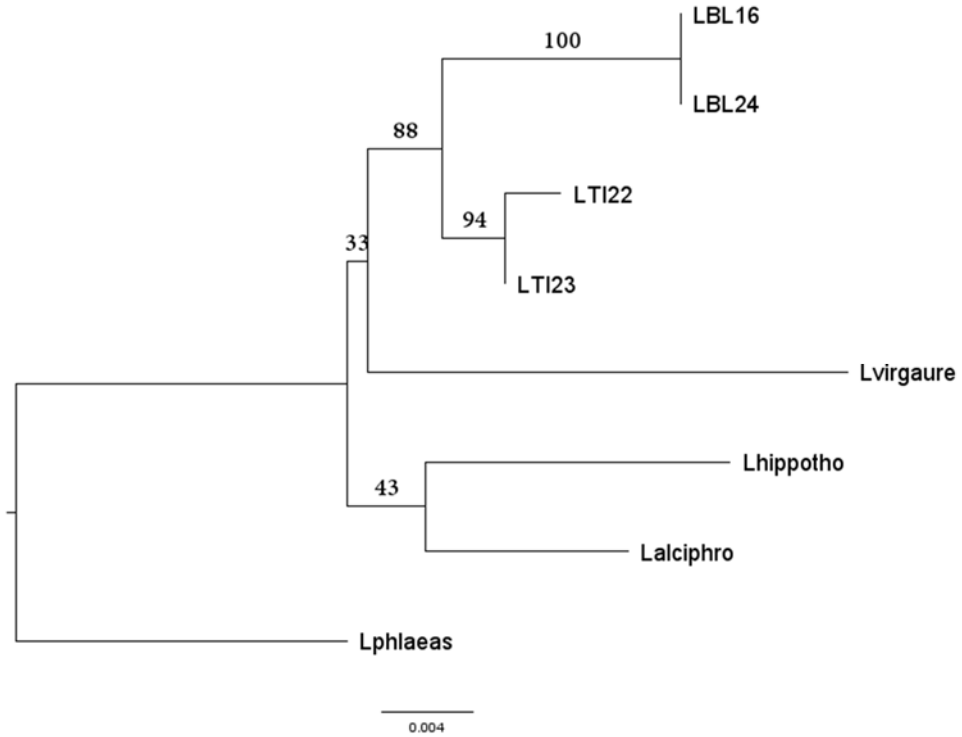

Figure S4.18 – Nuclear gene (Wingless, EF-1α + CAD2) Maximum likelihood phylogeny of the Sooty Coppers ingroup clade (Datasets 7 + 8 + 10). Bootstrap values above 50 are shown along branches. The names of the taxa are shown at the tip of the topology.

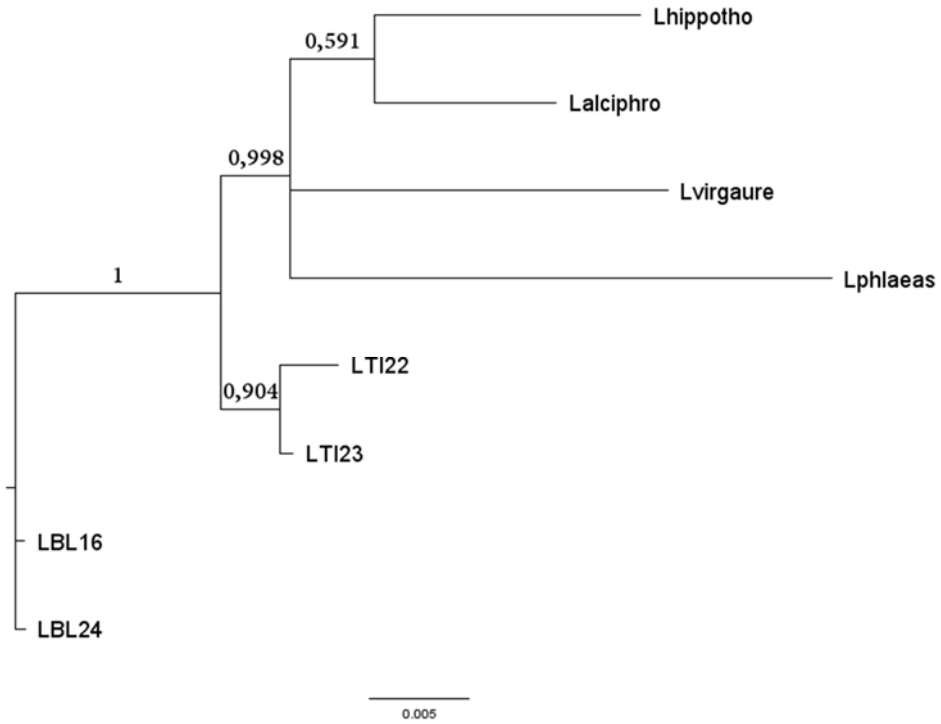

Figure S4.19 – Nuclear gene (Wingless, EF-1α + CAD2) Bayesian inference phylogeny of the Sooty Coppers ingroup clade (Datasets 7 + 8 + 10). Bayesian posterior probabilities higher than 0.7 are shown along branches. The names of the taxa are shown at the tip of the topology.

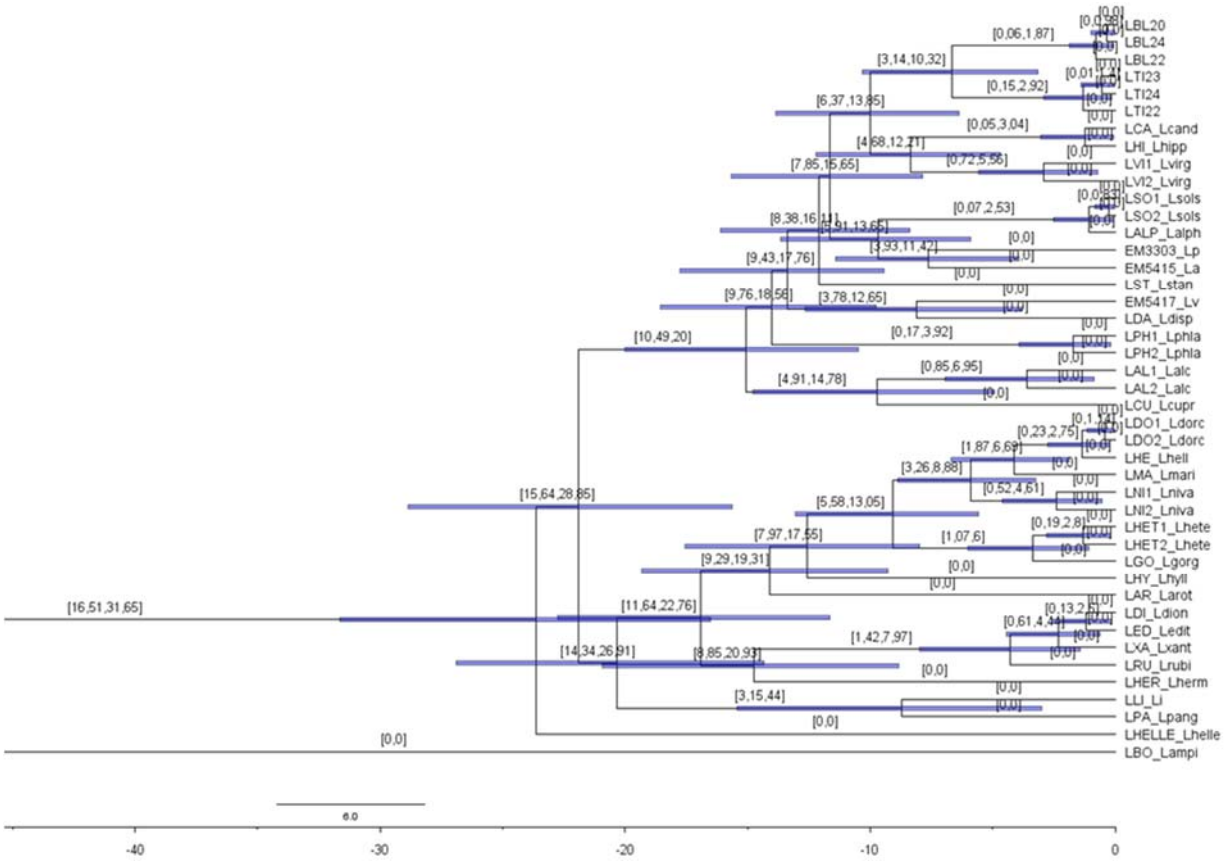

Figure S4.20 – Bayesian phylogeny with BEAST divergence time 95% HPD intervals of *Lycaena* based on the combined analysis of COI and EF-1α gene haplotypes (Datasets 3 + 5). The names of all taxa included are shown at the tip of the topology.

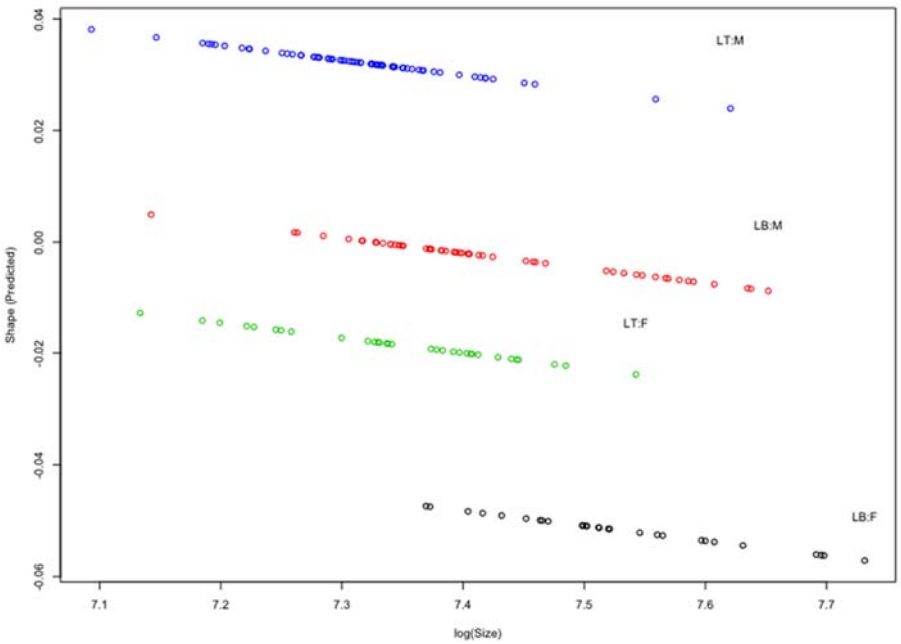

Figure S4.21 – Graphic representation of centroid size vectors between groups for the allometric inference: LT:M – *Lycaena tityrus* males; LB:M – *Lycaena bleusei* males; LT:F – *Lycaena tityrus* females; LB:F – *Lycaena bleusei* females.

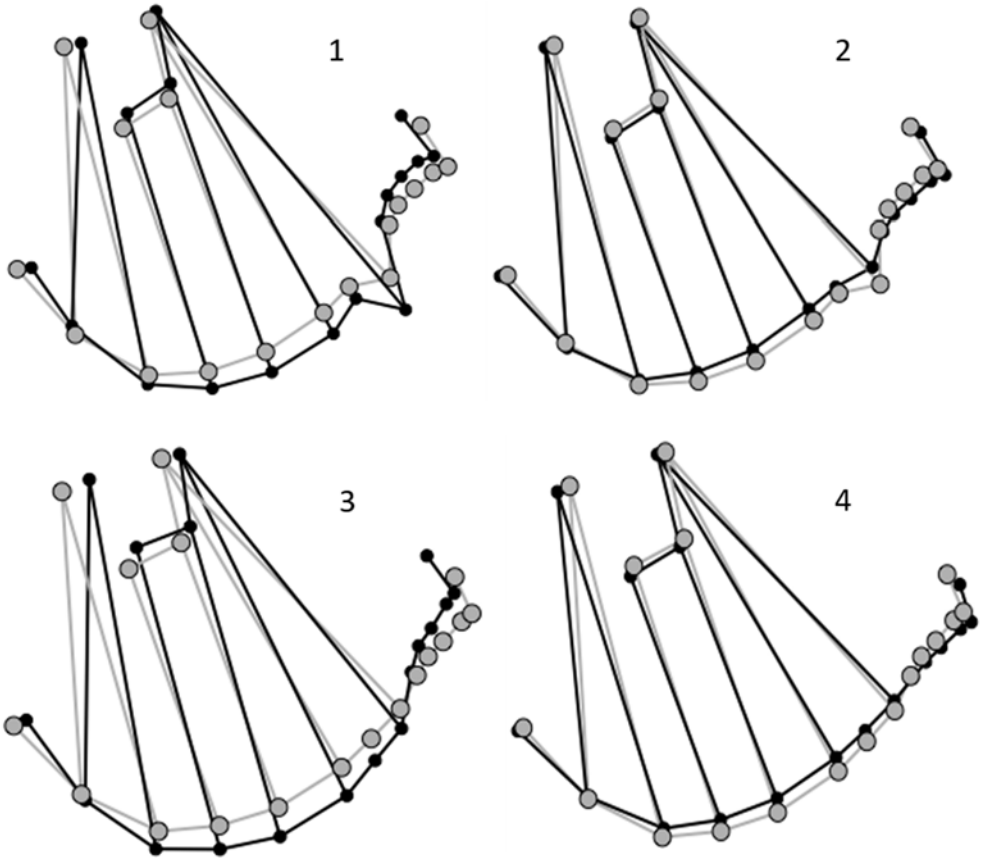

Figure S4.22 – Wing shape comparison between sexes. Differences between means of each species individuals (females + males; grey lines) against individual sexes (black lines). A – Mean of all *L. bleusei* individuals against the mean of *L. bleusei* females. B - Mean of all *L. bleusei* individuals against the mean of *L. bleusei* males. C - Mean of all *L. tityrus* individuals against the mean of *L. tityrus* females. D - Mean of all *L. tityrus* individuals against the mean of *L. tityrus* males.

Pairwise comparisons using t tests with pooled SD

data: CS and gr2

	LB_F P	LB_F V	LB_M P	LB_M V	LT_F P	LT_F V	LT_M P
LB_F V	1.00000	-	-	-	-	-	-
LB_M P	1.00000	0.00081	-	-	-	-	-
LB_M V	0.34910	1.2e-05	1.00000	-	-	-	-
LT_F P	0.01569	3.5e-08	0.20271	1.00000	-	-	-
LT_F V	0.00048	1.7e-08	0.00524	0.18384	1.00000	-	-
LT_M P	1.3e-05	1.4e-14	1.0e-05	0.04060	1.00000	1.00000	-
LT_M V	5.4e-05	7.5e-11	0.00039	0.05416	0.93749	1.00000	1.00000

P value adjustment method: bonferroni

Figure S4.23 – Pairwise t-test with Bonferroni correction for multiple comparison of centroid size between groups in Geometric Morphometric analyses.

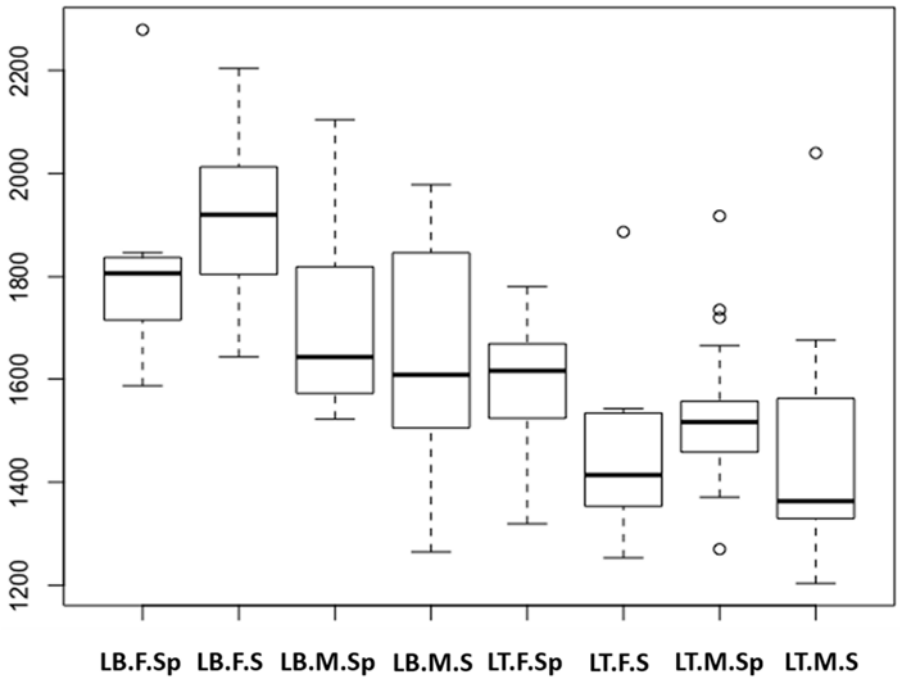

Figure S4.24 – Boxplot graphic of hindwing centroid size variation comparing species, sexes within species and specimens between seasons. LB.F.Sp – *Lycaena bleusei* females from Spring; LB.F.S – *Lycaena bleusei* females from Summer; LB.M.Sp – *Lycaena bleusei* males from Spring; LB.M.S – *Lycaena bleusei* males from Summer; LT.F.Sp – *Lycaena tityrus* females from Spring; LT.F.S - *Lycaena tityrus* females from Summer; LT.M.Sp – *Lycaena tityrus* males from Spring; LT.M.S – *Lycaena tityrus* males from Summer.

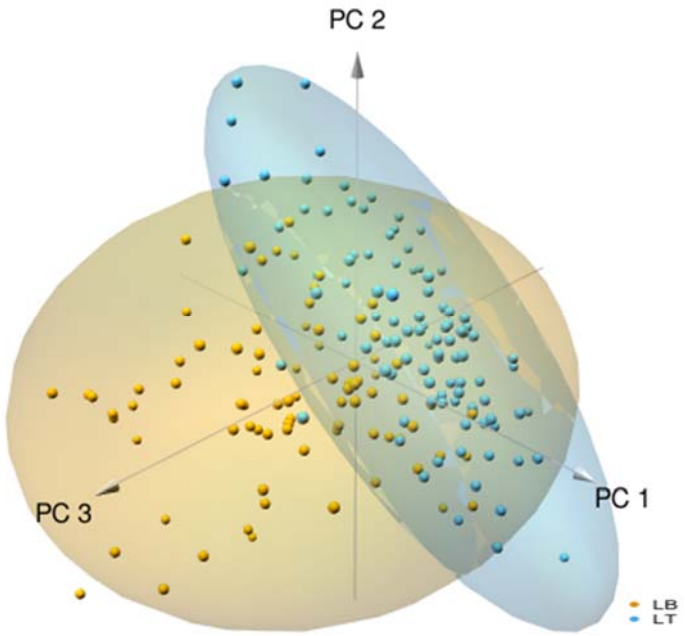

Figure S4.25 – Principal Component Analysis (PCA) of hindwing centroid size data from both taxa. LB – *Lycaena bleusei*; LT – *Lycaena tityrus*.

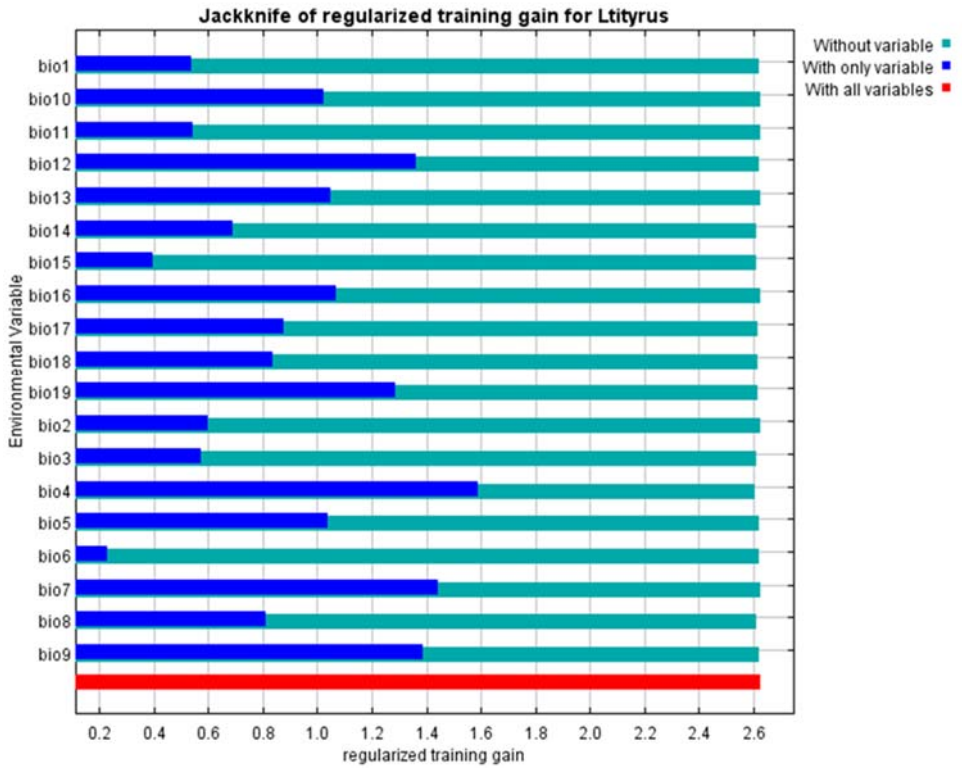

Figure S4.26 – Bioclimatic variables impact on *L. tityrus* distribution obtained with Maxent.

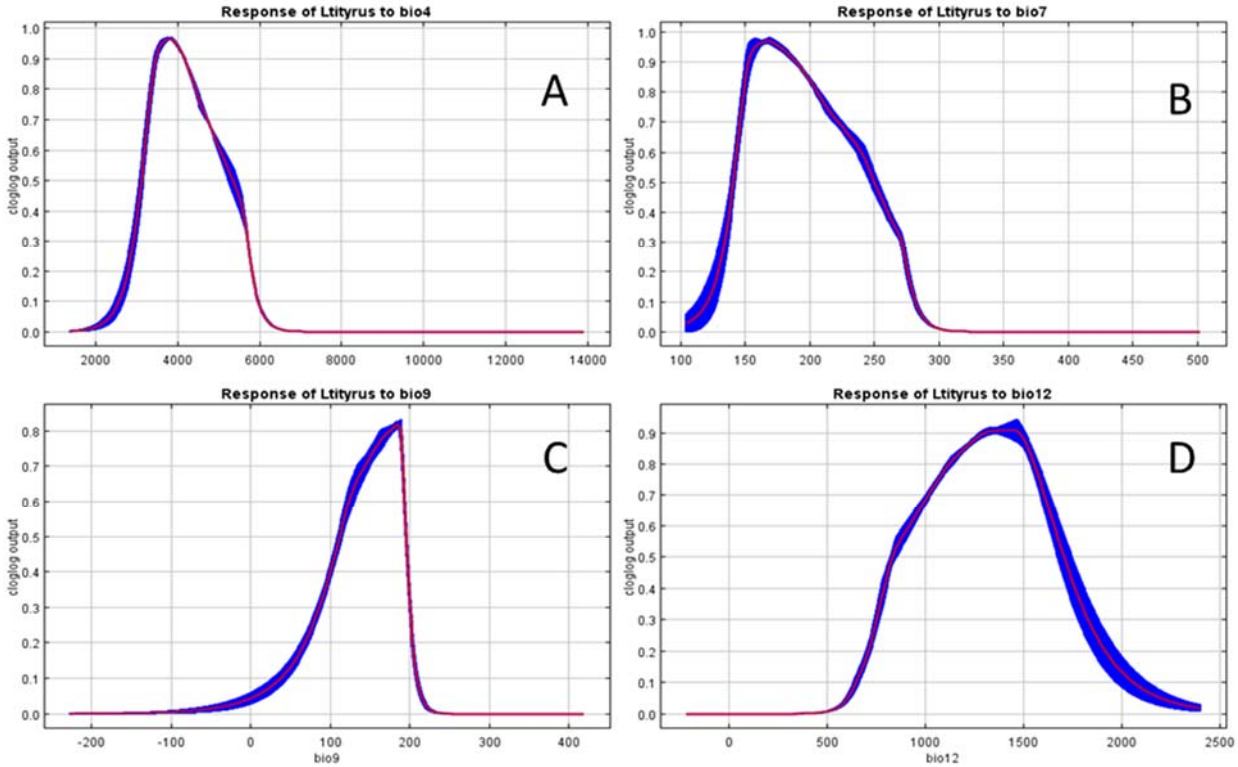

Figure S4.27 – Most influent bioclimatic variables for *L. tityrus* distribution obtained with Maxent. Response of *L. tityrus* to: (A) – Bio4; (B) – Bio7; (C) – Bio9; (D) – Bio12.

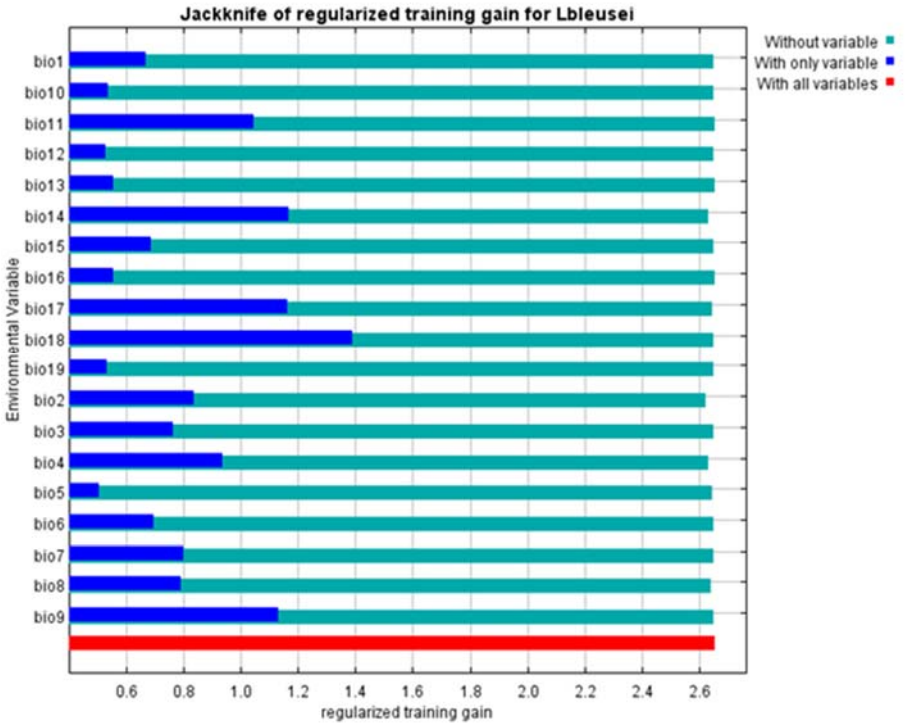

Figure S4.28 – Bioclimatic variables impact on *L. bleusei* distribution obtained with Maxent.

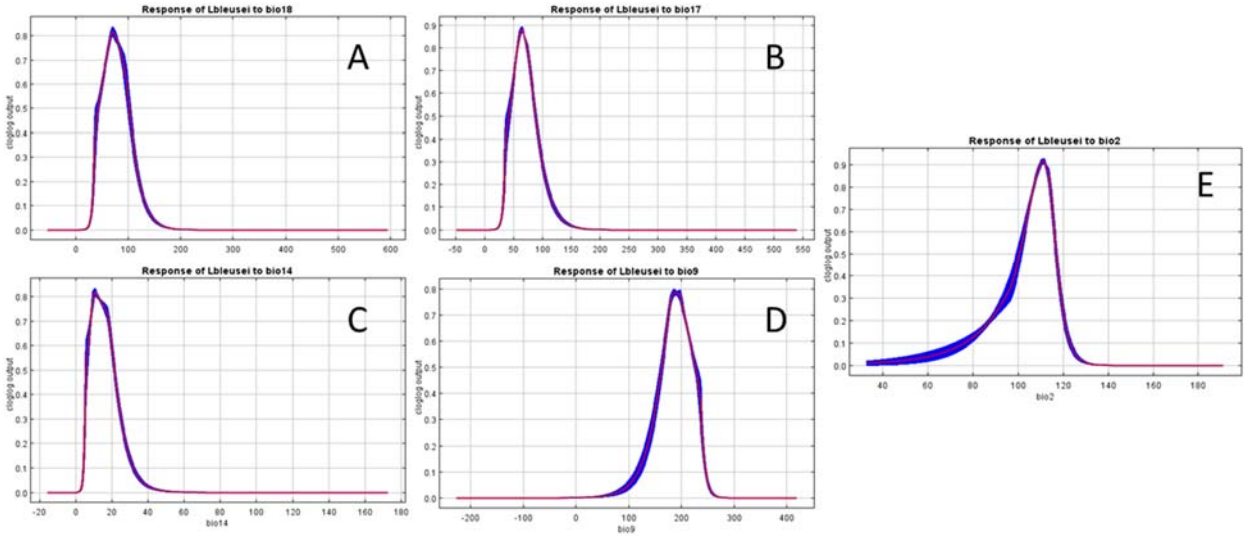

Figure S4.29 – Most influent bioclimatic variables for *L. bleusei* distribution obtained with Maxent. Response of *L. bleusei* to: (A) – Bio18; (B) – Bio17; (C) – Bio14; (D) – Bio9; (E) – Bio2.

	1	2	3	4	5	6	7	8	9	10	11	12	13	14	15
1. M.ines NS															
2. M.ines CS	0.005														
3. M.ines SS	0.003	0.005													
4. M.ines MA	0.049	0.047	0.049												
5. M.ines HA	0.046	0.044	0.046	0.012											
6. M.ines AA	0.047	0.046	0.047	0.014	0.002										
7. M.occi NI	0.075	0.076	0.075	0.088	0.088	0.090									
8. M.occi Fr	0.075	0.076	0.075	0.088	0.088	0.090	0.000								
9. M.occi NI	0.079	0.081	0.079	0.093	0.093	0.094	0.008	0.008							
10. M.occi CI	0.079	0.081	0.079	0.093	0.093	0.094	0.009	0.009	0.002						
11. M.occi SI	0.079	0.081	0.079	0.090	0.090	0.091	0.009	0.009	0.005	0.006					
12. M.occi MA	0.073	0.075	0.073	0.084	0.084	0.085	0.026	0.026	0.026	0.027	0.024				
13. M.o.pherusa	0.082	0.084	0.082	0.084	0.084	0.085	0.035	0.035	0.035	0.037	0.033	0.009			
14. M.arge	0.085	0.087	0.085	0.090	0.090	0.088	0.037	0.037	0.038	0.040	0.037	0.033	0.040		
15. M.jurtina	0.079	0.081	0.078	0.102	0.099	0.100	0.097	0.097	0.099	0.097	0.099	0.094	0.104	0.104	

Figure S6.1 – *Melanargia* COI pairwise distances using Dataset 1.

	1	2	3	4	5	6	7	8	9	10	11	12	13	14	15
1. M.ines NS															
2. M.ines CS	n/c														
3. M.ines SS	n/c	0.000													
4. M.ines MA	n/c	0.004	0.004												
5. M.ines HA	n/c	0.027	0.027	0.031											
6. M.ines AA	n/c	0.004	0.004	0.004	0.031										
7. M.occi NI	n/c	n/c	n/c	n/c	n/c	n/c									
8. M.occi Fr	n/c	0.025	0.025	0.029	0.029	0.029	n/c								
9. M.occi NI	n/c	n/c	n/c	n/c	n/c	n/c	n/c	n/c							
10. M.occi CI	n/c	n/c	n/c	n/c	n/c	n/c	n/c	n/c	n/c						
11. M.occi SI	n/c	n/c	n/c	n/c	n/c	n/c	n/c	n/c	n/c	n/c					
12. M.occi MA	n/c	0.022	0.022	0.025	0.027	0.025	n/c	0.008	n/c	n/c	n/c				
13. M.o.pherusa	n/c	0.023	0.023	0.027	0.027	0.027	n/c	0.006	n/c	n/c	n/c	0.002			
14. M.arge	n/c	0.020	0.020	0.023	0.029	0.023	n/c	0.010	n/c	n/c	n/c	0.010	0.012		
15. M.jurtina	n/c	0.068	0.068	0.068	0.083	0.065	n/c	0.068	n/c	n/c	n/c	0.070	0.070	0.070	

Figure S6.2 – *Melanargia* 16S pairwise distances using Dataset 2.

	1	2	3	4	5	6	7	8	9	10	11	12	13	14	15
1. M.ines NS															
2. M.ines CS	0.000														
3. M.ines SS	0.004	0.000													
4. M.ines MA	n/c	n/c	n/c												
5. M.ines HA	0.009	0.002	0.007	n/c											
6. M.ines AA	0.009	0.002	0.007	n/c	0.000										
7. M.occi NI	n/c	n/c	n/c	n/c	n/c	n/c									
8. M.occi Fr	0.040	0.032	0.036	n/c	0.031	0.031	n/c								
9. M.occi NI	0.042	0.033	0.038	n/c	0.033	0.033	n/c	0.002							
10. M.occi CI	0.042	0.033	0.038	n/c	0.033	0.033	n/c	0.002	0.003						
11. M.occi SI	0.042	0.033	0.038	n/c	0.033	0.033	n/c	0.002	0.003	0.000					
12. M.occi MA	0.045	0.036	0.040	n/c	0.036	0.036	n/c	0.004	0.005	0.005	0.005				
13. M.o.pherusa	n/c	n/c	n/c	n/c	n/c	n/c	n/c	n/c	n/c	n/c	n/c	n/c			
14. M.arge	0.047	0.039	0.040	n/c	0.038	0.038	n/c	0.014	0.016	0.016	0.016	0.012	n/c		
15. M.jurtina	0.088	0.089	0.094	n/c	0.091	0.091	n/c	0.102	0.102	0.104	0.105	0.107	n/c	0.104	

Figure S6.3 – *Melanargia* EF-1α pairwise distances using Dataset 3.

	1	2	3	4	5	6	7	8	9	10	11	12	13	14	15
1. M.ines NS															
2. M.ines CS	n/c														
3. M.ines SS	n/c	n/c													
4. M.ines MA	0.023	n/c	n/c												
5. M.ines HA	n/c	n/c	n/c	n/c											
6. M.ines AA	0.015	n/c	n/c	0.008	n/c										
7. M.occi NI	n/c	n/c	n/c	n/c	n/c	n/c									
8. M.occi Fr	n/c	n/c	n/c	n/c	n/c	n/c	n/c								
9. M.occi NI	0.049	n/c	n/c	0.086	n/c	0.076	n/c	n/c							
10. M.occi CI	n/c	n/c	n/c	n/c	n/c	n/c	n/c	n/c	n/c						
11. M.occi SI	n/c	n/c	n/c	n/c	n/c	n/c	n/c	n/c	n/c	n/c					
12. M.occi MA	0.040	n/c	n/c	0.045	n/c	0.041	n/c	n/c	0.055	n/c	n/c				
13. M.o.pherusa	n/c	n/c	n/c	n/c	n/c	n/c	n/c	n/c	n/c	n/c	n/c	n/c			
14. M.arge	0.030	n/c	n/c	0.038	n/c	0.028	n/c	n/c	0.049	n/c	n/c	0.020	n/c		
15. M.jurtina	0.081	n/c	n/c	0.079	n/c	0.074	n/c	n/c	0.086	n/c	n/c	0.060	n/c	0.065	

Figure S6.4 – *Melanargia* Wingless pairwise distances using Dataset 4.

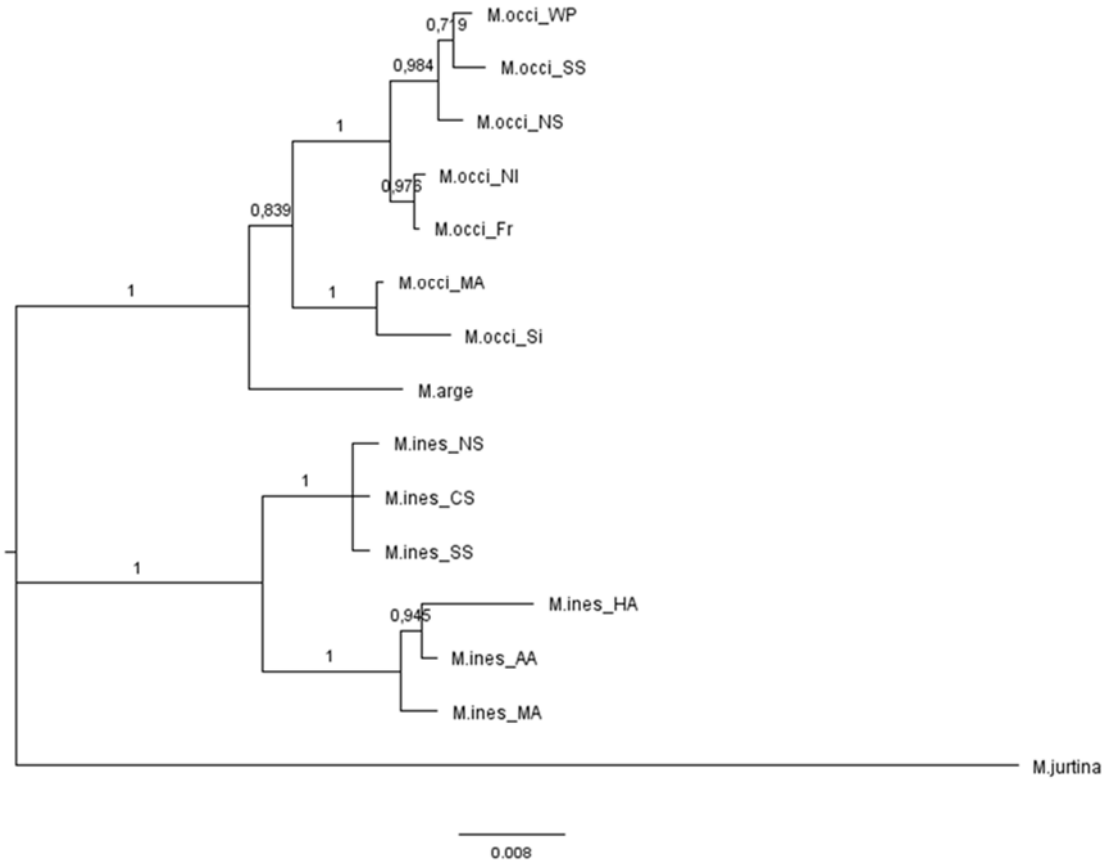

Figure S6.5 – *Melanargia* Bayesian phylogenetic tree using the concatenated dataset of 2 nuclear and 2 mitochondrial genes (Datasets 1 + 2 + 3 + 4). SS = South of Spain; CS = Central Spain; NS =North of Spain; WP = Western Portugal; NI = North Italy; MA = Middle Atlas; AA = Anti Atlas; HA = High Atlas;

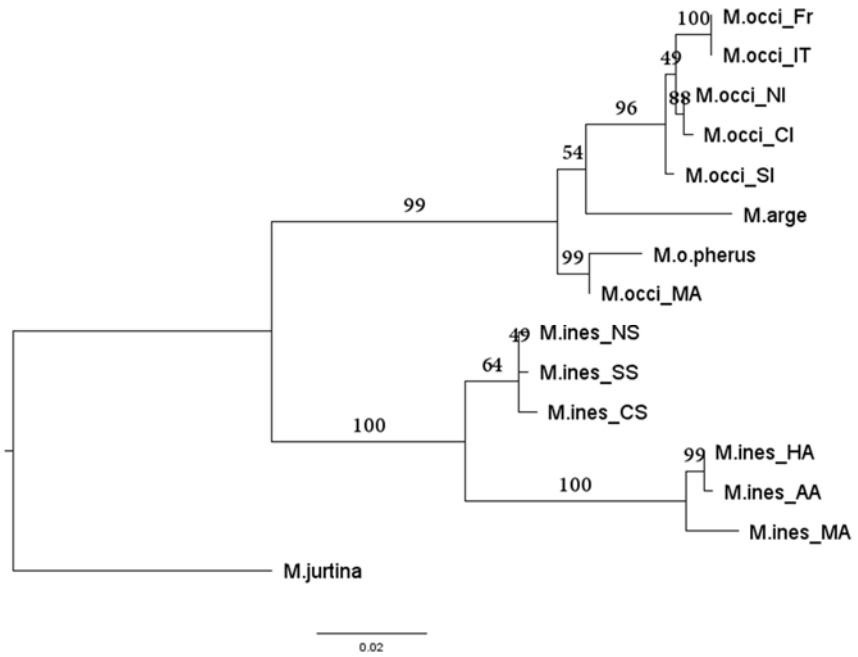

Figure S6.6 – *Melanargia* Maximum likelihood phylogenetic tree using COI gene haplotypes (Dataset 1). NI = North Iberia; CI = Central Iberial; SI = South Iberia; NS =North of Spain; SS = South of Spain; CS = Central Spain; IT = Italy (Liguria); MA = Middle Atlas; HA = High Atlas; AA = Anti Atlas.

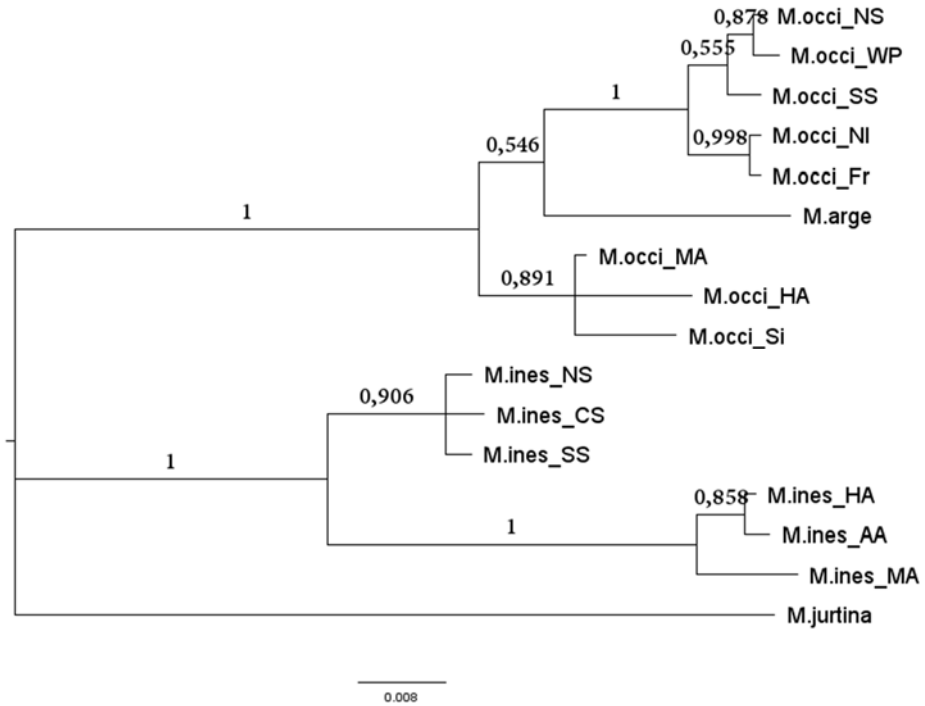

Figure S6.7 – *Melanargia* Bayesian phylogenetic tree using COI gene haplotypes (Dataset 1). SS = South of Spain; CS = Central Spain; NS =North of Spain; WP = Western Portugal; NI = North Italy; MA = Middle Atlas; AA = Anti Atlas; HA = High Atlas;

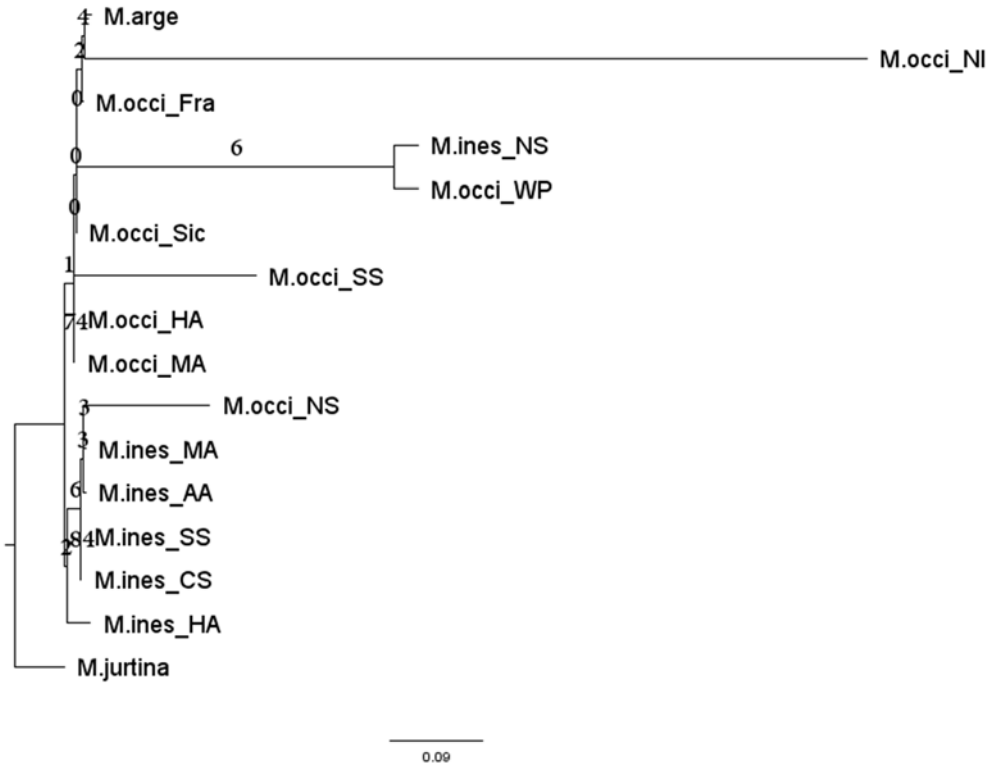

Figure S6.8 – *Melanargia* Maximum likelihood phylogenetic tree using 16S gene haplotypes (Dataset 2). SS = South of Spain; CS = Central Spain; NS =North of Spain; WP = Western Portugal; NI = North Italy; Fra = France; Sic = Sicily; MA = Middle Atlas; AA = Anti Atlas; HA = High Atlas.

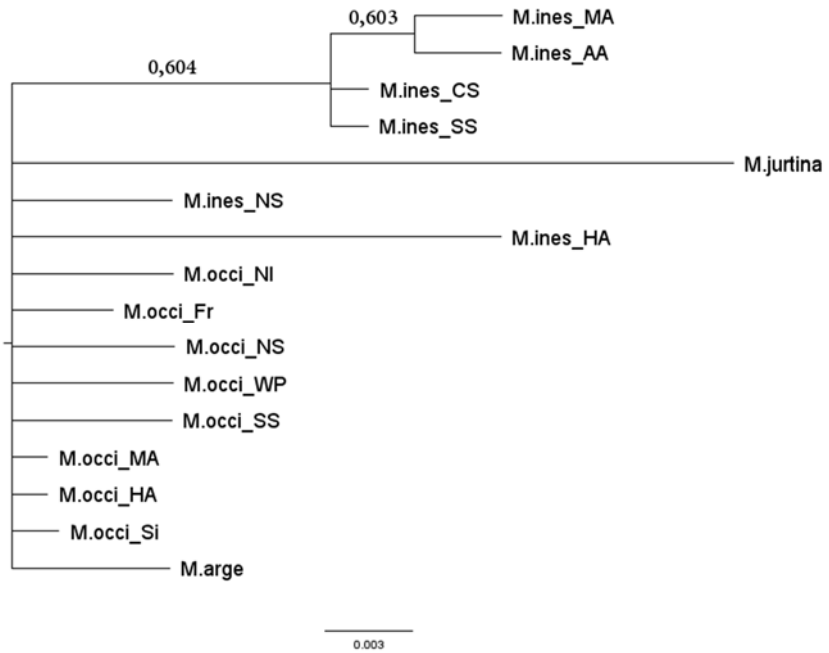

Figure S6.9 – *Melanargia* Bayesian phylogenetic tree using 16S gene haplotypes (Dataset 2). SS = South of Spain; CS = Central Spain; NS =North of Spain; WP = Western Portugal; NI = North Italy; Fr = France; Si = Sicily; MA = Middle Atlas; AA = Anti Atlas; HA = High Atlas.

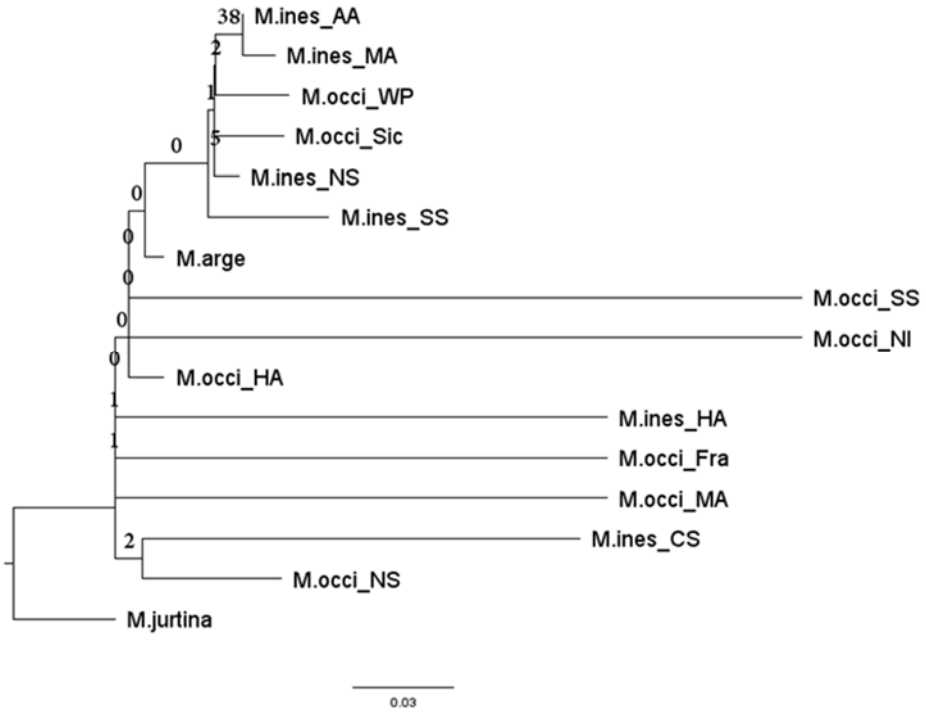

Figure S6.10 – *Melanargia* Maximum likelihood phylogenetic tree using EF-1α gene haplotypes (Dataset 3). SS = South of Spain; CS = Central Spain; NS =North of Spain; WP = Western Portugal; NI = North Italy; FR = France; Sic = Sicily; MA = Middle Atlas; AA = Anti Atlas; HA = High Atlas.

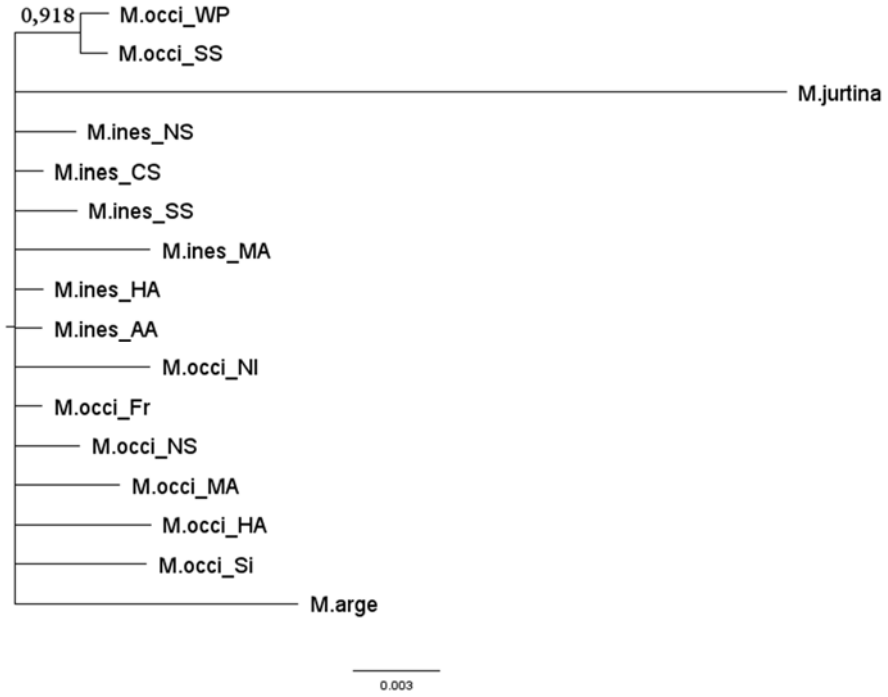

Figure S6.11 – *Melanargia* Bayesian phylogenetic tree using EF-1α gene haplotypes (Dataset 3). SS = South of Spain; CS = Central Spain; NS =North of Spain; WP = Western Portugal; NI = North Italy; Fr = France; Si = Sicily; MA = Middle Atlas; AA = Anti Atlas; HA = High Atlas.

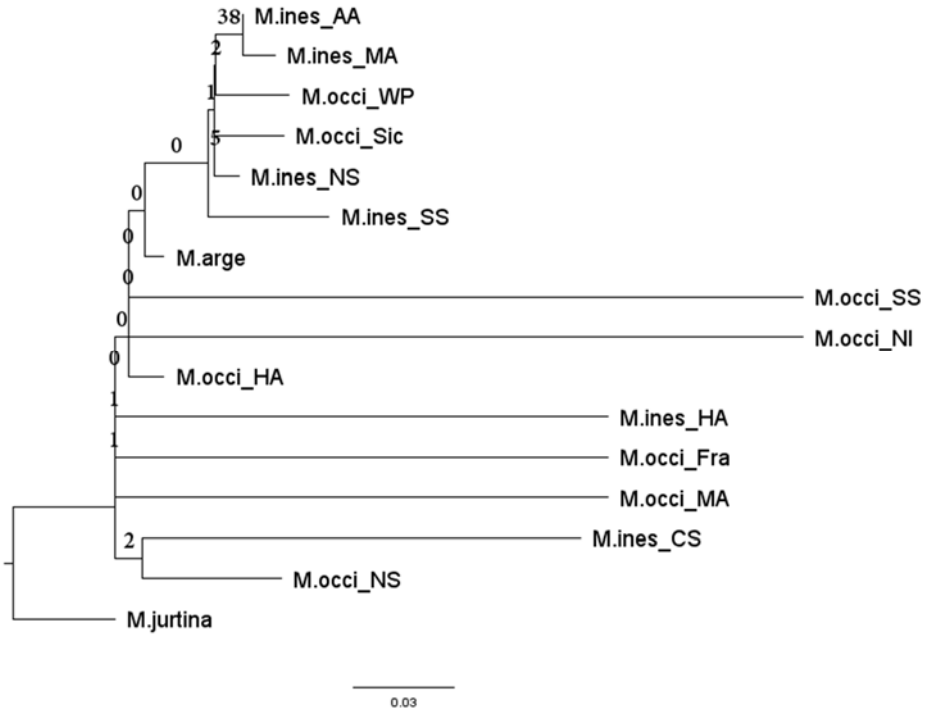

Figure S6.12 – *Melanargia* Maximum likelihood phylogenetic tree using Wingless gene haplotypes (Dataset 4). SS = South of Spain; CS = Central Spain; NS =North of Spain; WP = Western Portugal; NI = North Italy; Fra = France; Sic = Sicily; MA = Middle Atlas; AA = Anti Atlas; HA = High Atlas.

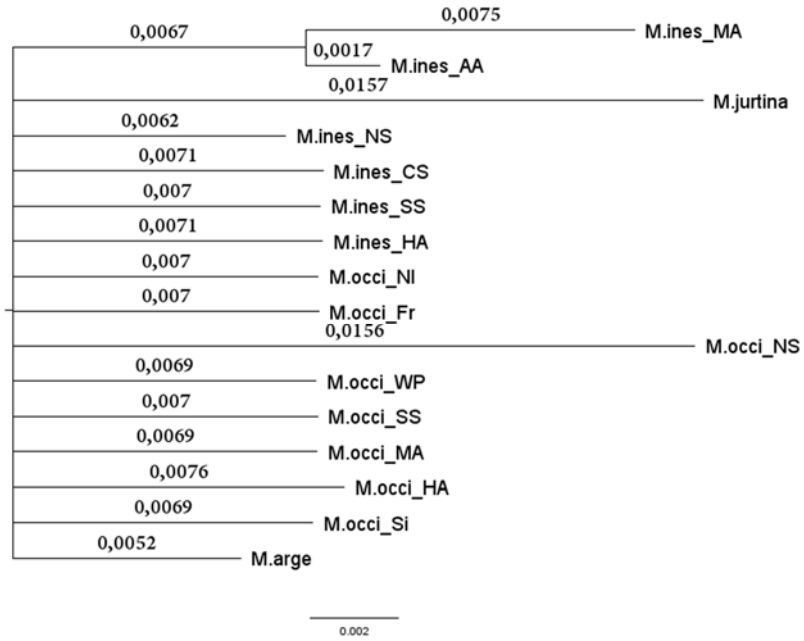

Figure S6.13 – *Melanargia* Bayesian phylogenetic tree using Wingless gene haplotypes (Dataset 4). SS = South of Spain; CS = Central Spain; NS =North of Spain; WP = Western Portugal; NI = North Italy; Fr = France; Si = Sicily; MA = Middle Atlas; AA = Anti Atlas; HA = High Atlas.

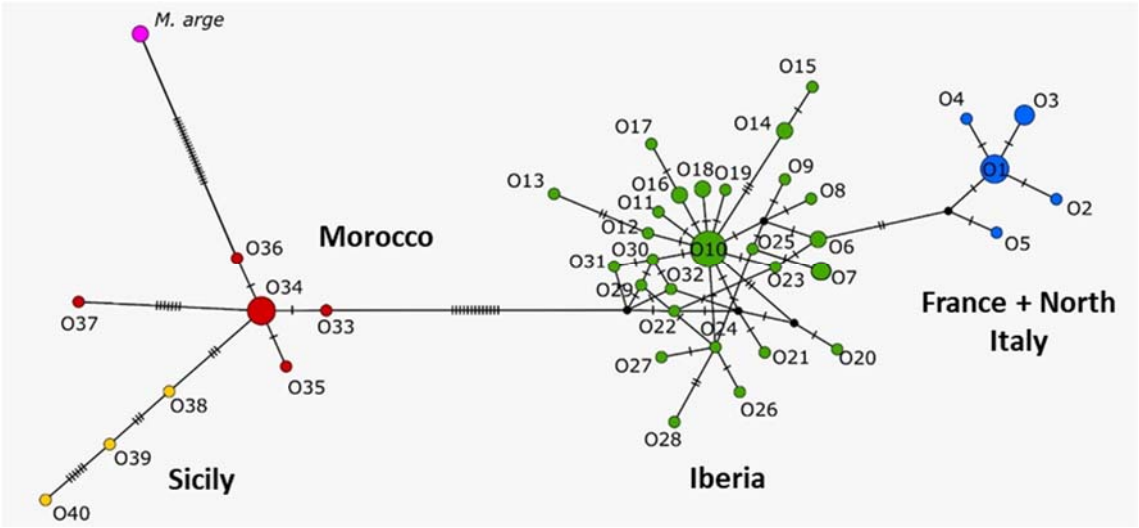

Figure S6.14 – Haplotype network of *Melanargia occitanica* for COI gene (Dataset 6) including one COI haplotype of *M. arge*.

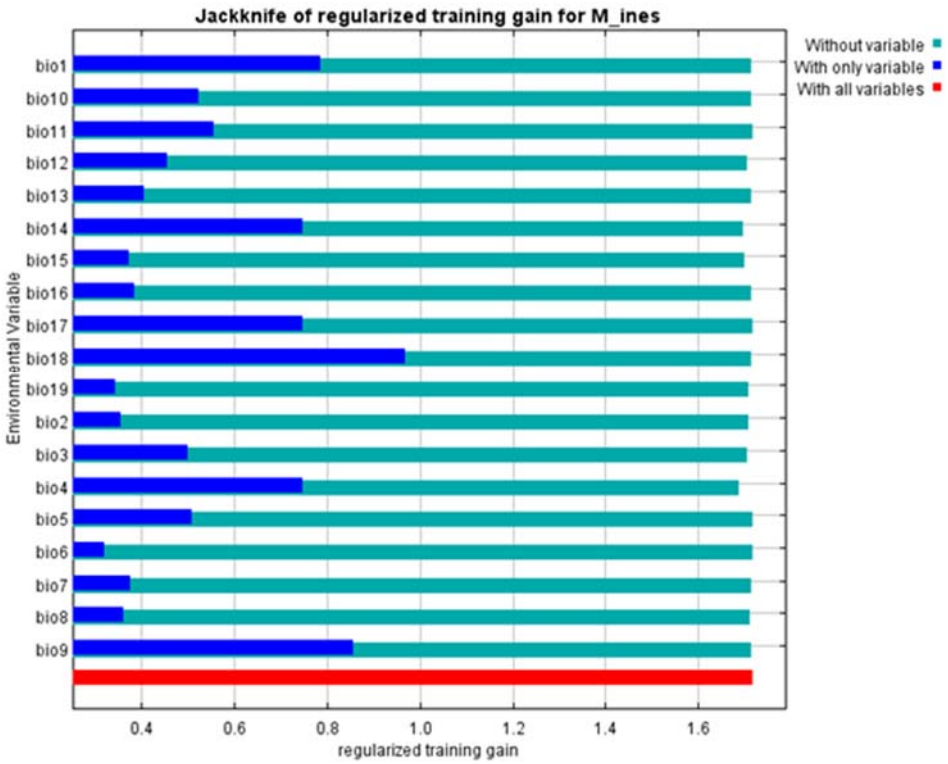

Figure S6.15 – Bioclimatic variables impact on *M. ines* distribution obtained with Maxent.

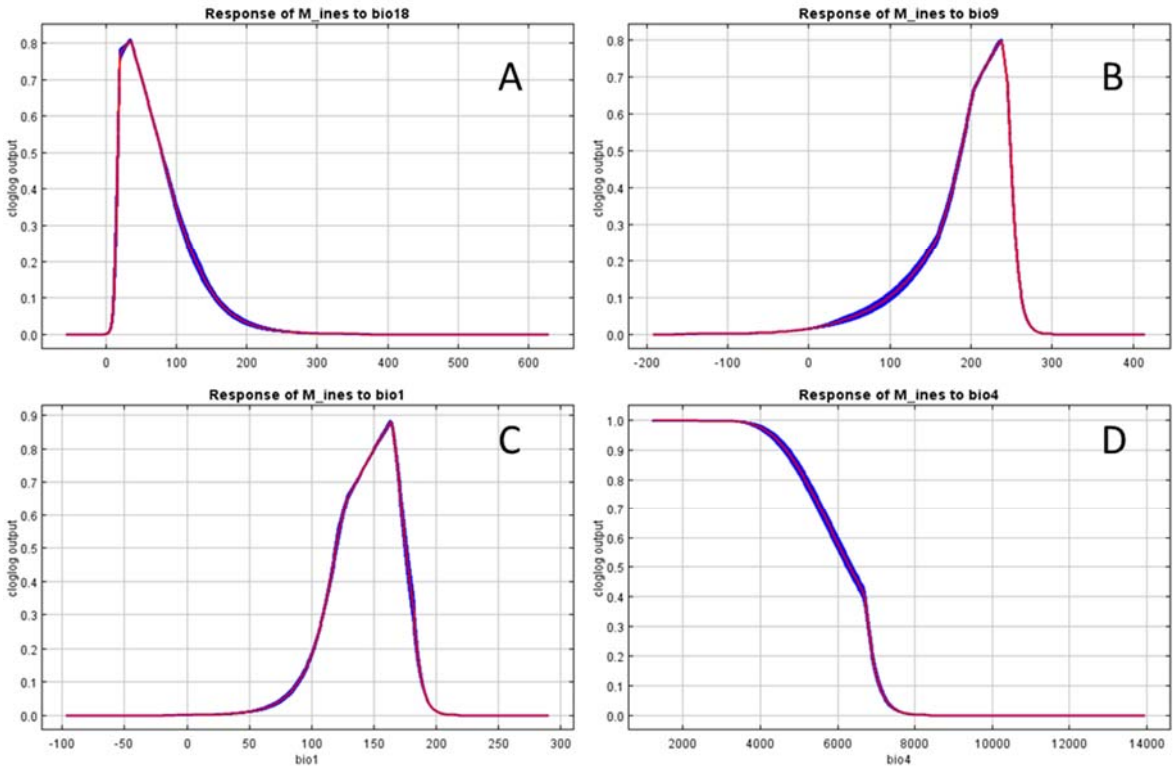

Figure S6.16 – Most influent bioclimatic variables for *M. ines* distribution obtained with Maxent. Response of *M. ines* to: (A) – Bio18; (B) – Bio9; (C) – Bio1; (D) – Bio4.

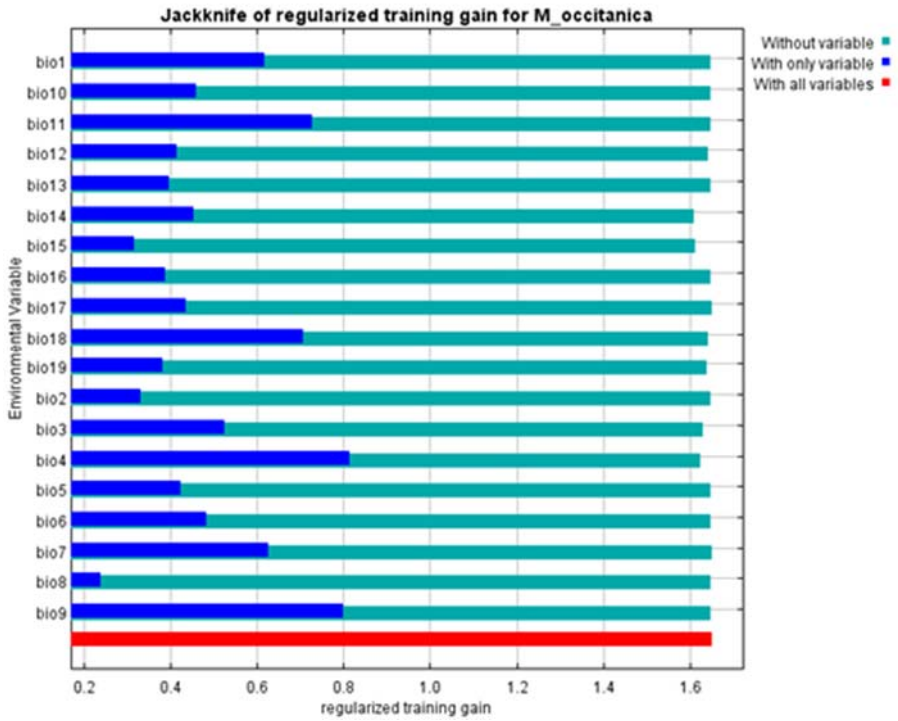

Figure S6.17 – Bioclimatic variables impact on *M. occitanica* distribution obtained with Maxent.

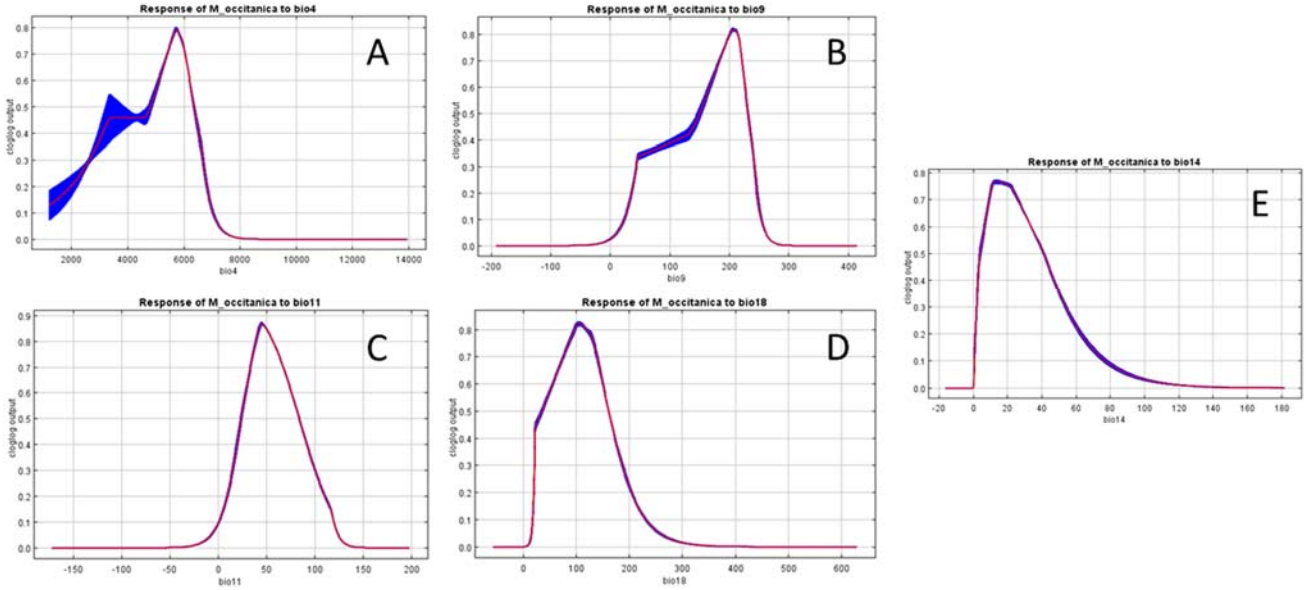

Figure S6.18 – Most influent bioclimatic variables for *M. occitanica* distribution obtained with Maxent. Response of *M. occitanica* to: (A) – Bio4; (B) – Bio9; (C) – Bio11; (D) – Bio18; (E) – Bio14.

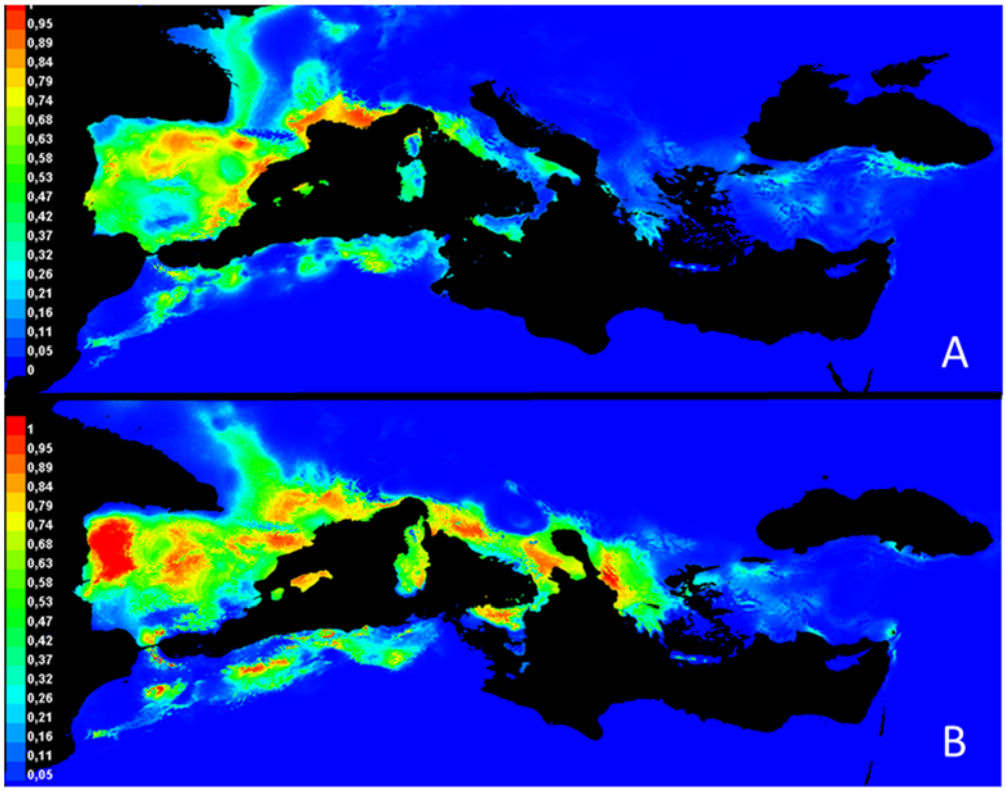

Figure S6.19 – SDM maps for *M. occitanica* Present (A) and LGM (B) distributions without accounting for the *M. o. pherusa* occurrence points in the input data.

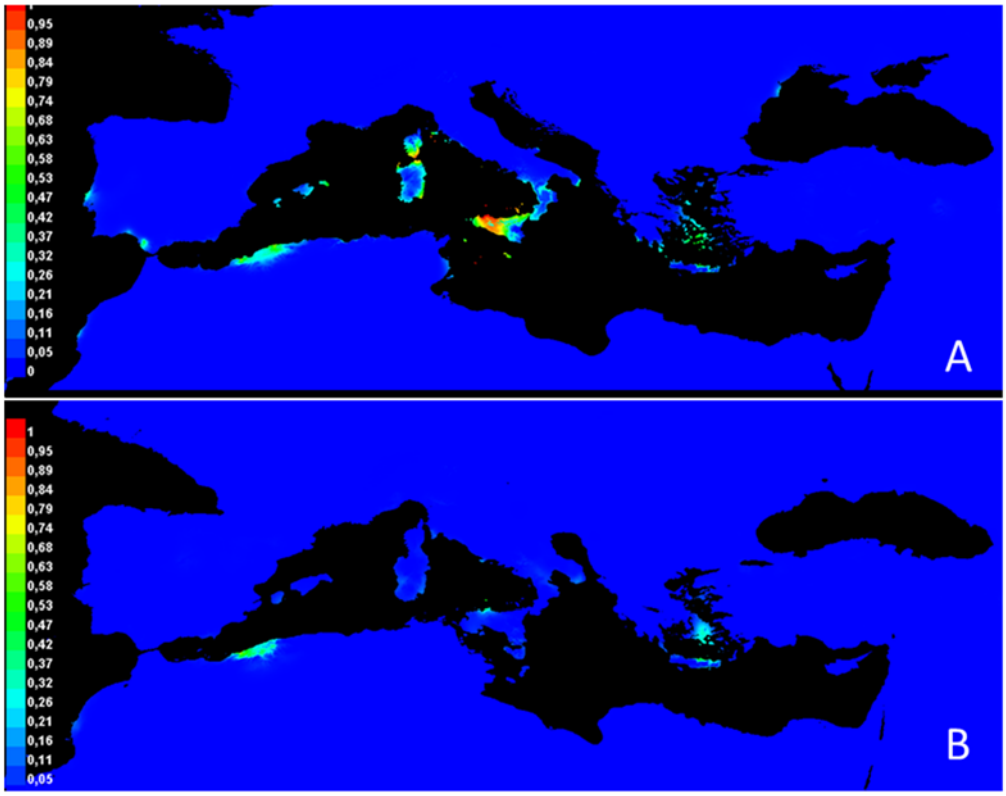

Figure S6.20 – SDM maps for *M. o. pherusa* Present (A) and LGM (B) distributions.

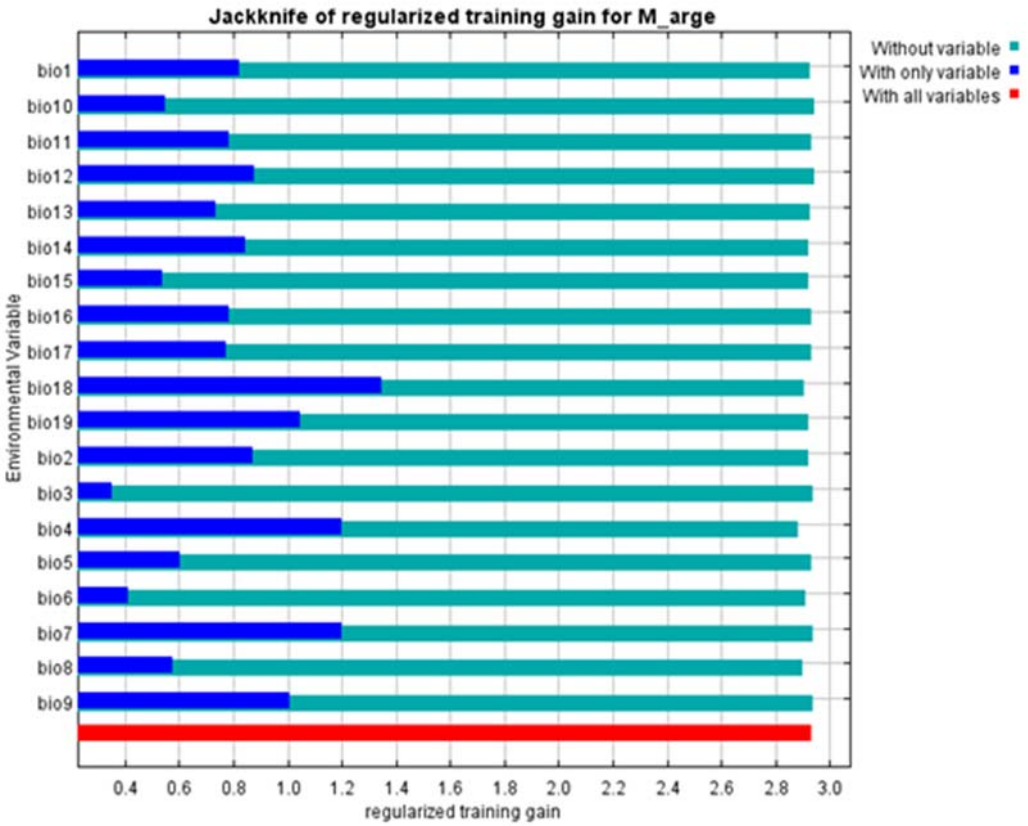

Figure S6.21 – Bioclimatic variables impact on *M. arge* distribution obtained with Maxent.

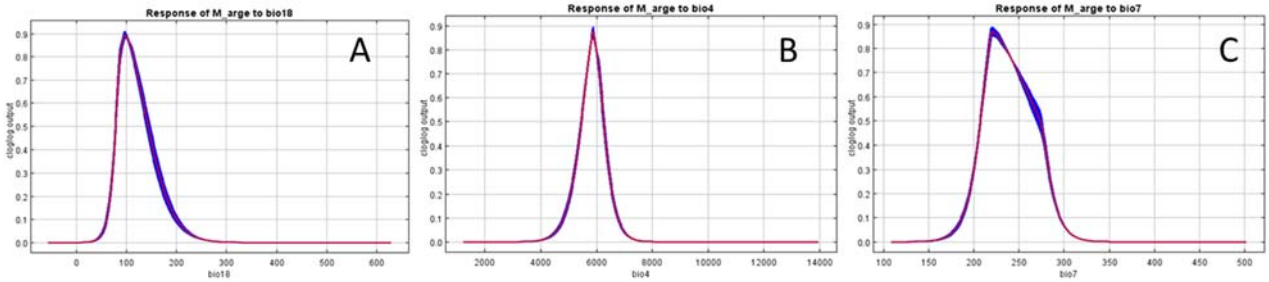

Figure S6.22 – Most influent bioclimatic variables for *M. arge* distribution obtained with Maxent. Response of *M. arge* to: (A) – Bio18; (B) – Bio4; (C) – Bio7.

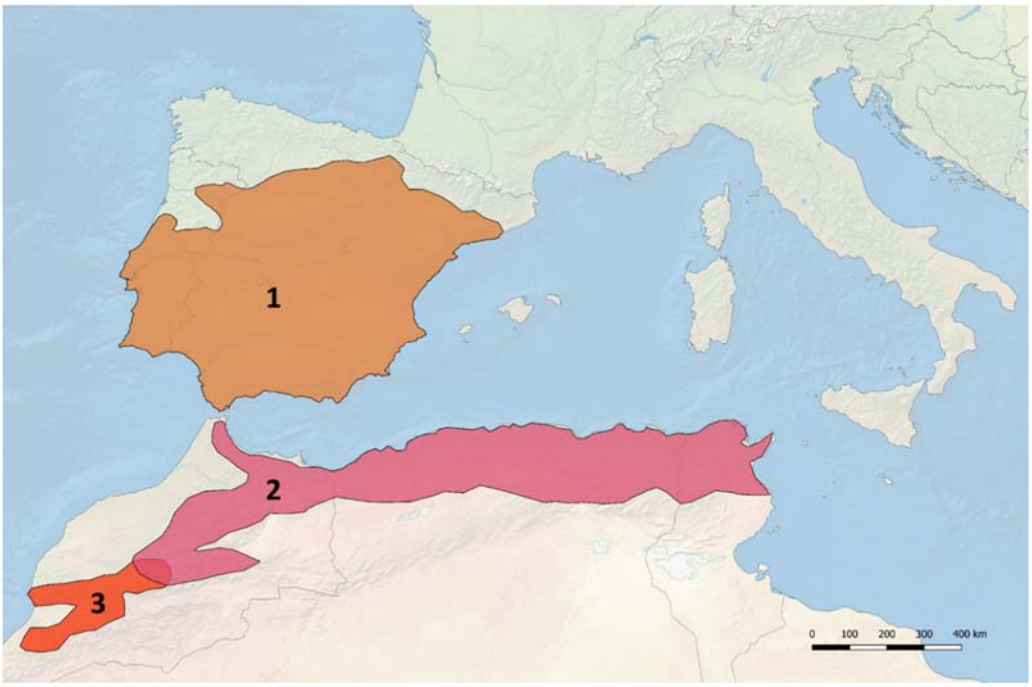

Figure S8.1 – Distribution range of *M. ines* potential subspecies: (1) *M. ines ines*; (2) *M. ines fathme* = *M. ines jahandiezi*; (3) *M. ines arahoui*.

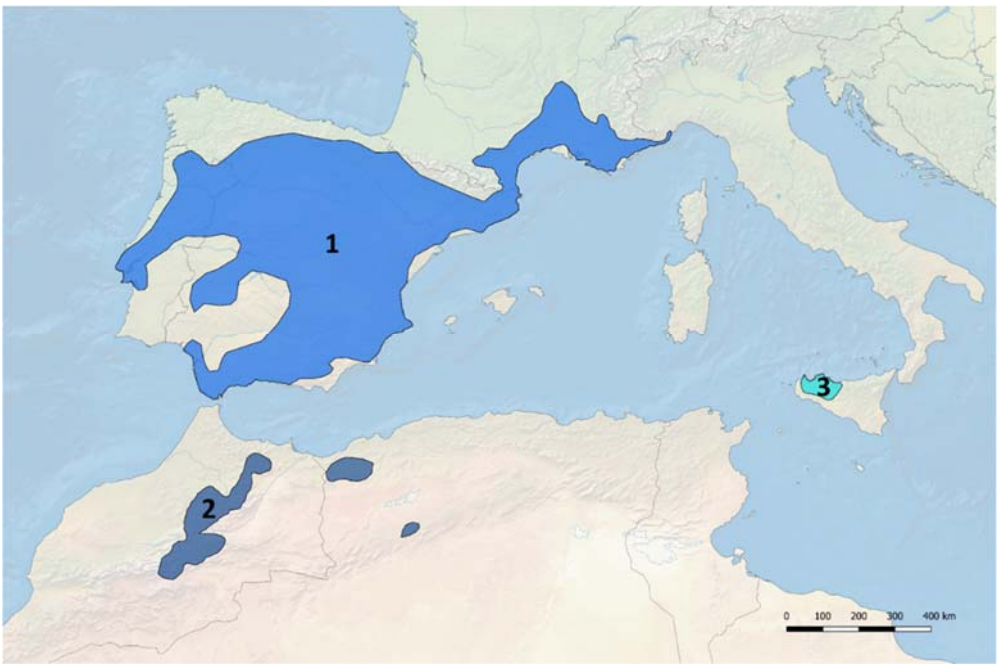

Figure S8.2 – Distribution range of *M. occitanica* potential subspecies: (1) *M. occitanica occitanica*; (2) *M. occitanica pelagia*; (3) *M. occitanica pherusa*.

10.2 Tables

Table S1.1 – List of current subspecies, authors and type localities of all *Argeformia* species.

Subspecies	**Type Locality**	**Author**	**Year**
M. ines ines	Belém, Portugal	Hoffmannsegg	1804
M. ines fathme	Tunisia	Wagner	1913
M. ines jahandiezi	Reraya, High Atlas, Morocco	Oberthur	1922
M. occitanica occitanica	Languedoc, France	Esper	1793
M. occitanica pelagia	Sebdou, Algeria	Oberthur	1911
M. occitanica pherusa	Sicily, Italy	Boisduval	1832

Table S3.1 – List of Lycaena (and outgroup taxa) specimens included in the phylogenetic analyses.

Name	Code	Collecting location	Collecting country	Coordenates	Date of collection	Acession number
Lycaena bleusei	LBL 7	Santa Eulália, Seia	Portugal	40.411250, -7.794900	05-mai-11	-
Lycaena bleusei	LBL 8	Santa Eulália, Seia	Portugal	40.411250, -7.794900	05-mai-11	-
Lycaena bleusei	LBL 9	Santa Eulália, Seia	Portugal	40.411250, -7.794900	05-mai-11	-
Lycaena bleusei	LBL 10	Manteigas	Portugal	40.383500, -7.546135	05-mai-11	-
Lycaena bleusei	LBL 11	Vale de Amoreira, Manteigas	Portugal	40.412410, -7.446730	05-mai-11	-
Lycaena bleusei	LBL 12	Vale de Amoreira, Manteigas	Portugal	40.412410, -7.446730	05-mai-11	-
Lycaena bleusei	LBL 13	Aldeia da Serra, Seia	Portugal	40.417080, -7.676740	05-mai-11	-
Lycaena bleusei	LBL 14	Santa Eulália, Seia	Portugal	40.411250, -7.794900	05-mai-11	-
Lycaena bleusei	LBL 15	Aldeia da Serra, Seia	Portugal	40.417080, -7.676740	05-mai-11	-
Lycaena bleusei	LBL 16	Penelas, Vila Real	Portugal	41.243333, -7.735333	03-ago-11	-
Lycaena bleusei	LBL 17	Penelas, Vila Real	Portugal	41.243333, -7.735333	03-ago-11	-
Lycaena bleusei	LBL 18	El Payo, San Martin Trevejo	Spain	40.299252, -6.729409	16-ago-11	-
Lycaena bleusei	LBL 19	El Payo, San Martin Trevejo	Spain	40.299252, -6.729409	16-ago-11	-
Lycaena bleusei	LBL 20	Cambrón	Spain	40.337842, -6.255551	17-ago-11	-
Lycaena bleusei	LBL 21	Cambrón	Spain	40.337842, -6.255551	17-ago-11	-
Lycaena bleusei	LBL 22	Cambrón	Spain	40.337842, -6.255551	17-ago-11	-
Lycaena bleusei	LBL 24	San Martin, Castañar	Spain	40.527549, -6.055500	17-ago-11	-
Lycaena bleusei	LBL 25	San Martin, Castañar	Spain	40.527549, -6.055500	17-ago-11	-
Lycaena bleusei	LBL 26	Mogarraz	Spain	40.498842, -6.047669	17-ago-11	-
Lycaena bleusei	LBL 27	Mogarraz	Spain	40.498842, -6.047669	17-ago-11	-
Lycaena bleusei	LBL 28	La Garganta	Spain	40.325040, -5.808280	18-ago-11	-
Lycaena bleusei	LBL 29	La Garganta	Spain	40.325040, -5.808280	18-ago-11	-
Lycaena bleusei	LBL 30	La Garganta	Spain	40.325040, -5.808280	18-ago-11	-
Lycaena bleusei	LBL 34	La Garganta	Spain	40.325040, -5.808280	18-ago-11	-
Lycaena bleusei	LBL 35	Candelario, Salamanca	Spain	40.368421, -5.735434	18-ago-11	-
Lycaena bleusei	LBL 36	Candelario, Salamanca	Spain	40.368421, -5.735434	18-ago-11	-
Lycaena bleusei	LBL 40	La Carrera, Gredos	Spain	40.343162, -5.556470	18-ago-11	-
Lycaena bleusei	LBL 41	La Carrera, Gredos	Spain	40.343162, -5.556470	18-ago-11	-
Lycaena bleusei	LBL 42	La Carrera, Gredos	Spain	40.343162, -5.556470	18-ago-11	-
Lycaena bleusei	LBL 45	Villuercas, Serra de Guadalupe	Spain	39.471676, -5.394915	19-ago-11	-
Lycaena bleusei	LBL 46	Villuercas, Serra de Guadalupe	Spain	39.471676, -5.394915	19-ago-11	-
Lycaena bleusei	LBL 47	Villuercas, Serra de Guadalupe	Spain	39.471676, -5.394915	19-ago-11	-
Lycaena bleusei	LBL 52	Villuercas, Serra de Guadalupe	Spain	39.471676, -5.394915	19-ago-11	-
Lycaena bleusei	LBL 53	Ariz, Moimenta da Beira	Portugal	40.908083, -7.651710	27-ago-11	-
Lycaena bleusei	LBL 54	Ariz, Moimenta da Beira	Portugal	40.908083, -7.651710	27-ago-11	-
Lycaena bleusei	LBL 55	Trinta, Guarda	Portugal	40.508450, -7.372150	07-ago-11	-
Lycaena bleusei	LBL 56	Trinta, Guarda	Portugal	40.508450, -7.372150	07-ago-11	-
Lycaena bleusei	LBL 57	Gosendinho, Castro Daire	Portugal	41.008714, -7.897170	27-ago-11	-
Lycaena bleusei	LTI 10*	Cabeça, Seia	Portugal	40.317560, -7.733050	04-mai-11	-
Lycaena bleusei	LTI 12*	Cabeça, Seia	Portugal	40.317560, -7.733050	04-mai-11	-
Lycaena bleusei	LTI 15*	Cabeça, Seia	Portugal	40.317560, -7.733050	04-mai-11	-
Lycaena bleusei	LTI 17*	Cabeça, Seia	Portugal	40.317560, -7.733050	04-mai-11	-
Lycaena bleusei	LTI 18*	Cabeça, Seia	Portugal	40.317560, -7.733050	04-mai-11	-
Lycaena bleusei	LTI 21*	Valezim, Seia	Portugal	40.357650, -7.715970	04-mai-11	-
Lycaena bleusei	EM1249	Minas de Sto. Adrião, Vimioso	Portugal	41.530270, -6.473990	18-mai-12	-
Lycaena bleusei	EM2775	Alcongosta, Fundão, Gardunha	Portugal	40.113013, -7.501667	18-mai-13	-
Lycaena bleusei	EM3504	Castrovido, Burgos	Spain	42.044499, -3.270998	15-mai-14	-
Lycaena bleusei	EM4700	Navaltoril, Toledo	Spain	39.572940, -4.787370	15-abr-16	-
Lycaena bleusei	EM5260	Guadramil, Rio de Onor	Portugal	41.917140, -6.573230	13-ago-16	-
Lycaena bleusei	EM5470	Serra da Nogueira	Portugal	41.750290, -6.862735	16-jul-15	-
Lycaena bleusei	-	Cebreros, Cebreros, Avila	Spain	40467, -4477	25-abr-08	EZSPN351-09
Lycaena bleusei	-	Pinar de Hoyocasero, Avila	Spain	40324, -5807	08-jun-08	EZSPC732-10
Lycaena bleusei	-	Candelario, Salamanca	Spain	40334, -5799	15-jun-08	EZSPC735-10
Lycaena bleusei	-	Soto del Real	Spain	40789, 3824	12-jun-08	EZSPC770-10
Lycaena bleusei	-	Candelario, Salamanca	Spain	40366, -5766	09-ago-08	EZSPC803-10

Lycaena bleusei	-	Los Angeles de San Rafael	Spain	40796, -4175	25-jul-09	EZSPC920-10
Lycaena bleusei	-	Candelario, Salamanca	Spain	40366, -5766	09-ago-08	EZSPM101-09
Lycaena bleusei	-	Candelario, Salamanca	Spain	40334, -5799	15-jun-08	EZSPN495-09
Lycaena bleusei	-	Pinar de Hoyocasero, Avila	Spain	40431, -4986	21-jun-08	EZSPN830-09
Lycaena bleusei	-	Soto del Real	Spain	40789, -3824	12-jun-08	EZSPN857-09
Lycaena bleusei	-	Soto del Real	Spain	40789, -3824	12-jun-08	EZSPN858-09
Lycaena tityrus	LTI 11	Cabeça, Seia	Portugal	40.317560, -7.733050	04-mai-11	-
Lycaena tityrus	LTI 13	Cabeça, Seia	Portugal	40.317560, -7.733050	04-mai-11	-
Lycaena tityrus	LTI 14	Cabeça, Seia	Portugal	40.317560, -7.733050	04-mai-11	-
Lycaena tityrus	LTI 16	Cabeça, Seia	Portugal	40.317560, -7.733050	04-mai-11	-
Lycaena tityrus	LTI 19	Cabeça, Seia	Portugal	40.317560, -7.733050	04-mai-11	-
Lycaena tityrus	LTI 20	Valezim, Seia	Portugal	40.357650, -7.715970	04-mai-11	-
Lycaena tityrus	LTI 22	Valezim, Seia	Portugal	40.357650, -7.715970	04-mai-11	-
Lycaena tityrus	LTI 23	Mount Vourinos	Greece	40.200200, 21.658380	20-jun-11	-
Lycaena tityrus	LTI 24	Mount Parnassus	Greece	38.578400, 22.575083	20-jun-11	-
Lycaena tityrus	LTI 25	Mount Parnassus	Greece	38.578400, 22.575083	20-jun-11	-
Lycaena tityrus	LTI 26	Mount Parnassus	Greece	38.578400, 22.575083	20-jun-11	-
Lycaena tityrus	LTI 27	Mount Parnassus	Greece	38.578400, 22.575083	20-jun-11	-
Lycaena tityrus	LTI 28	Castro Laboreiro, Melgaço	Portugal	42.017003, -8.166625	mai/11	-
Lycaena tityrus	LTI 29	Castro Laboreiro, Melgaço	Portugal	42.017003, -8.166625	mai/11	-
Lycaena tityrus	LTI 30	Penelas, Vila Real	Portugal	41.238340, -7.737710	03-ago-11	-
Lycaena tityrus	LTI 31	Moinho Fresulfe, Vinhais	Portugal	41.896751, -6.938015	08-jul-11	-
Lycaena tityrus	LTI 32	Boticas, Alto Trás os Montes	Portugal	41.668390, -7.761620	23-jul-11	-
Lycaena tityrus	LTI 33	Boticas, Alto Trás os Montes	Portugal	41.668390, -7.761620	23-jul-11	-
Lycaena tityrus	LTI 34	Serra do Caramulo, Viseu	Portugal	40.550350, -8.187280	26-ago-11	-
Lycaena tityrus	LTI 35	Ariz, Moimenta da Beira	Portugal	40.908083, -7.651710	26-ago-11	-
Lycaena tityrus	LTI 36	Gosendinho, Castro Daire	Portugal	41.008714, -7.897170	26-ago-11	-
Lycaena tityrus	LTI 37	Gosendinho, Castro Daire	Portugal	41.008714, -7.897170	26-ago-11	-
Lycaena tityrus	LTI 38	Gosendinho, Castro Daire	Portugal	41.008714, -7.897170	26-ago-11	-
Lycaena tityrus	LTI 39	Gosendinho, Castro Daire	Portugal	41.008714, -7.897170	26-ago-11	-
Lycaena tityrus	LTI 40	Caín de Valdeón, León	Spain	43.213863, -4.902654	23-set-11	-
Lycaena tityrus	LTI 41	A Riba, Vigo, Pontevedra	Spain	42.732050, -8.543478	25-set-11	-
Lycaena tityrus	LTI 42	A Riba, Vigo, Pontevedra	Spain	42.732050, -8.543478	25-set-11	-
Lycaena tityrus	LTI 43	Arcos de Valdevez	Portugal	41.934987, -8.459646	25-set-11	-
Lycaena tityrus	LTI 44	Arcos de Valdevez	Portugal	41.934987, -8.459646	25-set-11	-
Lycaena tityrus	LTI 45	Lourenzá, Lugo	Spain	43.467151, -7.301881	24-set-11	-
Lycaena tityrus	LTI 46	Lourenzá, Lugo	Spain	43.467151, -7.301881	24-set-11	-
Lycaena tityrus	LTI 47	Mestas de Com, Cangas de Onís	Spain	43.348530, -5.020370	22-set-11	-
Lycaena tityrus	LTI 49	Lourenzá, Lugo	Spain	43.467151, -7.301879	25-set-11	-
Lycaena tityrus	LTI 50	Lourenzá, Lugo	Spain	43.467151, -7.301879	25-set-11	-
Lycaena tityrus	LTI 51	Lloreda, Avilés	Spain	43.522050, -5.923880	24-set-11	-
Lycaena tityrus	LTI 52	Lloreda, Avilés	Spain	43.522050, -5.923880	24-set-11	-
Lycaena tityrus	LTI 53	A Riba, Vigo, Pontevedra	Spain	42.732051, -8.543481	25-set-11	-
Lycaena tityrus	LTI 54	A Riba, Vigo, Pontevedra	Spain	42.732051, -8.543481	25-set-11	-
Lycaena tityrus	LTI 55	A Riba, Vigo, Pontevedra	Spain	42.732051, -8.543481	25-set-11	-
Lycaena tityrus	LTI 56	Lloreda, Avilés	Spain	43.522050, -5.923880	24-set-11	-
Lycaena tityrus	LTI 57	Lloreda, Avilés	Spain	43.522050, -5.923880	24-set-11	-
Lycaena tityrus	LTI 58	Lloreda, Avilés	Spain	43.522050, -5.923880	24-set-11	-
Lycaena tityrus	LTI 59	Lloreda, Avilés	Spain	43.522050, -5.923880	24-set-11	-
Lycaena tityrus	LTI 61	Mestas de Com, Cangas de Onís	Spain	43.348530, -5.020370	22-set-11	-
Lycaena tityrus	LTI 62	Mestas de Com, Cangas de Onís	Spain	43.348530, -5.020370	22-set-11	-
Lycaena tityrus	EM1302	Queralbs	Spain	42.353420, 2.169455	24-mai-12	-
Lycaena tityrus	EM1334	Castrelos, PN Montesinho	Portugal	41.838822, -6.887835	15-mai-12	-
Lycaena tityrus	EM5258	Guadramil, Rio de Onor	Portugal	41.917140, -6.573230	13-ago-16	-
Lycaena tityrus	EM5261	Couços, Chaves	Portugal	41.683210, -7.360300	15-ago-16	-
Lycaena tityrus	EM6402	Monterrubio de la Demanda, Burgos	Spain	42.148333, -3.131667	15-mai-14	-
Lycaena tityrus	EM6404	Villasur Herreros, Burgos	Spain	42.311660, -3.392833	15-mai-14	-
Lycaena tityrus	EM6406	Pineda de la Sierra, Burgos	Spain	42.230750, -3.309833	15-mai-14	-
Lycaena tityrus	EM6418	Velilla rio Carrión, Palencia	Spain	42.833920, -4.855840	14-mai-14	-
Lycaena tityrus	EM6420	Paramo del Sil, León	Spain	42.813833, -6.511167	12-mai-14	-
Lycaena tityrus	-	Padron, Picarana-Rio Tinto	Spain	42.95, -6628	06-abr-08	EZSPM252-09
Lycaena tityrus	-	Ribeira de Varzea, Fafe	Portugal	42913, -4079	12-jun-08	EZSPN570-09
Lycaena tityrus	-	Valle (Valle-Zurea), Lena	Spain	43154, ?	02-ago-08	EZSPM142-09

Lycaena tityrus	-	Fondos de Vega, Degana	Spain	46767, 25683	16-ago-11	EZSPM769-12
Lycaena tityrus	-	San Andres, Valdeprado del Rio	Spain	42448, 1781	16-mai-08	EZSPN391-09
Lycaena tityrus	-	Posada de Valdeon	Spain	42612, 1075	21-jul-08	EZSPM297-09
Lycaena tityrus	-	Gheorgheni, Valea Belchia	Romania	42367, 1883	20-jul-06	EZROM268-08
Lycaena tityrus	-	Meranges, Girona	Spain	42367, 1883	29-jun-07	EZSPC504-09
Lycaena tityrus	-	Planes de Son, Pallars Sobira, Lleida	Spain	42.35, 1.85	07-set-08	EZSPC505-09
Lycaena tityrus	-	Torre de Riu, Ribera d`Alp, Cerdanya	Spain	46311, 11326	12-ago-08	EZSPC506-09
Lycaena tityrus	-	Torre de Riu, Ribera d`Alp, Cerdanya	Spain	491279, 721885	12-ago-08	EZSPC507-09
Lycaena tityrus	-	La Valira (near Urus), Cerdanya	Spain	479333, 110833	19-ago-08	EZSPC508-09
Lycaena tityrus	-	Muehlen/ Truden SW, Suedtirol	Italy	48946, 12855	12-ago-14	ABOLB032-15
Lycaena tityrus	-	Gersheim, Buchenberg	Germany	400839, 157297	08-mai-12	GBLAB132-13
Lycaena tityrus	-	Diessen, Oberbayern	Germany	47.36, 9.92	30-jul-08	GWORK519-09
Lycaena tityrus	-	Grandsberg, Niederbayern	Germany	534833, 107333	03-mai-07	GWORA2468-09
Lycaena tityrus	-	Moor bei Rivello, Potenza	Italy	46031, 25366	09-set-92	GWORZ040-10
Lycaena tityrus	-	Bizau	Austria	45574, 24614	20-Jun-13	PHLAW038-13
Lycaena tityrus	-	Fortkrug	Germany	46483, 23717	02-ago-13	GBLAA381-14
Lycaena tityrus	-	Racos, Transylvania	Romania	45583, 24617	28-mai-07	EZRMN058-08
Lycaena tityrus	-	Fagaras Mts., Muntenia	Romania	?	19-jul-08	EZRMN061-08
Lycaena tityrus	-	Badeni, Transylvania	Romania	?	14-mai-06	EZROM267-08
Lycaena tityrus	-	Cabana Capra, Muntenia	Romania	56133, 28667	06-ago-07	EZROM270-08
Lycaena tityrus	-	Laensi Viro	Estonia	?	27-mai-07	LEFID122-10
Lycaena tityrus	-	Tartu, Konguta	Estonia	46.84, 9361	26-mai-11	LEFIJ1005-11
Lycaena tityrus	-	Osyno	Russia	47.44, 11.29	01-jul-01	LOWA289-06
Lycaena tityrus	-	Saimbeyli Falls (1500 M)	Turkey	442508, 6.75	29-jul-98	GBGL0888-06
Lycaena tityrus	-	Waltensburg/Vuorz, Spinatsch	Switzerland	?	14-jun-09	PHLAB312-10
Lycaena tityrus	-	Mittenwald, Hasellaehne	Germany	474597, 136181	20-ago-10	GWOSF854-10
Lycaena tityrus	-	Col de la Cayolle S	France	470678, 128011	26-jul-09	PHLAA644-09
Lycaena tityrus	-	Kohlmaier Huette	Austria	470678, 128011	?	EULEP4171-16
Lycaena tityrus	-	Southern side of Dachstein	Austria	47.66, 115125	18-jul-15	EULEP4173-16
Lycaena tityrus	-	GR Glockner, Guttal / Brennkogel	Austria	46963, 10592	01-set-13	LEASS547-17
Lycaena tityrus	-	GR Glockner, Guttal / Brennkogel	Austria	46.52, 10.48	01-set-13	LEASS522-17
Lycaena tityrus	-	Hinteres Laengental	Germany	47131, 11719	20-jun-11	GWOTF674-12
Lycaena tityrus	-	Pfunds, Greit, Tscheywiesen	Austria	47066, 12091	22-jun-12	PHLAI505-13
Lycaena tityrus	-	Franzenshoehe/ Stilfserjoch	Italy	46833, 9633	08-jul-13	LEATD296-13
Lycaena tityrus	-	Lanersbach S: Loschbodenalm	Austria	47138, 10194	16-jul-09	LEATG007-14
Lycaena tityrus	-	Sauwipfel, Suedtirol	Italy	?	12-jun-07	LEATG427-14
Lycaena tityrus	-	Chur, Pagig	Switzerland	473527, 102217	14-jun-09	PHLAB361-10
Lycaena tityrus	-	Arlberg W, Alpe Rauz	Austria	46731, 10929	24-jul-12	PHLAH697-12
Lycaena tityrus	-	Risstal, Schafreuther, Oberbayern	Germany	46.65, 9597	16-jul-10	GWOSF850-10
Lycaena tityrus	-	Oberstdorf, Fellhorn/Schlappoltsee	Germany	43095, -5858	03-ago-04	ODOPE749-11
Lycaena tityrus	-	Vorderkaser S, Suedtirol	Italy	?	07-jul-14	LEATH781-14
Lycaena tityrus	-	Tiefencastel S/ Salouf, Got Grond	Switzerland	489886, 125253	20-jul-09	PHLAB286-10
Lycaena tityrus	-	Valle (Valle-Zurea), Lena	Spain	45299, 22894	02-ago-08	EZSPM143-09
Lycaena tityrus	-	Zellwies TOEL	Germany	44048, 27411	21-mai-09	GWORO791-09
Lycaena tityrus	-	Saulburg, Niederbayern	Germany	44638, 22589	21-jul-78	FBLMU496-09
Lycaena tityrus	-	Scorota (Retezat Mts.), Transylvania	Romania	45167, 22.3	21-jul-08	EZRMN062-08
Lycaena tityrus	-	Esechioi forest, Dobrogea	Romania	41.981040, -6.795770	29-jun-08	EZRMN059-08
Lycaena tityrus	-	4 Km W of Drobeta Turnu-Severin	Romania		08-jul-08	EZRMN060-08
Lycaena tityrus	-	Teregova, Banat	Romania	42.079950, -2.545720	05-jun-07	EZROM269-08
Lycaena virgaureae	LVI 1	Lama Grande, Serra de Montesinho	Portugal	41.981040, -6.795770	08-jul-11	-
Lycaena virgaureae	LVI 2	?	?	?	?	FJ490505
Lycaena hippothoe	EM6352	Sierra Cebollera, La Rioja	Spain	42.079950, -2.545720	22-jun-17	-
Lycaena candens	LCA	?	?	?	?	KJ671879
Lycaena alciphron	LAL 1	Lama Grande, Serra de Montesinho	Portugal	41.981040, -6.795770	09-jul-11	-
Lycaena alciphron	LAL 2	PN ITI, Ftiótide	Greece	38.731917, 22.343667	14-jun-11	-
Lycaena phlaeas	LPH 2	?	?	?	?	FJ490517
Lycaena phlaeas	LPH 1	Parâmio, Serra de Montesinho	Portugal	41.898090, -6.852940	08-jul-11	-
Lycaena violacea	EM5417	Mondy, Tunkinsky range, E. Sayan	Russia	51.691070, 101.007070	24-jun-09	-
Lycaena aeolides	EM5415	Obburdon Pass, Turkestan Mts	Tajikistan	39.501994, 69.135332	10-jul-15	-
Lycaena phoebus	EM3303	Tizi-n-Tarakatine, Tafraoute	Morocco	29.769170, -8.837667	19-abr-13	-
Lycaena alpherakyi	LALP	?	?	?	?	FJ490521
Lycaena solski	LSO 1	?	?	?	?	FJ490520
Lycaena solski	LSO 2	?	?	?	?	FJ490519

Lycaena li	LLI	?	?	?	?	FJ490501
Lycaena hermes	LHER	?	?	?	?	FJ490502
Lycaena nivalis	LNI 1	Gunnison County, Colorado	USA	?	?	EU326288
Lycaena nivalis	LNI 2	?	?	?	?	FJ490496
Lycaena dione	LDI	?	?	?	?	FJ490508
Lycaena mariposa	LMA	?	?	?	?	FJ490516
Lycaena gorgon	LGO	?	?	?	?	FJ490494
Lycaena hyllus	LHY	?	?	?	?	FJ490507
Lycaena cupreus	LCU	?	?	?	?	FJ490499
Lycaena editha	LED	?	?	?	?	FJ490504
Lycaena dorcas	LDO 1	?	?	?	?	FJ490513
Lycaena dorcas	LDO 2	?	?	?	?	FJ490514
Lycaena heteronea	LHET 1	?	?	?	?	FJ490497
Lycaena heteronea	LHET 2	Gunnison County, Colorado	USA	?	?	EU326289
Lycaena dispar aurata	LDA	Pocheon, Gyeonggi	South Korea	?	?	GU372655
Lycaena helloides	LHE	Lost Man Creek, Pitkin County	USA	?	?	AY954622
Lycaena arota	LAR	Topaz Lake, Mono County	USA	?	27-jun-92	KT286158
Lycaena rubidus	LRU	?	?	?	?	FJ490495
Lycaena xanthoides	LXA	?	?	?	?	FJ490503
Lycaena helle	EM5406	Mondy, Tunkinsky range, E. Sayan	Russia	51.691070, 101.007070	17-jun-16	-
Lycaena virgaureae	LVI 2	Buron, Leon	Spain	?	26-jul-08	EZSPM083-09
Lycaena candens	LCA	Shemshak ,Tehran	Iran	?	13-jul-00	GBGL0767-06
Lycaena phlaeas	LPH 2	Cantoblanco, Comunidad de Madrid	Spain	?	28-mar-08	EZSPN375-09
Lycaena alpherakyi	LALP	Murgab v., Pshart Mts., East-Pamir	Tajikistan	?	20-jul-96	LOWA386-06
Lycaena solski	LSO 1	Karatau Mts, Tchimkent Region	Kazakhstan	?	19-jun-00	LOWA044-06
Lycaena solski	LSO 2	Karatau Mts, Tchimkent Region	Kazakhstan	?	19-jun-00	LOWA045-06
Lycaena li	LLI	Yunnan	China	?	25-jul-09	BOAA256-13
Lycaena hermes	LHER	California	USA	?	21-jun-98	ABLCU255-09
Lycaena nivalis	LNI 1	Duck Lake Area, Lassen, California	USA	40.3581, -121.995	11-jun-08	JMMMB550-13
Lycaena nivalis	LNI 2	Washington	USA	48.625, -120.4	24-jul-05	RDBBC486-05
Lycaena dione	LDI	East Block badlands, Grasslands NP	Canada	49.071, -106.531	16-jul-08	LPSK369-08
Lycaena mariposa	LMA	Coppermine Creek, Waterton Lakes	Canada	49.104, -113.959	28-jul-08	LPAB195-08
Lycaena gorgon	LGO	Jackson County, Oregon	USA	42.229, -123.184	10-mai-04	EZBNB354-08
Lycaena hyllus	LHY	Lindale, Alberta	Canada	53.2, -114.615	27-jul-06	EZBNB093-08
Lycaena cupreus	LCU	Mt. Tripoli, Cardinal Divide, Alberta	Canada	52.896, -117.248	29-jul-03	EZBNB080-08
Lycaena editha	LED	Teepee Ck. FSR at Oke Ck.	Canada	49.253, -115.686	09-ago-04	EZBNB088-08
Lycaena dorcas	LDO 1	Great Valley Grasslands State Park	USA	37.309, -120.93	31-jul-11	BBLOC1962-11
Lycaena dorcas	LDO 2	Lindale, Alberta	Canada	53.2, -114.615	27-jul-06	EZBNB092-08
Lycaena heteronea	LHET 1	Apex Mtn Rd., W of Penticton	Canada	49.419, -119.828	04-jul-03	EZBNB070-08
Lycaena heteronea	LHET 2	Red Rock Canyon, Waterton Lakes	Canada	49.11, -113.984	09-ago-08	LPABC735-09
Lycaena dispar aurata	LDA	?	?	?	?	GBMIN38013-13
Lycaena helloides	LHE	Waterton Lakes, Blakiston Ck fan	Canada	?	14-ago-06	EZBNB090-08
Lycaena arota	LAR	Topaz Lake, Mono County, Califórnia	USA	?	27-jun-92	GBMIN81717-17
Lycaena rubidus	LRU	Nevada	USA	41.1154, -117.698	08-jun-06	ABLCU275-09
Lycaena xanthoides	LXA	California	USA	37.4089, -121.415	18-jun-07	LWUSA316-08
Lycaena helle	LHELLE	Dumbrava Vadului, Vad, Transylvani	Romania	45.767, 25.1	27-mai-07	EZROM256-08
Lycaena standfussi	EM6465	Halihatu gorge, Qinghai	China	37.062930, 98.656330	22-jul-17	-
Lycaena pang	EM6468	Shangri-La, Yunnan	China	27.853000, 99.692700	02-jul-17	-
Curetis barsine	CBA	Wafi River, Morobe Province	P. N. Guinea	?	?	JN204954.1
Lampides boeticus	LBO	Yewol, Jeju	Korea	?	?	GU372584.1
Papilio paris	PPA	Guangzhou	China	?	?	AY457574.1
Curetis barsine	CBA	Wafi River, Morobe Province	P. N. Guinea	?	?	JN204973.1
Lampides boeticus	LBO	Yewol, Jeju	Korea	?	?	GU372675.1
Papilio paris	PPA	Guangzhou	China	?	?	AY457605.1

**Lycaena bleusei* individuals incorrectly identified as *L. tityrus* when collected

Table S3.2 – List of Melanargia (and outgroup taxon) specimens included in the phylogenetic analyses.

Name	Code	Collecting location	Collecting country	Coordenates	Acession number
Melanargia ines	EM1419	Cerro de Meias, Loulé, Faro	Portugal	37.150865, -8.097720	-
Melanargia ines	EM2796	Caroucha, Castro Marim, Faro	Portugal	37.254140, -7.459410	-
Melanargia ines	EM4265	Laje, Porto Salvo, Oeiras, Lisboa	Portugal	38.709700, -9.320600	-
Melanargia ines	EM4985	Sierra Martés, Yátova, Buñol	Spain	39.329400, -0.938900	-
Melanargia ines	EM4356	Loeches, Madrid	Spain	40.371700, -3.382180	-
Melanargia ines	EM4410	Balsamão, Chacim, Macedo Cavaleiros	Portugal	41.478631, -6.857165	-
Melanargia ines	EM4180	Brotas, Mora, Évora	Portugal	38.858000, -8.156900	-
Melanargia ines	EM1404	Valcuerna, Monegros, Aragão	Spain	41.459420, 0.031640	-
Melanargia ines	EM1406	La Luz, Alcornocales, Tarifa, Cádiz	Spain	36.123300, -5.641610	-
Melanargia ines	EM2864	Horta, Vila Nova Foz Côa, Guarda	Portugal	41.069780, -7.330670	-
Melanargia ines	EM4393	Douro, Ligares, Freixo Espada a Cinta	Portugal	41.031890, -6.943570	-
Melanargia ines	EM4179	Brotas, Mora, Évora	Portugal	38.858000, -8.156900	-
Melanargia ines	EM4181	Brotas, Mora, Évora	Portugal	38.858000, -8.156900	-
Melanargia ines	EM6565	Ras El Ma, Taza, Djbel Tazekka	Morocco	34.143640, -4.014230	-
Melanargia ines	EM6567	Idardar, Taourirt, Oriental	Morocco	34.029380, -2.614540	-
Melanargia ines	EM6568	Idardar, Taourirt, Oriental	Morocco	34.029380, -2.614540	-
Melanargia ines	EM6569	Idardar, Taourirt, Oriental	Morocco	34.029380, -2.614540	-
Melanargia ines	EM6571	Ouled Ben Tahar, Beni Snassen, Oriental	Morocco	34.830600, -2.141900	-
Melanargia ines	EM6572	Ouled Ben Tahar, Beni Snassen, Oriental	Morocco	34.830600, -2.141900	-
Melanargia ines	EM6575	Tinissane, Beni Snassen, Oriental	Morocco	34.834970, -2.166000	-
Melanargia ines	EM6594	Tighezratine, Aknoul, Rif	Morocco	34.690270, -3.902720	-
Melanargia ines	EM6588	Tizi Ouasli, Ichellahane, Rif	Morocco	34.747540, -3.810820	-
Melanargia ines	EM6582	Kassita, Driouch	Morocco	34.915200, -3.798030	-
Melanargia ines	EM1416	Djebel Tisouka, Chefchaouen	Morocco	35.175280, -5.259940	-
Melanargia ines	EM3325	Ait Saleh, Imouzzer, Middle Atlas	Morocco	33.789100, -4.986670	-
Melanargia ines	EM3326	Ait Saleh, Imouzzer, Middle Atlas	Morocco	33.789100, -4.986670	-
Melanargia ines	EM1417	Ito – planalto, Middle Atlas	Morocco	33.529260, -5.307100	-
Melanargia ines	EM6564	Ras El Ma, Taza, Djbel Tazekka	Morocco	34.143640, -4.014230	-
Melanargia ines	EM6581	Al Hoceima	Morocco	35.233950, -3.923300	-
Melanargia ines	EM6576	Tinissane, Beni Snassen, Oriental	Morocco	34.834970, -2.166000	-
Melanargia ines	EM1412	Tizi-n-Test – South, High Atlas	Morocco	30.857230, -8.375470	-
Melanargia ines	EM1413	Tizi-n-Test – South, High Atlas	Morocco	30.857230, -8.375470	-

Melanargia ines	EM1415	Tizi-n-Test – South, High Atlas	Morocco	30.854160, -8.380730	-
Melanargia ines	EM5684	Tizi-n-Test, High Atlas	Morocco	30.862500, -8.377000	-
Melanargia ines	EM1418	Ito – planalto, Middle Atlas	Morocco	33.529260, -5.307100	-
Melanargia ines	EM6552	Ait Ourir, SE Marrakech	Morocco	31.547000, -7.564720	-
Melanargia ines	EM6553	Imlil, Demnate, High Atlas	Morocco	31.759300, -7.006700	-
Melanargia ines	EM6559	Sour El Aiz, Imlil, Demnate, High Atlas	Morocco	31.834600, -7.015600	-
Melanargia ines	EM3314	Tifghalt, Tafraoute, Anti-Atlas	Morocco	29.612420, -9.490490	-
Melanargia ines	EM3321	Col Kerdous, Tafraoute, Anti-Atlas	Morocco	29.546850, -9.332840	-
Melanargia ines	EM3324	Tizi-n-Tarakatine, Tafraoute, Anti-Atlas	Morocco	29.771930, -8.849840	-
Melanargia ines	-	Almaraz, Caceres, Extremadura	Spain	39.777, -5.697	EZSPC1129-10
Melanargia ines	-	N. Logrosan, Caceres, Extremadura	Spain	39.333, -5.483	VNMB458-08
Melanargia ines	-	Venta del Molinillo, Huetor de Santillan	Spain	37.313, ?	EZSPN710-09
Melanargia ines	-	Porches, Lagoa, Algarve	Portugal	37.135, -8.387	EZSPM716-12
Melanargia ines	-	Porches, Lagoa, Algarve	Portugal	37.135, -8.387	EZSPM717-12
Melanargia ines	-	Alrededores de Almedijar, Castellon	Spain	39.875, ?	EZSPN620-09
Melanargia ines	-	Jaboneros, Malaga, Andalusia	Spain	36.731, -4.373	VNMB426-08
Melanargia ines	-	Romangordo, Caceres, Extremadura	Spain	39.746, -5.695	EZSPC1131-10
Melanargia ines	-	La Mata, Toledo, Castílla-La Mancha	Spain	39.93, -4.474	EZSPC1133-10
Melanargia ines	-	Sierra de Alhamilla/Almeria, Andalusia	Spain	37.167, -2.333	VNMB234-08
Melanargia ines	-	N. Logrosan, Caceres, Extremadura	Spain	39.333, -5.483	VNMB459-08
Melanargia ines	-	Arroyo de los Molinillos, Viso del Marques	Spain	38.516, -3.597	EZSPM975-12
Melanargia ines	-	Plasencia, Caceres, Extremadura	Spain	40.03, -6.129	EZSPN523-09
Melanargia ines	-	Baix Cinca, Huesca, Aragão	Spain	41.5, 0.067	VNMB571-08
Melanargia ines	-	El Montgo _ Nivel Medio, Xavia, Alicante	Spain	38.802, 0.138	EZSPM780-12
Melanargia ines	-	El Campello, Alicante	Spain	38.433, ?	EZSPM609-12
Melanargia ines	-	Jaboneros, Malaga, Andalusia	Spain	36.731, -4.373	VNMB424-08
Melanargia ines	-	Jaboneros, Malaga, Andalusia	Spain	36.731, -4.373	VNMB425-08
Melanargia ines	-	Ubrique, Puerto de la Vibora, Cadiz	Spain	36.638, -5.455	EZSPN453-09
Melanargia ines	-	El Gastor, Cadiz, Andalusia	Spain	36.856, -5.339	EZSPN438-09
Melanargia ines	-	Porches, Lagoa, Algarve	Portugal	37.135, -8.387	EZSPM715-12
Melanargia ines	-	Faro, Algarve	Portugal	37.167, ?	VNMB233-08
Melanargia ines	-	Faro, Algarve	Portugal	37.167, ?	VNMB140-08
Melanargia ines	-	Sierra de Alhamilla/Almeria, Andalusia	Spain	37.167, -2.333	VNMB141-08
Melanargia ines	-	Aldeire, Granada, Andalusia	Spain	37.154, -3.075	EZSPC1138-10
Melanargia ines	-	Ferreira to Puerto de La Ragua, Granada	Spain	37.154, -3.049	EZSPC972-10
Melanargia ines	-	Djebel Ayachi, Tizi-n-Oufraou, Meknes	Morocco	32.6, ?	VNMB370-08

Melanargia ines	-	Djebel Ayachi, Tizi-n-Oufraou, Meknes	Morocco	32.6, ?	VNMB371-08
Melanargia ines	-	Djebel Ayachi, Tizi-n-Oufraou, Meknes	Morocco	32.6, ?	VNMB372-08
Melanargia ines	-	S vic Afourer, Beni-Mellal, Tadla-Azilal	Morocco	32.33, ?	VNMB143-08
Melanargia ines	-	S vic Afourer, Beni-Mellal, Tadla-Azilal	Morocco	32.21, ?	VNMB239-08
Melanargia ines	-	S vic Afourer, Beni-Mellal, Tadla-Azilal	Morocco	32.21, ?	VNMB238-08
Melanargia ines	-	Tizi-n Tichka, S Taddert, Marrakech	Morocco	31.287, -7.381	VNMB241-08
Melanargia ines	-	Tizi-n-Mlil, Tafraoute, Tiznit	Morocco	29.71, -9	VNMB237-08
Melanargia ines	-	Tizi-n-Mlil, Tafraoute, Tiznit	Morocco	29.71, -9	VNMB142-08
Melanargia ines	-	Tizi-n Tichka, S Taddert, Marrakech	Morocco	31.287, -7.381	VNMB240-08
Melanargia occitanica	EM6461	Diano Castello, Imperia, Liguria	Italy	43.925, 8.064	-
Melanargia occitanica	EM6462	Conna, Andora, Savona, Liguria	Italy	43.983, 8.105	-
Melanargia occitanica	EM1472	Cazevieilles, Montpellier, Gard	France	43.746960, 3.769410	-
Melanargia occitanica	EM1473	Cazevieilles, Montpellier, Gard	France	43.746960, 3.769410	-
Melanargia occitanica	EM1480	Signes, Var, Provence-Alpes-Côte-d'Azur	France	43.280790, 5.822670	-
Melanargia occitanica	EM1474	Cazevieilles, Montpellier, Gard	France	43.746960, 3.769410	-
Melanargia occitanica	EM4653	Serrella, Alicante, Comunidad Valenciana	Spain	38.692900, -0.290150	-
Melanargia occitanica	EM4560	Sierra Maria, Almeria, Andalusia	Spain	37.694300, -2.174800	-
Melanargia occitanica	EM4561	Sierra Maria, Almeria, Andalusia	Spain	37.694300, -2.174800	-
Melanargia occitanica	EM3049	Rodeno, Albarracín, Teruel, Aragão	Spain	40.378540, -1.393570	-
Melanargia occitanica	EM4355	Loeches, Madrid	Spain	40.371700, -3.382180	-
Melanargia occitanica	EM3050	Rodeno, Albarracín, Teruel, Aragão	Spain	40.383237, -1.409343	-
Melanargia occitanica	EM3051	Rodeno, Albarracín, Teruel, Aragão	Spain	40.383237, -1.409343	-
Melanargia occitanica	EM3673	Castronuevo Esgueva, Valladolid	Spain	41.686530, -4.596970	-
Melanargia occitanica	EM3674	Castronuevo Esgueva, Valladolid	Spain	41.686530, -4.596970	-
Melanargia occitanica	EM1465	Valcuerna, Monegros, Aragão	Spain	41.459420, 0.031640	-
Melanargia occitanica	EM4563	Sierra Maria, Almeria, Andalusia	Spain	37.694300, -2.174800	-
Melanargia occitanica	EM3578	Torcal de Antequera, Antequera, Málaga	Spain	36.960530, -4.526850	-
Melanargia occitanica	EM3579	Torcal de Antequera, Antequera, Málaga	Spain	36.960530, -4.526850	-
Melanargia occitanica	EM3580	Torcal de Antequera, Antequera, Málaga	Spain	36.960530, -4.526850	-
Melanargia occitanica	EM3838	Germanelo, Rabaçal, Penela, Coimbra	Portugal	40.031850, -8.435720	-
Melanargia occitanica	EM2717	Zambujeiro, Cascais	Portugal	38.743310, -9.429670	-
Melanargia occitanica	EM3839	Germanelo, Rabaçal, Penela, Coimbra	Portugal	40.031850, -8.435720	-
Melanargia occitanica	EM3840	Germanelo, Rabaçal, Penela, Coimbra	Portugal	40.031850, -8.435720	-
Melanargia occitanica	EM3827	Zambujeiro, Cascais	Portugal	38.742945, -9.430706	-
Melanargia occitanica	EM3828	Zambujeiro, Cascais	Portugal	38.742945, -9.430706	-
Melanargia occitanica	EM1466	Valcuerna, Monegros, Aragão	Spain	41.459420, 0.031640	-

Melanargia occitanica	EM1467	Valcuerna, Monegros, Aragão	Spain	41.459420, 0.031640	-
Melanargia occitanica	EM4624	Serrella, Alicante, Comunidad Valenciana	Spain	38.698900, -0.309100	-
Melanargia occitanica	EM4652	Serrella, Alicante, Comunidad Valenciana	Spain	38.692900, -0.290150	-
Melanargia occitanica	EM3672	Castronuevo Esgueva, Valladolid	Spain	41.686530, -4.596970	-
Melanargia occitanica	EM5742	Portela, Folgosinho, Gouveia, Guarda	Portugal	40.481330, -7.514670	-
Melanargia occitanica	EM5743	Portela, Folgosinho, Gouveia, Guarda	Portugal	40.481330, -7.514670	-
Melanargia occitanica	EM6602	Djebel Hebri, Middle Atlas	Morocco	33.358, -5.140	-
Melanargia occitanica	-	Rollo, Capo Mimosa, Liguria	Italy	43.9442, 8.13344	VNMB565-08
Melanargia occitanica	-	Col de Madeleine, Provence-Alpes	France	44.167, 5.283	VNMB144-08
Melanargia occitanica	-	Col de Madeleine, Provence-Alpes	France	44.167, 5.283	VNMB145-08
Melanargia occitanica	-	Pouzilhac, Languedoc-Roussillon, Occitanie	France	44.05, 4.583	VNMB235-08
Melanargia occitanica	-	Pouzilhac, Languedoc-Roussillon, Occitanie	France	44.05, 4.583	VNMB236-08
Melanargia occitanica	-	Fortuna,Fortuna, Murcia	Spain	38.156, -1.118	EZSPC1342-10
Melanargia occitanica	-	Barranco de Valcuerna, Candasnos, Huesca	Spain	41.465, 0.02	EZSPN132-09
Melanargia occitanica	-	El Burgo Ranero, Castilla y Leon	Spain	42.433, -5.202	EZSPM318-09
Melanargia occitanica	-	Collet de la Tina, La Mussara, Catalonia	Spain	41.276, 1.032	EZSPN202-09
Melanargia occitanica	-	Els Motllats, Vilaplana, Catalonia	Spain	41.271, 1.05	EZSPN339-09
Melanargia occitanica	-	Sierra de Javalambre, Alpuente	Spain	39.917, -1.027	EZSPN361-09
Melanargia occitanica	-	La Calahorra, Andalusia	Spain	37.176, ?	EZSPC1136-10
Melanargia occitanica	-	Arroyo de los Molinillos, Viso del Marques	Spain	38.516, -3.597	EZSPM974-12
Melanargia occitanica	-	Alrededores de Almedijar, Almedijar	Spain	39.875, ?	EZSPN624-09
Melanargia occitanica	-	Candasnos, Huesca, Aragão	Spain	41.5, 0.067	VNMB570-08
Melanargia occitanica	-	Colmenar Viejo, Comunidad de Madrid	Spain	40.642, -3.815	EZSPC1009-10
Melanargia occitanica	-	Campo Real, Comunidad de Madrid	Spain	40.358, -3.364	EZSPN393-09
Melanargia occitanica	-	Barranco de Valcuerna, Candasnos, Aragão	Spain	41.465, 0.02	EZSPC1187-10
Melanargia occitanica	-	Camino de Sa a Portela de Homen, Galicia	Spain	41.863, -8.096	EZSPM257-09
Melanargia occitanica	-	Inifife, Meknes-Tafilalet Region	Morocco	33.1, ?	VNMB361-08
Melanargia occitanica	-	Inifife, Meknes-Tafilalet Region	Morocco	33.1, ?	VNMB362-08
Melanargia occitanica	-	Inifife, Meknes-Tafilalet Region	Morocco	33.1, ?	VNMB363-08
Melanargia occitanica	-	Midelt, Meknes-Tafilalet Region	Morocco	32.68, ?	VNMB146-08
Melanargia occitanica	-	Djebel Ayachi, Tizi-n-Oufraou	Morocco	32.6, ?	VNMB365-08
Melanargia occitanica	-	Midelt, Meknes-Tafilalet Region	Morocco	32.68, ?	VNMB147-08
Melanargia occitanica	-	Djebel Ayachi, Tizi-n-Oufraou	Morocco	32.5999984, -4.8000001	VNMB364-08
Melanargia occitanica	-	Djebel Ayachi, Tizi-n-Oufraou	Morocco	32.5999984, -4.8000001	VNMB366-08
Melanargia occitanica	-	Racca Busambra, Sicily	Italy	37.85, 13.4	VNMB563-08
Melanargia occitanica	-	Busambra, Palermo, Sicily	Italy	37.85, 13.4	VNMB564-08

Melanargia occitanica	-	Racca Busambra, Fieuzza mt., Sicily	Italy	37.85, 13.4	VNMB455-08
Melanargia arge	EM5317	Civita, Castrovillari, Cosenza, Calabria	Italy	39.842720, 16.308650	-
Maniola jurtina	-	?	France	?	KP032276.1
Melanargia ines	-	Caceres, 40 km W Trujillo, Extremadura	Spain	39.3330001, -5.4829998	SalkML02
Melanargia ines	-	Malaga, Jaboneros, Andalusia	Spain	36.7309989, -4.3730001	GQ201286.1
Melanargia ines	-	S vic Afourer, Beni-Mellal, Tadla-Azilal	Morocco	32.3300018, -6.3499999	GQ201279.1
Melanargia ines	-	Meknes, W. Midelt, Djebel Ayachi	Morocco	32.5999984, -4.8000001	GQ201284.1
Melanargia ines	-	Tizi-n-Mlil, Tafraoute, Tiznit	Morocco	29.7099990, -9	GQ201280.1
Melanargia occitanica	-	Pouzilhac, Languedoc-Roussillon	France	44.0499992, 4.5830001	GQ201333.1
Melanargia occitanica	-	Inifife, Meknes-Tafilalet Region	Morocco	33.0999984, -5.0300002	GQ201328.1
Melanargia occitanica	-	Busambra, Palermo, Sicily	Italy	37.8499984, 13.3999996	GQ201334.1
Melanargia arge	-	Salerno, Amalfi, valle delle Ferriere	Italy	40.6329994, 14.6000003	GQ201236.1
Maniola jurtina	-	?	?	?	AF214592.1
Maniola jurtina	-	?	France	?	KP032629.1
Melanargia ines	-	Huesca, Candasnos, Baix Cinca, Aragão	Spain	41.5, 0.0670000	GQ201392.1
Melanargia ines	-	S vic Afourer, Beni-Mellal, Tadla-Azilal	Morocco	32.2099990, -6.5	GQ201391.1
Melanargia ines	-	Tizi-n-Mlil, Tafraoute, Tiznit	Morocco	29.70999908, -9	GQ201390.1
Melanargia occitanica	-	Huesca, Candasnos, Aragão	Spain	41.5, 0.067000002	GQ201406.1
Melanargia occitanica	-	Meknes, W. Midelt, Djebel Ayachi	Morocco	32.5999984, -4.8000001	GQ201405.1
Melanargia arge	-	Salerno, Amalfi, valle delle Ferriere	Italy	40.6329994, 14.6000003	GQ201377.1
Maniola jurtina	-	?	France	?	KP032488.1

Table S3.3 – List of primers, PCR mixture and PCR protocols for each gene analysed. Numbers in brackets represent different trials amplifying that gene for different samples.

Gene	Primers	Final volume of PCR mixture	PCR protocol
COI	LEPF (5'- AAT CAA CCA ATC ATA AAG ATA TTG G -3') and LEPR (5'- TAA ACT TCT GGA TGT CCA AAA AAT -3') (Hajibabaei *et al.* 2006)	Final volume is of 20 µL, comprising 2.5 µL DNA (10-50 ng/µL), 4 µL Colorless GoTaq® Flexi Buffer, 0.16 µL GoTaq® DNA Polymerase, 1.44 µL 1.8 mM $MgCl_2$, 0.8 µL 0.1 mM of dNTPs and 0.8 µL 4 µM of each primer	Initial denaturation step of 5 min at 94ºC, followed by 35 cycles at 94ºC for 30 sec, 53ºC for 45 sec and 72ºC for 1 min, with a final extension step of 72ºC for 7 min
EF1α (1)	ef44 (5'- GCY GAR CGY GAR CGT GGT ATY AC -3') and ELF1R (5'- GTT TCA ACT CTG CCT ACK GGC AC -3') (Kim *et al.* 2010)	Same as COI	Initial denaturation step of 94ºC for 7 min, followed by 35 cycles of 94ºC for 20 sec, 56ºC for 30 sec and 72ºC for 40 sec, with a final extension step of 72ºC for 7 min
EF1α (2)	ef44 (5'- GCY GAR CGY GAR CGT GGT ATY AC -3') and ELF1R (5'- GTT TCA ACT CTG CCT ACK GGC AC -3') (Kim *et al.* 2010)	Same as COI	Same as EF1α (1)
EF1α (3)	ef44 (5'- GCY GAR CGY GAR CGT GGT ATY AC -3') and ELF1R (5'- GTT TCA ACT CTG CCT ACK GGC AC -3') (Kim *et al.* 2010)	Same as COI	Same as EF1α (1)
Wingless (1) Samples: LBL16 and LBL24	WG1 (5′– GART-GYAARTGYCAYGGYATGTCTGG – 3′) and WG2 (5′- ACTICGCARCACCART-GGAATGTRCA – 3′) (Brower & De Salle 1998)	Final volume is of 20 µL, comprising 5 µL DNA (10-50 ng/µL), 4 µL Colorless GoTaq® Flexi Buffer, 0.16 µL GoTaq® DNA Polymerase, 1.44 µL 1.8 mM $MgCl_2$, 0.8 µL 0.1 mM of dNTPs and 0.8 µL 4 µM of each primer	Initial denaturation step of 95ºC for 5 min, followed by 40 cycles of 94ºC for 30 sec, 50ºC for 30 sec and 72ºC for 1:30 min, with a final extension step of 72ºC for 10 min
Wingless (2) Samples: *L. hippothoe*, *L. phlaeas*, *L. virgaureae*	WG1 (5′– GART-GYAARTGYCAYGGYATGTCTGG – 3′) and	Same as COI	Same as Wingless (1) but with anneling temperature of 47ºC

and *L. alciphron*	WG2 (5′- ACTICGCARCACCART-GGAATGTRCA – 3′) (Brower & De Salle 1998)		
Wingless (3) Samples: LTI22	WG1 (5′– GART-GYAARTGYCAYGGYATGTCTGG – 3′) and WG2 (5′- ACTICGCARCACCART-GGAATGTRCA – 3′) (Brower & De Salle 1998)	Final volume is of 20 µL, comprising 5 µL DNA (10-50 ng/µL), 4 µL Colorless GoTaq® Flexi Buffer, 0.16 µL GoTaq® DNA Polymerase, 3 µL 1.8 mM $MgCl_2$, 0.8 µL 0.1 mM of dNTPs a nd 0.8 µL 4 µM of each primer	Same as Wingless (1) but with anneling temperature of 45ºC
Wingless (4) Samples: LBL57	WG1 (5′– GARTGYAARTGYCAYGGYAT-GTCTGG – 3′) and WG2 (5′- ACTICGCAR-CACCARTGGAATGTRCA – 3′) (Brower & De Salle 1998)	Same as Wingless (3)	Same as Wingless (1) but with anneling temperature of 44ºC
16S	16S1_F (5'- AATATTTRATCCTTTCG-TAC20 -3') and 16S1_R (5'- CTT-GTTTATCAAAAACATGTC21 -3') (Wan *et al.* 2013)	Same as Wingless (1)	Initial denaturation step of 94ºC for 7 min, followed by 35 cycles of 94ºC for 1 min, 56ºC for 1 min and 72ºC for 2 min, with a final extension step of 72ºC for 7 min
CAD2	CADmidF (5' - KGGATTYTCNGAYAA-ACAAATNGC24 -3') and CAD1028R (5'-TTRTTNGGNARYTGNCCNCCCAT -3') (Wahlberg & Wheat 2008)	Same as Wingless (1)	Initial denaturation step of 95ºC for 2 min, followed by 40 cycles of 95ºC for 45 sec, 45ºC for 1 min and 72ºC for 1 min, with a final extension step of 72ºC for 5 min

Table S3.4 – List of *Lycaena* datasets with detailed information of dataset type, specimens included and total number of individuals.

Dataset	Type of dataset	Specimens included	No. of individuals included
Dataset 1	All *L. tityrus* + *L. bleusei* COI sequences from our own specimens and online database sequences	EM1249, EM2775, EM3504, EM4700, EM5260, EM5470, LBL 7-22, LBL 24-30, LBL 34-36, LBL40-42, LBL 46-47, LBL 52-57, LTI 10 Ble, LTI 12 Ble, LTI 15 Ble, LTI 17 Ble, LTI 18 Ble, LTI 21 Ble, EZSPN351-0, EZSPC732-1, EZSPC735-1, EZSPC770-1, EZSPC803-1, EZSPC920-1, EZSPM101-0, EZSPN495-0, EZSPN830-0, EZSPN857-0, EZSPN858-0, EM1302, EM1334, EM5258, EM5261, EM6402, EM6404, EM6406, EM6418, EM6420, LTI 11, LTI 13-14, LTI 16, LTI 19-20, LTI 22-47, LTI 49-59, LTI 61-62, EZSPM252-0, EZSPN570-0, EZSPM142-0, EZSPM769-1, EZSPN391-0, EZSPM297-0, EZROM268-0, EZSPM143-0, EZSPC504-0, EZSPC505-0, EZSPC506-0, EZSPC507-0, EZSPC508-0, ABOLB032-1, FBLMU496-0, GBLAB132-1, GWORK519-0, GWORA2468, GWORZ040-1, PHLAW038-1, GBLAA381-1, EZRMN058-0, EZRMN059-0, EZRMN060-0, EZRMN061-0, EZRMN062-0, EZROM267-0, EZROM269-0, EZROM270-0, LEFID122-1, LEFIJ1005, LOWA289-06, GWORO791-0, GBGL0888-0, GWOSF954-1, PHLAA644-0, PHLAB286-1, PHLAB361-1, PHLAH697-1, GWOSF850-1, ODOPE749-1, PHLAB312-1, EULEP4171-16, EULEP4173-16, LEASS522-17, LEASS547-17, GWOTF674-1, PHLAI505-1, LEATH781-1, LEATD296-1, LEATG007-1, LEATG427-1	166
Dataset 2	All *L. tityrus* + *L. bleusei* COI sequences from our own specimens	EM1249, EM2775, EM3504, EM4700, EM5260, EM5470, LBL 7-22, LBL 24-30, LBL 34-36, LBL40-42, LBL 46-47, LBL 52-57, LTI 10 Ble, LTI 12 Ble, LTI 15 Ble, LTI 17 Ble, LTI 18 Ble, LTI 21 Ble, EM1302, EM1334, EM5258, EM5261, EM6402, EM6404, EM6406, EM6418, EM6420, LTI 11, LTI 13-14, LTI 16, LTI 19-20, LTI 22-	103

		47, LTI 49-59, LTI 61-62, (LVI2), (LCA), (LPH2)	
Dataset 3	All *Lycaena* species COI sequences available from our own specimens and online database DNA sequences + outgroup species COI sequences from online databases	LBL 20, LBL 22, LBL 24, LTI 22-24, LVI 1-2, LCA, LHI, LAL 1-2, LLI, LED, LDI, LXA, LRU, LCU, EM5415, EM5417, EM3303, LDA, LSO 1-2, LALP, LAR, LST, LPH 1-2, LDO 1-2, LHE, LMA, LNI 1-2, LHY, LGO, LHET 1-2, LHER, LHELLE, LPA, LBO, CBA, PPA	45
Dataset 4	All *L. tityrus* + *L. bleusei* EF-1α sequences from our own specimens	EM1249, EM2775, EM3504, EM4700, EM5260, EM5470, LBL 7-22, LBL 24-30, LBL 34-36, LBL40-42, LBL 46-47, LBL 52-57, LTI 10 Ble, LTI 12 Ble, LTI 15 Ble, LTI 17 Ble, LTI 18 Ble, LTI 21 Ble, EM1302, EM1334, EM5258, EM5261, EM6402, EM6404, EM6406, EM6418, EM6420, LTI 11, LTI 13-14, LTI 16, LTI 19-20, LTI 22-47, LTI 49-59, LTI 61-62, (LVI2), (LCA), (LPH2)	103
Dataset 5	All *Lycaena* species EF-1α sequences available from our own specimens and online database DNA sequences + outgroup species EF-1α sequences from online databases	LBL 20, LBL 22, LBL 24, LTI 22-24, LVI 1-2, LCA, LHI, LAL 1-2, LLI, LED, LDI, LXA, LRU, LCU, EM5415, EM5417, EM3303, LDA, LSO 1-2, LALP, LAR, LST, LPH 1-2, LDO 1-2, LHE, LMA, LNI 1-2, LHY, LGO, LHET 1-2, LHER, LHELLE, LPA, LBO, CBA, PPA	45
Dataset 6	16S sequences of the Sooty Coppers phylogenetic clade species	LBL16, LBL 24, LTI 22, LTI 23, *L. virgaureae*, *L. hippothoe*, *L. alciphron*, *L. phlaeas*	8
Dataset 7	Wingless sequences of the Sooty Coppers phylogenetic clade species	LBL16, LBL 24, LTI 22, *L. virgaureae*, *L. hippothoe*, *L. alciphron*, *L. phlaeas*	7
Dataset 8	CAD2 sequences of the Sooty Coppers phylogenetic clade species	LBL16, LBL 24, LTI 22, LTI 23, *L. virgaureae*, *L. alciphron*	6
Dataset 9	COI sequences of the Sooty Coppers phylogenetic clade species	LBL16, LBL 24, LTI 22, LTI 23, *L. virgaureae*, *L. hippothoe*, *L. alciphron*, *L. phlaeas*	8
Dataset 10	EF-1α sequences of the Sooty Coppers phylogenetic clade species	LBL16, LBL 24, LTI 22, LTI 23, *L. virgaureae*, *L. hippothoe*, *L. alciphron*, *L. phlaeas*	8

Table S3.5 – List of *Melanargia* datasets with detailed information of dataset type, specimens included and total number of individuals.

Dataset	**Type of dataset**	**Specimens included**	**No. of individuals included**
Dataset 1	Representative COI haplotype sequences from the main populations of *Melanargia ines* and *Melanargia occitanica* + Melanargia arge + outgroup taxon (*M. jurtina*) using our own genetic sequences and online database sequences	EM 1404, EZSPN523-09, EM 1406, EM1417, EM 6553, EM 3314, EM 6461, EM 1473, EM 1465, EM 2717, EM 3580, EM 6602, VNMB455-08, EM 5317, KP032276.1	15
Dataset 2	Representative 16S haplotype sequences from the main populations of *Melanargia ines* and *Melanargia occitanica* + Melanargia arge + outgroup taxon (*M. jurtina*) using our own genetic sequences and online database sequences	SalkML02, GQ201286.1, GQ201279.1, GQ201284.1, GQ201280.1, GQ201333.1, GQ201328.1, GQ201334.1, GQ201236.1, AF214592.1	10
Dataset 3	Representative EF-1α haplotype sequences from the main populations of *Melanargia ines* and *Melanargia occitanica* + Melanargia arge + outgroup taxon (*M. jurtina*) using our own genetic sequences and online database sequences	EM 1404, EM 4410, EM 6553, EM 3314, EM 1473, EM 3673, EM 2717, EM 3580, EM 6602, EM 5317, KP032629.1	11
Dataset 4	Representative Wingless haplotype sequences from the main populations of *Melanargia ines* and *Melanargia occitanica* + Melanargia arge + outgroup taxon (*M. jurtina*) using our own genetic sequences and online database sequences	GQ201392.1, GQ201391.1, GQ201390.1, GQ201406.1, GQ201405.1, GQ201377.1, KP032488.1	7
Dataset 5	All *Melanargia ines* COI sequences available from our own data + online sequences database	EM 1419, EM 2796, EM4265, EM 4985, EM4356, EM 4410, EM 4180, EZSPC1129-10, VNMB458-08, EZSPN710-09, EZSPM716-12, EZSPM717-12, EZSPN620-09, VNMB426-08, EZSPC1131-10, VNMB459-08, EZSPC1133-10, VNMB234-08, EZSPM975-12, EM 4179, EZSPN523-09, EM 4181, EM2864, EM 4393, EM1404, VNMB571-08, EZSPM780-12,	77

		EZSPM609-12, EM1406, VNMB424-08, VNMB424-08, EZSPN453-09, EZSPN438-09, EZSPM715-12, VNMB233-08, VNMB140-08, VNMB141-08, EZSPC1138-10, EZSPC972-10, EM6564, EM6565, EM6567, EM6568, EM6569, EM6571, EM6572, EM6575, EM6594, EM6588, EM6582, EM1416, VNMB370-08, VNMB371-08, EM6581, EM6576, VNMB372-08, EM3325, EM3326, EM1417, EM1418, EM6552, EM6552, EM6559, VNMB143-08, VNMB239-08, VNMB238-08, VNMB241-08, EM3314, EM3321, EM3324, VNMB237-08, EM1412, EM1413, EM1415, EM5684, VNMB142-08, VNMB240-08	
Dataset 6	All *Melanargia occitanica* COI sequences available from our own data + online sequences database	EM 6461, EM 6462, EM 1472, EM 1473, VNMB565-08, VNMB144-08, VNMB145-08, VNMB235-08, VNMB236-08, EM 1480, EM 1474, EM 4653, EZSPC1342-10, EM 4560, EM 4561, EM 3049, EM 4355, EM 3050, EM 3051, EM 3673, EM 3674, EM 1465, EZSPN132-09, EZSPM318-09, EZSPN202-09, EZSPN339-09, EZSPN361-09, EM 4563, EZSPC1136-10, EZSPM974-12, EM 3578, EM 3580, EM 3579, EM 3838, EM 2717, EM 3840, EM 3839, EM 3827, EM 3828, EZSPN624-09, VNMB570-08, EM 1466, EM 1467, EZSPC1009-10, EZSPN393-09, EM 4624, EM 4652, EZSPC1187-10, EM 3672, EZSPM257-09, EM 5742, EM 5743, VNMB363-08, EM6602, VNMB361-08, VNMB362-08, VNMB146-08, VNMB365-08, VNMB147-08, VNMB364-08, VNMB366-08, VNMB563-08, VNMB455-08, VNMB564-08	65

Table S3.6 – List of *Lycaena* specimens included in each population group (region) defined.

Region	Specimens included	Total no. of indivi-duals
Lycaena tityrus		
Estrela **(Western Iberia – AMOVA)**	LTI 11, LTI 13-14, LTI 16, LTI 19-20, LTI 22	7
South of Douro* **(Western Iberia – AMOVA)**	LTI 34-39	6
North of Douro + Galicia **(Western Iberia – AMOVA)**	LTI 28-33, LTI 41-44, LTI 53-55, EM1334, EM5258, EM5261, EZSPM252-09, EZSPN570-09	18
Cantabrian **(Western Iberia – AMOVA)**	LTI 40, LTI 45-47, LTI 49-52, LTI 56-59, LTI 61-62, EM6420, EZSPM142-09, EZSPM769-12, EZSPN391-09, EZSPM297-09, EZSPM143-09	20
Eastern Spain **(Eastern Iberia – AMOVA)**	EM1302, EM6402, EM6404, EM6406, EM6418, EZSPC504-09, EZSPC505-09, EZSPC506-09, EZSPC507-09, EZSPC508-09	10
Western Europe **(Western Europe – AMOVA)**	ABOLB032-15, GBLAB132-13, GWORK519-09, GWORA2468-09, GWORZ040-10, PHLAW038-13, GBLAA381-14, GWORO791-09, FBLMU496-09	9
Eastern Europe **(Eastern Europe – AMOVA)**	LTI 23-27, EZROM268-08, EZRMN058-08, EZRMN061-08, EZROM267-08, EZROM270-08, LEFID122-10, LEFIJ1005-11, LOWA289-06, GBGL0888-06, EZRMN062-08, EZRMN059-08, EZRMN060-08, EZROM269-08	18
L. t. subalpinus **(*L.t. subalpinus* – AMOVA)**	PHLAB312-10, GWOSF854-10, PHLAA644-09, EULEP4171-16, EULEP4173-16, LEASS547-17, LEASS522-17, GWOTF674-12, PHLAI505-13, LEATD296-13, LEATG007-14, LEATG427-14, PHLAB361-10, PHLAH697-12, GWOSF850-10, ODOPE749-11, LEATH781-14, PHLAB286-10	18
Lycaena bleusei		
Western CIMS	LBL 7-15, LBL 55-56, LTI 10 Ble, LTI 12 Ble, LTI 15 Ble, LTI 17 Ble, LTI 18 Ble, LTI 21 Ble, EM2775	18
Douro	LBL 16-17, LBL 53-54, LBL 57	5
Bragança	EM1249, EM5260, EM5470	3
Central CIMS	LBL 18-22, LBL 24-30, LBL 34-36, LBL 40-42, EZSPC732-10, EZSPC735-10, EZSPC803-10, EZSPM101-09, EZSPN495-09, EZSPN830-09	24

Eastern CIMS	EZSPN351-09, EZSPC770-10, EZSPC920-10, EZSPN857-09, EZSPN858-09	5
Toledo Mountains	LBL 46-47, LBL 52, EM4700	4
Burgos	EM3504	1

Table S3.7 – List of *Melanargia* specimens included in each population group (region) defined.

Region	**Specimens included**	**Total no. of individuals**
Melanargia ines		
North Iberia **(Iberia – AMOVA)**	EM4410, EM1404, VNMB571-08	3
Central Iberia **(Iberia – AMOVA)**	EM4265, EM4985, EM4356, EM4180, EM2864, EM4393, EM4179, EM4181, EZSPC1129-10, VNMB458-08, EZSPN620-09, EZSPC1131-10, EZSPC1133-10, VNMB459-08, EZSPM975-12, EZSPN523-09, EZSPM780-12	17
South Iberia **(Iberia – AMOVA)**	EM1419, EM2796, EM1406, EZSPN710-09, EZSPM716-12, EZSPM717-12, VNMB426-08, VNMB234-08, EZ-SPM609-12, VNMB424-08, VNMB425-08, EZSPN453-09, EZSPN438-09, EZ-SPM715-12, VNMB233-08, VNMB140-08, VNMB141-08, EZSPC1138-10, EZ-SPC972-10	19
Rif Mountain range **(Above High Atlas/Morocco – AMOVA)**	EM6594, EM6588, EM6582, EM1416, EM6581	5
Oriental Moroccan region **(Above High Atlas/Morocco – AMOVA)**	EM6567, EM6568, EM6569, EM6571, EM6572, EM6575, EM6576	7
Northern Middle Atlas **(Above High Atlas/Morocco – AMOVA)**	EM6565, EM3325, EM3326, EM1417, EM6564, EM1418	6
Southern Middle Atlas **(Above High Atlas/Morocco – AMOVA)**	EM6552, EM6553, EM6559, VNMB370-08, VNMB371-08, VNMB372-08, VNMB143-08, VNMB239-08, VNMB238-08	9
Southern High Atlas border	EM1412, EM1413, EM1415, EM5684, VNMB241-08, VNMB240-08	6

(Below High Atlas/Morocco – AMOVA)		
Anti Atlas **(Below High Atlas/Morocco – AMOVA)**	EM3314, EM3321, EM3324, VNMB237-08, VNMB142-08	5
Melanargia occitanica		
North Italy **(Above Pyrenees/Above + below Pyrenees – AMOVA)**	EM6461, EM6462, VNMB565-08	3
France **(Above Pyrenees/Above + below Pyrenees – AMOVA)**	EM1472, EM1473, EM1480, EM1474, VNMB144-08, VNMB145-08, VNMB235-08, VNMB236-08	8
North Iberia **(Iberia/Above + below Pyrenees – AMOVA)**	EM3673, EM3674, EM1465, EM1466, EM1467, EM3672, EZSPN132-09, EZSPM318-09, EZSPN202-09, EZSPN339-09, VNMB570-08, EZSPC1187-10, EZSPM257-09	13
Central Iberia **(Iberia/Above + below Pyrenees – AMOVA)**	EM4653, EM3049, EM4355, EM3050, EM3051, EM3838, EM2717, EM3840, EM3839, EM3827, EM3828, EM4624, EM4652, EM5742, EM5743, EZSPC1342-10, EZSPN361-09, EZSPM974-12, EZSPN624-09, EZSPC1009-10, EZSPN393-09,	21
South Iberia **(Iberia/Above + below Pyrenees – AMOVA)**	EM4560, EM4561, EM4563, EM3578, EM3580, EM3579, EZSPC1136-10	7
Middle Atlas **(Middle Atlas – AMOVA)**	EM6602, VNMB363-08, VNMB361-08, VNMB362-08, VNMB146-08, VNMB365-08, VNMB147-08, VNMB364-08, VNMB366-08	9
Sicily **(Sicily – AMOVA)**	VNMB563-08, VNMB455-08, VNMB564-08	3

Table S3.8 – List of parameters and priors used in the divergence time estimates analysis with BEAST for the *Lycaena* case-study.

Parameters / Genes	"Site Models"	"Clock Model"	"Priors"	MCMC
COI	Substitution Model: JC69+I+G • Substitution Rate = 1.0 (not estimated); • "Gamma Category Count" = 4; • "Shape"= 0.76 (estimated); • "Proportion Invariant" = 0.54;	"Relaxed Clock Log Normal" Model with clock rate = 0.0115, (not estimated).	Gene partitions "linked" to share the same topology and branch times. Tree prior: "Birth Death Model" with default parameters. Outgroup calibrated with monophyly and an uniform distribution: [57, 63] Mya.	20M iterations, sampling every 1000. Log and tree files sampled every 100 iterations.
EF-1α	Substitution Model: TIM2+I+G • Substitution Rate = 1.0 (not estimated); • "Gamma Category Count" = 4; • "Shape"= 1.21 (estimated); • "Proportion Invariant" = 0.57;	"Relaxed Clock Log Normal" Model with clock rate = 0.001277, (not estimated).		

Table S3.9 – List of parameters and priors used in the divergence time estimates analysis with BEAST for the *Melanargia* case-study.

Parameters / Genes	"Site Models"	"Clock Model"	"Priors"	MCMC
16S	Substitution Model: TPM2uf • Substitution Rate = 1.0 (not estimated);	"Relaxed Clock Log Normal" Model with clock rate = 0.0086, (not estimated).	Gene partitions "linked" to share the same topology and branch times. Tree prior: "Yule Model" with default parameters. Outgroup calibrated with monophyly and an uniform distribution: [32, 36] Mya.	20M iterations, sampling every 1000. Log and tree files sampled every 100 iterations.
COI	• Substitution Model: JC69+G; • Substitution Rate = 1.0 (not estimated); • "Gamma Category Count" = 4; • "Shape"= 0.16 (estimated);	"Relaxed Clock Log Normal" Model with clock rate = 0.0115, (not estimated).		

EF-1α	• Substitution Model: TN93+G • Kappa 1 e 2 = 2.0 (estimated); • Substitution Rate = 1.0 (not estimated); • "Gamma Category Count" = 4; • "Shape"= 0.3 (estimated);	"Relaxed Clock Log Normal" Model with clock rate = 0.001277, (not estimated).		
Wingless	Substitution Model: HKY+G • Kappa= 2.0 (estimated) • Substitution Rate = 1.0 (not estimated); • "Gamma Category Count" = 4; • "Shape"= 0,19 (estimated);	"Relaxed Clock Log Normal" Model with clock rate = 0.007044, (not estimated).		

Table S3.10 – List of *L. bleusei* specimens included in the Geometric Morphometric analyses. Season: V = Summer; P = Spring.

Species	Specimen	♂ | ♀	Season
L. bleusei	LB_EM5751	M	V
L. bleusei	LB_EM4428	M	P
L. bleusei	LB_EM4445	M	P
L. bleusei	LB_EM4728	M	P
L. bleusei	LB_EM1257	F	V
L. bleusei	LB_EM4451	M	P
L. bleusei	LB_EM4446	F	P
L. bleusei	LB_EM1271	M	V
L. bleusei	LB_EM4406	M	P
L. bleusei	LB_EM4449	M	P
L. bleusei	LB_EM4412	M	P
L. bleusei	LB_EM4396	F	P
L. bleusei	LB_EM5471	M	V
L. bleusei	LB_EM1250	M	P
L. bleusei	LB_EM4405	F	P
L. bleusei	LB_EM4429	M	P
L. bleusei	LB_EM4413	F	P
L. bleusei	LB_EM4447	M	P
L. bleusei	LB_EM4450	M	P
L. bleusei	LB_EM4448	M	V
L. bleusei	LB_EM5280	M	V
L. bleusei	LB_EM5291	F	V
L. bleusei	LB_EM5289	F	V
L. bleusei	LB_EM5290	F	V

L. bleusei	LB_EM5278	M	V
L. bleusei	LB_EM5279	M	V
L. bleusei	LB_EM5255	F	V
L. bleusei	LB_EM5256	M	V
L. bleusei	LB_SC1	M	P
L. bleusei	LB_SC2	F	P
L. bleusei	LB_EM2853	F	P
L. bleusei	LB_EM4172	M	P
L. bleusei	LB_EM2775	F	P
L. bleusei	LB_EM5470	F	V
L. bleusei	LB_EM1236	M	P
L. bleusei	LB_EM1235	F	P
L. bleusei	LB_EM3504	F	P
L. bleusei	LB_EM1238	M	P
L. bleusei	LB_EM1237	M	P
L. bleusei	LB_EM4136	M	V
L. bleusei	LB_SC3	F	P
L. bleusei	LB_LBL17	M	V
L. bleusei	LB_EM2854	M	P
L. bleusei	LB_SC4	M	P
L. bleusei	LB_EM1226	M	P
L. bleusei	LB_EM4699	M	P
L. bleusei	LB_EM4700	M	P
L. bleusei	LB_EM4175	M	P
L. bleusei	LB_EM4251	M	V
L. bleusei	LB_LBL08	M	P
L. bleusei	LB_LBL09	M	P
L. bleusei	LB_LBL10	M	P
L. bleusei	LB_LBL11	M	P
L. bleusei	LB_LBL12	M	P
L. bleusei	LB_LBL14	F	P
L. bleusei	LB_LBL15	M	P
L. bleusei	LB_SEB3	M	P
L. bleusei	LB_SEB4	-	P
L. bleusei	LB_SEB12	M	P
L. bleusei	LB_SEB13	M	P
L. bleusei	LB_SEB14	F	V
L. bleusei	LB_SEB15	F	V
L. bleusei	LB_SEB16	F	V
L. bleusei	LB_SEB18	M	v
L. bleusei	LB_SEB19	F	V
L. bleusei	LB_SEB20	F	V
L. bleusei	LB_SEB22	F	V
L. bleusei	LB_SEB21	M	V
L. bleusei	LB_SEB23	M	V
L. bleusei	LB_SEB24	M	V
L. bleusei	LB_SEB25	M	V
L. bleusei	LB_SEB26	F	V
L. bleusei	LB_SEB34	M	V
L. bleusei	LB_SEB35	M	V
L. bleusei	LB_SEB36	F	V
L. bleusei	LB_EM6425	F	V
L. bleusei	LB_EM6422	M	V
L. bleusei	LB_EM6423	M	V

L. bleusei	LB_EM6424	M	V
L. bleusei	LB_LTI10	M	V
L. bleusei	LB_LTI12	F	V
L. bleusei	LB_LTI15	F	V
L. bleusei	LB_LTI21	M	V

Table S3.11 – List of *L. tityrus* specimens included in the Geometric Morphometric analyses. V = Summer; P = Spring.

Species	Specimen	♂ | ♀	Season
L. tityrus	LT_EM6404	F	P
L. tityrus	LT_EM6398	F	P
L. tityrus	LT_EM6418	M	P
L. tityrus	LT_EM6402	M	P
L. tityrus	LT_EM6403	M	P
L. tityrus	LT_EM6406	M	P
L. tityrus	LT_EM6396	M	P
L. tityrus	LT_EM6397	F	P
L. tityrus	LT_EM6410	M	P
L. tityrus	LT_EM6420	M	P
L. tityrus	LT_EM6409	F	P
L. tityrus	LT_EM1302	M	P
L. tityrus	LT_EM6395	M	P
L. tityrus	LT_EM6415	M	P
L. tityrus	LT_EM6419	M	P
L. tityrus	LT_EM6405	M	P
L. tityrus	LT_EM6417	M	P
L. tityrus	LT_EM6411	F	P
L. tityrus	LT_EM6412	M	P
L. tityrus	LT_EM6416	F	P
L. tityrus	LT_EM6408	F	P
L. tityrus	LT_EM6399	M	P
L. tityrus	LT_EM6413	M	P
L. tityrus	LT_EM6407	M	P
L. tityrus	LT_EM6390	F	P
L. tityrus	LT_EM6401	M	P
L. tityrus	LT_EM6393	F	P
L. tityrus	LT_EM6414	F	P
L. tityrus	LT_EM6394	F	P
L. tityrus	LT_EM6400	M	P
L. tityrus	LT_EM1334	M	P
L. tityrus	LT_EM6391	M	P
L. tityrus	LT_EM6421	M	P
L. tityrus	LT_EM5257	M	V
L. tityrus	LT_EM5258	F	V
L. tityrus	LT_EM5262	F	V
L. tityrus	LT_EM4164	M	V
L. tityrus	LT_EM1325	M	P
L. tityrus	LT_EM1321	M	P
L. tityrus	LT_SC5	M	P
L. tityrus	LT_SC6	M	P
L. tityrus	LT_EM1324	M	P
L. tityrus	LT_EM4156	M	V

L. tityrus	LT_EM3617	M	P
L. tityrus	LT_EM4157	F	V
L. tityrus	LT_EM1313	M	P
L. tityrus	LT_EM1315	M	P
L. tityrus	LT_EM1340	M	P
L. tityrus	LT_EM3611	F	P
L. tityrus	LT_EM5266	M	V
L. tityrus	LT_EM5265	M	V
L. tityrus	LT_EM4135	M	V
L. tityrus	LT_SC7	M	P
L. tityrus	LT_EM1323	M	P
L. tityrus	LT_EM1356	M	P
L. tityrus	LT_EM3771	F	P
L. tityrus	LT_EM3770	F	P
L. tityrus	LT_EM4282	M	V
L. tityrus	LT_EM1355	F	P
L. tityrus	LT_EM1354	M	P
L. tityrus	LT_EM1344	M	V
L. tityrus	LT_EM1319	M	P
L. tityrus	LT_EM1322	M	P
L. tityrus	LT_EM6146	M	P
L. tityrus	LT_EM1337	M	P
L. tityrus	LT_EM1338	M	P
L. tityrus	LT_EM1342	M	P
L. tityrus	LT_EM4134	M	V
L. tityrus	LT_EM1314	F	P
L. tityrus	LT_EM4163	M	V
L. tityrus	LT_EM4159	F	V
L. tityrus	LT_EM1320	M	P
L. tityrus	LT_EM1361	F	P
L. tityrus	LT_EM1336	M	P
L. tityrus	LT_EM1333	F	P
L. tityrus	LT_EM1335	F	P
L. tityrus	LT_EM1318	F	P
L. tityrus	LT_EM4798	M	P
L. tityrus	LT_EM2859	M	P
L. tityrus	LT_EM3752	M	P
L. tityrus	LT_EM3751	F	P
L. tityrus	LT_EM1358	M	P
L. tityrus	LT_EM3511	M	P
L. tityrus	LT_EM2859	M	P
L. tityrus	LT_EM6154	M	P
L. tityrus	LT_EM1317	F	P
L. tityrus	LT_SC8	F	P
L. tityrus	LT_SC9	M	P
L. tityrus	LT_EM5509	M	P
L. tityrus	LT_EM4865	M	P
L. tityrus	LT_EM5263	F	V
L. tityrus	LT_EM5264	F	V
L. tityrus	LT_EM5276	M	V
L. tityrus	LT_EM5277	F	V
L. tityrus	LT_LTI13	F	P
L. tityrus	LT_LTI14	M	P
L. tityrus	LT_LTI22	M	P
L. tityrus	LT_SE1T	M	V
L. tityrus	LT_SE2T	M	V

Table S4.1 – *Lycaena* COI Pairwise distances using Dataset 9.

	1	2	3	4	5	6	7	8
1. LBL 16	-	-	-	-	-	-	-	-
2. LBL 24	0,002	-	-	-	-	-	-	-
3. LTI 22	0,026	0,027	-	-	-	-	-	-
4. LTI 23	0,026	0,027	0,003	-	-	-	-	-
5. L. virgaureae	0,038	0,037	0,029	0,032	-	-	-	-
6. L. hippothoe	0,038	0,041	0,034	0,037	0,036	-	-	-
7. L. alciphron	0,042	0,039	0,038	0,041	0,050	0,049	-	-
8. L. phlaeas	0,050	0,048	0,046	0,049	0,056	0,056	0,052	-

Table S4.2 – *Lycaena* 16S Pairwise distances using Dataset 6.

	1	2	3	4	5	6	7	8
1. LBL 16	-	-	-	-	-	-	-	-
2. LBL 24	0	-	-	-	-	-	-	-
3. LTI 22	0,018	0,024	-	-	-	-	-	-
4. LTI 23	0,016	0,020	0,010	-	-	-	-	-
5. L. virgaureae	0,031	0,040	0,031	0,032	-	-	-	-
6. L. hippothoe	0,042	0,049	0,041	0,042	0,046	-	-	-
7. L. alciphron	0,052	0,067	0,055	0,058	0,056	0,059	-	-
8. L. phlaeas	0,050	0,067	0,051	0,059	0,055	0,050	0,045	-

Table S4.3 – *Lycaena* EF-1α Pairwise distances using Dataset 10.

	1	2	3	4	5	6	7	8
1. LBL 16	-	-	-	-	-	-	-	-
2. LBL 24	0	-	-	-	-	-	-	-
3. LTI 22	0,012	0,012	-	-	-	-	-	-
4. LTI 23	0,010	0,010	0,002	-	-	-	-	-
5. L. virgaureae	0,022	0,024	0,021	0,019	-	-	-	-
6. L. hippothoe	0,017	0,017	0,015	0,012	0,022	-	-	-
7. L. alciphron	0,022	0,024	0,022	0,019	0,027	0,019	-	-
8. L. phlaeas	0,026	0,026	0,024	0,021	0,029	0,017	0,029	-

Table S4.4 – *Lycaena* Wingless Pairwise distances using Dataset 7.

	1	2	3	5	6	7	8
1. LBL 16	-	-	-	-	-	-	-
2. LBL 24	0	-	-	-	-	-	-
3. LTI 22	0,021	0,021	-	-	-	-	-
4. L. virgaureae	0,025	0,026	0,023	-	-	-	-
5. L. hippothoe	0,035	0,036	0,039	0,030	-	-	-
6. L. alciphron	0,022	0,023	0,021	0,012	0,027	-	-
7. L. phlaeas	0,041	0,041	0,033	0,033	0,041	0,033	-

Table S4.5 – *Lycaena* CAD2 Pairwise distances using Dataset 8.

	1	2	3	4	5	6
1. LBL 16	-	-	-	-	-	-
2. LBL 24	0	-	-	-	-	-
3. LTI 22	0,009	0,009	-	-	-	-
4. LTI 23	0,009	0,009	0	-	-	-
5. L. virgaureae	0,048	0,048	0,036	0,036	-	-
6. L. alciphron	0,025	0,025	0,016	0,016	0,051	-

Table S4.6 – COI Pairwise distances for *Lycaena* sister taxa using Dataset 3.

	L. hippothoe	*L. alpheraki*	*L. helloides*	*L. gorgon*	*L. xanthoides*
L. candens	0,012	-	-	-	-
L. solski	-	0,002	-	-	-
L. dorcas	-	-	0,008	-	-
L. heteronea	-	-	-	0,027-0,029	-
L. editha	-	-	-	-	0,020

Table S4.7 – EF-1α Pairwise distances for *Lycaena* sister taxa using Dataset 5.

	L. hippothoe	*L. alpheraki*	*L. helloides*	*L. gorgon*	*L. xanthoides*
L. candens	0	-	-	-	-
L. solski	-	0-0,002	-	-	-
L. dorcas	-	-	0-0,002	-	-
L. heteronea	-	-	-	0,003-0,009	-
L. editha	-	-	-	-	0,002

Table S4.8 – List of all *Lycaena* species included in our phylogenies, their current subgenus attribution and biogeographic region of occurrence.

Name	Current Subgenus	Biogeographic region
Lycaena bleusei	Lycaena - Virgaureae species group (Bozano & Weidenhoffer 2001)	Palaearctic
Lycaena tityrus	Lycaena - Virgaureae species group (Bozano & Weidenhoffer 2001)	Palaearctic
Lycaena candens	Lycaena - Hippothoe species group (Bozano & Weidenhoffer 2001)	Palaearctic
Lycaena hippothoe	Lycaena - Hippothoe species group (Bozano & Weidenhoffer 2001)	Palaearctic
Lycaena virgaureae	Lycaena - Virgaureae species group (Bozano & Weidenhoffer 2001)	Palaearctic
Lycaena solski	Lycaena - Thersamon species group (Bozano & Weidenhoffer 2001)	Palaearctic
Lycaena alpherakyi	Lycaena - Thersamon species group (Bozano & Weidenhoffer 2001)	Palaearctic
Lycaena phoebus	Lycaena - Thersamon species group (Bozano & Weidenhoffer 2001)	Palaearctic
Lycaena aeolides	Lycaena - Dispar species group (Bozano & Weidenhoffer 2001)	Palaearctic
Lycaena dispar	Lycaena - Dispar species group (Bozano & Weidenhoffer 2001)	Palaearctic
Lycaena violacea	Lycaena - Dispar species group (Bozano & Weidenhoffer 2001)	Palaearctic
Lycaena standfussi	Lycaena - Dispar species group (Bozano & Weidenhoffer 2001)	Oriental
Lycaena alciphron	Lycaena - Virgaureae species group (Bozano & Weidenhoffer 2001)	Palaearctic
Lycaena phlaeas	Lycaena - Phlaeas species group (Bozano & Weidenhoffer 2001)	Holarctic
Lycaena cupreus	Lycaena (Pelham 2016)	Nearctic
Lycaena dorcas	Epidemia (Pelham 2016)	Nearctic
Lycaena helloides	Epidemia (Pelham 2016)	Nearctic
Lycaena mariposa	Epidemia (Pelham 2016)	Nearctic
Lycaena nivalis	Epidemia (Pelham 2016)	Nearctic
Lycaena heteronea	Chalceria (Pelham 2016)	Nearctic
Lycaena gorgon	Chalceria (Pelham 2016)	Nearctic
Lycaena hyllus	Epidemia (Pelham 2016)	Nearctic
Lycaena arota	Tharsalea (Pelham 2016)	Nearctic
Lycaena editha	Chalceria (Pelham 2016)	Nearctic
Lycaena xanthoides	Chalceria (Pelham 2016)	Nearctic
Lycaena dione	Chalceria (Pelham 2016)	Nearctic
Lycaena rubidus	Chalceria (Pelham 2016)	Nearctic
Lycaena hermes	Hermelycaena (Pelham 2016)	Nearctic
Lycaena helle	Lycaena - Helle species group (Bozano & Weidenhoffer 2001)	Palaearctic
Lycaena li	Lycaena - Helle species group (Bozano & Weidenhoffer 2001)	Oriental
Lycaena pang	Lycaena - Helle species group (Bozano & Weidenhoffer 2001)	Oriental

Table S4.9 – List of all *L. tityrus* and *L. bleusei* specimens included in our study and their respective morphotype (for *L. tityrus*) and haplotypes.

Name	Code	Morphotype	Haplotype COI	Haplotype EF-1α	Collecting country	Acession number
Lycaena tityrus	LTI 11	Praebleusei	T1	T2	Portugal	-
Lycaena tityrus	LTI 13	Praebleusei	T1	T1 and T2	Portugal	-
Lycaena tityrus	LTI 14	Praebleusei	T1	T1	Portugal	-
Lycaena tityrus	LTI 16	Praebleusei	T1	T2 and T3	Portugal	-
Lycaena tityrus	LTI 19	Praebleusei	T1	T1 and T2	Portugal	-
Lycaena tityrus	LTI 20	Praebleusei	T1	T1	Portugal	-
Lycaena tityrus	LTI 22	Praebleusei	T1	T1 and T2	Portugal	-
Lycaena tityrus	LTI 23	EAST	T8	T6 and T7	Greece	-
Lycaena tityrus	LTI 24	EAST	T9	T6	Greece	-
Lycaena tityrus	LTI 25	EAST	T3	T7	Greece	-
Lycaena tityrus	LTI 26	EAST	T3	T6 and T7	Greece	-
Lycaena tityrus	LTI 27	EAST	T3	T6 and T7	Greece	-
Lycaena tityrus	LTI 28	Praebleusei	T1	T1	Portugal	-
Lycaena tityrus	LTI 29	Praebleusei	T1	T1 and T2	Portugal	-
Lycaena tityrus	LTI 30	Praebleusei	T1	T1 and T3	Portugal	-
Lycaena tityrus	LTI 31	Praebleusei	T1	T1	Portugal	-
Lycaena tityrus	LTI 32	Praebleusei	T1	B2 and B4 Hybrid	Portugal	-
Lycaena tityrus	LTI 33	Praebleusei	T1	B2 and B4 Hybrid	Portugal	-
Lycaena tityrus	LTI 34	Praebleusei	T1	T1	Portugal	-
Lycaena tityrus	LTI 35	Praebleusei	T1	T1	Portugal	-
Lycaena tityrus	LTI 36	Praebleusei	T1	T1	Portugal	-
Lycaena tityrus	LTI 37	Praebleusei	T1	T1	Portugal	-
Lycaena tityrus	LTI 38	Praebleusei	T1	T1 and T3	Portugal	-
Lycaena tityrus	LTI 39	Praebleusei	T1	T2	Portugal	-
Lycaena tityrus	LTI 40	Pallidepicta	T1	T1 and T2	Spain	-
Lycaena tityrus	LTI 41	Praebleusei	T1	T1	Spain	-
Lycaena tityrus	LTI 42	Praebleusei	T1	T1 and T2	Spain	-
Lycaena tityrus	LTI 43	Praebleusei	T1	T1 and T6	Portugal	-
Lycaena tityrus	LTI 44	Praebleusei	T1	-	Portugal	-
Lycaena tityrus	LTI 45	Praebleusei	T1	T2 and T6	Spain	-
Lycaena tityrus	LTI 46	Praebleusei	T1	T1 and T2	Spain	-
Lycaena tityrus	LTI 47	?	T2	T1 and T5	Spain	-
Lycaena tityrus	LTI 49	Praebleusei	T1	T1	Spain	-
Lycaena tityrus	LTI 50	Praebleusei	T2	T1 and T2	Spain	-
Lycaena tityrus	LTI 51	Praebleusei	T2	T2	Spain	-
Lycaena tityrus	LTI 52	Praebleusei	T1	T1 and T2	Spain	-
Lycaena tityrus	LTI 53	Praebleusei	T1	T1	Spain	-
Lycaena tityrus	LTI 54	Praebleusei	T1	T2 and T6	Spain	-
Lycaena tityrus	LTI 55	Praebleusei	T1	T1 and T2	Spain	-
Lycaena tityrus	LTI 56	Praebleusei	T1	T1 and T6	Spain	-
Lycaena tityrus	LTI 57	Praebleusei	T1	T1 and T2	Spain	-
Lycaena tityrus	LTI 58	Praebleusei	T1	T1 and T2	Spain	-
Lycaena tityrus	LTI 59	Praebleusei	T1	T1 and T2	Spain	-
Lycaena tityrus	LTI 61	?	T1	T1 and T2	Spain	-
Lycaena tityrus	LTI 62	?	T1	T1	Spain	-
Lycaena tityrus	EM1302	Pallidepicta	T3	T1	Spain	-
Lycaena tityrus	EM1334	Praebleusei	T1	T1 and T4	Portugal	-
Lycaena tityrus	EM5258	Praebleusei	T1	T2	Portugal	-
Lycaena tityrus	EM5261	Praebleusei	T1	T2 and T4	Portugal	-
Lycaena tityrus	EM6402	Praebleusei	T1	T1	Spain	-
Lycaena tityrus	EM6404	FEMALE - Bright phenotype	T1	T1 and T4	Spain	-
Lycaena tityrus	EM6406	Pallidepicta	T1	T1	Spain	-
Lycaena tityrus	EM6418	Praebleusei	T1	T1	Spain	-
Lycaena tityrus	EM6420	Praebleusei	T1	T2	Spain	-
Lycaena tityrus	-	Praebleusei	T1	-	Spain	EZSPM252-09
Lycaena tityrus	-	FEMALE - Bright phenotype	T1	-	Portugal	EZSPN570-09

Lycaena tityrus	-	Praebleusei	T1	-	Spain	EZSPM142-09
Lycaena tityrus	-	FEMALE - Bright phenotype	T1	-	Spain	EZSPM769-12
Lycaena tityrus	-	FEMALE - Bright phenotype	T1	-	Spain	EZSPN391-09
Lycaena tityrus	-	Praebleusei	T1	-	Spain	EZSPM297-09
Lycaena tityrus	-	FEMALE - Bright phenotype	T1	-	Romania	EZROM268-08
Lycaena tityrus	-	Pallidepicta	T3	-	Spain	EZSPC504-09
Lycaena tityrus	-	Pallidepicta	T3	-	Spain	EZSPC505-09
Lycaena tityrus	-	? No image available	T3	-	Spain	EZSPC506-09
Lycaena tityrus	-	Pallidepicta	T3	-	Spain	EZSPC507-09
Lycaena tityrus	-	Pallidepicta	T3	-	Spain	EZSPC508-09
Lycaena tityrus	-	Northern dark phenotype	T3	-	Italy	ABOLB032-15
Lycaena tityrus	-	FEMALE - Bright phenotype	T3	-	Germany	GBLAB132-13
Lycaena tityrus	-	FEMALE - Dark phenotype	T3	-	Germany	GWORK519-09
Lycaena tityrus	-	Dark phenotype	T3	-	Germany	GWORA2468-09
Lycaena tityrus	-	Dark phenotype	T3	-	Italy	GWORZ040-10
Lycaena tityrus	-	Dark phenotype	T3	-	Austria	PHLAW038-13
Lycaena tityrus	-	FEMALE - Bright phenotype	T3	-	Germany	GBLAA381-14
Lycaena tityrus	-	Dark phenotype	T3	-	Romania	EZRMN058-08
Lycaena tityrus	-	Dark phenotype	T3	-	Romania	EZRMN061-08
Lycaena tityrus	-	Dark phenotype	T3	-	Romania	EZROM267-08
Lycaena tityrus	-	Dark phenotype	T3	-	Romania	EZROM270-08
Lycaena tityrus	-	? No image available	T3	-	Estonia	LEFID122-10
Lycaena tityrus	-	Dark phenotype	T3	-	Estonia	LEFIJ1005-11
Lycaena tityrus	-	Dark phenotype	T3	-	Russia	LOWA289-06
Lycaena tityrus	-	? No image available	T3	-	Turkey	GBGL0888-06
Lycaena tityrus	-	Dark phenotype	T3	-	Switzerland	PHLAB312-10
Lycaena tityrus	-	Dark phenotype	T6	-	Germany	GWOSF854-10
Lycaena tityrus	-	Dark phenotype	T6	-	France	PHLAA644-09
Lycaena tityrus	-	Dark phenotype	T6	-	Austria	EULEP4171-16
Lycaena tityrus	-	Dark phenotype	T6	-	Austria	EULEP4173-16
Lycaena tityrus	-	Dark phenotype	T6	-	Austria	LEASS547-17
Lycaena tityrus	-	FEMALE - Dark phenotype	T6	-	Austria	LEASS522-17
Lycaena tityrus	-	Dark phenotype	T6	-	Germany	GWOTF674-12
Lycaena tityrus	-	Dark phenotype	T6	-	Austria	PHLAI505-13
Lycaena tityrus	-	Dark phenotype	T6	-	Italy	LEATD296-13
Lycaena tityrus	-	Dark phenotype	T6	-	Austria	LEATG007-14
Lycaena tityrus	-	Dark phenotype	T6	-	Italy	LEATG427-14
Lycaena tityrus	-	Dark phenotype	T7	-	Switzerland	PHLAB361-10
Lycaena tityrus	-	Dark phenotype	T7	-	Austria	PHLAH697-12
Lycaena tityrus	-	Dark phenotype	T7	-	Germany	GWOSF850-10
Lycaena tityrus	-	Dark phenotype	T7	-	Germany	ODOPE749-11
Lycaena tityrus	-	Dark phenotype	T7	-	Italy	LEATH781-14
Lycaena tityrus	-	Dark phenotype	T7	-	Switzerland	PHLAB286-10
Lycaena tityrus	-	Praebleusei (darker)	T2	-	Spain	EZSPM143-09
Lycaena tityrus	-	Dark phenotype	T5	-	Germany	GWORO791-09
Lycaena tityrus	-	Dark phenotype	T4	-	Germany	FBLMU496-09
Lycaena tityrus	-	Dark phenotype	T10	-	Romania	EZRMN062-08
Lycaena tityrus	-	? No valid image available	T8	-	Romania	EZRMN059-08
Lycaena tityrus	-	? No valid image available	T8	-	Romania	EZRMN060-08
Lycaena tityrus	-	Dark phenotype	T8	-	Romania	EZROM269-08
Lycaena bleusei	LBL 7	-	B1	B1 and B2	Portugal	-
Lycaena bleusei	LBL 8	-	B2	B1 and B2	Portugal	-
Lycaena bleusei	LBL 9	-	B2	B1 and B3	Portugal	-
Lycaena bleusei	LBL 10	-	B1	B5	Portugal	-
Lycaena bleusei	LBL 11	-	B1	B1 and B2	Portugal	-
Lycaena bleusei	LBL 12	-	B1	B1 and B2	Portugal	-
Lycaena bleusei	LBL 13	-	B1	B2 and B4	Portugal	-
Lycaena bleusei	LBL 14	-	B2	B2 and B4	Portugal	-
Lycaena bleusei	LBL 15	-	B2	B1 and B3	Portugal	-
Lycaena bleusei	LBL 16	-	B2	B3 and B4	Portugal	-
Lycaena bleusei	LBL 17	-	B2	B3 and B4	Portugal	-
Lycaena bleusei	LBL 18	-	B1	B5	Spain	-
Lycaena bleusei	LBL 19	-	B2	-	Spain	-

Lycaena bleusei	LBL 20	-	B2	B2 and B6	Spain	-
Lycaena bleusei	LBL 21	-	B2	B6 and B7	Spain	-
Lycaena bleusei	LBL 22	-	B2	B7	Spain	-
Lycaena bleusei	LBL 24	-	B1	B2 and B5	Spain	-
Lycaena bleusei	LBL 25	-	B2	B2 and B5	Spain	-
Lycaena bleusei	LBL 26	-	B2	B5	Spain	-
Lycaena bleusei	LBL 27	-	B1	B5	Spain	-
Lycaena bleusei	LBL 28	-	B1	B5 and B6	Spain	-
Lycaena bleusei	LBL 29	-	B2	B2 and B5	Spain	-
Lycaena bleusei	LBL 30	-	B2	B1	Spain	-
Lycaena bleusei	LBL 34	-	B2	B2 and B5	Spain	-
Lycaena bleusei	LBL 35	-	B2	B5 and B6	Spain	-
Lycaena bleusei	LBL 36	-	B1	B5	Spain	-
Lycaena bleusei	LBL 40	-	B2	B5 and B6	Spain	-
Lycaena bleusei	LBL 41	-	B2	B5	Spain	-
Lycaena bleusei	LBL 42	-	B2	B5 and B6	Spain	-
Lycaena bleusei	LBL 45	-	?	?	Spain	-
Lycaena bleusei	LBL 46	-	B2	B5 and B6	Spain	-
Lycaena bleusei	LBL 47	-	B2	B5	Spain	-
Lycaena bleusei	LBL 52	-	B2	B5 and B6	Spain	-
Lycaena bleusei	LBL 53	-	B1	B1 and B2	Portugal	-
Lycaena bleusei	LBL 54	-	B2	B6	Portugal	-
Lycaena bleusei	LBL 55	-	B1	B2 and B3	Portugal	-
Lycaena bleusei	LBL 56	-	B1	B5 and B6	Portugal	-
Lycaena bleusei	LBL 57	-	B2	B2 and B4	Portugal	-
Lycaena bleusei	LTI 10*	-	B2	B2 and B3	Portugal	-
Lycaena bleusei	LTI 12*	-	B2	B2 and B3	Portugal	-
Lycaena bleusei	LTI 15*	-	B1	B1 and B2	Portugal	-
Lycaena bleusei	LTI 17*	-	B1	B2 and B4	Portugal	-
Lycaena bleusei	LTI 18*	-	B1	B2	Portugal	-
Lycaena bleusei	LTI 21*	-	B1	B5	Portugal	-
Lycaena bleusei	EM1249	-	B1	B2 and B5	Portugal	-
Lycaena bleusei	EM2775	-	B1	B2 and B5	Portugal	-
Lycaena bleusei	EM3504	-	B2	B3 and B5	Spain	-
Lycaena bleusei	EM4700	-	B2	B3 and B5	Spain	-
Lycaena bleusei	EM5260	-	B1	B5	Portugal	-
Lycaena bleusei	EM5470	-	B2	B5	Portugal	-
Lycaena bleusei	-	-	B2	-	Spain	EZSPN351-09
Lycaena bleusei	-	-	B1	-	Spain	EZSPC732-10
Lycaena bleusei	-	-	B2	-	Spain	EZSPC735-10
Lycaena bleusei	-	-	B2	-	Spain	EZSPC770-10
Lycaena bleusei	-	-	B1	-	Spain	EZSPC803-10
Lycaena bleusei	-	-	B2	-	Spain	EZSPC920-10
Lycaena bleusei	-	-	B2	-	Spain	EZSPM101-09
Lycaena bleusei	-	-	B2	-	Spain	EZSPN495-09
Lycaena bleusei	-	-	B2	-	Spain	EZSPN830-09
Lycaena bleusei	-	-	B1	-	Spain	EZSPN857-09
Lycaena bleusei	-	-	B1	-	Spain	EZSPN858-09

Table S4.10 – Number of individuals, number of haplotypes, haplotypic diversity, nucleotide diversity and neutrality tests Tajima's D and Fu's Fs for each population group (region) defined.

Region	No. of individuals	No. of haplotypes	h	π	Tajima's D	Fu' Fs
Lycaena tityrus						
Estrela **(Western Iberia – AMOVA)**	7	1	0.0000 +/- 0.0000	0.000000 +/- 0.000000	0.00000	N/A
South of Douro* **(Western Iberia – AMOVA)**	6	1	0.0000 +/- 0.0000	0.000000 +/- 0.000000	0.00000	N/A
North of Douro + Galicia **(Western Iberia – AMOVA)**	18	2	0.1111 +/- 0.0964	0.000169 +/- 0.000321	-1.16467	-0.79427
Cantabrian **(Western Iberia – AMOVA)**	19	2	0.2807 +/- 0.1163	0.000427 +/- 0.000535	-0.03486	0.42138
Eastern Spain **(Eastern Iberia – AMOVA)**	11	2	0.5455 +/- 0.0722	0.000830 +/- 0.000833	1.44272	1.13653
Western Europe **(Western Europe – AMOVA)**	9	3	0.4167 +/- 0.1907	0.000676 +/- 0.000749	-1.36240	-1.08110
Eastern Europe (Eastern Europe – AMOVA)	18	5	0.6013 +/- 0.1126	0.001091 +/- 0.000966	-1.19565	-2.19487
L. t. subalpinus **(*L.t. subalpinus* – AMOVA)**	18	3	0.5425 +/- 0.0861	0.001055 +/- 0.000936	-0.57029	0.33588
Lycaena bleusei						
Western CIMS	18	2	0.4706 +/- 0.0823	0.000716 +/- 0.000731	1.16615	1.21483
Douro	5	2	0.4000 +/- 0.2373	0.000609 +/- 0.000774	-0.81650	0.09021
Bragança	3	2	0.6667 +/- 0.3143	0.001015 +/- 0.001266	0.00000	0.20067
Central CIMS	24	2	0.4312 +/- 0.0812	0.000656 +/- 0.000683	1.02682	1.22968
Eastern CIMS	5	2	0.6000 +/- 0.1753	0.000913 +/- 0.001000	1.22474	0.62615
Toledo Mountains	4	1	0.0000 +/- 0.0000	0.000000 +/- 0.000000	0.00000	N/A
Burgos	1	1	1.0000 +/- 0.0000	0.000000 +/- 0.000000	0.00000	N/A

*South of Douro except Estrela

Table S4.11 – Analysis of Molecular Variance (AMOVA) between populations of *Lycaena tityrus*.

	AMOVA 1	Degrees of freedom	Sum of squares	Variance components	Percentage of variation
Lycaena tityrus • Western Iberia • Eastern Iberia • Western Europe • Eastern Europe ***Lycaena t. subalpinus***	Among groups	1	16.428	0.32017 Va	38.16
	Among populations within groups	3	17.780	0.32053 Vb	38.21
	Within populations	101	20.018	0.19820 Vc	23.63
	Total	105	54.226	0.83890	100
	AMOVA 2	**Degrees of freedom**	**Sum of squares**	**Variance components**	**Percentage of variation**
Lycaena tityrus • Western Iberia • Eastern Iberia • *Lycaena t. subalpinus* • Western Europe • Eastern Europe	Among populations	4	34.208	0.44915 Va	69.38
	Within populations	101	20.018	0.19820 Vb	30.62
	Total	105	54.226	0.64735	100
	AMOVA 3	**Degrees of freedom**	**Sum of squares**	**Variance components**	**Percentage of variation**
L. tityrus* Iberia** • Iberia ***L. tityrus* Europe** • Western Europe + Catalonian specimens • Eastern Europe ***Lycaena t. subalpinus	Among groups	2	36.265	0.54091 Va	73.60
	Among populations within groups	1	0.553	0.02334 Vb	3.18
	Within populations	102	17.409	0.17068 Vc	23.22
	Total	105	54.226	0.73493	100

Table S4.12 – Analysis of Molecular Variance (AMOVA) between populations of *Lycaena bleusei*.

	AMOVA 1	Degrees of freedom	Sum of squares	Variance components	Percentage of variation
L. bleusei • Western CIMS • Douro • Bragança • Central CIMS • Eastern CIMS • Toledo Mountains • Burgos	Among populations	6	2.775	0.03336 Va	13.20
	Within populations	53	11.625	0.21934 Vb	86.80
	Total	59	14.400	0.25270	100

Table S4.13 – Pairwise F_{st} between *Lycaena bleusei* populations. Values above 0.5 are highlighted.

Lycaena bleusei	Western CIMS	Douro	Bragança	Central CIMS	Eastern CIMS	Toledo Mountains	Bur-gos
Western CIMS	-						
Douro	0.25850	-					
Bragança	- 0.24138	0.15167	-				
Central CIMS	0.20970	-0.11251	0.11111	-			
Eastern CIMS	0.01557	-0.13636	-0.17978	-0.10510	-		
Toledo Mountains	0.48936	-0.05263	**0.57895**	0.07167	0.19463	-	
Burgos	0.29412	-1.00000	0.00000	-0.47826	-0.50000	0.00000	-

Table S4.14 – Pairwise comparisons of wing shape between groups: *L. bleusei* F – *Lycaena bleusei* females; *L. bleusei* M – *Lycaena bleusei* males; *L. tityrus* F – *Lycaena tityrus* females; *L. tityrus* M – *Lycaena tityrus* males.

Group	*L. bleusei* F	*L. bleusei* M	*L. tityrus* F
L. bleusei F	-	-	-
L. bleusei M	0.0509	-	-
L. tityrus F	0.0494	0.0460	-
L. tityrus M	0.0844	0.0395	0.0575

Table S4.15 – Centroid sizes of each boxplot group from Figure 4.9.

Group	**Centroid size**
Lycaena bleusei females	1871.487
Lycaena bleusei males	1684.607
Lycaena tityrus females	1561.097
Lycaena tityrus males	1511.172

Table S4.16 – Centroid sizes of each boxplot group from Figure S4.24.

Group	Code	Centroid size
Lycaena bleusei females (Spring)	LB.F.Sp	1797.828
Lycaena bleusei females (Summer)	LB.F.S	1919.149
Lycaena bleusei males (Spring)	LB.M.Sp	1710.924
Lycaena bleusei males (Summer)	LB.M.S	1649.136
Lycaena tityrus females (Spring)	LT.F.Sp	1592.222
Lycaena tityrus females (Summer)	LT.F.S	1467.724
Lycaena tityrus males (Spring)	LT.M.Sp	1520.039
Lycaena tityrus males (Summer)	LT.M.S	1473.655

Table S4.17 – List of WorldClim bioclimatic variables and respective codes.

Code	Bioclimatic Variable
BIO1	Annual Mean Temperature
BIO2	Mean Diurnal Range (Mean of monthly (max temp - min temp))
BIO3	Isothermality (BIO2/BIO7) (* 100)
BIO4	Temperature Seasonality (standard deviation *100)
BIO5	Max Temperature of Warmest Month
BIO6	Min Temperature of Coldest Month
BIO7	Temperature Annual Range (BIO5-BIO6)
BIO8	Mean Temperature of Wettest Quarter
BIO9	Mean Temperature of Driest Quarter
BIO10	Mean Temperature of Warmest Quarter
BIO11	Mean Temperature of Coldest Quarter
BIO12	Annual Precipitation
BIO13	Precipitation of Wettest Month
BIO14	Precipitation of Driest Month
BIO15	Precipitation Seasonality (Coefficient of Variation)
BIO16	Precipitation of Wettest Quarter
BIO17	Precipitation of Driest Quarter
BIO18	Precipitation of Warmest Quarter
BIO19	Precipitation of Coldest Quarter

Table S5.1 – Demographic tests of Tajima D and Fu' Fs for *Lycaena bleusei* in Iberia and *Lycaena tityrus* in Iberia and Europe.

	Iberia				Europe			
Species	Tajima D	Fu' FS	Gene copies	No. of sequences	Tajima D	Fu' FS	Gene copies	No. of sequences
Lycaena tityrus	-0.48791	-0.49997	61	3	-1.12659	-3.50569	88	8
Lycaena bleusei	1.63801	1.98947	60	2	-	-	-	-

Table S6.1 – List of Melanargia specimens included in the analyses with their respective haplotype and sampling location.

Name	Code	Haplotype COI	Collecting location	Collecting country	Acession number
Melanargia ines	EM1419	I1	Cerro de Meias, Loulé, Faro	Portugal	-
Melanargia ines	EM2796	I1	Caroucha, Castro Marim, Faro	Portugal	-
Melanargia ines	EM4265	I1	Laje, Porto Salvo, Oeiras, Lisboa	Portugal	-
Melanargia ines	EM4985	I1	Sierra Martés, Yátova, Buñol	Spain	-
Melanargia ines	EM4356	I1	Loeches, Madrid	Spain	-
Melanargia ines	EM4410	I1	Balsamão, Chacim, Macedo Cavaleiros	Portugal	-
Melanargia ines	EM4180	I1	Brotas, Mora, Évora	Portugal	-
Melanargia ines	EM1404	I8	Valcuerna, Monegros, Aragão	Spain	-
Melanargia ines	EM1406	I10	La Luz, Alcornocales, Tarifa, Cádiz	Spain	-
Melanargia ines	EM2864	I7	Horta, Vila Nova Foz Côa, Guarda	Portugal	-
Melanargia ines	EM4393	I7	Douro, Ligares, Freixo Espada a Cinta	Portugal	-
Melanargia ines	EM4179	I4	Brotas, Mora, Évora	Portugal	-
Melanargia ines	EM4181	I6	Brotas, Mora, Évora	Portugal	-
Melanargia ines	EM6565	I18	Ras El Ma, Taza, Djbel Tazekka	Morocco	-
Melanargia ines	EM6567	I18	Idardar, Taourirt, Oriental	Morocco	-
Melanargia ines	EM6568	I18	Idardar, Taourirt, Oriental	Morocco	-
Melanargia ines	EM6569	I18	Idardar, Taourirt, Oriental	Morocco	-
Melanargia ines	EM6571	I18	Ouled Ben Tahar, Beni Snassen, Oriental	Morocco	-
Melanargia ines	EM6572	I18	Ouled Ben Tahar, Beni Snassen, Oriental	Morocco	-
Melanargia ines	EM6575	I18	Tinissane, Beni Snassen, Oriental	Morocco	-
Melanargia ines	EM6594	I18	Tighezratine, Aknoul, Rif	Morocco	-
Melanargia ines	EM6588	I18	Tizi Ouasli, Ichellahane, Rif	Morocco	-
Melanargia ines	EM6582	I18	Kassita, Driouch	Morocco	-
Melanargia ines	EM1416	I18	Djebel Tisouka, Chefchaouen	Morocco	-
Melanargia ines	EM3325	I22	Ait Saleh, Imouzzer, Middle Atlas	Morocco	-
Melanargia ines	EM3326	I22	Ait Saleh, Imouzzer, Middle Atlas	Morocco	-
Melanargia ines	EM1417	I23	Ito – planalto, Middle Atlas	Morocco	-
Melanargia ines	EM6564	I17	Ras El Ma, Taza, Djbel Tazekka	Morocco	-
Melanargia ines	EM6581	I19	Al Hoceima	Morocco	-
Melanargia ines	EM6576	I20	Tinissane, Beni Snassen, Oriental	Morocco	-
Melanargia ines	EM1412	I28	Tizi-n-Test – South, High Atlas	Morocco	-
Melanargia ines	EM1413	I28	Tizi-n-Test – South, High Atlas	Morocco	-
Melanargia ines	EM1415	I28	Tizi-n-Test – South, High Atlas	Morocco	-

Melanargia ines	EM5684	I28	Tizi-n-Test, High Atlas	Morocco	-
Melanargia ines	EM1418	I24	Ito – planalto, Middle Atlas	Morocco	-
Melanargia ines	EM6552	I24	Ait Ourir, SE Marrakech	Morocco	-
Melanargia ines	EM6553	I24	Imlil, Demnate, High Atlas	Morocco	-
Melanargia ines	EM6559	I24	Sour El Aiz, Imlil, Demnate, High Atlas	Morocco	-
Melanargia ines	EM3314	I27	Tifghalt, Tafraoute, Anti-Atlas	Morocco	-
Melanargia ines	EM3321	I27	Col Kerdous, Tafraoute, Anti-Atlas	Morocco	-
Melanargia ines	EM3324	I27	Tizi-n-Tarakatine, Tafraoute, Anti-Atlas	Morocco	-
Melanargia ines	-	I1	Almaraz, Caceres, Extremadura	Spain	EZSPC1129-10
Melanargia ines	-	I1	N. Logrosan, Caceres, Extremadura	Spain	VNMB458-08
Melanargia ines	-	I1	Venta del Molinillo, Huetor de Santillan	Spain	EZSPN710-09
Melanargia ines	-	I1	Porches, Lagoa, Algarve	Portugal	EZSPM716-12
Melanargia ines	-	I1	Porches, Lagoa, Algarve	Portugal	EZSPM717-12
Melanargia ines	-	I1	Alrededores de Almedijar, Castellon	Spain	EZSPN620-09
Melanargia ines	-	I1	Jaboneros, Malaga, Andalusia	Spain	VNMB426-08
Melanargia ines	-	I2	Romangordo, Caceres, Extremadura	Spain	EZSPC1131-10
Melanargia ines	-	I2	La Mata, Toledo, Castílla-La Mancha	Spain	EZSPC1133-10
Melanargia ines	-	I2	Sierra de Alhamilla/Almeria, Andalusia	Spain	VNMB234-08
Melanargia ines	-	I2	N. Logrosan, Caceres, Extremadura	Spain	VNMB459-08
Melanargia ines	-	I3	Arroyo de los Molinillos, Viso del Marques	Spain	EZSPM975-12
Melanargia ines	-	I5	Plasencia, Caceres, Extremadura	Spain	EZSPN523-09
Melanargia ines	-	I8	Baix Cinca, Huesca, Aragão	Spain	VNMB571-08
Melanargia ines	-	I8	El Montgo _ Nivel Medio, Xavia, Alicante	Spain	EZSPM780-12
Melanargia ines	-	I9	El Campello, Alicante	Spain	EZSPM609-12
Melanargia ines	-	I10	Jaboneros, Malaga, Andalusia	Spain	VNMB424-08
Melanargia ines	-	I10	Jaboneros, Malaga, Andalusia	Spain	VNMB425-08
Melanargia ines	-	I11	Ubrique, Puerto de la Vibora, Cadiz	Spain	EZSPN453-09
Melanargia ines	-	I11	El Gastor, Cadiz, Andalusia	Spain	EZSPN438-09
Melanargia ines	-	I12	Porches, Lagoa, Algarve	Portugal	EZSPM715-12
Melanargia ines	-	I13	Faro, Algarve	Portugal	VNMB233-08
Melanargia ines	-	I14	Faro, Algarve	Portugal	VNMB140-08
Melanargia ines	-	I15	Sierra de Alhamilla/Almeria, Andalusia	Spain	VNMB141-08
Melanargia ines	-	I15	Aldeire, Granada, Andalusia	Spain	EZSPC1138-10
Melanargia ines	-	I16	Ferreira to Puerto de La Ragua, Granada	Spain	EZSPC972-10
Melanargia ines	-	I18	Djebel Ayachi, Tizi-n-Oufraou, Meknes	Morocco	VNMB370-08
Melanargia ines	-	I18	Djebel Ayachi, Tizi-n-Oufraou, Meknes	Morocco	VNMB371-08
Melanargia ines	-	I21	Djebel Ayachi, Tizi-n-Oufraou, Meknes	Morocco	VNMB372-08

Melanargia ines	-	I24	S vic Afourer, Beni-Mellal, Tadla-Azilal	Morocco	VNMB143-08
Melanargia ines	-	I24	S vic Afourer, Beni-Mellal, Tadla-Azilal	Morocco	VNMB239-08
Melanargia ines	-	I25	S vic Afourer, Beni-Mellal, Tadla-Azilal	Morocco	VNMB238-08
Melanargia ines	-	I26	Tizi-n Tichka, S Taddert, Marrakech	Morocco	VNMB241-08
Melanargia ines	-	I27	Tizi-n-Mlil, Tafraoute, Tiznit	Morocco	VNMB237-08
Melanargia ines	-	I28	Tizi-n-Mlil, Tafraoute, Tiznit	Morocco	VNMB142-08
Melanargia ines	-	I29	Tizi-n Tichka, S Taddert, Marrakech	Morocco	VNMB240-08
Melanargia occitanica	EM6461	O1	Diano Castello, Imperia, Liguria	Italy	-
Melanargia occitanica	EM6462	O1	Conna, Andora, Savona, Liguria	Italy	-
Melanargia occitanica	EM1472	O1	Cazevieilles, Montpellier, Gard	France	-
Melanargia occitanica	EM1473	O1	Cazevieilles, Montpellier, Gard	France	-
Melanargia occitanica	EM1480	O4	Signes, Var, Provence-Alpes-Côte-d'Azur	France	-
Melanargia occitanica	EM1474	O5	Cazevieilles, Montpellier, Gard	France	-
Melanargia occitanica	EM4653	O6	Serrella, Alicante, Comunidad Valenciana	Spain	-
Melanargia occitanica	EM4560	O7	Sierra Maria, Almeria, Andalusia	Spain	-
Melanargia occitanica	EM4561	O7	Sierra Maria, Almeria, Andalusia	Spain	-
Melanargia occitanica	EM3049	O8	Rodeno, Albarracín, Teruel, Aragão	Spain	-
Melanargia occitanica	EM4355	O9	Loeches, Madrid	Spain	-
Melanargia occitanica	EM3050	O10	Rodeno, Albarracín, Teruel, Aragão	Spain	-
Melanargia occitanica	EM3051	O10	Rodeno, Albarracín, Teruel, Aragão	Spain	-
Melanargia occitanica	EM3673	O10	Castronuevo Esgueva, Valladolid	Spain	-
Melanargia occitanica	EM3674	O10	Castronuevo Esgueva, Valladolid	Spain	-
Melanargia occitanica	EM1465	O10	Valcuerna, Monegros, Aragão	Spain	-
Melanargia occitanica	EM4563	O11	Sierra Maria, Almeria, Andalusia	Spain	-
Melanargia occitanica	EM3578	O14	Torcal de Antequera, Antequera, Málaga	Spain	-
Melanargia occitanica	EM3579	O14	Torcal de Antequera, Antequera, Málaga	Spain	-
Melanargia occitanica	EM3580	O15	Torcal de Antequera, Antequera, Málaga	Spain	-
Melanargia occitanica	EM3838	O16	Germanelo, Rabaçal, Penela, Coimbra	Portugal	-
Melanargia occitanica	EM2717	O16	Zambujeiro, Cascais	Portugal	-
Melanargia occitanica	EM3839	O17	Germanelo, Rabaçal, Penela, Coimbra	Portugal	-
Melanargia occitanica	EM3840	O18	Germanelo, Rabaçal, Penela, Coimbra	Portugal	-
Melanargia occitanica	EM3827	O18	Zambujeiro, Cascais	Portugal	-
Melanargia occitanica	EM3828	O19	Zambujeiro, Cascais	Portugal	-
Melanargia occitanica	EM1466	O22	Valcuerna, Monegros, Aragão	Spain	-
Melanargia occitanica	EM1467	O23	Valcuerna, Monegros, Aragão	Spain	-
Melanargia occitanica	EM4624	O26	Serrella, Alicante, Comunidad Valenciana	Spain	-

Melanargia occitanica	EM4652	O27	Serrella, Alicante, Comunidad Valenciana	Spain	-
Melanargia occitanica	EM3672	O29	Castronuevo Esgueva, Valladolid	Spain	-
Melanargia occitanica	EM5742	O31	Portela, Folgosinho, Gouveia, Guarda	Portugal	-
Melanargia occitanica	EM5743	O32	Portela, Folgosinho, Gouveia, Guarda	Portugal	-
Melanargia occitanica	EM6602	O34	Djebel Hebri, Middle Atlas	Morocco	-
Melanargia occitanica	-	O1	Rollo, Capo Mimosa, Liguria	Italy	VNMB565-08
Melanargia occitanica	-	O2	Col de Madeleine, Provence-Alpes	France	VNMB144-08
Melanargia occitanica	-	O3	Col de Madeleine, Provence-Alpes	France	VNMB145-08
Melanargia occitanica	-	O3	Pouzilhac, Languedoc-Roussillon, Occitanie	France	VNMB235-08
Melanargia occitanica	-	O3	Pouzilhac, Languedoc-Roussillon, Occitanie	France	VNMB236-08
Melanargia occitanica	-	O6	Fortuna,Fortuna, Murcia	Spain	EZSPC1342-10
Melanargia occitanica	-	O10	Barranco de Valcuerna, Candasnos, Huesca	Spain	EZSPN132-09
Melanargia occitanica	-	O10	El Burgo Ranero, Castilla y Leon	Spain	EZSPM318-09
Melanargia occitanica	-	O10	Collet de la Tina, La Mussara, Catalonia	Spain	EZSPN202-09
Melanargia occitanica	-	O10	Els Motllats, Vilaplana, Catalonia	Spain	EZSPN339-09
Melanargia occitanica	-	O10	Sierra de Javalambre, Alpuente	Spain	EZSPN361-09
Melanargia occitanica	-	O12	La Calahorra, Andalusia	Spain	EZSPC1136-10
Melanargia occitanica	-	O13	Arroyo de los Molinillos, Viso del Marques	Spain	EZSPM974-12
Melanargia occitanica	-	O20	Alrededores de Almedijar, Almedijar	Spain	EZSPN624-09
Melanargia occitanica	-	O21	Candasnos, Huesca, Aragão	Spain	VNMB570-08
Melanargia occitanica	-	O24	Colmenar Viejo, Comunidad de Madrid	Spain	EZSPC1009-10
Melanargia occitanica	-	O25	Campo Real, Comunidad de Madrid	Spain	EZSPN393-09
Melanargia occitanica	-	O28	Barranco de Valcuerna, Candasnos, Aragão	Spain	EZSPC1187-10
Melanargia occitanica	-	O30	Camino de Sa a Portela de Homen, Galicia	Spain	EZSPM257-09
Melanargia occitanica	-	O33	Inifife, Meknes-Tafilalet Region	Morocco	VNMB361-08
Melanargia occitanica	-	O34	Inifife, Meknes-Tafilalet Region	Morocco	VNMB362-08
Melanargia occitanica	-	O34	Inifife, Meknes-Tafilalet Region	Morocco	VNMB363-08
Melanargia occitanica	-	O34	Midelt, Meknes-Tafilalet Region	Morocco	VNMB146-08
Melanargia occitanica	-	O34	Djebel Ayachi, Tizi-n-Oufraou	Morocco	VNMB365-08
Melanargia occitanica	-	O35	Midelt, Meknes-Tafilalet Region	Morocco	VNMB147-08
Melanargia occitanica	-	O36	Djebel Ayachi, Tizi-n-Oufraou	Morocco	VNMB364-08
Melanargia occitanica	-	O37	Djebel Ayachi, Tizi-n-Oufraou	Morocco	VNMB366-08
Melanargia occitanica	-	O38	Racca Busambra, Sicily	Italy	VNMB563-08
Melanargia occitanica	-	O39	Busambra, Palermo, Sicily	Italy	VNMB564-08
Melanargia occitanica	-	O40	Racca Busambra, Fieuzza mt., Sicily	Italy	VNMB455-08

Table S6.2 – Number of individuals, number of haplotypes, haplotypic diversity, nucleotide diversity and neutrality tests Tajima's D and Fu's Fs for each population group (region) defined.

Region	No. of individuals	No. of haplotypes	h	π	Tajima's D	Fu' Fs
Melanargia ines						
North Iberia	3	2	0.6667 +/- 0.3143	0.001013 +/- 0.001264	0.00000	0.20067
Central Iberia	17	8	0.8162 +/- 0.0815	0.001997 +/- 0.001471	-1.29553	-4.39197
South Iberia	19	10	0.8830 +/- 0.0563	0.002417 +/- 0.001678	-1.04344	-6.06464
Rif Mountain range	5	2	0.4000 +/- 0.2373	0.000644 +/- 0.000819	-0.81650	0.09021
Oriental Moroccan region	7	2	0.2857 +/- 0.1964	0.000908 +/- 0.000948	-1.23716	0.85642
Northern Middle Atlas	6	5	0.9333 +/- 0.1217	0.006080 +/- 0.004106	-0.21398	-0.83934
Southern Middle Atlas	9	4	0.6944 +/- 0.1470	0.003911 +/- 0.002645	0.46802	0.82623
Southern High Atlas border	6	3	0.6000 +/- 0.2152	0.004863 +/- 0.003366	-1.12062	1.94878
Anti Atlas	5	2	0.4000 +/- 0.2373	0.000608 +/- 0.000773	-0.81650	0.09021
Melanargia occitanica						
North Italy	3	1	0.0000 +/- 0.0000	0.000000 +/- 0.000000	0.00000	N/A
France	8	5	0.8571 +/- 0.1083	0.002334 +/- 0.001772	-0.92337	-1.74756
North Iberia	14	8	0.7692 +/- 0.1198	0.003240 +/- 0.002150	-1.25391	-3.10145
Central Iberia	18	14	0.9673 +/- 0.0298	0.004785 +/- 0.002926	-1.63386	-9.66096
South Iberia	11	8	0.9455 +/- 0.0535	0.006632 +/- 0.004003	-0.38374	-1.83937
Middle Atlas	9	5	0.7222 +/- 0.1592	0.003419 +/- 0.002355	-1.84361	-0.61358
Sicily	3	3	1.0000 +/- 0.2722	0.009160 +/- 0.007479	0.00000	0.58779